Department of Electrical and Computer Engineering

Hierarchical Optimization of Voltages, VArs and Real Power in Distribution Networks

Xiangjing Su

This thesis is presented for the Degree of

Doctor of Philosophy

at

Curtin University

August 2015

Declaration

To the best of my knowledge and belief this thesis contains no material previously published by any other person except where due acknowledgment has been made.

This thesis contains no material which has been accepted for the award of any other degree or diploma in any university.

Signature : 

Date : 29/08/2015

Abstract

The distribution networks are often of high complexity with a large system scale and diverse load types. Moreover, they are also expanding at a staggering rate in terms of complexity. All nations face a significant investment challenge to build, expand or refurbish their electrical power networks to meet the increasing loads. Meanwhile, network operators are also reporting a significant and growing demand for the connections of renewable energy systems such as solar and wind generators as well as smart devices such as electric vehicles and distributed storage batteries. In Smart Grid era, intelligent algorithms are presupposed to exist to control networks of high complexity. However, in reality a significant practical and fundamental knowledge gap exists. Although highly automated and integrated control systems have been proposed, systems with coverage from the zone substation to the low-voltage (LV) feeders practically do not exist. By studying the physical structure of distribution networks, this research is dedicated to propose a hierarchical optimization strategy that could fully exploit the capabilities of both traditional and emerging devices, expand the network load capacity and accommodate more renewable connections.

Chapter 1 of this thesis will first review the recent changes within distribution networks, especially in Smart Grid era, and their impacts on system control. Then, the advanced hierarchical control theory which can effectively handle system complexity is introduced with a brief review on its applications in power systems to identify the knowledge gap. After that, by studying the physical structure of distribution networks under the background of Smart Grid, a novel hierarchical control strategy is proposed to optimize distribution networks of high complexity. In addition, the objectives, methodologies and contributions of the thesis are also presented.

Chapter 2 will present a comprehensive review on some most popular algorithms for solving the optimization problems of power systems which generally fall into two categories: constrained nonlinear programming problem (CNLP) and mixed integer nonlinear programming problem (MINLP). Based on careful comparison, two most promising methods are selected to support the hierarchical optimization proposed. Besides, optimization problems of distribution networks usually involve multiple mutually conflicting objectives. Thus, a review on the strategies and methods which can effectively handle multi-objective optimization problems is also presented.

Chapter 3 focuses on the formulation of LV controllers of the proposed hierarchical control. Specifically, based on the reactive capability and real power curtailment of inverters, a comprehensive PV control strategy as well as a multi-objective optimization model is proposed to improve the performance of unbalanced three-phase four-wire LV distribution networks of high residential PV penetrations.

Chapter 4 builds up the medium-voltage (MV) controller of the proposed hierarchical control. Specifically, a comprehensive optimization based sequential strategy and a multi-objective optimization based real-time strategy is presented for the placement and control of delta switched capacitors in unbalanced MV distribution networks.

In Chapter 5, an effective coordination interface for the LV and MV controllers is presented based on the detailed analysis of a most common delta-grounded wye distribution transformer. Then, by combing this interface with the LV and MV controllers of Chapters 3 and 4, a three-step hierarchical control strategy is proposed to coordinate the control on LV and MV levels and optimize the operation of the whole distribution network at an affordable computational cost.

Chapter 6 of the thesis presents the complete optimization models for each stage of the proposed three-step hierarchical control based on Chapters 3, 4 and 5. Then a detailed simulation on a real unbalanced Western Australian distribution network of high complexity is performed over 24 hours. The analysis and comparison on the results in terms of both optimality and efficiency demonstrate the feasibility, effectiveness and superiority of the proposed hierarchical optimization.

Dedication

To my loved wife Jing and daughter Zihan,

and my parents.

Acknowledgment

Firstly, I would like to express my sincere gratitude to my Ph.D. supervisor, Professor Mohammad A.S. Masoum for his invaluable supervision, encouragement, and suggestions throughout this research. He is such a wonderful advisor and mentor. I thank him for every piece of his intensive efforts that have been put into this project. I also would like to thank my associate Ph.D. supervisor, Professor Peter J. Wolfs. I am very grateful that he continued to supervise me and meet me online every week till the submission of this thesis even though he relocated back to Central Queensland University in the middle of my Ph.D. study. He is such a great person, and I appreciate everything he has done for me.

I would like to thank Margaret Pittuck, Robyn Cornwell and Mark Fowler for their kind assistance. I am grateful to the other Ph.D. students in my office who have helped me during my study. Their emotional support and friendship is something I shall never forget.

I also would like to express my deepest gratitude to Chinese government and Curtin University for the China State Scholarship and the Curtin International Postgraduate Research Scholarship that provides financial support throughout my Ph.D. research.

Let me reserve my final appreciation to my family. Without the care and love from my parents, I definitely could not have completed my doctoral study. They have always offered me so much but asked for so little. Special thanks to my wife, whose sincerest love has given me courage to face difficulties in the way of pursuing my dream. I am very proud of my daughter, who newly joined the family. She has been giving me huge pleasure and keeping me so energised throughout the final stage of my Ph.D. study.

Contents

List of Figures

List of Tables

Chapter 1. Introduction

1.1 STATEMENT OF THE PROBLEM

The distribution networks are often characterized by high complexity. In Australia, a zone substation can typically supply up to a dozen feeders and a feeder could feed as many as 5,000 homes over a length of tens of kilometres. Moreover, distribution networks are also expanding at a staggering rate in terms of complexity. Energy and peak demand are increasing in the developing world. In the first world peak demand still grows albeit with declining energy consumption. All nations face a significant investment challenge to build, expand or refurbish electrical power networks, especially in the distribution area. The Australian Energy Regulator (AER) approved investments of $7.4B and $36.1B in the transmission and distribution networks, respectively, during the current five-year regulatory period [1]. As network investment is responsible for more than half of Australian retail electricity cost, Australia's Federal Government has released its Energy White Paper 2012 [2] which sets out a strategic policy framework focused on the affordable supply of reliable electric power. Meanwhile, distribution network operators are also reporting a significant and growing demand for the connections of renewable energy systems such as solar [3-6] and wind [7-9] energy generators. Additionally, smart devices such as plug-in electric vehicles [10-13] and distributed storage batteries [14-16] have also already demonstrated their promising application prospects in distribution networks.

In Smart Grid era, intelligent algorithms are presupposed to exist to optimize power networks of high complexity [17, 18]. However, in reality a significant practical and fundamental knowledge gap exists. Although highly automated and integrated control systems have been proposed, systems with coverage from the zone substation to the low-voltage (LV) feeder level practically do not exist. The primary barrier is,

with the significant increase of complexity of distribution networks, the problem dimension is also getting much larger. As a result, it becomes unfeasible to develop a control system using a model representation of the whole distribution network, which is both computationally complex and expensive and unlikely to be robust.

1.2 RESEARCH MOTIVATION

To deal with the control problems of complex power systems, some advanced control theories have been introduced over the last decades. Among them, hierarchical control is the most promising and has shown its effectiveness in reducing the problem complexity in practice. Hierarchical control was first proposed around 1970 by M. D. Mesarovic, etc. with the aim to reduce the computational effort of large-scale control systems [19]. Since then, it has been further improved by many researchers and an influential complete description of hierarchical control concepts can be found in [20, 21].

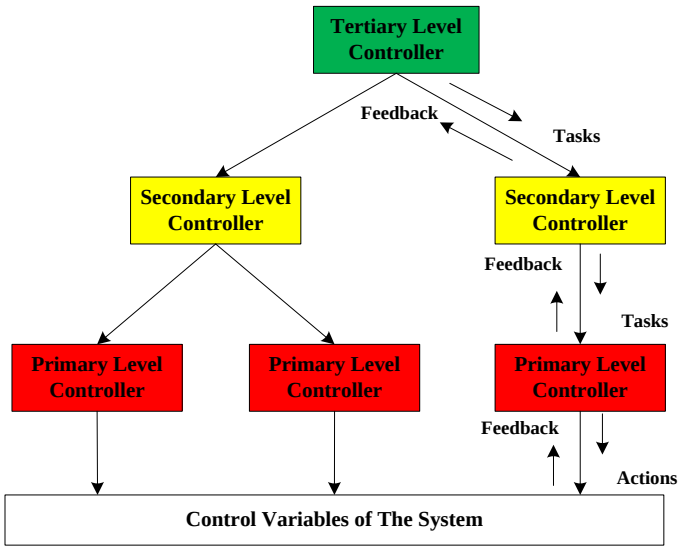

Figure 1.1 Hierarchical control system.

As shown in figure 1.1, in hierarchical control, the control system of a complex network is decomposed into two or more levels where controllers on each level send control tasks to controllers on the lower level and feedback to controllers on the upper level. Basically, among the controllers on different levels of the hierarchy,

only part of them have access to the control variables of the problem while the others, at a higher level, define the tasks and coordinate the lower-level controllers.

In hierarchical control theory, decomposition is a key concept and it directly impacts both the accuracy and efficiency. By far, many types of decomposition techniques have been proposed according to the system characteristics and problems of interest. Basically, three kinds of decomposition are commonly found in the previous studies, including level decomposition, time decomposition and mode decomposition [22]. By decomposing a complex system into some simpler subsystems, hierarchical control could significantly reduce the dimension of problem and therefore the computation time as well as communication burden. Besides, the introduction of parallel computing technologies can further improve the computation performance of hierarchical control. Additionally, with an effective coordination between controllers of different levels, hierarchical control can also retain high solution optimality.

Hierarchical control has been first adopted to solve the control problems of electric transmission systems which are usually of a large scale and high complexity [23-27]. Recently, with the proliferation of micro-grid, some studies also attempted to apply hierarchical control in micro-grids to mimic the existing control behaviours on the transmission level with some superior performance obtained [28-32]. However, only a few hierarchical studies have been conducted in the distribution area with a focus on the network reconfiguration problems [33-35]. As the distribution network is getting more complicated than ever before, especially with the increasing connections of renewable energy systems and smart devices in Smart Grid era, there is a real and urgent demand to apply hierarchical control in distribution networks to achieve various control tasks with both accuracy and efficiency.

In fact, distribution networks have a hierarchical physical structure and are naturally suited to hierarchical control approaches. Figure 1.2 shows the likely developmental path for intelligent distribution networks in Smart Grid age. Specifically, multiple medium-voltage (MV) feeders are supplied from an on-line tap changer (OLTC) equipped zone substation transformer. The first MV feeder includes a combination of state estimation and direct state measurement with coverage of a robust

communication medium either through Nation Broadband Network (NBN), Advanced Metering Infrastructures (AMI) or other means. Low cost and robust communication and computational capability will improve our knowledge of the network [36]. The next evolutionary stage in the second MV feeder is the deployments of intelligent devices. Voltage regulators and capacitor banks are widely deployed but traditionally respond to local voltages and currents. A robust communication network raises the possibility of remote control. The third feeder incorporates intelligent devices at the low-voltage (LV) consumer premises. The proliferation of rooftop solar systems has resulted in power quality issues, which have resulted in calls for changes to the interconnection standards [37]. Besides, the emergence of electric vehicles (EV) with vehicle to grid (V2G) regeneration capability or the availability of large numbers of "second-use" EV batteries raises the possibility of household level energy storage [38]. There is a potential to aggregate the storage and reactive capabilities of residential systems to provide grid support.

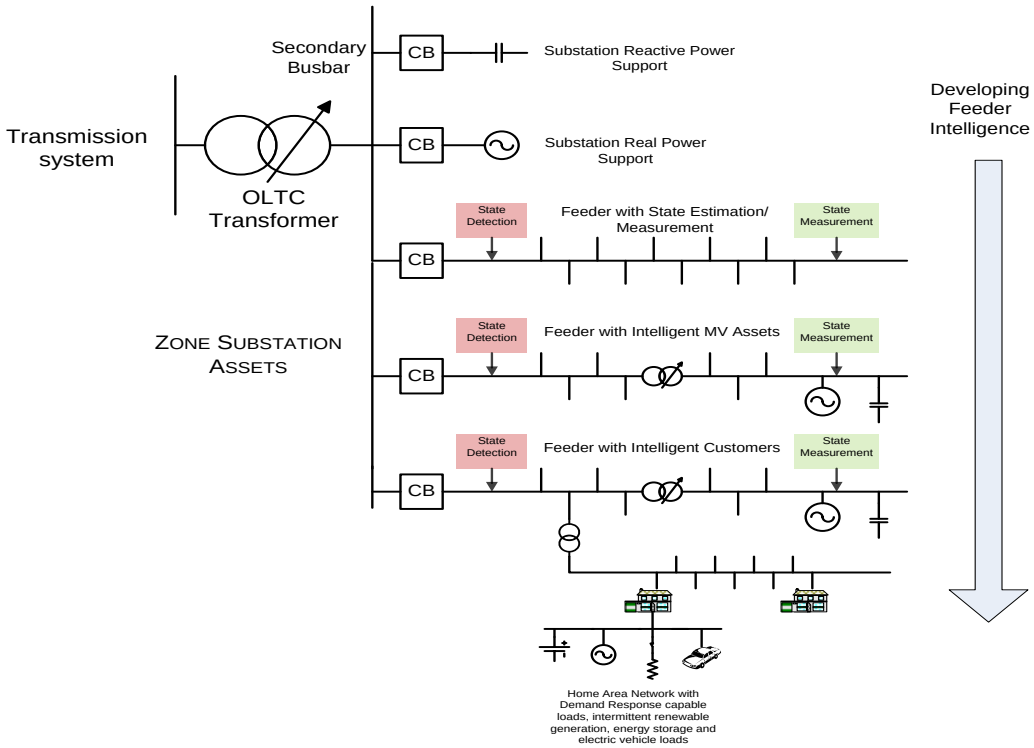

Figure 1.2 Hierarchy and the evolution of intelligent feeders.

In addition, although hierarchical control has been utilized in transmission systems and micro-grids, some technical challenges still exist especially when applying it in distribution networks. Specifically, firstly all the existing hierarchical control studies assume a balanced network model [23-35], which is reasonable on the transmission level. However, due to non-uniform load allocations and non-even conductor spacing among phases, distribution networks are naturally unbalanced. Therefore, hierarchical control with an unbalanced distribution network model is required for a better control accuracy and effect. Moreover, the existing hierarchical researches often focus on one single objective each time [23-35]. Nevertheless, control problems of power systems usually involve multiple objectives which are mutually conflicting. To generate a feasible and reasonable network solution after control, a multi-objective hierarchical control, which can effectively balance different goals while the constraints of practical networks exist, is desired.

1.3 RESEARCH OBJECTIVES

By studying the physical structure of distribution networks, this research is dedicated to propose a hierarchical optimization strategy with a complete system coverage, which could fully exploit the capabilities of traditional and emerging devices to expand network load capacity and accommodate increasing renewable connections, at an affordable computational cost.

A set of more specific objectives of this study are listed as follows:

1) A hierarchical control strategy will be proposed for distribution networks of high complexity to improve both the operational and computational performance;
2) The grid support capabilities of the traditional (e.g. delta switched capacitors) and emerging (e.g. rooftop PV systems) devices in terms of voltages, VArs and real power will be fully exploited and coordinated within distribution networks;
3) Typical multi-objective optimization problems will be studied on each level of the proposed hierarchical control to effectively manage the mutually conflicting objectives and achieve the desired network operational performance after control;

4) Unbalanced network model will be employed throughout this study to depict the physical features of real distribution networks of high complexity for a higher control accuracy;
5) This research will also improve the system control flexibility by supporting different sets of objectives and solution algorithms on different levels of the proposed hierarchical control.

1.4 RESEARCH METHODOLOGIES

In this research, based on the natural voltage level decomposition (i.e. MV and LV) of distribution networks, a novel hierarchical control strategy will be proposed to reduce the problem complexity and improve both the operational and computational performance. Figure 1.3 below describes the brief idea of the proposed hierarchical control of complex distribution networks.

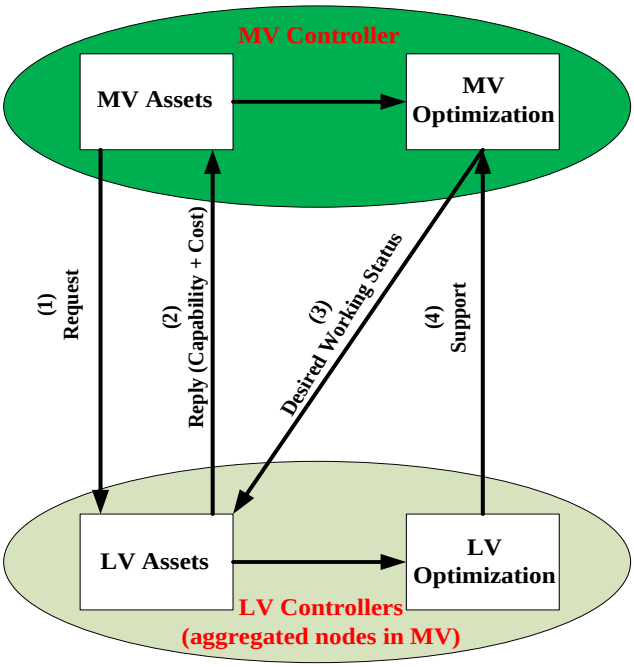

Figure 1.3 Brief of the proposed hierarchical control strategy.

Specifically, when doing the hierarchical control, the top-level MV controller installed on the substation transformer will first send a request to the bottom-level LV controllers installed on distribution transformers for their voltages, VArs and real power support capabilities and the corresponding costs. Once receive these

information, the MV controller will treat the LV feeders supplied by distribution transformers as aggregated nodes in the MV network. Together with the MV controllable devices, these aggregated LV nodes will be optimally controlled by the MV optimization to improve the MV operational performance with the desired working status for each LV feeder generated. Finally, LV optimization will be performed within each LV feeder by controlling the LV active devices to meet the MV support request as well as improve the LV operational performance. The full version of this hierarchical control strategy will be presented in Chapter 5 where some related technical challenges such as control interface will also be addressed.

To perform the proposed hierarchical optimization above and fulfill the control objectives of Section 1.3, the following methodologies are utilized in this research:

1) Due to the existence of both continuous (e.g. LV rooftop PVs) and discrete (e.g. MV switched capacitors) control variables, sub-problems of hierarchical optimization generally falls into two categories: constrained nonlinear programming problem (CNLP) and mixed integer nonlinear programming problem (MINLP). Therefore, a comprehensive review and comparison on some most popular optimization algorithms will be conducted to select the most promising methods for the two problems above.
2) As the optimization of distribution networks often involves multiple mutually conflicting objectives, strategies which can effectively manage the various objectives will be studied to support the multi-objective hierarchical optimization of distribution networks.
3) On the LV level, considering the proliferation of residential PV systems in Australia, a comprehensive multi-objective optimization of unbalanced LV distribution feeders based on the latent reactive capability and active real power curtailment of PV inverters will be presented, which forms the LV controllers of the proposed hierarchical control.
4) On the MV level, the optimal placement and real-time control problems of delta-connected switched capacitors will be studied in the unbalanced MV network

based on multi-objective optimization. This builds up the MV controller of the proposed hierarchical control.

5) The most critical part of the proposed hierarchical control is how to effectively and efficiently coordinate the MV and LV controllers to achieve the operation optimization of the whole distribution network. In this study, based on detailed analysis on the voltages, currents and power relationships of the most common delta-grounded wye distribution transformer, an efficient coordination interface will be presented to support the hierarchical control proposed.
6) The proposed LV controller, MV controller and coordination interface will finally form the hierarchical control strategy proposed in this research and the individual and overall performance be studied based on detailed simulations over 24 hours on a real Western Australian distribution network .

1.5 THESIS STRUCTURE

Overall, this thesis comprises seven chapters with organization as follows:

1) Chapter 1 provides the motivation, objectives, methodologies and organization of this research as well as a summary of the contributions.
2) Chapter 2 presents a comprehensive review on some most popular optimization algorithms for solving both the CNLP problem and MINLP problem with the most promising methods selected. Besides, a brief review on the strategies to effectively handle multi-objective optimization problems is also presented.
3) Chapter 3 focuses on the LV controller of the proposed hierarchical control. Specifically, based on the reactive capability and real power curtailment of inverters, a comprehensive PV control strategy as well as a multi-objective optimization model is proposed to enhance the performance of unbalanced three-phase four-wire LV distribution networks of high residential PV penetrations.
4) Chapter 4 aims to form the MV controller of the proposed hierarchical control. More exactly, a comprehensive optimization based sequential strategy and a multi-objective optimization based real-time strategy is presented for the optimal

placement and control of delta-connected switched capacitors in unbalanced MV distribution networks.

5) In Chapter 5, a detailed coordination interface for the LV and MV controllers is proposed based on the analysis of the voltages, currents and power relationships between the MV and LV sides of a most common distribution transformer of delta-grounded wye connection. Then, by combing the coordination interface and the LV and MV controllers of Chapters 3 and 4, a complete three-step hierarchical control strategy is finally presented to coordinate the control on both LV and MV levels and to optimize the whole distribution network operation at an affordable computational cost.
6) Chapter 6 of the thesis presents the multi-objective optimization models for each step of the proposed hierarchical control based on the Chapters 3, 4 and 5. Then detailed simulations on a real unbalanced Western Australian distribution network of high complexity are performed over 24 hours. The analysis and comparison of the results in terms of optimality and efficiency demonstrates the feasibility, validity and efficiency of the proposed hierarchical control.
7) Finally, conclusion and contributions as well future research work are presented in Chapter 7.

1.6 LIST OF AUTHOR'S PUBLICATIONS

The main content of the thesis is based on the following published/submitted articles:

- **Journal papers:**

J1. **X. Su**, M.A.S. Masoum, P. Wolfs, "Multi-Objective Hierarchical Control of Unbalanced Distribution Networks to Accommodate More Renewable Connections in the Smart Grid Era," **Submitted to IEEE Transactions on Power Systems**, Manuscript ID: TPWRS-00665-2015, 2015.

J2. **X. Su**, M.A.S. Masoum, P. Wolfs, "PSO and Improved BSFS Based Sequential Comprehensive Placement and Real-time Multi-objective Control of Delta-connected Switched Capacitors in Unbalanced Radial MV

Distribution Networks," **IEEE Transactions on Power Systems**, Paper Number: TPWRS-01222-2014, **In Press**, 2015.

J3. **X. Su**, M.A.S. Masoum, P. Wolfs, "Optimal PV Inverter Reactive Power Control and Real Power Curtailment to Improve Performance of Unbalanced Four-Wire LV Distribution Networks," **IEEE Transactions on Sustainable Energy**, Vol.5, No.3, pp.967-977, 2014.

J4. **X. Su**, M.A.S. Masoum, P. Wolfs, "Comprehensive Optimal PV Inverter Control Strategy in Unbalanced Three-Phase Four-Wire LV Distribution Networks," **IET Generation, Transmission & Distribution**, Vol.8, No.11, pp.1848-1859, 2014.

- **Conference papers:**

C1. **X. Su**, M.A.S. Masoum and P. Wolfs. "PSO Based Multi-objective Optimization of Unbalanced LV Distribution Network by PV Inverter Control," 6th International Conference on Electricity Distribution (CICED2014), Shenzhen, China, pp. 1-4, Sep. 23-26, 2014.

C2. **X. Su**, M.A.S Masoum and P. Wolfs. "Comprehensive Optimization of PV Inverter Reactive and Real Power Flows in Unbalanced Four Wire LV Distribution Network Operations," IEEE Power & Energy Society General Meeting (PES), Vancouver, Canada, pp. 1-5, Jul. 21-25, 2013.

C3. **X. Su**, P. Wolfs, M.A.S. Masoum, "Optimal Operation of Multiple Unbalanced Distributed Generation Sources in Three-Phase Four-Wire LV Distribution Networks," Australasian Universities Power Engineering Conference (AUPEC2012), Bali, Indonesia, pp. 1-6, Sep. 26-29, 2012.

Chapter 2. Optimization Algorithms in Power Systems: A Review and Selection

2.1 INTRODUCTION

Optimization plays a very important role in the control of power systems, especially for the hierarchical control proposed in this research. Due to the nonlinear network characteristics, control of power systems is often formulated as a nonlinear optimization problem with nonlinear objectives and (or) constraints. Based on the types of control variables, power optimization problems can be roughly divided into the following two categories: constrained nonlinear programming (CNLP) problem and mixed integer nonlinear programming (MINLP) problem. For CNLP problems, the objective and constraints are nonlinear functions of control variables which all have a continuous solution range. Devices with continuous control variables are common in power networks such as renewable solar and wind generators and most types of loads. On the other hand, if parts of the control variables are limited to only take an integer value, the corresponding optimization problem is often known as a MINLP problem. Devices with discrete control variables are also widely used in power systems, such as transformers equipped with load tap changers, switched capacitor banks and voltage regulators. For the above-mentioned two typical optimization problems, many solution algorithms have been proposed and implemented in practice with various performance obtained. To support the potential optimization on both LV and MV levels of the proposed hierarchical control, a comprehensive review on the existing most popular optimization algorithms will first be conducted. After careful comparison, two most promising methods will be selected for solving the CNLP and MINLP problems in this hierarchical study. Besides, as optimization problems of power systems usually involve multiple objectives which are mutually contradicting. Therefore, at the end of this chapter, the

concept of Pareto Optimization is introduced to describe the solutions of multi-objective optimization and a most popular and efficient strategy to solve multi-objective optimization problems is also presented.

2.2 ALGORITHMS REVIEW FOR CNLP AND MINLP PROBLEMS

In the past decades, numerous studies have been performed to propose and develop optimization methods for various control aims of power systems. For example, for the CNLP problems, classical optimization techniques such as penalty function (PF) methods, interior point (IP) methods and sequential quadratic programming (SQP) method have shown their effectiveness with a long history of successful applications. Meanwhile, for the more complicated MINLP problems, heuristic methods such as evolutionary programming (EP), simulated annealing (SA), tabu search (TS), genetic algorithm (GA) and particle swarm optimization (PSO) have been gradually demonstrating their superior performance. In this research, as optimization directly impacts the performance of the proposed hierarchical control in terms of both accuracy and efficiency, a comprehensive review on the most popular approaches for CNLP and MINLP problems is conducted to identify the advantages and disadvantages of each.

2.2.1 Classical Optimization Techniques for CNLP Problems

The classical optimization methods for CNLP problems are usually an iterative process to locate the optima. The basic idea is that, given an initial point $\boldsymbol{X_0}$, the optimization generates a sequence $\boldsymbol{X_i}$ of evaluation points, by means of a specified iterative rule, such that when $\boldsymbol{X_i}$ is finite, the last point is the optimal solution of the problem. A typical behaviour of a classical optimization algorithm is that the evaluation point $\boldsymbol{X_i}$ moves steadily towards the neighbourhood of the local optima $\boldsymbol{X}^*$ and then rapidly converges to this point. When a predefined convergence criteria is met, the iteration process will be terminated.

As a most common and most historical concern of power systems, CNLP problems have been well researched with a variety of solution approaches proposed and

applied. Several most popular methods are briefly reviewed below with their advantages and disadvantages identified.

A. Penalty Function Methods

The penalty function methods are an important class of algorithms for CNLP problems. In this class of methods, the original constrained problem is replaced with an unconstrained one by adding a penalty term to the objective function. Specifically, a high cost is imposed on the objective function when the constraints are violated while zero cost added when the constraints are feasible. Because they are simple in theory and capable to handle all types of constraints, penalty function methods have been widely used for solving CNLP problems of power systems [39-43].

In practice, penalty function methods often cooperate with other unconstrained optimization methods. By removing the complicated constraints, penalty function methods pave the way for the applications of various unconstrained optimization approaches. Among them, three classical methods including Newton's method, conjugate gradient method and quasi-Newton method are presented.

1) Newton's Method

The basic idea of Newton's method for unconstrained nonlinear optimization is to iteratively use the quadratic approximation of the objective function throughout the whole process. Therefore, for problems with a positive definite quadratic objective function, Newton's method can reach the optima within several iterations. In addition, when the starting point is properly selected, the Newton's method which has a quadratic convergence rate can converge rapidly.

In [44-48], researchers explored the applications of Newton's method in power systems with some satisfactory results generated. Specifically, Newton's method is used in [44] to solve the nonlinear optimization problem of the incorporation of unified power flow controllers in optimal power flow (OPF) with considerable progress achieved. Besides, references [45, 46] propose to apply Newton's method for the power flow calculation of power systems by minimizing the square sum of

discrepancies of nodal capacities. In [47], the classical optimal power flow problem is solved by an explicit Newton's approach with efficient and robust solutions obtained. Then, this Newton-OPF program developed in [47] is implemented for optimal reactive power scheduling in the Taiwan power systems [48].

However, Newton's method also has some noticeable drawbacks which limit its application range and capability. Firstly, Newton's method is based on the calculation of Hessian matrix which offers useful curvature information. But, for various practical problems of large scale, computing the Hessian matrix is highly expensive and the Hessian is also not available analytically in some cases. Besides, Newton's method is sensitive to the selection of initial point. Precisely, when the starting point is close to the optima, it will converge quickly while when the starting point is far from the solution, the convergence of Newton's method is not guaranteed. To alleviate or overcome these disadvantages of Newton's method, some other methods e.g. conjugate gradient method and quasi-Newton method are proposed.

2) Conjugate Gradient Method

The conjugate gradient method was originally proposed by Hestenes and Stiefel in the 1950s [49] and then developed by Fletcher and Reeves in the 1960s [50] for unconstrained optimization. The conjugate gradient method deflects the descent direction by adding to it a positive multiple of the direction used in the last step. By means of conjugacy, this method only requires the first-order instead of the second-order derivatives which are required by Newton's method, and thus it does not need to calculate the Hessian matrix. With a higher efficiency and reliability as well as quadratic convergence rate, conjugate gradient method is applicable to large-scale optimization problems in power systems [51-55]. Specifically, in [51, 52], together with the penalty function method, the conjugate gradient method is used to deal with the optimal compensation of distribution networks which is approached and solved as a nonlinear optimization problem. To damp low-frequency power oscillations of an interconnected power system, the conjugate gradient method is employed in [53]

to optimally assess the parameters of power system stabilizers. A conjugate gradient method based strategy is also presented in [54] for the most economical operation of a hydrothermal power system over a one-year time span. Additionally, the problem of hydroelectric scheduling is solved as an unconstrained nonlinear optimization problem in [55] with the penalty function method used for the constraints and the conjugated gradient method for the optimization.

3) Quasi Newton Method

Due to the difficulty of computation of Hessian matrix in Newton's method, another classical algorithm, quasi-Newton method, which only uses the function value and the gradient of the objective function is proposed [56, 57] and it is closely related to the Newton's method. Quasi-Newton is such a method which needs not to compute the Hessian, but generates a series of Hessian approximations and at the same time maintains a fast rate of super-linear convergence. The key point of the quasi-Newton method is to produce Hessian approximations by the use of some convenient techniques so that the quasi-Newton equation holds.

Since proposed, quasi-Newton method has been used for various optimization purposes in power systems [58-62]. Specifically, by using quasi-Newton algorithm, a generalized nonlinear predictive controller is developed in [58] for the application of power plants load-frequency control. In [59], quasi-Newton method together with augmented Lagrangian functions are utilized for power system voltage optimization and the efficiency of quasi-Newton method is proved by the simulation results. Moreover, to support the application of advanced distribution management system in Smart Grid era, reference [60] proposes a quasi-Newton based methodology for unbalanced three-phase optimal power flow of distribution systems. Quasi-Newton algorithm is also put forward to support the proposed framework in [61] for optimal load-frequency control in deregulated power systems with objectives to optimize both the indices of economy and stability. Additionally, in [62] the quasi-Newton algorithm under the direction of the suggested control strategy is employed for the

layered parameter optimization of power system stabilizers and HVDC damping controllers in China southern power grid.

The aforementioned three classical methods for the CNLP problem have strict requirements on choosing penalty function. However, due to the introduction of penalty function, their solutions have a high risk to be infeasible. Meanwhile, their computation also converges more slowly as they cannot effectively deal with inequality constraints. To address these disadvantages, another two classical optimization algorithms, which can effectively handle the constraints with no need of penalty function, are presented below.

B. Interior Point Methods

Another important class of optimization techniques for the CNLP problems is the interior point (IP) methods. Although it was originally proposed to solve linear programming (LP) problems, because of its superb performance displayed, the IP methods have been further extended to tackle nonlinear programming problems. The earliest ideas of the IP methods can be traced back to 1955 when Frisch proposed a log-barrier function to replace the linear inequality constraints [63]. The term 'interior point methods' was firstly introduced by Fiacco and McCormick in their book [64]. However, the optimization area has not been significantly influenced by the introduction of IP methods until the publication of Karmarkar's landmark paper in 1984 [65].

Usually, IP methods can be divided into three main categories: projective methods, affine-scaling methods and primal-dual methods [66, 67]. Projective methods including Karmarkar's original work are responsible for the great interests in this area. As the simplification of projective methods, affine-scaling methods became very popular at their time due to the reduced computational complexity. Nevertheless, it is the primal-dual interior point methods that are, at present, accepted as the most computationally effective IP algorithms.

The basic primal-dual interior point method usually consists of four main steps [68-70]. Firstly, slack variables are introduced to convert inequality constraints into

equality constraints. Then, the slack variables are added to the objective function as soft constraints using logarithmic barrier functions. After that, a Lagrangian function is formed by integrating all constraints to the modified objective function. Consequently, the constrained optimization problem is converted into an unconstrained one. Finally, the Karush Kuhn Tucker (KKT) first order optimality conditions are applied to obtain a set of nonlinear equations which are then solved by the Newton's method.

By far, IP methods have shown attractive traits in terms of fast convergence and numeric robustness. Specifically, besides the strong capability in treatment of inequality constraints, they converge in polynomial time as well as can handle the numerical ill conditioning. Additionally, unlike Newton's methods which are sensitive to initial point, IP algorithms allow an infeasible starting point. Due to the above-mentioned advantages, IP methods have computationally proven to be a viable alternative for a wide range of optimization problems in electric power systems. According to our literature review, several typical applications of IP methods in power systems include: load flow [71, 72], Volt/VAr control [69, 73], optimal power flow [70, 74], maximum load-ability [68] and economic dispatch [75].

Although a great variation of IP methods have been proposed and implemented in power systems with good performance obtained, their drawbacks are also noticeable. More exactly, the biggest issue is that IP methods require high computational effort at each iteration as a result of solving a large, sparse linear system. Besides, although its superb performance in solving the linear programming problems has been widely proved, the convergence of IP methods on nonlinear programming problems, especially non-convex problems, is not guaranteed. Additionally, other issues such as initialization of the algorithm, pre-processing of the data, handling of free variables, computing the step lengths, reducing the barrier parameter, and termination criteria also need great attention.

C. Sequential Quadratic Programming Method

By far, the most powerful and the most widely used method for the CNLP problems is the sequential quadratic programming (SQP) method and it represents the state of the art in nonlinear programming methods [56, 57, 76, 77]. The basic idea is that, at each iteration, a Taylor's quadratic approximation is made of the Hessian of the Lagrangian function using a quasi-newton updating method. It is then used to generate a quadratic programming sub-problem whose solution is used to form a search direction for a linear search procedure which in turn leads to a better approximation. By solving a sequence of the aforementioned quadratic programming sub-problems, the solution of the CNLP problem can be obtained.

The earliest idea of SQP-type method has been proposed by Wilson in 1963 [78]. Since its popularization in the late 1970s, SQP has arguably become the most successful method for solving the CNLP problems. This view was further reinforced by the work of Hock and Schittkowscki [79] where they implemented and tested the SQP method that outperforms every other competitor in terms of efficiency, accuracy and percentage of successful solutions over a large number of test problems.

The greatest strength of SQP is that equality, inequality as well as nonlinear constraints and limitation on the state variables can be handled high effectively. Besides, the SQP is deterministic and free from any heuristic internal parameters and therefore it is a very robust and transparent optimization technique. Compared with other classical CNLP methods such as Newton's method, conjugate gradient method and quasi-Newton method, SQP is comparatively more accurate, efficient and reliable with an excellent convergence rate. Additionally, if the objective function is properly chosen, the global optima can be obtained and then the local convergence can be extended to global convergence.

All the above-mentioned advantages of SQP have made it one of the most prominent algorithms in constrained nonlinear programming and it has been widely applied for various CNLP problems in power systems. A most common application of SQP is for the problem of optimal power flow (OPF). For example, in [80], a new SQP with

an outer linearization loop and an inner optimization loop is proposed to efficiently solve the OPF problem. SQP is also used in [81] to solve an OPF problem including models of FACT devices to reduce power losses and power transmission cost. Reference [82] proposes a trust-region SQP method to investigate the OPF problem for distribution networks with the integration of distribution generation. Besides, SQP is also often applied for the volt/VAr control problems. For instance, a CNLP problem is formulated and solved by SQP to support a coordinated voltage control strategy proposed in [83]. To investigate the coordinated voltage control problem for smart distribution grid with penetrations of distributed generation, another trust-region SQP method integrated with the branch and bound approach is also presented [84]. Additionally, SQP is employed to solve the optimal distributed generation sizing problem in [85].

D. Summary of Classical CNLP Optimization Techniques

Classical methods above all have a long history of applications to the CNLP problems of power systems with various performances obtained. Despite significant advancements have been made in these algorithms, majority of them still suffer from the following drawbacks, which make their implementations in power systems, especially in more complex smart grid, intractable and problematic.

1) The classical algorithms are sensitive to initial point and when the starting point is not properly chosen e.g. far from the optima, a slow convergence even divergence may occur because of zigzagging in the search direction;
2) As the classical methods start from a single point, when the optimization problem has a solution space of multiple basins, they cannot guarantee the global optimality of the solution and are more likely to be trapped into a local optima;
3) When the problem size grows, solution process becomes more difficult with an expensive computational cost and convergence problem occurs in some serious cases (curse of dimensionality);

4) These algorithms often require some preconditions such as continuity, differentiability of objective function and convexity of problem, which are hard to meet in most cases.

2.2.2 Heuristic Optimization Techniques for MINLP Problems

Power system itself is a highly complicated system, especially with the increasing integrations of renewable energy sources in smart grid age, and classical methods are becoming insufficient to deal with various optimization problems of power systems. Moreover, for the MINLP problems with discrete variables, conventional mathematical programming techniques have collapsed for large-scale problems as consideration of discrete variables will cause the computation time much longer and the algorithms less robust. Classical optimization methods such as penalty function methods, interior point methods and SQP method have no chance to handle the aforementioned MINLP problems unless significant assumptions are made.

For the MINLP problems, the latest heuristic methods have been proved to be both effective and efficient for finding the global or near global optima. Heuristics are techniques which seek optimal solutions with a population-based and stochastic-based manner and inspired by biological or human intelligence phenomenon. In one single simulation, they can locate and maintain multiple solutions. Comparing with the classical methods, heuristic algorithms have a better computational performance, are more flexible, do not require preconditions such as convexity, continuity and differentiability of objective function. All of the heuristic approaches can provide satisfactory solutions for power systems with a more exact modelling of the problem.

The following of this section will be dedicated to present and review several most popular heuristic methods including evolutionary programming (EP), simulated annealing (SA), tabu search (TS), genetic algorithm (GA) and particle swarm optimization (PSO) methods and their applications in power systems. On this basis, a most promising algorithm will be chosen to support the MINLP problem in the proposed hierarchical optimization.

A. Evolutionary Programming

Evolutionary programming (EP) is an artificial intelligence method which is an optimization algorithm based on the mechanism of natural selection, including mutation, recombination, reproduction and selection [86, 87]. Mutation randomly perturbs a candidate solution; recombination randomly mixes their parts to form a novel solution; reproduction replicates the most successful solutions found in a population; whereas selection purges poor solutions from a population. Starting from an initial generation of candidate solutions, this process produces advanced generations with candidates that are successively better suited to their environment. It has been proven that optimization with EP is more efficient and effective than the classical methods. Specifically, comparing with the conventional algorithms, EP has the following features:

1) EP searches from a population of points rather than a single point. Therefore, the population can move over hills and across valleys to discover the global optima.
2) EP uses objective function information as the search direction instead of derivatives or other auxiliary knowledge. Thus it can deal with non-smooth, non-continuous and non-differentiable problems.
3) EP uses probabilistic transition rules to select generations, not deterministic rules so it can search a complicated and uncertain area for the global optima. Therefore, EP is more flexible and robust than the classical methods.

On the other hand, as the computation of each individual in the population is independent on others, EP needs more generations to converge to the global optima.

Because of it superior performance over classical optimization techniques, EP has been well employed by researchers to address power system optimization problems. For example, reference [88] proposes a hybrid EP method for the reactive power planning problem with the objective function of minimization of operating cost by reducing real power loss, improving the voltage profile and minimizing the allocation cost of reactive power sources. Besides, in [89], three evolutionary algorithms including EP are applied to solve the optimal reactive power

programming problem to minimize both the operation cost and the investment cost and the superior performance of EP is proved by simulation and comparison with the other two methods. To address the optimal reactive power dispatch and voltage control problems of large-scale power systems, EP is also implemented in both [90] and [86] where by comparing with convention optimization methods, the advantages of applications of EP are demonstrated.

B. Simulated Annealing

Simulated Annealing (SA) is one of the most important and common probabilistic heuristic methods for the MINLP problems. This method was independently introduced by Kirkpatrick et al. in 1983 [91] and by Černý in 1985 [92] respectively. The name and inspiration come from annealing in metallurgy, a technique involving heating and controlled cooling of a material to enhance the size of its crystals and decline their defects [93]. The heat causes the atoms to become unstuck from their initial positions and wander randomly through states of higher energy; the slow cooling gives them more chances of finding configuration with lower internal energy than the initial one. By analogy with this physical process, each step of the SA method replaces the current solution by a random "nearby" solution, chosen with a probability that depends on the difference between the corresponding function values and also on a global parameter called the temperature that is gradually reduced during the procedure. The dependency is such that the current solution changes almost randomly when the temperature is high but increasingly "downhill" as the temperature goes to zero. The allowance for "uphill" moves saves the method from becoming stuck in local optima.

SA is often used to settle problems with discrete variables [93, 94]. For instance, considering the advantages in terms of robustness and initial point, SA is presented for the design of multi-machine power system stabilizer in [95]. SA is also introduced in [96] to solve the power distribution phase balancing problem. Furthermore, in [97], an improved SA is proposed to work with fuzzy clustering method and the modified Gray code for solving the voltage stability constrained reactive power planning problem in power systems. Additionally, reference [98]

presents a novel energy management strategy for a hybridized power source electric vehicle and SA is exploited to accomplish the global optimization of the energy management system proposed.

It should be noticed that the slower the cooling is, the more likely that SA is to find an optimal or near-optimal solution, which however will cause the speed of SA to deteriorate. Therefore, in most cases, the aim of this method is to find an acceptably good solution within a limited amount of time rather than the best possible solution. Besides, SA, although as the oldest heuristic optimization method applied to power systems, has shown limited capacity for dealing with large-scale problems [99].

C. Tabu Search

Tabu Search (TS) method was first proposed independently by Glover and Hansen both in 1986 for solving the MINLP problems [100]. It is a heuristic mathematical optimization algorithm, belonging to the class of local search techniques. By using flexible memory structures, TS method is able to eliminate local minima and search areas beyond a local minimum. The basic components of the tabu search are the moves, tabu list and aspiration level [101, 102]. Specifically, TS goes from some initial feasible solutions to another by making moves. It makes several candidate moves and selects the one producing the best solution for the current iteration. The set of admissible moves forms a candidate list and the best candidate solution becomes the current solution. There is a possibility of cycling as TS may visit the same solution again in latter iterations. To avoid such cycling, tabu list is used by making the current solution tabu, i.e. forbidden. Tabu list contains forbidden solutions (moves) and it is banned to accept the same solution as long as it is on the list. Since tabu list avoids returning to the solutions just visited, so TS has a capability to escape from a local optima. The aspiration level is often introduced to speed up the tabu search process by temporarily overriding the tabu status of a move if it is sufficiently good. The simplest aspiration level is to override the tabu status of a move and allow it out of the tabu list if it leads to a better solution than the best obtained so far.

Similar as SA, TS method is capable to deal with discrete, nonlinear and non-smooth optimization problems with a global convergence for which the classical algorithms turn to be insufficient. Another noticeable advantage of TS is that comparing with conventional and even some heuristic methods, it has only one parameter called tabu length to be tuned up, making it easier for applications. By far, TS has got great attention in the power system optimization applications. For example, based on parallelism, an improved TS algorithm is developed in [103] for the problem of economic dispatch with non-continuous and non-smooth cost functions and a reasonable performance is obtained. Besides, to address the capacitor control problem in distribution systems, reference [104] proposes a dual TS method which makes use of the dual code for the initial value. TS algorithm is also employed by [102] to support the robust tuning of power system stabilizers in multi-machine systems. Additionally, to enhance the power system operation, TS method is used in [105] to address the optimization problem formulated to solve the voltage/reactive control strategy satisfying the trade-off problem concerning security and economy.

Although TS has been implemented in power systems for quite a few years, it still has some drawbacks which limit it from more wide-spread applications. Firstly, as the deterministic technique is employed to evaluate a new solution in the search process, TS is still sensitive to the selection of initial points [106]. If the initial solution is not good, the optimization result may be far from satisfaction. Besides, the size of tabu list should also be carefully set [102]. If the size is too small, the search may start cycling while if it is too large, the search may be too restrictive with a low quality of the solution. Additionally, TS performance deteriorates as the problem size increases because the number of candidate solutions dramatically increases making the solution search inefficient [104].

D. Genetic Algorithm

Genetic algorithm (GA) is the most common heuristic method used to find an optimal or near optimal solution for the MINLP problems. Basically, GA searches for an optimal solution using the principles of evolution and heredity [94, 107, 108]. It operates on populations that consist of a number of individuals, each representing a

particular selection of the values of the variables. The initial population is randomly generated. Each individual is evaluated to obtain a measure of its fitness in terms of the objective function to be optimized. Then a new population is formed by selecting the fittest individuals. Some members of the new population undergo transformations by genetic operators to form new solutions. Such operators include "crossover" and "mutation". Crossover creates new individuals by combining substrings from the parent individuals and takes place according to a given probability value. Mutation creates a new individual by changing randomly selected bits in its coding.

Generally GA can be stated in the following three steps:

1) Create a population of randomly generated individuals.
2) Evaluate fitness of all members of the population by the objective function. This allows estimation of the probability of each individual to be selected for reproduction.
3) Select individuals for reproduction. Apply crossover and mutation, each with a given probability. Create the new population and go back to step 2.

As a robust and parallel method, GA can adaptively search for the global optimal or near-global optimal point. Some obvious advantages of GA include:

1) It does not require detailed information of the objective function and also does not need discretization, convexity and differentiability of the objective function. Therefore, GA is a general-purpose optimization technique and effective to handle MINLP problems [108].
2) Unlike TS method and other conventional algorithms, optimization solution by GA is not influenced by start points, as after generating initial points randomly, stochastic genetic operators are implemented.

One noticeable point about GA is that it has some parameters of genetic operators which should be selected optimally to have a good computational performance [108]. For example, if the mutation rate is too high, the computation time increases significantly while if mutation rate is too low, GA is likely to get trapped in local

optima. Besides, for optimization problems of large-scale systems, a larger population size is often required to ensure the optimal point reached, which however will increase the computational complexity and reduce the efficiency of GA due to the use of probabilistic methods [101].

By far, GA is the most popular method for solving the MINLP problems in power systems. For example, a GA based procedure is designed in [107] for the topological optimization of the power network against parallel (or loop) flows by optimally controlling substation breakers and phase-shift transformers. Besides, reference [109] proposes an integer-coded, multi-objective GA applied to the full reactive power compensation planning problem considering both intact and contingent operating states. In order to decide the optimal locations of automatic voltage regulators in electric distribution networks, GA is also used in [110] to solve a multi-objective optimization problem for the minimization of both power losses and voltage drops. Additionally, an adaptive hybrid GA is proposed in [111] for loss reduction in distribution networks under variable demands.

E. Particle Swarm Optimization

Particle Swarm Optimization (PSO) is a modern population-based heuristic optimization technique developed by Kennedy and Eberhart [112] and inspired by social behaviours of birds flocking, fish schooling and swarm theory. PSO is similar with other heuristic methods e.g. GA in the way that the system is initialized with a population (swarm) of random solutions and searches for the global optimum by updating generations. Nevertheless, different from GA, PSO has no genetic operators such as crossover and mutation [108, 113]. Specifically, in PSO, a possible solution for the optimization problem is treated as a particle in a multi-dimensional searching space. Each individual particle is evaluated based on the objective function to seek a better experience for itself as well as the whole population. Each particle updates its searching direction in term of velocity and position based on two experiences at each iteration. The first one is the best experience/solution encountered by the individual itself so far and named as P_{best} while the other is the best experience obtained so far by the entire population and named as G_{best}. After that, PSO will evaluate the

solutions at each iteration until the global optimum is located or termination conditions are met. By doing so, the probability for each particle to arrive at the target is enhanced. Besides, there are also several random variables such as inertia weight to prevent the method from being trapped into local optima. A more detailed description of PSO can be found in [114, 115].

PSO is considered as the most powerful method for solving the MINLP problems. Comparing with other heuristic algorithms and classical methods, it has the following main advantages [116]:

1) A differentiable-free technique as no gradient is used;
2) Easy in concept and coding;
3) Few number of parameters to adjust;
4) Less sensitive to the nature of the objective function;
5) Less dependent on initial points;
6) Generate high-quality solutions with a shorter computation time as well as more stable and robust convergence.

Due to the aforementioned advantages, PSO outperforms other existing heuristic optimization methods as well as classical mathematical algorithms in many terms such as memory and computation time requirements [116-119]. The PSO is a relatively new technique that has been empirically shown to perform well on many optimization problems of power systems. For example, PSO is used for the optimal reactive power and voltage control problem of power systems in [120], considering voltage security assessment. To reduce power loss, a hybrid PSO is proposed in [121] by using the tangent vector technique. Besides, through integrating the multi-agent system and PSO, a novel PSO approach is presented in [122] for the MINLP problem of reactive power dispatch in power systems. Additionally, a hybrid discrete PSO method is also presented in [123] to optimally control the outputs of distributed generators and the size of capacitors installation in distribution networks. A comprehensive overview of PSO and its applications in power systems can be found

in [115] which also demonstrates its advantages such as fast convergence speed over other heuristic methods.

2.3 ALGORITHMS SELECTION FOR HIERARCHICAL CONTROL

Optimization plays a critical role in the hierarchical control of distribution networks proposed in this study. Therefore, a careful selection of appropriate optimization methods for the control problems involved should be conducted. Usually, the correct selection of optimization algorithms depends on two factors. The first one is the nature of the objective function and constraints and the other is the nature and number of the control variables. As analysed in Section 2.1, the optimization problems of power systems generally fall into the following two categories: CNLP and MINLP. Based on the review and comparison performed in Section 2.2 on the most popular algorithms for these two typical problems, SQP and PSO, which have shown a more promising performance, are finally selected to solve the CNLP and MINLP problems involved in the proposed hierarchical control of this study respectively.

It should be noticed that for the CNLP problems, classical SQP method rather than the global heuristic PSO is used. This is because all the control variables in CNLP are continuous and if PSO is selected, a larger size of population and more particles will be needed to ensure the optimality of solutions, which however leads to a more expensive computational cost as well as a slow convergence rate. Besides, as analysed in Section 2.2, although SQP outperforms other classical mathematical methods, it is a local search method and cannot handle complex problems with multiple optimal points. In this research, this drawback of SQP is overcome by running with multiple initial points. With multiple initial points given in each basin of the solution space, SQP can thoroughly search the whole space for the global optima. A detailed description of this mechanism can be found in [124].

Additionally, to have a better understanding on the optimization performed in this study, more detailed mathematical descriptions of SQP and PSO are presented as follows.

2.3.1 Sequential Quadratic Programming

As demonstrated in Section 2.2, generally SQP method iteratively derives search directions at each iteration by solving quadratic programming sub-problems which are obtained through linearization of the optimization problem based on Taylor's approximation. The objective function is reduced along each search direction to ensure convergence from an initial point.

Mathematically, a general CNLP problem can be expressed as:

$$\min \ f(x) \tag{2.1}$$

$$subject\ to \qquad h_i(x) = 0; \ \ i = 1,2,\dots,m$$

$$g_j(x) \le 0; \ \ j = 1,2,\dots,n$$

where $f(x)$ is the objective function while $h_i(x)$ and $g_j(x)$ are the equality and inequality constraints respectively. Additionally, m and n are the number of equality and inequality constraints.

This CNLP problem is solved by means of the SQP method considering a quadratic approximation of the Lagrangian function as follows:

$$L(x,\lambda,\mu) = f(x) + \sum_{i=1}^{m} \lambda_i h_i(x) + \sum_{j=1}^{n} \mu_j g_j(x) \tag{2.2}$$

where $f(x)$ is the objective function described in equation (2.1) while $h_i(x)$ are the equality constraints of the power flow equations and $g_j(x)$ are the inequality constraints. Besides, λ and μ are the Lagrangian multipliers. Starting from the solution x_r defined in the previous iteration $(r-1)$, at each new step the SQP algorithm provides an appropriate search direction d_r towards the solution of the following quadratic programming sub-problem:

$$\begin{cases} \min \ f(x_r) + \nabla f(x_r)^T d + \frac{1}{2} d^T \nabla_{rr}^2 L(x_r,\lambda_r,\mu_r)d \\ \nabla h_i(x_r)^T d + h_i(x_r) = 0; \quad i = 1,2,\dots,m \\ \nabla g_j(x_r)^T d + g_j(x_r) = 0; \quad j = 1,2,\dots,n \end{cases} \tag{2.3}$$

where $\nabla h_i(x_r)^T$ and $\nabla g_j(x_r)^T$ are the Jacobian matrices corresponding to the equality and inequality constraints respectively while $\nabla_{rr}^2 L(x_r,\lambda_r,\mu_r)$ is the Hessian

matrix of the Lagrangian. The contribute d_r is used to create a starting solution for the next iteration as follows:

$$x_{r+1} = x_r + \alpha_r d_r \tag{2.4}$$

where α_r is the step length parameter determined by using an appropriate line search procedure so that a sufficient decrease in the objective function is obtained [83].

2.3.2 Particle Swarm Optimization

In PSO, a population called a swarm is randomly generated. The swarm consists of individuals called particles, representing a potential solution of the optimization problem. Each particle search through a multi-dimensional space for the optimal solution by updating its velocity and position based on its own experience and its companions' experience as follows:

$$V_i^{k+1} = \omega V_i^k + c_1 r_1 \left(P_{besti}^k - X_i^k\right) + c_2 r_2 \left(G_{best}^k - X_i^k\right) \tag{2.5}$$

$$X_i^{k+1} = X_i^k + V_i^{k+1} \tag{2.6}$$

where,

ω inertia weight;

c_1, c_2 acceleration constants with identical typical values of 2 [114];

r_1, r_2 two random numbers in the range of [0, 1];

P_{besti}^k best position searched by particle i at kth iteration;

G_{best}^k best position ever searched by the entire swarm.

2.4 MULTI-OBJECTIVE OPTIMIZATION AND SOLUTION

Power system optimization inherently involves multiple objectives which are usually mutually conflicting. For example, a significant reactive power injection into power networks can generate a better voltage magnitude profile. At the same time, it may also cause more serious network losses due to local overcompensation. For such multi-objective optimization (MOO) problems with multiple conflicting control targets, a solution that minimizes all the objectives simultaneously does not exist. A

common practice is to introduce the notion of Pareto optimality to describe the solutions of MOO problems.

2.4.1 Pareto Optimality

Generally, a multi-objective optimization problem can be mathematically defined as:

$$\min \ \boldsymbol{F}(\boldsymbol{X}) = [f_1(\boldsymbol{X}), f_2(\boldsymbol{X}), \cdots, f_k(\boldsymbol{X})]^T \tag{2.7}$$

Subject to:

$$\boldsymbol{h}(\boldsymbol{X}) = \boldsymbol{0};$$

$$\boldsymbol{g}(\boldsymbol{X}) \leq \boldsymbol{0};$$

$$\boldsymbol{X_{LB}} \leq \boldsymbol{X} \leq \boldsymbol{X_{UB}}.$$

Where $k \geq 2$ is the number of objective functions and $\boldsymbol{X}$ is a vector of control variables and $\boldsymbol{F}(\boldsymbol{X})$ is a vector of objective functions $f_i(\boldsymbol{X})$. Besides, $\boldsymbol{h}$ and $\boldsymbol{g}$ are the equality and inequality constraints, while $\boldsymbol{X_{LB}}$ and $\boldsymbol{X_{UB}}$ are the lower and upper bounds on the control variables respectively.

Based on the MOO problem defined above, the definition of Pareto optimality is described as: a point $\boldsymbol{X}^* \in \boldsymbol{\Omega}$ is Pareto optimal if for every $\boldsymbol{X} \in \boldsymbol{\Omega}$ and $I = 1, 2 \ldots, k$ either, $\forall_{i \in I}(f_i(\boldsymbol{X}) = f_i(\boldsymbol{X}^*))$ or there is at least one $i \in I$ such that $f_i(\boldsymbol{X}) \geq f_i(\boldsymbol{X}^*)$, where $\boldsymbol{\Omega}$ is the feasible region [125]. In other words, a solution is called Pareto optimal, if none of the objective functions can be improved in value without detriment to any other objective functions.

Thus, the solution of such a MOO problem is a set of favourable trade-off alternatives, i.e. a solution is better than another one in some objectives but worse in others [126, 127]. This optimum set of non-dominated solutions is termed as a Pareto-optimal set. In terms of their objectives, the Pareto set is referred as to the Pareto front, and these terms are sometimes used interchangeably. Due to the fact that the number of non-dominated solutions on the Pareto optimal front can be infinite, in practice a strategy of decision making is needed to find the most preferable Pareto optimal solution according to the decision maker's preference.

2.4.2 Weighted-Sum Method

Popular approaches for solving the MOO problems can be categorized into three groups: weighted-sum method, ε -constrained method and Pareto-based multi-objective evolutionary algorithm [128]. Among them, the most widely used and also the most efficient is the weighted-sum method [129, 130].

$$F = \sum_{i=1}^{k} w_i f_i(\boldsymbol{X}) \tag{2.8}$$

As shown above, the weighted sum method transforms multiple objectives into an aggregated single objective by multiplying each objective with a weighting factor and summing up all the weighted objectives. To ensure the Pareto optimality of solution(s), it is suggested that the weights be set such that $\sum_{i=1}^{k} w_i = 1$ and $\boldsymbol{w} \geq 0$, which also generates a convex combination of objectives [131].

The value of a weight is significant not only relative to other weights but also relative to its own objective function magnitude, which is a critical idea but often overlooked. Thus when using weights to represent the relative importance of the objectives, scaling each objective function by being divided by a scale factor sf_i so that they all have similar magnitudes and do not naturally dominate the aggregated objective function can help a decision maker choose the weights to reflect preferences more accurately. Common practice is to choose the maxima of each objective as the scale factor, i.e. $sf_i = f_i^{max}$ [129]. Accordingly, equation (2.8) can be improved as:

$$F = \sum_{i=1}^{k} w_i f_i(\boldsymbol{X}) \,/ sf_i \tag{2.9}$$

After scaling, multi-objective optimization then takes place in a non-dimensional, unit-less space. At the end, recover the original objective function values by reverse scaling.

2.5 CONCLUSION

In this chapter, based on the nature of objective function, constraints and control variables, optimization problems of power systems are divided into two categories: CNLP and MINLP. For each type of these optimization problems, several most

popular algorithms and their applications in power networks are presented and reviewed in terms of both advantages and disadvantages. On this basis, considering the optimization requirements of the proposed hierarchical control, two most promising methods, i.e. SQP and PSO, are selected for solving the CNLP and MINLP problems respectively in this study. Additionally, as power system optimization problems often involve multiple mutually conflicting objectives, the notion of Pareto optimality is introduced to describe the solutions of MOO problems and weighted-sum method, which is the most widely used and the most efficient approach for solving the MOO problems, is also presented.

Chapter 3. Optimization by PV Inverters Control in Unbalanced LV Distribution Networks

3.1 INTRODUCTION

The MV and LV controllers of the proposed hierarchical control in section 1.4 are fully based on operation optimization by controlling active devices on the corresponding level. In this chapter, for the LV distribution networks, considering the proliferation of residential photovoltaic (PV) systems in Australia, operation optimization is conducted by controlling the reactive and real outputs of PV inverters, which is a CNLP problem. The content of this chapter is based on our work of [132-136].

Specifically, rooftop PV systems are being increasingly installed in LV distribution networks by consumers to reduce the cost of electricity supply. However the expanding scale of residential PV connections leads to detrimental impacts on the network operation. Two of the foremost issues are voltage regulation [137] and voltage unbalance [138]. During high PV generation periods, there is a possibility of significant reverse power flow and consequent voltage rises on the LV feeder. On the other hand, serious voltage drops may occur due to the intermittent loss of PV generation during cloudy days. Furthermore, the increasing installation of single-phase rooftop PV units at random locations with various ratings is further worsening the already poor phase balance profile of LV distribution networks.

Traditional approaches to address voltage regulation and unbalance problems are utilizing secondary LV transformer online tap changer (OLTC), auto-transformers, voltage regulators and switched capacitors, as well as increasing conductor sizes and adding energy storage devices [139-141]. However, tap positions cannot be changed frequently, auto-transformers, voltage regulators and switched capacitors introduce

additional failure points into the system while upgrading the conductors and adding energy storage devices are very effective but expensive approaches that are usually not justified due to low cost benefit ratios [141].

The more recent approaches to overcome the voltage regulation problem in LV networks with high PV generation penetrations involve inverter based reactive power control [142-148]. Compared with the above-mentioned traditional approaches, PV inverter reactive power control is more effective, has superior transient performance and does not require extra investments. Generally, existing control schemes based on reactive power capability of PV inverters are presented mainly in two forms. One is the centralized control where optimal PV reactive outputs are determined by solving a network-wide optimal power flow (OPF) [149, 150] problem for the best operational performance. For example, the Volt/VAR control is formulated as a radial OPF problem in [142]. Subject to voltage and PV inverter reactive power limit constraints, the objective is to minimize line losses, energy consumption through Conservation Voltage Reduction (CVR) and inverter losses. Moreover, a systematic method for determining both the real- and reactive- power set points of PV inverters in residential system is proposed in [143] by solving an OPF problem with objectives of optimizing the system operation and ensuring voltage regulation. Additionally, an economic dispatch problem for unbalanced distribution networks is defined and solved in [144]. The objective is to minimize the overall real power cost with constrains on the voltage magnitudes and on the power factor at both the substation and the nodes with capacitors. By contrast, the other control approach is distributed control where control actions of each PV are decided based on local measurements. For instance, in [145], a simple OPF problem is defined to minimize network losses by PV inverter reactive power control. As the cost function is separable, a distributed on-line approach is then introduced for optimality of reactive power flows in distribution systems. A decentralized reactive power control is also presented in [146], based on voltage sensitivity analysis, to achieve grid voltage support with less total reactive power consumption by assigning a location-dependent power factor to each PV unit. Additionally, distributed Volt/VAR controls have been used in [147]

and [148] to maintain voltage within acceptable range through local PV reactive managements.

Distributed control with local variable requires less communication but is inherently locally optimal due to the lack of the full network information. As for the centralized control, the majority of the existing studies (e.g. [142-144]) are based on a balanced network model which, however, will result in incorrect predictions and conclusions as most practical distribution networks are naturally unbalanced. Besides, some existing PV controllers are only based on reactive power control without considering real power management (e.g. [142]), which is not an effective approach in distribution networks with high R/X ratios. Furthermore, the multiple objectives of inverter reactive power control tend to be mutually conflicting and the challenge that how to implement a PV control approach which can balance different goals and constraints of practical networks still exists (e.g. [142-144]).

Based on both optimal reactive power control and real power curtailment of single-phase inverters, this chapter proposes a comprehensive PV control strategy to improve the operational performance of significantly unbalanced four-wire LV distribution networks. The proposed multi-objective OPF problem, that simultaneously improves voltage magnitude and balance profiles and minimizes network losses and generation costs, is converted into an aggregated single-objective problem using the weighted sum method and then solved by the global SQP approach with multiple starting points in Matlab. Simulations are performed and analysed for two extreme operating scenarios over 24 hours on a real four-wire unbalanced LV distribution system. Smart meter readings are used to justify the validity and accuracy of the proposed optimization model and considerations on the practical applications of the proposed PV control strategy are also presented.

3.2 PV CONTROL STRATEGY

3.2.1 Reactive Power Capability of PV Inverters

Many PV inverters have a reactive power capability [151]. In figure 3.1, the inverter's capacity and real power are represented by vectors with magnitudes S and P. The semicircle with radius S denotes the boundary of the inverter's operating range in PQ space. The amount of reactive power (Q) available from the inverter is constrained by $-\sqrt{S^2 - P^2} \leq Q \leq \sqrt{S^2 - P^2}$.

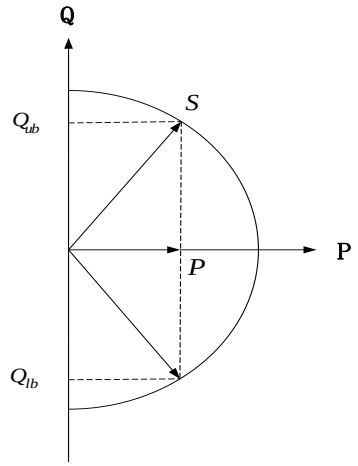

Figure 3.1 Inverter reactive power capability.

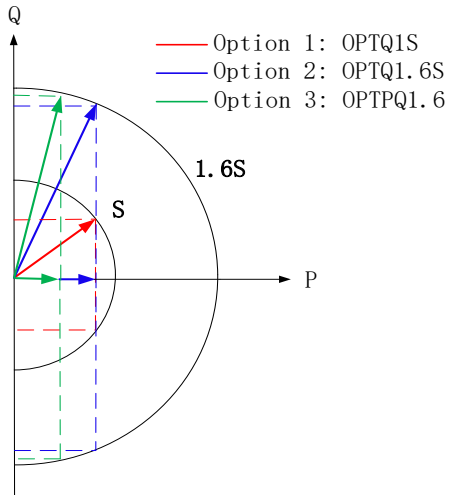

Figure 3.2 Proposed control strategy.

3.2.2 The Proposed PV Inverter Control Strategy

Based on the reactive power capability and real power curtailment of the PV inverters [152], one of the following proposed three control options could be selected for the desired network performance (figure 3.2):

Control Option 1 - OPTQ1S (Optimal Q-Control with Rated Inverter Capacity): this option is selected for normal operating conditions. As the inverter real power generation is usually below its rating and therefore, the inverter will have the capability to supply reactive power, at a cost of incremental inverter losses.

Control Option 2 - OPTQ1.6S (Optimal Q-Control with Increased Inverter Capacity): this option could be selected if the desired network performance is not achieved after Option 1 due to limited inverter reactive power availability (e.g. in high generation cases). Thus the sizes of PV inverters can be increased to allow more active reactive power control.

Control Option 3 - OPTPQ1.6S (Optimal PQ-Control with Increased Inverter Capacity): this option could be selected if the network performance is still not satisfactory with Option 2. This could be due to the limited effect of reactive power management in distribution networks with high R/X ratios. Then a comprehensive control can be implemented where real power curtailment is available to each inverter to allow both reactive power and real power controls. Curtailment incurs a relatively higher cost in the optimization process and partial curtailment allows all the users to share the network resources when constraints exist.

Table 3.1 PV inverter capacity expansion.

Used/Rated Capacity Ratio	(0,1]	(1,1.2]	(1.2,1.4]	(1.4,1.6]	(1.6,1.8]	(1.8,2.0]
PVs Number	16	5	3	3	4	3

It is known that with inverter capacity increased, the performance related cost will be reduced. To decide the suitable proportion by which the inverter capacity should be increased, multi-objective OPF (proposed in Section 3.3) calculation is carried out for the peak demand case (18:45 pm, 25/01/2012) of network in figure 3.3 with a dramatic inverter size expansion of 100%. As shown in table 3.1, out of total 34

inverters, only 18 have their increased capacity partially used. To effectively show the potential reactive power benefits of inverters while considering the cost associated with inverter upgrade, 60% is finally chosen in this study.

3.3 MULTI-OBJECTIVE OPF PROBLEM AND SOLUTION

A multi-objective model is proposed to ensure reasonable operational performance after optimization. The network is described by a nonlinear load flow model with constant-power loads. Bus 1 at the secondary side of distribution transformer is taken as the slack bus.

3.3.1 Optimization Objectives

A. Network Losses

$$J_1 = \sum_{p=1}^{4} \sum_{i=1}^{n-1} \sum_{j=i+1}^{n} {I_{ij}^p}^2 R_{ij}^p \tag{3.1}$$

where $i, j = 1, 2, \cdots n$ is the bus number and $p = 1, 2, 3, 4$ represents the phase and neutral designations (a, b, c and n), respectively. As the network is unbalanced, both the bus number i and the phase designation p are required to identify a node i^p. Accordingly, I_{ij}^p and R_{ij}^p are the current through and resistance of the branch between nodes i^p and j^p.

B. Voltage Magnitude Profile

To ensure voltage magnitude within the limits provided by utilities, a dead band based objective is proposed below.

$$J_2 = \sum_{p=1}^{3} \sum_{i=1}^{n} {\Delta V_{idb}^p}^2 \tag{3.2}$$

where ${\Delta V_{idb}^p}^2 = \left(V_i^p - V_{db}^{lower}\right)^2$, 0 and $\left(V_i^p - V_{db}^{upper}\right)^2$ for $V_i^p < V_{db}^{lower}$, $V_{db}^{lower} \le V_i^p \le V_{db}^{upper}$ and $V_i^p > V_{db}^{upper}$, respectively.

According to the Australian standard AS61000 [153] which is based on IEC61000, the preferred voltage dead band $[V_{db}^{lower}, V_{db}^{upper}]$ should be around half of the permissible tolerance of nominal voltage in LV distribution networks.

C. Voltage Balance Profile

Generally network unbalance is quantified by voltage unbalance factor (VUF). In this study, the IEC developed and IEEE recommended definition of $\%VUF = |V_-/V_+|$ as the ratio of the negative-sequence voltage magnitude to positive-sequence voltage magnitude is used [154]. A dead band based objective is also formed to achieve the desired balance profile.

$$J_3 = \sum_{i\in\lambda} \Delta VUF_{idb}{}^2 \tag{3.3}$$

where $\Delta VUF_{idb}{}^2 = 0$ and $(VUF_i - VUF_{db})^2$ for $0 \le VUF_i \le VUF_{db}$ and $VUF_i > VUF_{db}$, respectively while λ represents the set of three-phase buses.

D. PV Generation Cost

The proposed PV control strategy is based on adjusting inverter real and reactive power generations. Inverter losses will rise with the generation increase, which can be approximated as the quadratic polynomial of the apparent power S_{PVi}^p with coefficients k_{i1}^p, k_{i2}^p and k_{i3}^p [155].

$$J_4 = \sum_{p=1}^{3} \sum_{i\in\delta} \left(k_{i1}^p S_{PVi}^p{}^2 + k_{i2}^p S_{PVi}^p + k_{i3}^p \right) \tag{3.4}$$

where δ denotes the set of buses with PV installation. The coefficients k_{i1}^p, k_{i2}^p and k_{i3}^p can be determined by curve fitting of each inverter's efficiency data (provided by manufacturer).

E. PV Real Power Curtailment Cost

When curtailing the PV real power generation from initial P_{PVi0}^p to P_{PVi}^p, consumers will suffer the loss of revenue from foregone energy sales.

$$J_5 = \sum_{p=1}^{3} \sum_{i\in\delta} \left(P_{PVi0}^p - P_{PVi}^p \right) \tag{3.5}$$

3.3.2 Multi-Objective Optimization by Weighted Sum Method

As analysed in section 2.4, optimization objectives above are mutually conflicting. For example, more reactive power injected locally by inverters can generate a better

voltage magnitude profile but also cause higher network losses. For multi-objective optimization (MOO) problems with multiple conflicting objectives, a solution that minimizes all objectives simultaneously does not exist. Consequently the notion of Pareto optimality is used to describe the solutions of MOO problems. A solution is called Pareto optimal, if none of the objectives can be improved in value without detriment to any other objectives [125].

In practice, the objective of solving a MOO problem is to support a decision maker in finding the most preferred Pareto optimal solution(s) according to his/her preferences. The most widely-used method for solving the MOO problems is the weighted sum method [129].

$$F = \sum_{i=1}^{k} w_i J_i(\boldsymbol{X}) \tag{3.6}$$

As shown above, the weighted sum method transforms multiple objectives into an aggregated single objective by multiplying each objective with a weighting factor and summing up all the weighted objectives. To ensure the Pareto optimality of solution(s), it is suggested that the weights be set such that $\sum_{i=1}^{k} w_i = 1$ and $\boldsymbol{w} \geq \boldsymbol{0}$, which also generates a convex combination of objectives.

The value of a weight is significant not only relative to other weights but also relative to its objective function magnitude, which is a critical idea but often overlooked. Thus when using weights to represent the relative importance of the objectives, scaling each objective function by being divided by a scale factor sf_i so that they all have similar magnitudes and do not naturally dominate the aggregated objective function can help one set the weights to reflect preferences more accurately. Common practice is to choose the maxima of each objective as the scale factor, i.e. $sf_i = J_i^{max}$ [129]. Accordingly, equation (3.6) can be improved as:

$$F = \sum_{i=1}^{k} w_i J_i(\boldsymbol{X}) \,/ sf_i \tag{3.7}$$

After scaling, multi-objective optimization then takes place in a non-dimensional, unit-less space. At the end, recover the original objective function values by reverse scaling.

3.3.3 The Proposed OPF Model

$$\min \ F$$

subject to:

$$P_{PVi}^{p} - P_{Li}^{p} - P_{i}^{p} = 0; \quad Q_{PVi}^{p} - Q_{Li}^{p} - Q_{i}^{p} = 0 \tag{3.8}$$

$$P_{PVi}^{p\ 2} + Q_{PVi}^{p\ 2} \leq S_{i}^{p2} \tag{3.9}$$

$$V_{ilb}^{p} \leq V_{i}^{p} \leq V_{iub}^{p} \tag{3.10}$$

where equality constraints in equation (3.8) are the power balance equations. Of these $P_{PVi}^{p}(Q_{PVi}^{p})$, $P_{Li}^{p}(Q_{Li}^{p})$ and $P_{i}^{p}(Q_{i}^{p})$ are the PV, load and network real (reactive) power, respectively. Inequality constraints in equation (3.9) indicate the capacity limits on inverter outputs. Besides, in line with the technical rules set by the network operator on nominal voltage and its permissible tolerance for LV networks, the boundary constraints on voltage magnitude are given in equation (3.10).

3.3.4 OPF Solution

Matlab codes for the multi-objective OPF problem above in unbalanced four-wire network have been developed to obtain the global optima, using Sequential Quadratic Programming (SQP) algorithm with multiple starting points [124, 156].

3.4 SIMULATION RESULTS AND ANALYSIS

3.4.1 Test Network Based on the Perth Solar City

The selected test network for simulations and analyses of this study is contained within the Perth Solar City [157]. As shown in figure 3.3 and table 3.2, the 415/240V network is supplied by a 200kVA 22kV/415V distribution transformer and includes 101 buses and 77 consumers. Of these, 51 consumers are single-phase and 34 consumers have single-phase roof-top PV systems with typical ratings of 1.59kW, 1.88kW and 2kW, etc. Total rated PV installation capacity is 63.81kW representing a network penetration of 31.9%. As the consumers have a mixture of single- and three-phase house connections the loading is inherently unbalanced.

The network under study is an aerial, 3-phase 4-wire construction with four equally sized conductors on a mixture of 0.9m and 1.2m cross arms. The consumer mains are 6mm^2 copper with R=3.7Ω/km and X=0.369Ω/km while the aerial mains are of two seven strand, all aluminium conductor types:

7/4.50 AAC – R=0.316Ω/km; X=0.292Ω/km;

7/3.75 AAC – R=0.452Ω/km; X=0.304Ω/km.

A more detailed description of the test network can be found in Appendix B. In this study, the four-wire test network above is simulated based on the proposed multi-objective OPF model in Section 3.3 by including its operational characteristics and requirements e.g. power balance equations, PV inverter capacity limit and acceptable voltage range etc., in the constraints of equations (3.8-3.10). Solution of the OPF problem automatically performs the simulation of the unbalanced test network.

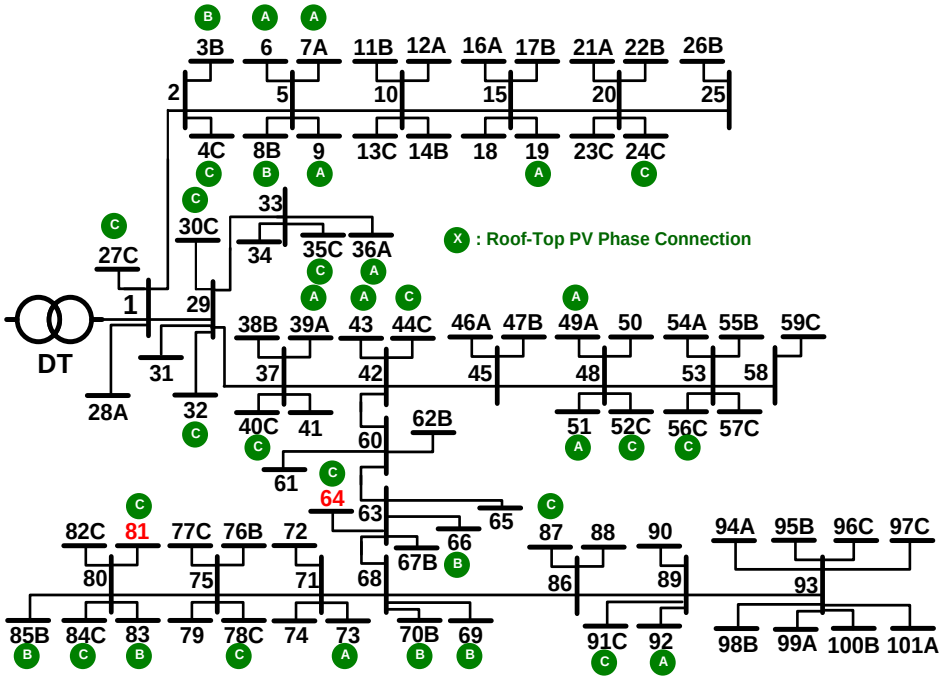

Figure 3.3 The 101 bus, 415/240V test network diagram based on the Perth Solar City [157]. Single-phase buses are represented with both bus and phase numbers (e.g., bus 3B is a single-phase bus connected to phase B).

Table 3.2 Load and PV system connections.

Phase	Consumers *	PV Connection	PV Capacity	Penetration
A	13	11	21.31kW	10.7%
B	18	7	13.07kW	6.5%
C	20	16	29.43kW	14.7%
3 Phase	26	---	---	---
Total	77	34	63.81kW	31.9%

*) Each house has a meter installed at the connection point to its switchboard. There are 24 three-phase and 51 single-phase smart meters, in addition to 2 mechanical meters (marked as red in figure 3.3).

3.4.2 Simulated Cases Studies

For the 101 bus network above, the following two network operational extremes are simulated:

1) The first scenario is characterized by the highest power flows (i.e. high load and low generation), which caused the most significant voltage drop in summer (25/01/2012).
2) The second scenario is related to the smallest grid power requirement (i.e. high generation and low load), which caused the most serious reverse power flow and voltage rise in late spring (28/11/2011). However, as a real network, even the most serious voltage rise was still within the permissible tolerance. Furthermore, according to the Australian Energy Market Operator (AEMO) forecast [158], the total installed capacity of rooftop PV in Australia will increase dramatically from 1,450 MW at the end of February 2012 to 5,100 MW by 2020 and 12,000 MW by 2031 (based on a moderate growth scenario). These forecasts have been recently supported by the installed PV base reaching 4,000 MW at the end of 2014. To prove the capability of the proposed PV control strategy on mitigating the coming more serious voltage rise, this scenario is redefined with the original PV generation doubled.

For each scenario, the proposed three-option control assessment strategy of Section 3.2 will be applied. A reference case is simulated based on the original network state

(ORIGINAL) without any inverter control. For all the control cases (ORIGINAL, OPTQ1S, OPTQ1.6S and OPTPQ1.6S), simulations are performed and analysed over 24-hour period. Due to space limitation, the effects of the proposed PV control strategy and MOO model on the network performance are studied mainly based on phase C, which has both the most load and the most PV connections.

3.4.3 Optimization Parameters Selection

According to the Electricity Act 1945, distribution system supply should function within the limits of ±6% of the nominated voltage [159]. Concurrently, in line with the IEC standard, in medium or low voltage network VUF should not exceed 2%. Accordingly, voltage dead band in J_2 is set as ±3% of the rated voltage (i.e. [232.8, 247.2]) and VUF dead band in J_3 is set to be 1% in this study. For the second scenario, considering conservation voltage reduction (CVR) for higher efficiency, voltage dead band is reduced to [-3%, 2%] (i.e. [232.8, 244.8]). Additionally, the relative importance of objectives is set to be decreasing in the order of voltage magnitude profile J_2, voltage balance profile J_3 /real power curtailment cost J_5 and network losses J_1 /PV generation cost J_4 with weights of 0.4, 0.2/0.2 and 0.1/0.1, respectively.

Table 3.3 Simulated scenarios and optimization parameters selection.

High Load & Low Generation					High Generation & Low Load				
Voltage DB			VUF DB		Voltage DB			VUF DB	
[-3%, +3%]/ [232.8, 247.2]			[0,1%]		[-3%,+2%]/ [232.8, 244.8]			[0,1%]	
w_1	w_2	w_3	w_4	w_5	w_1	w_2	w_3	w_4	w_5
0.1	0.4	0.2	0.1	0.2	0.1	0.4	0.2	0.1	0.2

3.4.4 Simulation Results for High Load and Low Generation

As demonstrated in figures 3.4-3.8 and table 3.4, originally the network load was much higher than the PV generation, especially between 17:00 and 23:00, causing dramatic voltage drop and serious unbalance along the feeder with the maximum

objective function value (F_{max}) of 90.32 at 21:00. Concurrently the poor network performance was not alleviated by the PV penetrations as the generation peak was not coincident with the load peak (figure 3.4). After applying the proposed three-option inverter control strategy, the network performance can be continuously improved with a smaller objective function value. Specifically, with capacitive reactive power injected using the latent capacity of inverters in OPTQ1S, the network performance has been significantly improved with F_{max} at 21:00 reduced to only 0.22178 (table 3.4). More reactive power can be available to support network by increasing the inverter capacity by 60%, with the smallest F_{max} of 0.177 for both OPTQ1.6S and OPTPQ1.6S (table 3.4). Similar results for OPTQ1.6S and OPTPQ1.6S indicate no real power is curtailed after control, which is because considerable load is connected at all times and reverse power flow, at the whole feeder level, does not occur.

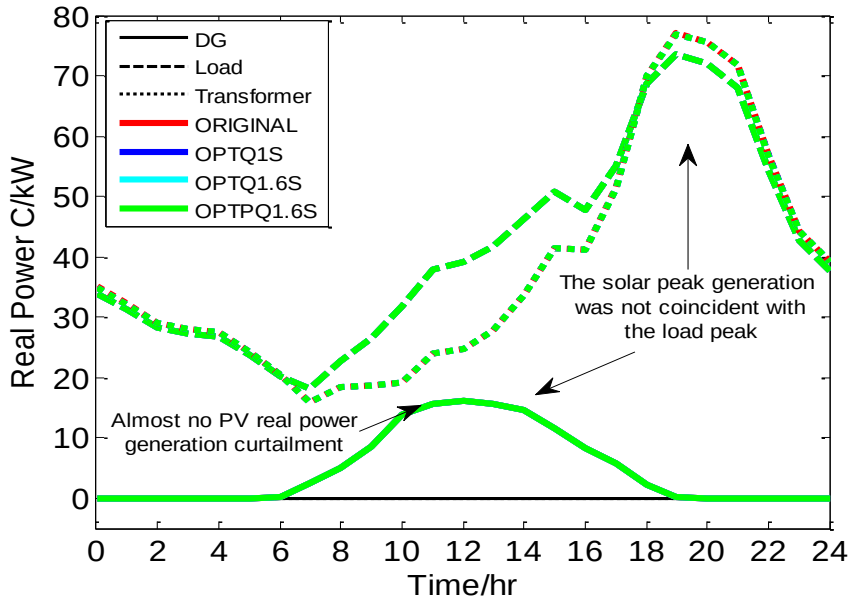

Figure 3.4 Phase C real power: transformer, load & PV/kW (HLLG). The results are presented based on the combination of line type and color.

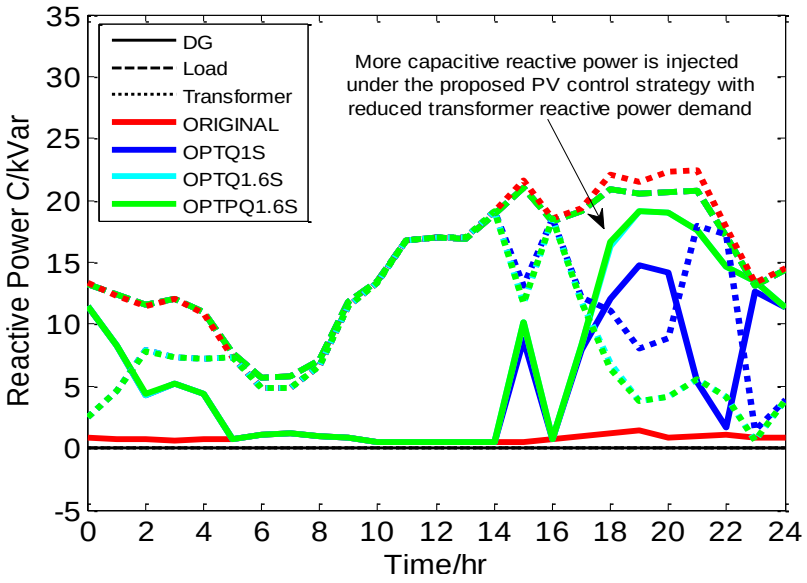

Figure 3.5 Phase C reactive power: transformer, load & PV/kVar (HLLG). The results are presented based on the combination of line type and color.

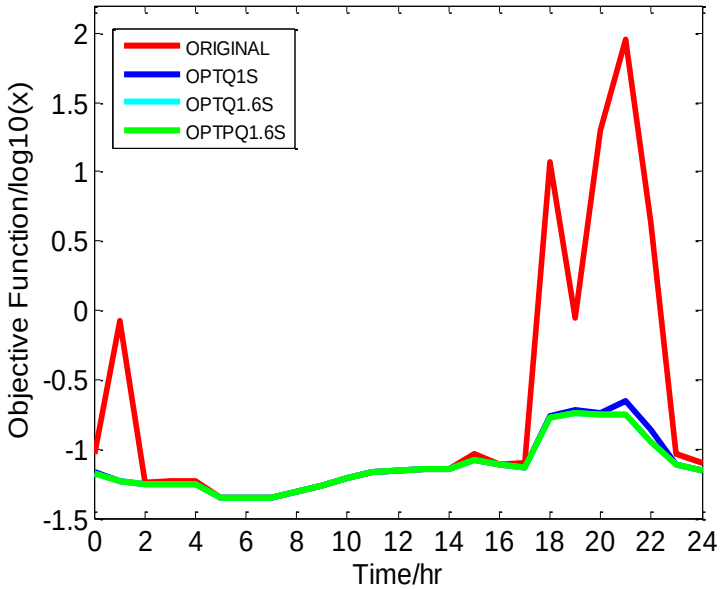

Figure 3.6 Objective function (table 3.4, column 2) under the proposed PV control (HLLG).

Table 3.4 Network optimization results over 24 hours (HLLG). The highlighted green/red cells indicate decrease/increase of the value compared with the pervious case.

Time	F	J1/0.1	J2/0.4	J3/0.2	J4/0.1	J5/0.2	Time	F	J1/0.1	J2/0.4	J3/0.2	J4/0.1	J5/0.2
ORIGINAL							**OPTQ1S**						
00:00	0.09179	2730.3	1356.8	6.7E-9	1016.0	0	**00:00**	0.06767	2463.0	359.7	0	1224.7	0
01:00	0.84417	2082.3	809.7	3.6E-7	1015.7	0	**01:00**	0.05914	1895.4	248.8	0	1151.0	0
02:00	0.05760	1860.2	482.3	0	1015.9	0	**02:00**	0.05588	1745.5	233.9	0	1097.2	0
03:00	0.05816	1839.6	530.2	0	1015.1	0	**03:00**	0.05592	1708.4	237.2	0	1104.5	0
04:00	0.05824	1880.6	515.3	0	1015.3	0	**04:00**	0.05631	1762.7	248.4	0	1099.6	0
05:00	0.04488	1092.8	20.9	0	1015.8	0	**05:00**	0.04488	1092.8	20.9	0	1015.8	0
06:00	0.04456	1034.7	2.1	0	1026.8	0	**06:00**	0.04456	1034.7	2.1	0	1026.8	0
07:00	0.04488	821.6	0.0	0	1080.2	0	**07:00**	0.04488	821.6	0.0	0	1080.2	0
08:00	0.04931	1022.0	14.2	0	1156.4	0	**08:00**	0.04931	1022.0	14.2	0	1156.4	0
09:00	0.05480	1074.0	1.5	0	1304.0	0	**09:00**	0.05480	1074.0	1.5	0	1304.0	0
10:00	0.06190	1287.3	3.7	0	1457.0	0	**10:00**	0.06190	1287.3	3.7	0	1457.0	0
11:00	0.06731	1630.6	4.8	0	1536.7	0	**11:00**	0.06731	1630.6	4.8	0	1536.7	0
12:00	0.06960	1729.7	18.7	0	1573.9	0	**12:00**	0.06960	1729.7	18.7	0	1573.9	0
13:00	0.07225	2061.2	68.8	0	1558.5	0	**13:00**	0.07225	2061.2	68.8	0	1558.5	0
14:00	0.07155	1984.0	155.4	0	1517.8	0	**14:00**	0.07155	1984.0	155.4	0	1517.8	0
15:00	0.09228	3282.5	1131.9	0	1412.3	0	**15:00**	0.08288	3001.9	376.1	0	1530.3	0
16:00	0.07733	3119.5	577.9	0	1265.9	0	**16:00**	0.07733	3119.5	577.9	0	1265.9	0
17:00	0.07850	3471.1	725.6	0	1163.3	0	**17:00**	0.07354	3342.7	222.4	0	1266.1	0
18:00	11.6357	7544.7	7479.8	5.3E-6	1056.0	0	**18:00**	0.17299	7259.4	4881.8	6.0E-13	1244.1	0
19:00	0.88445	8652.7	9791.0	2.9E-7	1026.9	0	**19:00**	0.19211	8245.2	5284.5	0	1402.3	0
20:00	19.7967	8110.4	8659.4	9.1E-6	1015.5	0	**20:00**	0.18090	7742.0	5019.6	5.9E-13	1306.6	0
21:00	**90.3188**	**7613.9**	**8627.5**	**4.2E-5**	**1019.7**	**0**	**21:00**	**0.22178**	**7624.6**	**8171.8**	**0**	**1124.2**	**0**
22:00	4.28506	5064.4	4261.6	1.9E-6	1018.6	0	**22:00**	0.13859	5059.1	4188.9	0	1033.3	0
23:00	0.09133	3438.6	1922.5	0	1016.8	0	**23:00**	0.07784	3172.9	616.2	0	1252.9	0
24:00	0.08013	2903.9	1448.9	0	1016.6	0	**24:00**	0.07052	2671.7	426.1	0	1232.9	0
OPTQ1.6S							**OPTPQ1.6S**						
00:00	0.06688	2435.3	312.2	0	1228.6	0	**00:00**	0.06688	2435.3	312.2	0	1228.6	0
01:00	0.05914	1895.4	248.8	0	1151.0	0	**01:00**	0.05914	1895.4	248.8	0	1151.0	0
02:00	0.05588	1745.5	233.9	0	1097.2	0	**02:00**	0.05588	1745.5	233.9	0	1097.2	0
03:00	0.05592	1708.4	237.2	0	1104.5	0	**03:00**	0.05592	1708.4	237.2	0	1104.5	0
04:00	0.05631	1762.7	248.4	0	1099.6	0	**04:00**	0.05631	1762.7	248.4	0	1099.6	0
05:00	0.04488	1092.8	20.9	0	1015.8	0	**05:00**	0.04488	1092.8	20.9	0	1015.8	0

06:00	0.04456	1034.7	2.1	0	1026.8	0	**06:00**	0.04456	1034.7	2.1	0	1026.8	0
07:00	0.04488	821.6	0.0	0	1080.2	0	**07:00**	0.04488	821.6	0.0	0	1080.2	0
08:00	0.04931	1022.0	14.2	0	1156.4	0	**08:00**	0.04931	1022.0	14.2	0	1156.4	0
09:00	0.05480	1074.0	1.5	0	1304.0	0	**09:00**	0.05480	1074.0	1.5	0	1304.0	0
10:00	0.06190	1287.3	3.7	0	1457.0	0	**10:00**	0.06190	1287.3	3.7	0	1457.0	0
11:00	0.06731	1630.6	4.8	0	1536.7	0	**11:00**	0.06731	1630.6	4.8	0	1536.7	0
12:00	0.06960	1729.7	18.7	0	1573.9	0	**12:00**	0.06960	1729.7	18.7	0	1573.9	0
13:00	0.07225	2061.2	68.8	0	1558.5	0	**13:00**	0.07225	2061.2	68.8	0	1558.5	0
14:00	0.07155	1984.0	155.4	0	1517.8	0	**14:00**	0.07155	1984.0	155.4	0	1517.8	0
15:00	0.08270	2986.0	299.0	0	1561.7	0	**15:00**	0.08270	2986.0	299.0	0	1561.7	0
16:00	0.07733	3119.5	577.9	0	1265.9	0	**16:00**	0.07733	3119.5	577.9	0	1265.9	0
17:00	0.07350	3334.0	221.0	0	1267.5	0	**17:00**	0.07350	3334.0	221.0	0	1267.5	0
18:00	0.16816	7311.6	4306.7	1.6E-12	1344.2	0	**18:00**	0.16691	7301.0	4209.3	1.4E-12	1352.1	6.4
19:00	0.18261	8316.3	4244.8	3.1E-13	1566.6	0	**19:00**	0.18261	8316.3	4244.8	3.1E-13	1566.6	0
20:00	0.17697	7830.2	4484.3	1.3E-12	1407.3	0	**20:00**	0.17697	7830.2	4484.3	1.3E-12	1407.3	0
21:00	**0.17714**	**7355.9**	**4896.9**	**6.5E-13**	**1333.5**	**0**	**21:00**	**0.17714**	**7355.9**	**4896.9**	**6.5E-13**	**1333.5**	**0**
22:00	0.11123	4823.3	1946.6	5.1E-13	1276.4	0	**22:00**	0.11123	4823.3	1946.6	5.1E-13	1276.4	0
23:00	0.07771	3172.6	559.7	4.3E-15	1273.4	0	**23:00**	0.07771	3172.6	559.7	4.3E-15	1273.4	0
24:00	0.07052	2671.7	426.1	0	1232.9	0	**24:00**	0.07052	2671.7	426.1	0	1232.9	0

The weighted sum method is used in this study to define the relative importance of each objective. As shown in table 3.3, the voltage magnitude profile J_2 is given the highest importance with w_2 =0.4. Therefore, a continuously declining J_2 can be observed from ORIGINAL to OPTPQ1.6S at all the time points (table 3.4). Additionally, as the objectives are mutually conflicting, therefore, as shown in table 3.4, objectives with lower importance (e.g. network losses w_1 =0.1 and voltage balance profile w_3 =0.2) may be sacrificed at some time points to ensure the improvement of voltage magnitude profile and the reduction of the total objective function value.

Dead band is introduced to constrain voltage magnitude and VUF within the given limits in table 3.3. As seen in figures 3.7-3.8, after inverter control, both voltage magnitude and VUF are significantly improved with the lowest voltage increased and the peak VUF decreased from 217.3V and 1.28% for ORIGINAL to 218.9V and 1%

for OPTQ1S and to 222.8V and 1% for both OPTQ1.6S and OPTPQ1.6S, respectively.

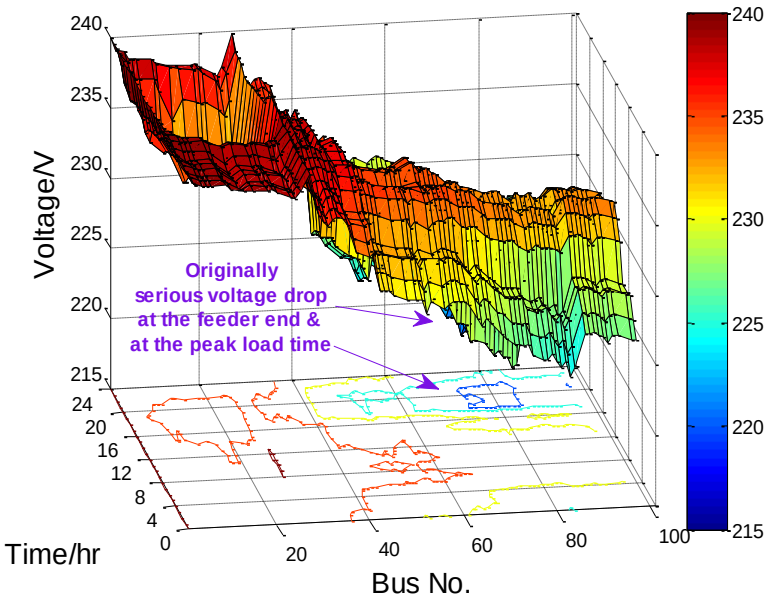

(a) ORIGINAL.

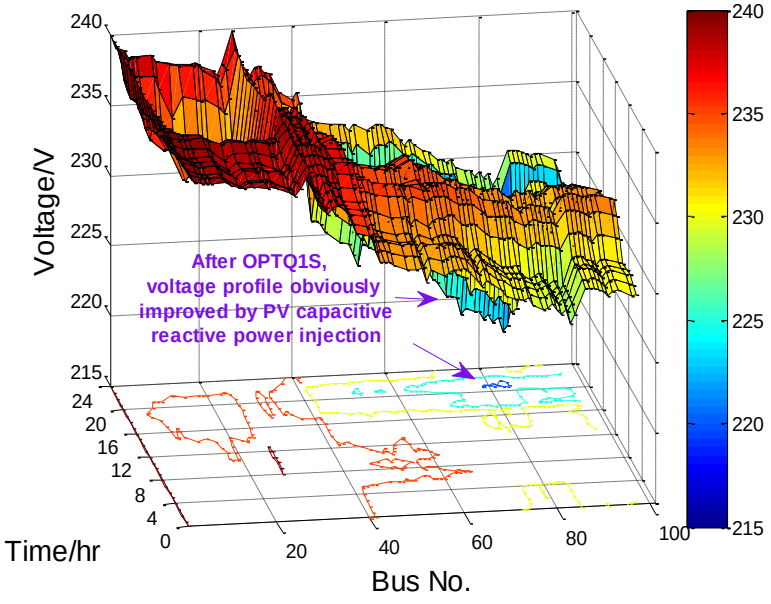

(b) OPTQ1S.

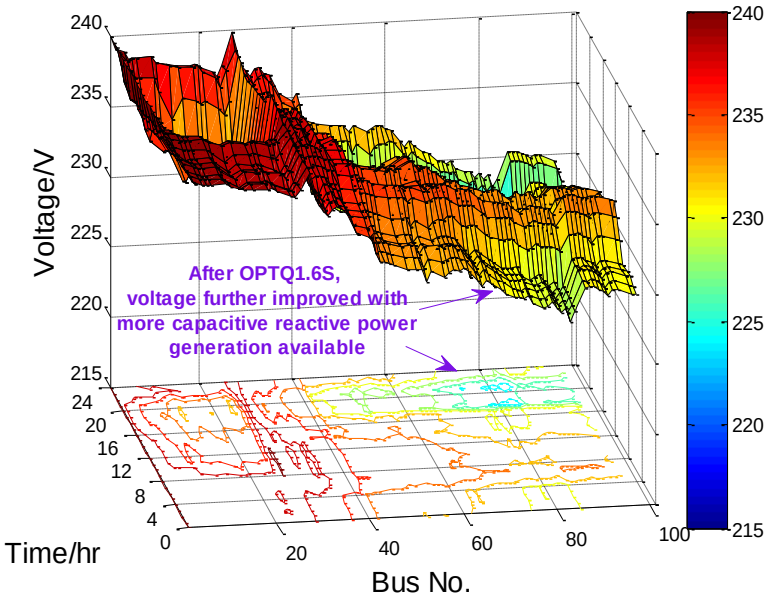

(c) OPTQ1.6S.

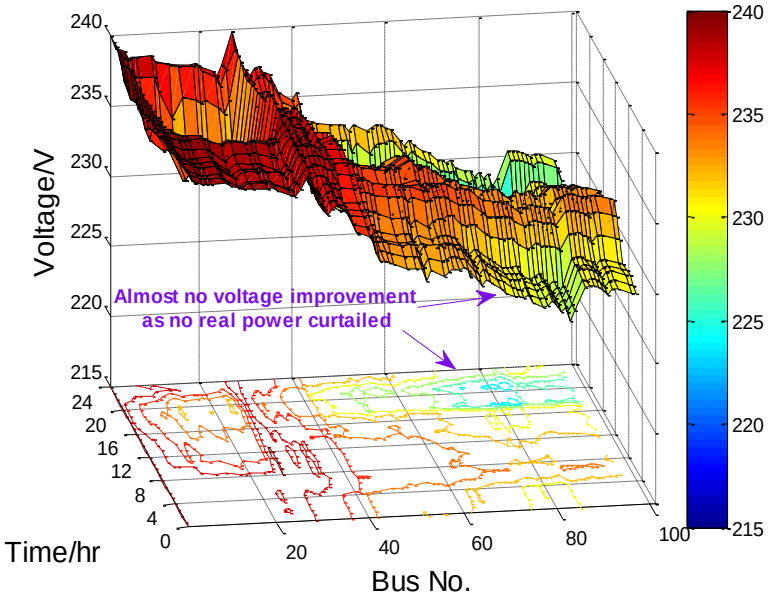

(d) OPTPQ1.6S.

Figure 3.7 Phase C voltage/V under the proposed PV control (HLLG).

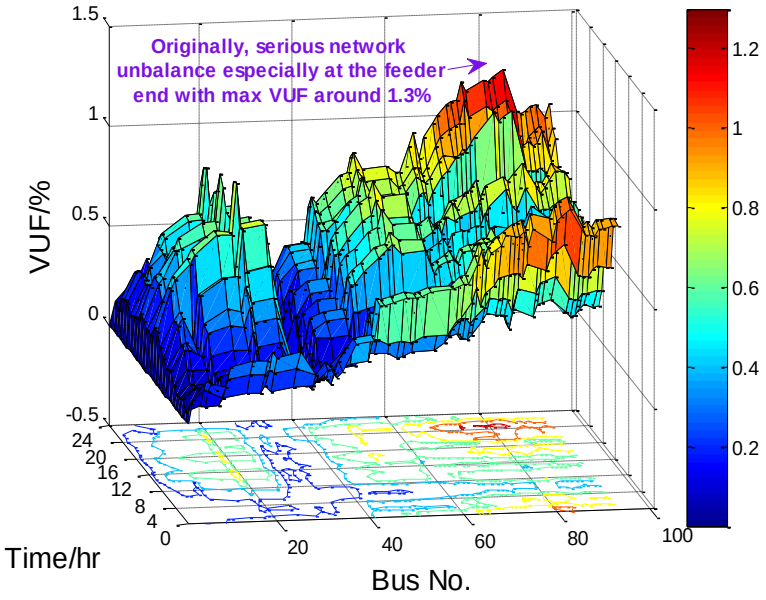

(a) ORIGINAL.

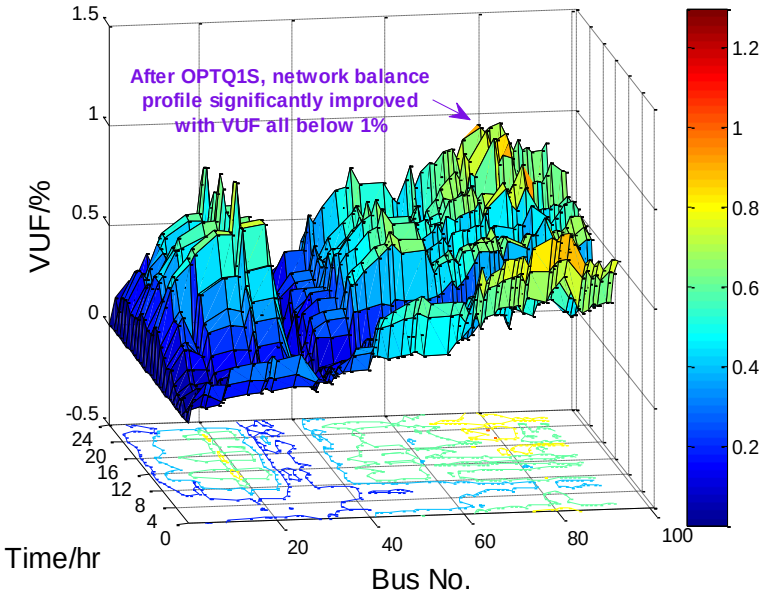

(b) OPTQ1S.

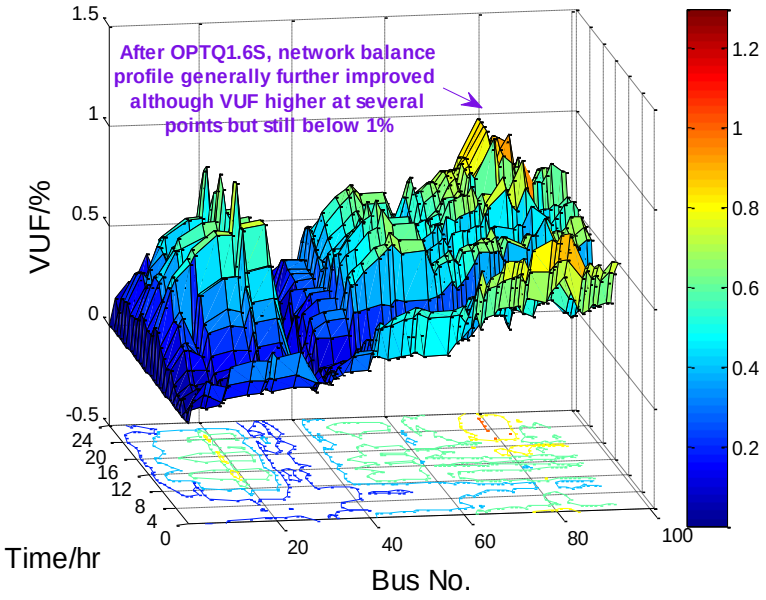

(c) OPTQ1.6S

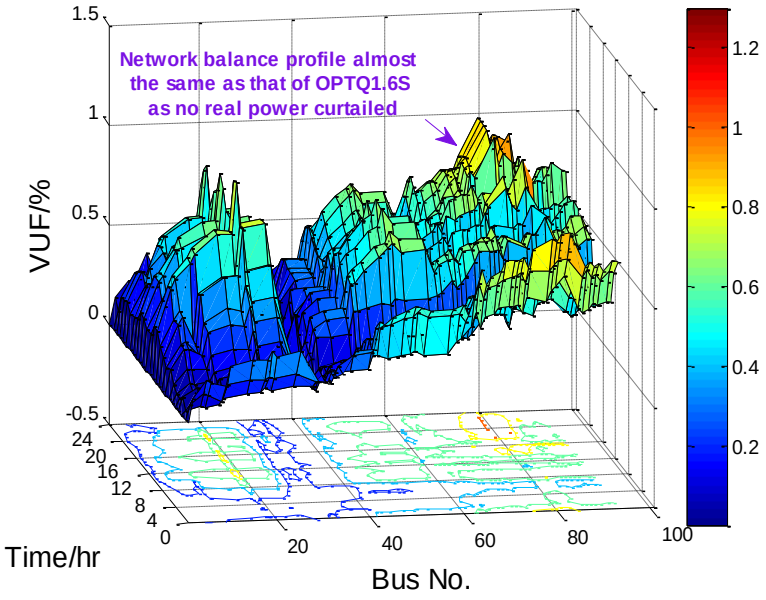

(d) OPTPQ1.6S.

Figure 3.8 Network VUF/% under the proposed PV control (HLLG).

3.4.5 Simulation Results for High Generation and Low Load

As shown in figures 3.9-3.13, by doubling the generation, a scenario with seriously high PV penetrations is formed to simulate the projected increased PV connections. Originally, as the generation is much higher than the load, especially during peak generation between 12:00 and 14:00 (figure 3.9), poor network performance, characterized by a significant reverse power flow, dramatic voltage rise and unbalance, is caused with the maximum objective function value (F_{max}) of 0.261 at 14:00 (table 3.5). To mitigate the voltage rise and improve the overall network quality, inductive reactive power is injected optimally by the PV inverters in OPTQ1S and OPTQ1.6S. As shown in table 3.5, comparing with the results of ORIGINAL, the objective function values show an obvious downward trend over 24 hours with F_{max} decreased significantly to 0.04259 for OPTQ1S and to 0.042 for OPTQ1.6S. However, the network performance has not been improved much by increasing inverter capacity, which is due to the limited effect of reactive power control on networks with high R/X ratio. Thus, real power curtailment is used in OPTPQ1.6S to work with reactive power control. As seen in figures 3.9-3.10 and table 3.5, with real power curtailed during the peak generation, further improved network performance can be observed with lower reactive power demand, alleviated reverse power flow and the smallest F_{max} of 0.04181.

As shown in tables 3.3 and 3.5, voltage magnitude profile with the highest weight w_2 =0.4 is ensured to be improved first, which is supported by the continuously decreasing J_2. J_3 and J_1 with lower importance may be sacrificed to support J_2 and the total objective function at some time points (table 3.5). Additionally, as J_3 has a higher weight than J_1, worse network losses are more likely to be observed.

As shown in figures 3.12-3.13, after applying the proposed three-option PV control, both the overvoltage and VUF are reduced to their corresponding dead band limits in table 3.3. Specifically, the highest voltage and the peak VUF are decreased from 249.3V and 1.33% for ORIGINAL to 247.1V and 1.02% for OPTQ1S and to

246.81V and 1.02% for OPTQ1.6S and to 246.8V and 1.00% for OPTPQ1.6S, respectively.

Table 3.5 Network optimization results over 24 hours (HGLL). The highlighted green/red cells indicate decrease/increase of the value compared with the pervious case.

Time	F	J1/0.1	J2/0.4	J3/0.2	J4/0.1	J5/0.2	Time	F	J1/0.1	J2/0.4	J3/0.2	J4/0.1	J5/0.2
ORIGINAL							**OPTQ1S**						
00:00	0.01270	347.3	0.0	0	1035.9	0.0	**00:00**	0.01270	347.3	0.0	0	1035.9	0.0
01:00	0.01209	226.7	0.0	0	1038.4	0.0	**01:00**	0.01209	226.7	0.0	0	1038.4	0.0
02:00	0.01202	216.5	0.0	0	1036.6	0.0	**02:00**	0.01202	216.5	0.0	0	1036.6	0.0
03:00	0.01211	235.0	0.0	0	1035.8	0.0	**03:00**	0.01211	235.0	0.0	0	1035.8	0.0
04:00	0.01192	198.7	0.0	0	1035.6	0.0	**04:00**	0.01192	198.7	0.0	0	1035.6	0.0
05:00	0.01271	348.8	0.0	0	1036.2	0.0	**05:00**	0.01271	348.8	0.0	0	1036.2	0.0
06:00	0.02642	634.1	16.8	4.3E-6	1096.1	0.0	**06:00**	0.01553	633.9	2.1	2.7E-9	1142.8	0.0
07:00	0.01575	457.7	0.2	2.4E-7	1215.1	0.0	**07:00**	0.01522	458.1	0.2	3.8E-10	1218.4	0.0
08:00	0.01903	287.8	0.0	0	1668.1	0.0	**08:00**	0.01903	287.8	0.0	0	1668.1	0.0
09:00	0.02187	412.6	0.0	0	1876.5	0.0	**09:00**	0.02187	412.6	0.0	0	1876.5	0.0
10:00	0.01694	190.9	0.0	0	1518.2	0.0	**10:00**	0.01694	190.9	0.0	0	1518.2	0.0
11:00	0.03022	741.9	19.0	0	2342.2	0.0	**11:00**	0.03022	741.9	19.0	0	2342.2	0.0
12:00	0.05477	1320.8	190.5	1.2E-7	2878.0	0.0	**12:00**	0.03931	1494.1	7.1	1.6E-9	2933.9	0.0
13:00	0.12307	1436.4	247.7	2.6E-5	3033.0	0.0	**13:00**	0.04433	1689.9	24.3	7.5E-8	3149.1	0.0
14:00	**0.26062**	**1411.9**	**252.9**	**8.6E-5**	**2876.5**	**0.0**	**14:00**	**0.04259**	**1757.8**	**14.4**	**4.2E-8**	**3043.1**	**0.0**
15:00	0.01947	304.8	0.0	0	1701.9	0.0	**15:00**	0.01947	304.8	0.0	0	1701.9	0.0
16:00	0.01932	276.0	0.0	0	1701.8	0.0	**16:00**	0.01932	276.0	0.0	0	1701.8	0.0
17:00	0.02841	1026.5	94.8	1.1E-6	1121.4	0.0	**17:00**	0.01886	1046.5	6.3	1.8E-9	1217.7	0.0
18:00	0.01712	893.7	8.8	0	1107.1	0.0	**18:00**	0.01712	893.7	8.8	0	1107.1	0.0
19:00	0.02504	1331.9	77.1	0	1050.8	0.0	**19:00**	0.02504	1331.9	77.1	0	1050.8	0.0
20:00	0.03305	1406.7	163.1	0	1031.6	0.0	**20:00**	0.01981	1396.3	4.0	1.9E-9	1153.0	0.0
21:00	0.03040	1304.4	140.0	0	1030.5	0.0	**21:00**	0.01886	1284.8	2.4	0	1132.2	0.0
22:00	0.01715	857.0	19.3	0	1036.9	0.0	**22:00**	0.01565	834.3	0.9	0	1065.3	0.0
23:00	0.01342	487.1	0.0	0	1034.5	0.0	**23:00**	0.01342	487.1	0.0	0	1034.5	0.0
24:00	0.01295	390.6	0.0	0	1038.1	0.0	**24:00**	0.01295	390.6	0.0	0	1038.1	0.0
OPTQ1.6S							**OPTPQ1.6S**						
00:00	0.01270	347.3	0.0	0	1035.9	0.0	**00:00**	0.01270	347.3	0.0	0	1035.9	0.0
01:00	0.01209	226.7	0.0	0	1038.4	0.0	**01:00**	0.01209	226.7	0.0	0	1038.4	0.0
02:00	0.01202	216.5	0.0	0	1036.6	0.0	**02:00**	0.01202	216.5	0.0	0	1036.6	0.0
03:00	0.01211	235.0	0.0	0	1035.8	0.0	**03:00**	0.01211	235.0	0.0	0	1035.8	0.0
04:00	0.01192	198.7	0.0	0	1035.6	0.0	**04:00**	0.01192	198.7	0.0	0	1035.6	0.0
05:00	0.01271	348.8	0.0	0	1036.2	0.0	**05:00**	0.01271	348.8	0.0	0	1036.2	0.0

06:00	0.01553	633.9	2.1	2.7E-9	1142.8	0.0	**06:00**	0.01553	633.9	2.1	2.7E-9	1142.8	0.2
07:00	0.01522	458.1	0.2	3.8E-10	1218.4	0.0	**07:00**	0.01522	458.1	0.2	3.8E-10	1218.4	0.4
08:00	0.01903	287.8	0.0	0	1668.1	0.0	**08:00**	0.01903	287.8	0.0	0	1668.1	0.5
09:00	0.02187	412.6	0.0	0	1876.5	0.0	**09:00**	0.02187	412.6	0.0	0	1876.5	0.6
10:00	0.01694	190.9	0.0	0	1518.2	0.0	**10:00**	0.01694	190.9	0.0	0	1518.2	0.0
11:00	0.03022	741.9	19.0	0	2342.2	0.0	**11:00**	0.03022	741.9	19.0	0	2342.2	1.0
12:00	0.03931	1494.1	7.1	1.6E-9	2933.9	0.0	**12:00**	0.03328	1120.2	4.1	0	2769.8	3949.1
13:00	0.04385	1750.2	14.3	3.2E-8	3170.4	0.0	**13:00**	0.04198	1057.6	8.0	0	2852.0	7483.8
14:00	**0.04247**	**1755.1**	**13.7**	**3.7E-8**	**3039.6**	**0.0**	**14:00**	**0.04181**	**1116.8**	**7.7**	**2.2E-9**	**2729.7**	**5369.0**
15:00	0.01947	304.8	0.0	0	1701.9	0.0	**15:00**	0.01947	304.8	0.0	0	1701.9	0.0
16:00	0.01932	276.0	0.0	0	1701.8	0.0	**16:00**	0.01932	276.0	0.0	0	1701.8	0.0
17:00	0.01886	1046.5	6.3	1.8E-9	1217.7	0.0	**17:00**	0.01886	1046.5	6.3	1.8E-9	1217.7	0.0
18:00	0.01712	893.7	8.8	0	1107.1	0.0	**18:00**	0.01712	893.7	8.8	0	1107.1	0.0
19:00	0.02504	1331.9	77.1	0	1050.8	0.0	**19:00**	0.02504	1331.9	77.1	0	1050.8	0.0
20:00	0.01981	1396.3	4.0	1.9E-9	1153.0	0.0	**20:00**	0.01981	1396.3	4.0	1.9E-9	1153.0	0.0
21:00	0.01886	1284.8	2.4	0	1132.2	0.0	**21:00**	0.01886	1284.8	2.4	0	1132.2	0.0
22:00	0.01565	834.3	0.9	0	1065.3	0.0	**22:00**	0.01565	834.3	0.9	0	1065.3	0.0
23:00	0.01342	487.1	0.0	0	1034.5	0.0	**23:00**	0.01342	487.1	0.0	0	1034.5	0.0
24:00	0.01295	390.6	0.0	0	1038.1	0.0	**24:00**	0.01295	390.6	0.0	0	1038.1	0.0

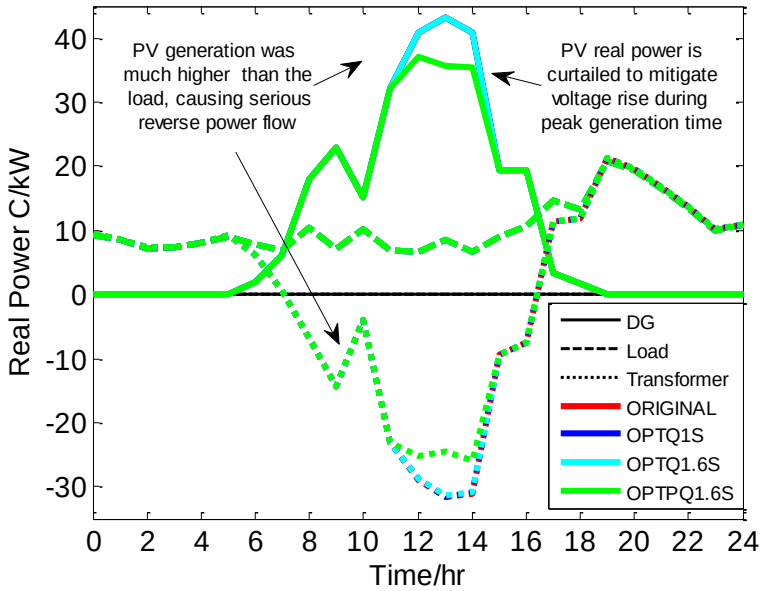

Figure 3.9 Phase C real power: transformer, load & PV/kW (HGLL). The results are presented based on the combination of line type and color.

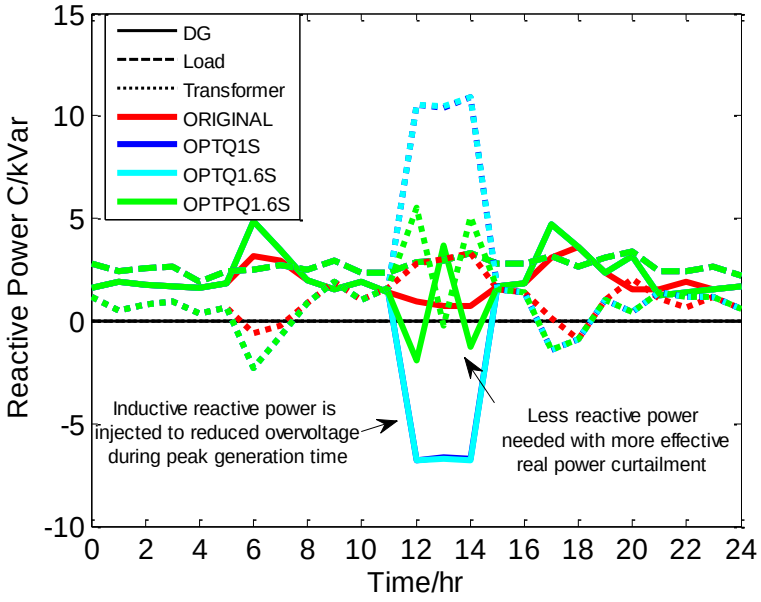

Figure 3.10 Phase C reactive power: transformer, load & PV/kVar (HGLL). The results are presented based on the combination of line type and color.

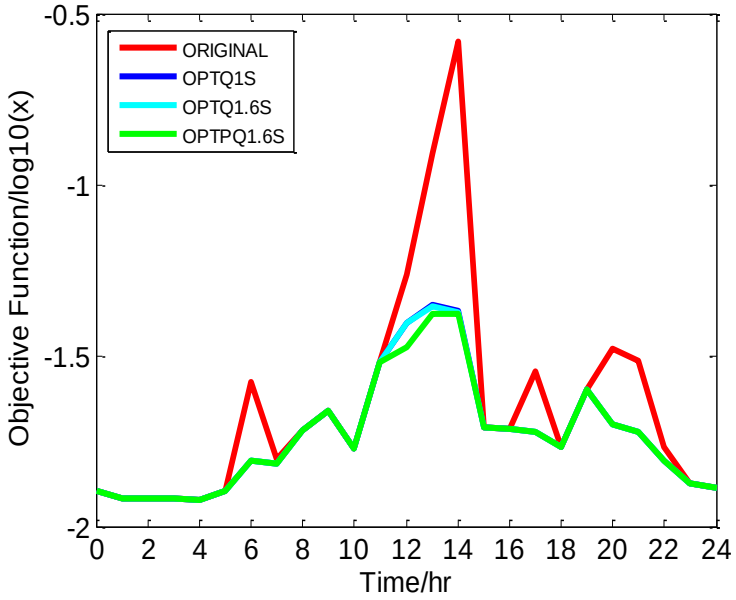

Figure 3.11 Objective function (table 3.5, column 2) under the proposed PV control (HGLL)

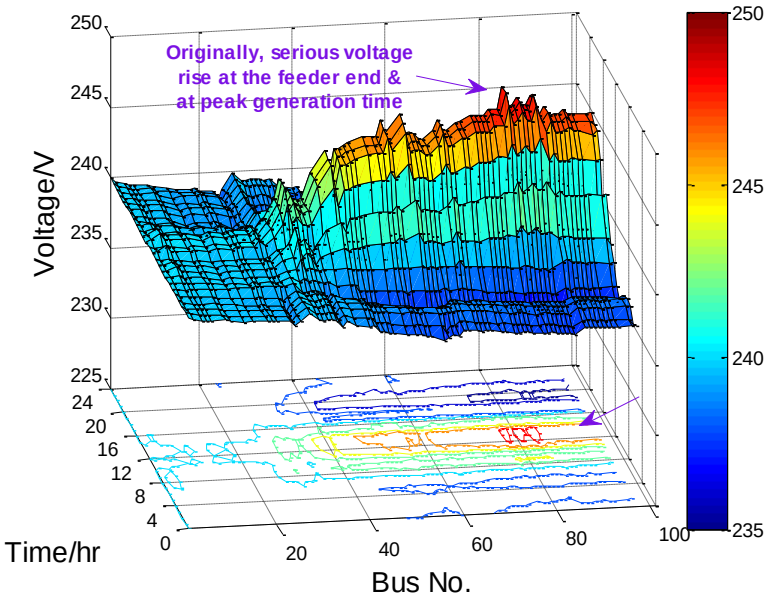

(a) ORIGINAL.

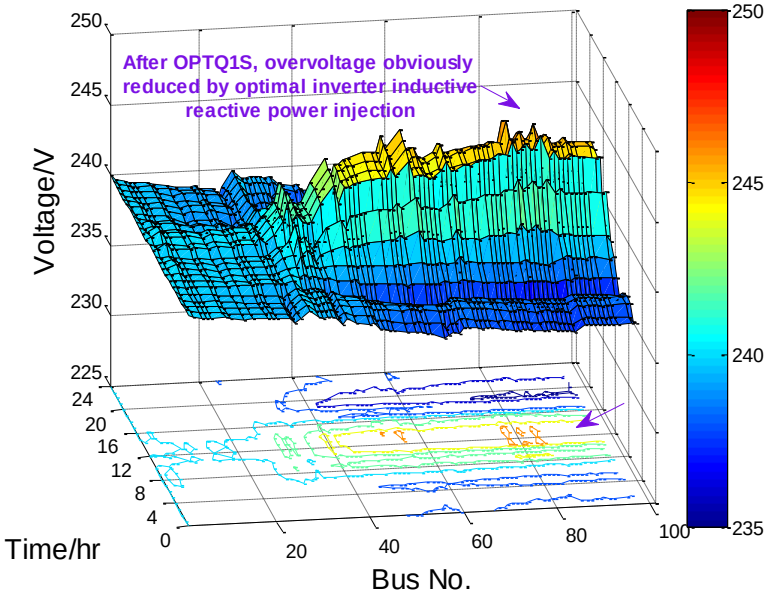

(b) OPTQ1S.

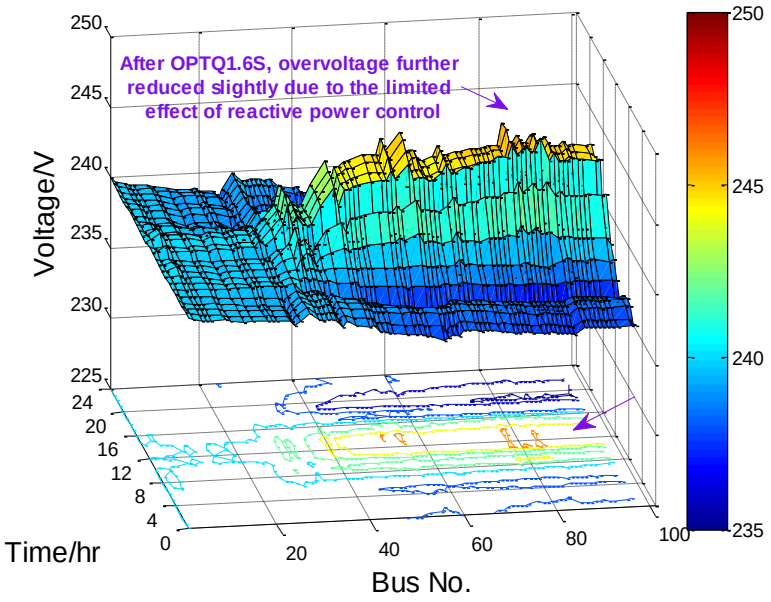

(c) OPTQ1.6S.

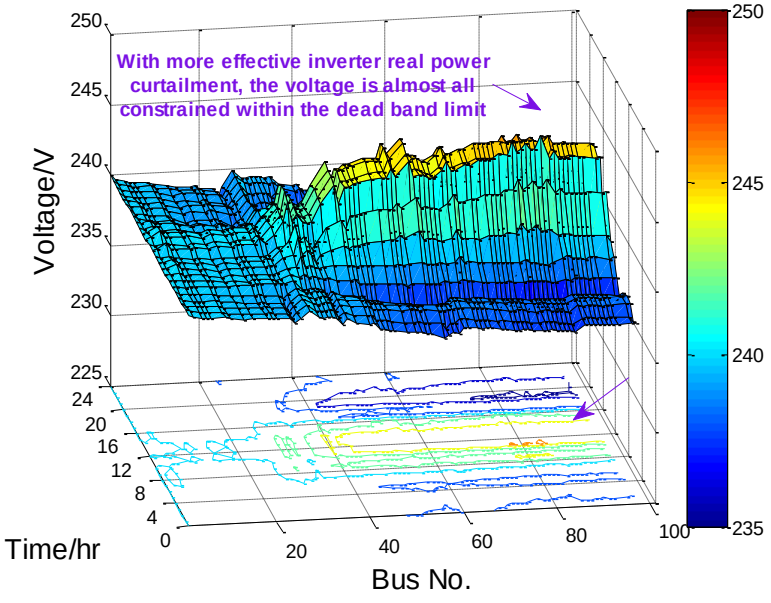

(d) OPTPQ1.6S.

Figure 3.12 Phase C voltage/V under the proposed PV control (HGLL).

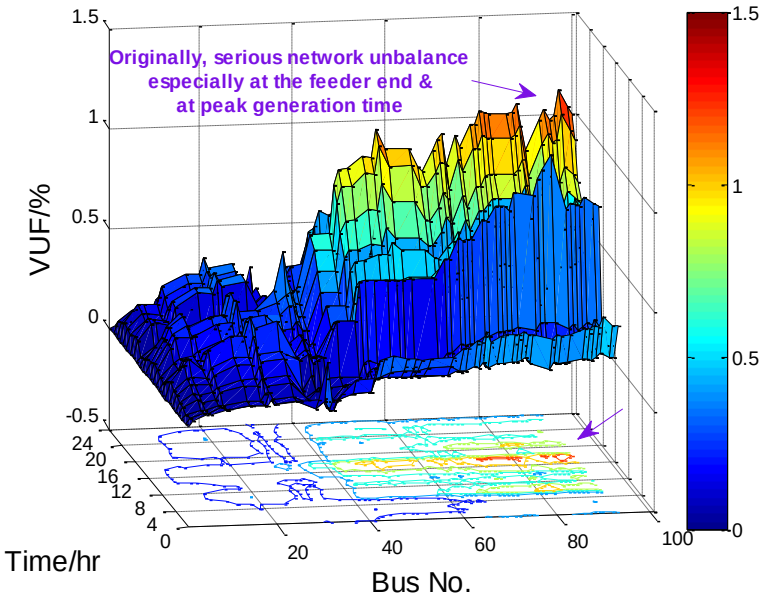

(a) ORIGINAL.

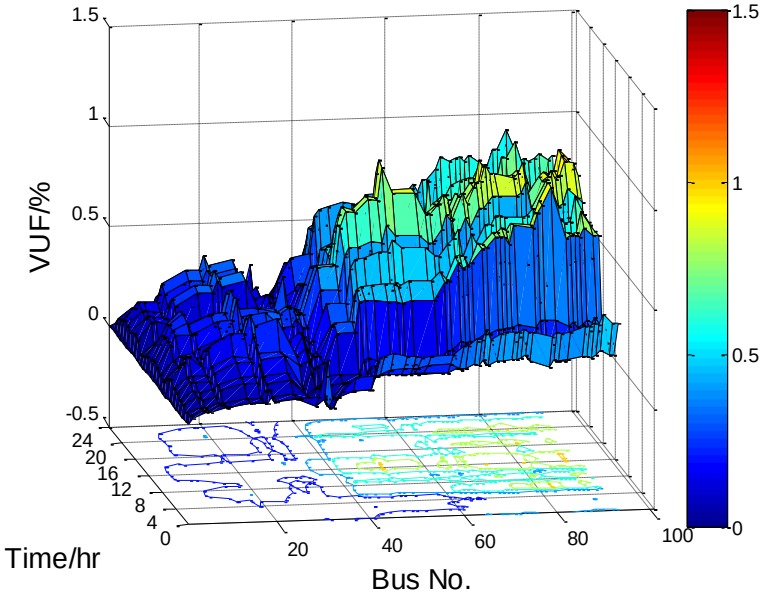

(b) OPTQ1S.

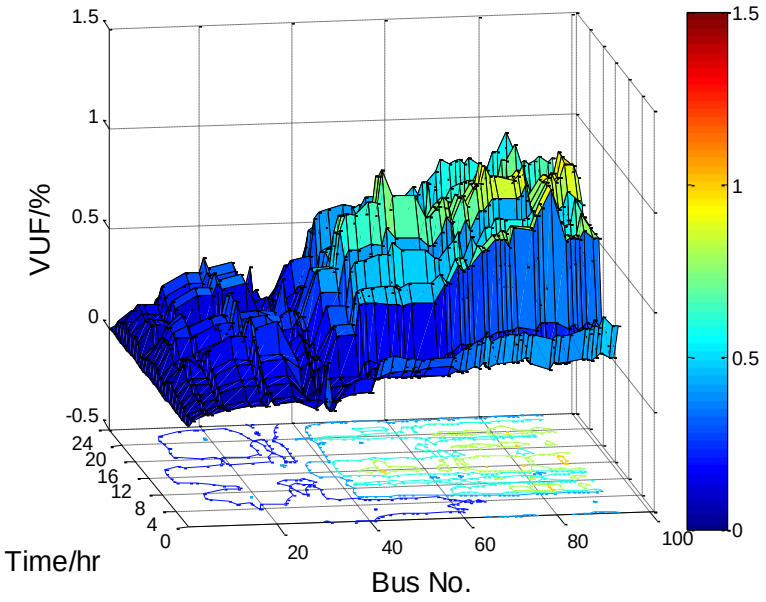

(c) OPTQ1.6S.

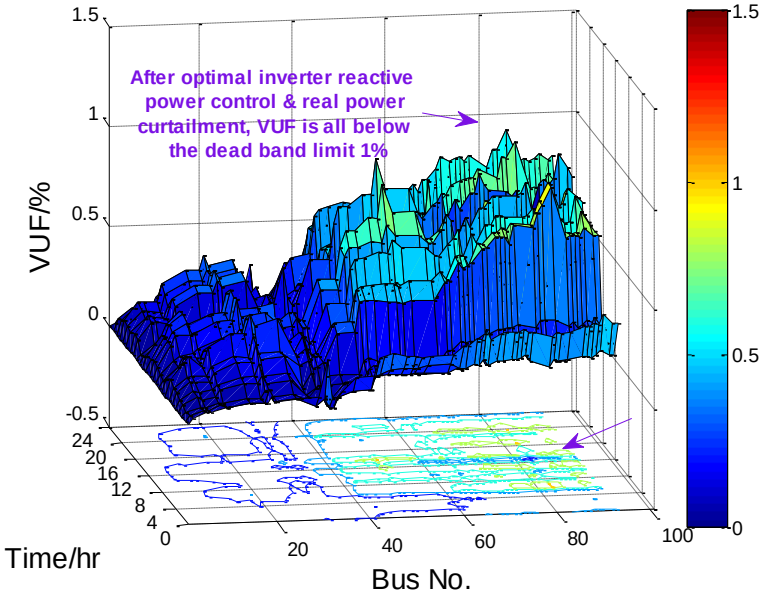

(d) OPTPQ1.6S.

Figure 3.13 Network VUF/% under the proposed PV control (HGLL).

3.4.6 Convergence Analysis and Computing Time

To ensure convergence of the proposed optimization problem, all objectives of equations (3.1-3.5) have been carefully defined as convex functions of the control variables. The utilization of dead band and global Matlab solver with multiple starting points also contributes to the convergence. The approach has proven robust with all of the simulations conducted to date converging.

Based on an unbalanced network model, solving the proposed OPF problem requires more time but still within an acceptable level. The average computing time for solving the test network used in this study is about 5 minutes (308 seconds) on a machine with an Intel Core i5 processor @3.2GHz. In this research, network data including PV generation, loads and voltages is measured and collected every 15 min through smart meters installed across the test network. Therefore, the simulation time is much less than the data measurement interval and the proposed multi-objective OPF model can support real-time applications. It should be noted that generally the network data collection time and the set points implementation time is limited by the physical communication infrastructure.

3.5 MODEL VALIDATION BASED ON SMART METER READING

To further investigate the validity and accuracy of the proposed Multi-objective OPF model coded in Matlab as well as the network model, unbalanced load flow calculations are carried out by imposing the actual loads and PV generations boundary limits recorded by the 24 three-phase and 51 single-phase smart meters installed on the test network. Detailed comparisons are performed between the recorded (measured) and simulation for typical days through the year (spring, summer, autumn and winter). Due to page limitation, only one set of results (peak demand case at 18:45 pm on 25/01/2012) is presented. As shown in figure 3.14, the maximum voltage error between the calculated values and the actual smarter meter data is 4.7V i.e. around 2% of the rated value. Considering the following factors, the error is acceptable and both the optimization and network models are valid and accurate:

1) Calculations are based on average values over the data collection interval (15 minutes) while the smart meter data is instantaneous;
2) Data collection by smart meters is not synchronous due to different time delays in communication;
3) Estimated data is used for the two buses with mechanical meters (marked red in figure 3.3).

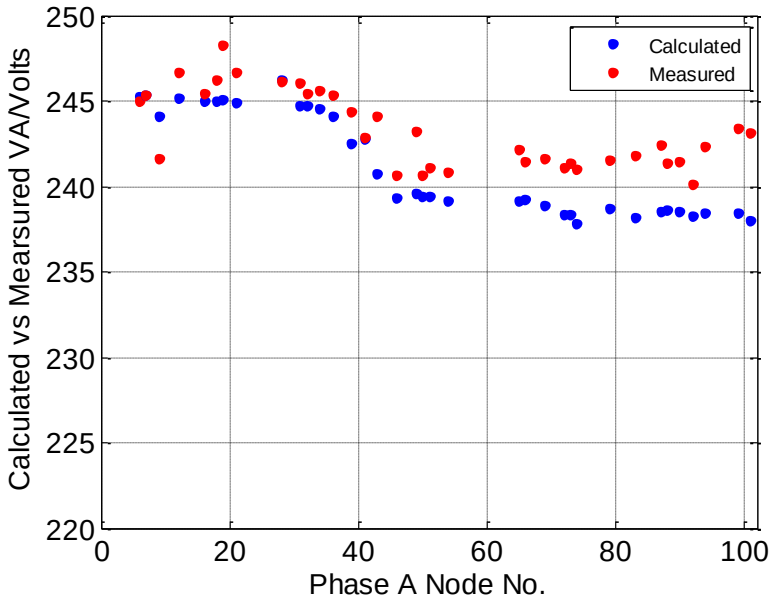

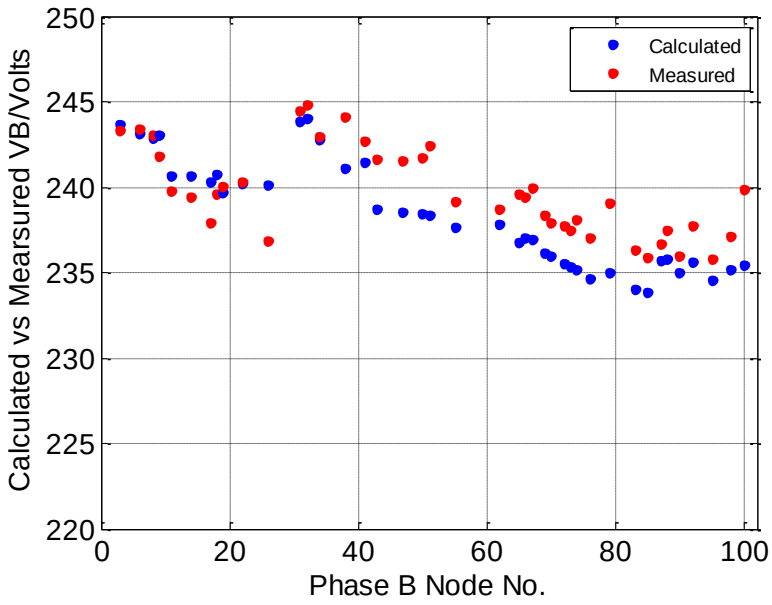

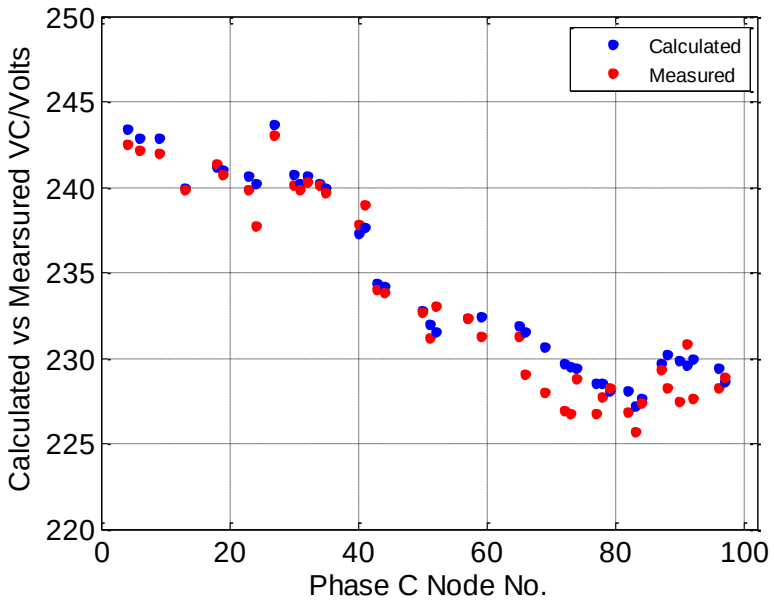

Figure 3.14 Phase voltage error analyses based on actual smart meter readings for a typical summer day (25/01/2012) in WA, Australia.

3.6 CONCLUSION AND APPLICATION CONSIDERATION

To form the LV controller of the proposed hierarchical control, this chapter makes a comprehensive study on PV inverter control to optimize the operational performance of unbalanced four-wire distribution networks with high PV penetrations. A PV control options assessment strategy is proposed based on the reactive power capability and real power curtailment of single-phase inverters. An OPF problem with multiple objectives of dead band based voltage magnitude and balance profiles, network losses, PV generation and real power curtailment costs is defined and then converted into an aggregated single-objective problem using the weighted sum method, which can be successfully solved by the SQP based global solver in Matlab. The performance of the proposed PV control strategy and multi-objective OPF model is demonstrated on a real distribution network over 24 hours. The validity and accuracy of the optimization model are also tested by comparing simulation results against the actual smart meter readings. The results demonstrate that the proposed PV control options assessment strategy and multi-objective OPF model are feasible and effective for improving the voltage regulation and balance of LV four-wire

distribution networks with high residential PV penetrations, which in turn increases the capability to simultaneously supply the increasing consumer loads and absorb higher fractions of renewable energy.

Despite some national standards (e.g. IEEE 1547 and AS4777) limiting the reactive power control of low-voltage inverters for voltage regulation, reactive control is mandated for larger PV systems. Furthermore, small solar inverters with reactive power control are already available in the European market. To implement the proposed PV control strategy in real distribution networks, the following several factors should be considered:

1) PV reactive power is controlled in this study to provide grid support. Thus, in a way similar to the existing real power feed-in tariff, feed-in policies on the inverter reactive power generation should be proposed and provide financial benefits for the consumers involved;
2) This study is carried out with the assumption of widespread two-way communication infrastructure availability. In fact, some latest Advanced Metering Infrastructures (AMI) already have the capability of collecting data from and sending control signals to inverters [160]. Research is currently underway to identify and standardize communication architecture for the next-generation PV inverters [143].
3) The control procedure: network information (e.g. loads and generations at each house) is collected and passed to the centralized feeder controller, where according to the network status, one of the three proposed control options (Section 3.2) is selected and the optimal set points of each controlled PV inverter are determined based on the proposed multi-objective OPF model. Then the set points will be sent to each inverter and implemented.

Chapter 4. Optimization by Delta Switched Capacitors Control in Unbalanced MV Networks

4.1 INTRODUCTION

To introduce controllability at the MV level as part of a hierarchical control, switched capacitors are considered in this chapter to optimize the operation of MV distribution networks. Within comparison to other MV controllable devices such as online tap changer equipped transformers and voltage regulators, switched capacitors are the most flexible and effective and therefore, the most popular. Besides, capacitor control is a most typical MINLP problem of distribution networks and the generated optimization model and strategy can be easily expanded to address other MINLP problems. Additionally, as the MV distribution network simulated in this research originally had no capacitors installed, the switched capacitor placement problem is also studied. The content of this chapter is supported by our publication of [161].

Specifically, switched capacitors have been widely used for reactive power compensation in distribution networks to provide benefits such as loss reduction, voltage profile improvement, power factor correction and network capacity release etc.. These benefits depend greatly on how the capacitors are placed along the feeder and controlled at different load levels.

The switched capacitor placement problem generally involves determining the location and size of capacitors to be installed in the distribution networks such that the maximum benefit is achieved while all the operational constraints are satisfied [162]. Optimal capacitor placement is often formulated as a MINLP problem and numerous optimization objectives and solution methods have been proposed in the last decades. More specifically, due to the availability of pricing information, the objective function of capacitor placement is often defined as the power loss reduction

[162-173] and capacitor purchase cost minimization [162-167, 169, 170, 172]. Additionally, other typical objectives, such as capacitor installation cost [162, 163, 165, 168, 169, 171-173], saving from system capacity release [166-168, 173], capacitor operation and maintenance cost [172, 173] have also been utilized in the previous studies. For the capacitor placement problem, many solution techniques have been proposed and they can be generally divided into three categories: analytical, numerical programming, heuristics and a comprehensive survey can be found in [170] and [174]. Among them, the latest heuristic methods [175] have been widely used as they are easy to implement and capable to locate the global optimal solution. So far, PSO [165, 171] and genetic algorithm (GA) [167, 169] are the two most popular heuristic techniques for the capacitor placement problem.

While the placement problem has been well researched, only a few studies have been dedicated to determining the operational control schemes of capacitors. Traditionally, strategies widely used by the utilities include voltage control, current control, VAr control, time control, temperature control and power factor control. These approaches including their advantages and limitations are analyzed in [176]. However, these strategies are not generally capable of handling frequently and significantly changed load profiles. To address this problem, in [176] and [177], the capacitor control problem was formulated as a constrained optimization problem with the objective of loss minimization and solved by a GA based two-stage algorithm and the exhaustive search approach respectively. Besides, a portioning method based distributed capacitor control is also presented in [178] with a focus on voltage spread reduction.

Despite the problems of capacitor placement and control have been studied for quite a long period, challenges still exist. In terms of placement, although various objectives have been defined [162-173], to our knowledge no paper has comprehensively included all these objectives in one study. Additionally, to efficiently decide the locations of capacitors in large-scale distribution networks, a common practice is to perform the sensitivity analysis once and then select a desired number of buses with the highest sensitivities. However, the selected buses are

usually geographically close to each other and will lead to an unreasonable clustered placement with over-compensation in a local area as the network sensitivity profile will significantly change after the last capacitor placement. In terms of control, all the existing studies are based on optimization of only one single objective. In fact, capacitor control involves multiple objectives that are normally mutually conflicting and a multi-objective control is needed to ensure a reasonable network performance after control. Even though multi-objective optimization has already been used for the capacitor placement in some studies [169, 170, 172], no study has applied it to the capacitor control problem. Besides, for both capacitor placement and control, the load flow is critical for the heuristic methods to evaluate and locate the optimal solution. Nevertheless, conventional load flow methods such as Newton or Gauss-Seidel usually become inefficient and even divergent in distribution networks due to the high R/X ratio [165]. Considering a huge population is required in the heuristic methods for the global optimal solution, a fast and reliable load flow is essential for both the capacitor placement and control problems. Moreover, majority of the studies are based on a balanced network model (e.g. [163-167, 169, 170, 172, 173]) which will result in non-optimal solutions as most practical distribution networks are naturally unbalanced. Most importantly, majority of the existing literature assumes a neutral connected star for the capacitors. This is quite common in American MV distribution networks typically with a three-phase four-wire physical structure. However, in Australia and most European countries, MV distribution networks are mostly three-phase three-wire without neutrals and delta-connected capacitors are more widely used. Studies on the optimal placement and control of delta-connected capacitors will have a great significance in terms of both theory and application.

For the unbalanced radial MV distribution networks, this chapter proposes both a comprehensive optimization based sequential placement strategy and a multi-objective optimization based real-time control strategy of delta-connected switched capacitors. Specifically, with all the typical objectives considered, a comprehensive optimization model is firstly formulated for capacitor placement with the objective function of maximizing the annual savings from energy loss reduction and network

capacity release while minimizing the annual costs of capacitor purchase, installation, operation and maintenance. For a higher efficiency of the unbalanced capacitor placement, unlike the widely used clustered strategy, a sequential strategy is then proposed based on the loss sensitivity analysis to identify the high benefit locations. On this basis, a multi-objective capacitor control strategy is proposed to simultaneously minimize network losses, voltage magnitude and voltage unbalance factor (VUF) deviations where weighted sum method is utilized to reflect the preferences on the mutual-conflicting control objectives. For the MINLP problems of both capacitor placement and control, the improved BSFS based PSO is used for the optimal solution and real-time applications. Finally, the feasibility, effectiveness and robustness of the proposed capacitor placement and control models and strategies are verified by comparing them with some existing popular schemes through detailed simulations over 24 hours on a real unbalanced Australian MV distribution network.

4.2 SEQUENTIAL COMPREHENSIVE CAPACITOR PLACEMENT

For the annual net saving maximization with all related objectives considered, a comprehensive optimization model of delta-connected switched capacitor placement is proposed.

4.2.1 Optimization Objectives

A. Annual Saving by Energy Loss Reduction (SER)

$$SER = K_E \sum_{i=1}^{nl} T_{li} \Delta P_{lossi} \tag{4.1}$$

where K_E is the energy cost with a typical value of \$50/MWh [166, 167] and nl represents the total number of typical load levels in a year. T_{li} is the duration of load level i and $\Delta P_{lossi} = P_{lossi} - P'_{lossi}$ represents the power loss reduction under load level i after capacitor placement.

B. Annual Saving by Network Capacity Release (SCR)

$$SCR = K_R \cdot \Delta P_{losspk} \cdot T_{lpk}/8760 \tag{4.2}$$

where K_R is the annual network capacity cost which is usually estimated at

$120,000/MW/year [166]. As network capacity release is more significant under heavy load, in this study only peak load capacity release ΔP_{losspk} is considered with a duration of T_{lpk}.

C. Annual Cost of Capacitor Purchase (CP)

$$CP = \sum_{i=1}^{N} \sum_{k=1}^{3} C_i^k \cdot Q_{Ci}^k \cdot K_{Pi}^k \tag{4.3}$$

As delta-connected capacitors are studied in unbalanced networks, both the bus number $i = 1,2,\cdots,N$ and phase-phase bridging designation $k = 1,2,3$ for ab, bc, ca are needed to identify a potential position for capacitor placement. Accordingly, C_i^k is the binary decision variable (0, 1) indicating whether to install a capacitor at position i^k. Besides, Q_{Ci}^k and K_{Pi}^k are the discrete capacitor size and the corresponding annual purchase cost with a group of typical commercial data shown in table 4.1 [166].

Table 4.1 Commercially available capacitor sizes and the corresponding purchase costs.

$\boldsymbol{Q_C}$ **[kVAr]**	**150**	**300**	**450**	**600**	**750**
K_P [$/kVAr/year]	0.500	0.350	0.253	0.220	0.276
$\boldsymbol{Q_C}$ **[kVAr]**	**900**	**1,050**	**1,200**	**1,350**	**1,500**
K_P [$/kVAr/year]	0.183	0.228	0.170	0.207	0.201

D. Annual Cost of Capacitor Installation (CI)

$$CI = \frac{1}{T} \sum_{i=1}^{N} C_i K_I \tag{4.4}$$

where K_I is the capacitor installation cost and often given at $1,600/position [165]. Thus the annual cost can be obtained based on the expected lifetime T (T=30 years in this study [179]).

E. Annual Cost of Capacitor Operation and Maintenance (COM)

$$COM = \sum_{i=1}^{N} C_i \cdot K_{OM} \tag{4.5}$$

where K_{OM} is the annual operation and maintenance cost and often set at $300/position/year [165].

4.2.2 Comprehensive Optimization Model

Based on the objectives above, the comprehensive optimization model of delta-connected switched capacitor placement can be formulated as follows for the maximization of net annual saving:

$$\min FP = CP + CI + COM - SER - SCR \tag{4.6}$$

subject to:

$$V_{min} \leq V_i^p \leq V_{max} \tag{4.7}$$

$$0 \leq Q_{Ci}^k \leq NC.Q_{C0} \tag{4.8}$$

where the boundary limits $[V_{min}, V_{max}]$ on the voltage magnitude V_i^p at bus i and phase p are specified in equation (4.7), which are to be kept throughout the optimization. According to AS 60038 [180], for MV distribution networks, voltage must be kept within ±6% of the nominal value. Additionally, commercially available switched capacitors consist of multiple smallest capacitor units and the number and size limits at bus i and phase-phase bridge k are given in equation (4.8), where NC is the maximum number of capacitor units of smallest size Q_{C0}. As shown in table 4.1, NC and Q_{C0} is set as 10 and 150kVAr respectively in this study.

4.2.3 Sequential Placement at High Benefit Buses

Although considering all the buses as the potential positions for capacitor placement will generate the most optimal results, the computation time will grow exponentially with the size increase of distribution networks and this issue becomes far more serious in unbalanced systems. To apply the proposed capacitor placement model to large and unbalanced distribution networks, selection of high benefit buses, can help with the reduction of search space, has been recommended in [165], [169] and [181]. However, the existing selection approaches often do the sensitivity analysis only once and then select a desired number of buses with highest sensitivities at one time. Consequently, the selected buses are usually geographically close to each other and will lead to an unreasonable clustered placement with over-compensation in a local area as the network sensitivity profile will be significantly changed after the last capacitor placement.

To solve this problem, a loss sensitivity analysis based sequential placement strategy is proposed in this study. A desired number of delta-connected switched capacitors are sequentially placed in unbalanced networks by repeating the following procedure:

Step 1: Based on equation (4.9) [169], with the previously placed capacitors kept, conduct a network loss sensitivity analysis for each phase-phase bridge of all buses.

$$dP_{loss}/dQ_C = \left|P_{loss}^{i} - P_{loss}^{i-1}\right| / \left|Q_C^{i} - Q_C^{i-1}\right| \tag{4.9}$$

where P_{loss}^{i} and P_{loss}^{i-1} are the values of network power loss corresponding to the sizes Q_C^{i} and Q_C^{i-1} at each position.

Step 2: Average the loss sensitivities of the three phase-phase bridges as the value of the corresponding bus in unbalanced networks and then locate the bus with the highest sensitivity.

Step 3: For the bus selected in step 2, perform the comprehensive optimization in equations (4.6-4.8) for the optimal capacitor sizes of the unbalanced three phase-phase bridges. As commercially available delta-connected capacitors have the same sizes for all three bridges, the final capacitor size at the bus is set as the maximum of the three bridge values.

4.3 REAL-TIME MULTI-OBJECTIVE CAPACITOR CONTROL

Control of switched capacitors usually involves multiple objectives which are mutually conflicting. To ensure a reasonable operational performance after control, a multi-objective and real-time capacitor control strategy is proposed.

4.3.1 Multi-Objective Optimization Model

A. Optimization Objectives

1) Network Power Loss:

$$J_1 = \sum_{l=1}^{N-1} \sum_{p=1}^{3} BLoss_l^p \tag{4.10}$$

where $BLoss_l^p$ is the power loss through phase p of branch l and can be calculated by equation (4.11) below.

$$\begin{bmatrix} BLoss_l^a \\ BLoss_l^b \\ BLoss_l^c \end{bmatrix} = \begin{bmatrix} R_{aa} & R_{ab} & R_{ac} \\ R_{ba} & R_{bb} & R_{bc} \\ R_{ca} & R_{cb} & R_{cc} \end{bmatrix} \begin{bmatrix} {I_l^a}^2 \\ {I_l^b}^2 \\ {I_l^c}^2 \end{bmatrix} \tag{4.11}$$

where $[R_{pp}]$ and $[I_l^p]$ are the real part of the total phase impedance matrix of and the currents through the branch (see section 4.4.2 for details).

2) Voltage Magnitude Profile

To improve the voltage magnitude profile, deviation from the nominal value V_N is defined as the objective.

$$J_2 = \sum_{i=1}^{N} \sum_{p=1}^{3} \left(V_i^p - V_N\right)^2 \tag{4.12}$$

3) Voltage Balance Profile

To ensure an acceptable balance profile after control, deviation of voltage unbalance factor (VUF) [154] from the desired value (e.g. 0) is also included in the objective function.

$$J_3 = \sum_{i=1}^{N} (VUF_i - VUF_{desired})^2 \tag{4.13}$$

B. Multi-Objective Optimization by Weighted Sum Method

For multi-objective optimization problems, a solution that minimizes all objectives simultaneously does not exist. Consequently, the notion of Pareto optimality was proposed to describe the solutions of multi-objective problems. A solution is called Pareto optimal if none of the objectives can be improved in value without detriment to any other objectives [125]. In practice, weighted sum method [129] is most widely used to reflect decision maker's preferences on objectives in the multi-objective optimization problems.

$$FC = \sum_{i=1}^{m} w_i J_i \tag{4.14}$$

As shown above, weighted sum method converts the multi-objective optimization problem into an integrated single-objective problem by multiplying each objective with a weighting factor and then summing up all the weighted objectives. To ensure the Pareto optimality of solution(s), it is recommended that the weights be set such that $\sum_{i=1}^{m} w_i = 1$ and $\boldsymbol{w} \geq \mathbf{0}$, which also generates a convex combination of objectives.

The value of a weight is significant not only relative to other weights but also relative to its objective function magnitude, which is a critical idea but often overlooked. Thus when using weights to reflect the relative preferences on the objectives, each objective function is divided by a scale factor sf_i so that they all have similar magnitudes and no objective dominates the aggregated objective function. Common practice is to choose the maxima of each objective as the scale factor, i.e. $sf_i = J_i^{max}$ [129]. Accordingly, equation (4.14) can be improved in equation (4.15). At the end, recover the original objective function values by reverse scaling.

$$FC = \sum_{i=1}^{m} w_i J_i / sf_i \tag{4.15}$$

C. Proposed Multi-Objective Optimization Model

$$\min \quad FC \tag{4.16}$$

subject to:

$$V_{min} \leq V_i^p \leq V_{max} \tag{4.17}$$

$$0 \leq Q_{Ci}^k \leq Q_{Cmaxi}^k \tag{4.18}$$

where constraints in equations (4.17) and (4.18) are the limits on the voltage magnitude and reactive capability decided by the capacitor sizes obtained from the placement in Section 4.2.

4.3.2 Real-Time Control Strategy

To improve network performance, a multi-objective real-time control strategy for switched capacitors is proposed in figure 4.1. Specifically, at any time point t, based on the capacitor settings passed down from the last hour t-1, load flow is conducted

and the objective function FC in equation (4.16) is calculated as well. After that, FC is checked against the preset limit FC_{max} with the following two options: $if\ FC < FC_{max}$, network performance is satisfactory based on the current capacitor settings which then will be kept and passed to the next hour t+1; $if\ FC > FC_{max}$, the network performance is not desired and the multi-objective optimization defined in equations (4.10-4.18) is performed for the optimal capacitor settings. This newly generated capacitor settings will be passed down to hour t+1.

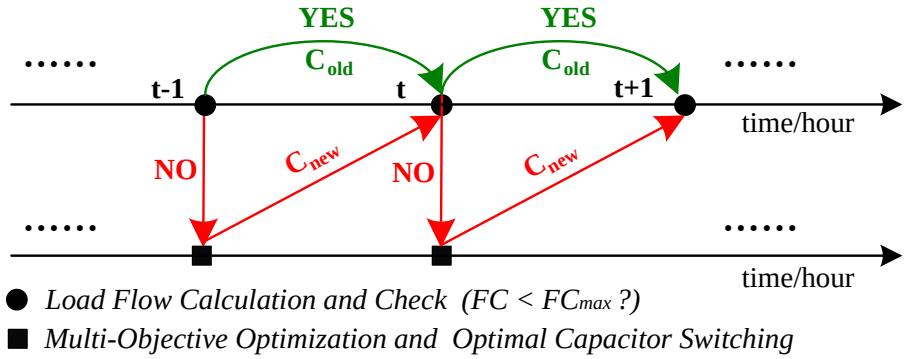

Figure 4.1 Proposed real-time capacitor control strategy.

4.4 PSO AND IMPROVED BSFS BASED SOLUTION METHOD

Both the capacitor placement and control problems in Sections 4.2 and 4.3 are MINLP problems. To efficiently solve this kind of problems and also support real-time applications, improved BSFS based PSO is utilized.

4.4.1 PSO

Since developed by Eberhart and Kennedy in 1995 [112], PSO has been widely used to solve various optimization problems in power systems. In PSO, a population called a swarm is randomly generated. The swarm consists of individuals called particles, representing a potential solution of the optimization problem. Each particle search through a multi-dimensional space for the optimal solution by updating its velocity and position based on its own experience and its companion's experience as follows:

$$V_i^{k+1} = \omega V_i^k + c_1 r_1 \left(P_{besti}^k - X_i^k\right) + c_2 r_2 \left(G_{best}^k - X_i^k\right) \tag{4.19}$$

$$X_i^{k+1} = X_i^k + V_i^{k+1} \tag{4.20}$$

where,

ω inertia weight;

c_1, c_2 acceleration constants;

r_1, r_2 two random numbers in the range of [0, 1];

P_{besti}^k best position searched by particle i at kth iteration;

G_{best}^k best position ever searched by the entire swarm.

As analyzed in Chapter 2, based on a simple concept, PSO is easy to implement with few parameters to adjust. Comparing with other heuristic methods e.g. GA, PSO has a better computational efficiency and more stable convergence [115, 122].

4.4.2 Improved BSFS and Delta Capacitor Model

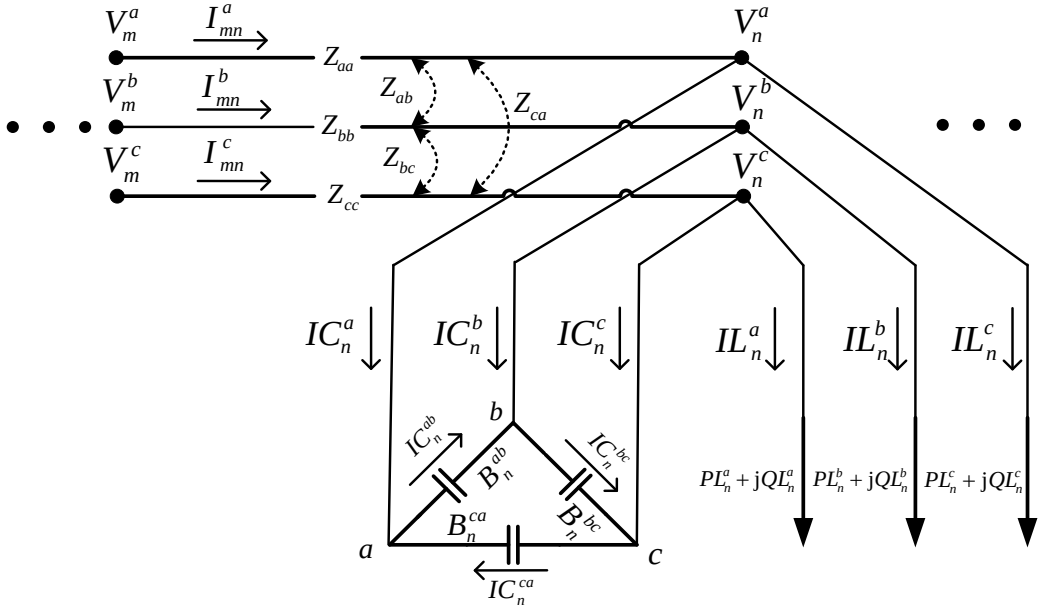

Figure 4.2 Generalized three-phase branch model with delta-connected capacitor.

Load flow is fundamental to PSO as the objective functions defined in equations (4.1-4.8) and (4.10-4.18) need to be evaluated for each particle at all iterations. So

far, many approaches for distribution network load flow analysis have been developed. Among them, a simple and efficient improved BSFS method was presented in [182]. However, it is only based on the balanced network model. In this study, this original method is expanded for the load flow analysis of unbalanced radial distribution networks with delta-connected switched capacitors.

As shown in figure 4.2, unbalanced load flow analysis based on the improved BSFS mainly involves the following steps:

Step 1: identify all buses beyond each branch;

Step 2: with an initial rated voltage, calculate the load current and capacitor charging current at each bus according to equations (4.21) and (4.22);

$$IL_n^p = (PL_n^p - jQL_n^p)/V_n^{p^*} \qquad p = a, b, c \tag{4.21}$$

$$\begin{bmatrix} IC_n^a \\ IC_n^b \\ IC_n^c \end{bmatrix} = \begin{bmatrix} j(B_n^{ab} + B_n^{ca}) & -jB_n^{ab} & -jB_n^{ca} \\ -jB_n^{ab} & j(B_n^{ab} + B_n^{bc}) & -jB_n^{bc} \\ -jB_n^{ca} & -jB_n^{bc} & j(B_n^{bc} + B_n^{ca}) \end{bmatrix} \begin{bmatrix} V_n^a \\ V_n^b \\ V_n^c \end{bmatrix} \tag{4.22}$$

where B is the constant susceptance of the phase-phase capacitor bridge and can be calculated from the rated capacity and rated phase-phase voltage as follows [183]:

$$B = kVAr/(kV_{pp}^2 \cdot 1000) \text{ S} \tag{4.23}$$

Step 3: according to Kirchhoff's Current Law (KCL), current through each branch equals the sum of load currents and capacitor charging currents of all the buses beyond that branch. That is,

$$I_{mn}^p = \sum_{i \in \varphi} \left(IL_i^p + IC_i^p \right) \qquad p = a, b, c \tag{4.24}$$

where φ is the set of buses beyond the branch mn including bus n.

Step 4: with branch currents and substation voltage at bus 1 available, voltage of each bus downstream can be calculated by equation (4.25).

$$\begin{bmatrix} V_n^a \\ V_n^b \\ V_n^c \end{bmatrix} = \begin{bmatrix} V_m^a \\ V_m^b \\ V_m^c \end{bmatrix} - \begin{bmatrix} Z_{aa} & Z_{ab} & Z_{ac} \\ Z_{ba} & Z_{bb} & Z_{bc} \\ Z_{ca} & Z_{cb} & Z_{cc} \end{bmatrix} \begin{bmatrix} I_{mn}^a \\ I_{mn}^b \\ I_{mn}^c \end{bmatrix} \tag{4.25}$$

where $[Z_{pp}]$ is the total phase impedance matrix with mutual coupling considered.

Step 5: Obtain new bus voltage values and check convergence of the solution. If the solution does not converge, go to Step 2 with the new voltages and repeat the whole process.

4.4.3 Flowchart of PSO and Improved BSFS Based OPF

In this study, PSO and the improved BSFS are combined to efficiently solve the sequential comprehensive placement and real-time multi-objective control problems of delta-connected switched capacitors. Specifically, as shown in figure 4.3, PSO is employed as a global optimization solver to optimally determine the capacitor size at each high benefit bus and the control schemes while the improved BSFS is used to support PSO by evaluating the objective/fitness function and also to meet the equality constraints of power flow equations.

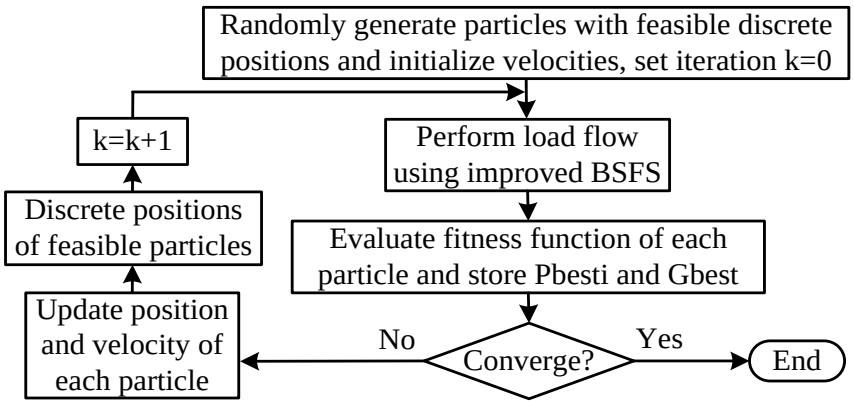

Figure 4.3 Flowchart of PSO and improved BSFS based optimization solver.

4.5 SIMULATION RESULTS AND ANALYSIS

4.5.1 Test Network

To verify the feasibility, effectiveness and robustness of the proposed placement and control strategies of delta-connected switched capacitors, a real MV radial distribution network in the district of Forrestfield, Western Australia is studied. As shown in figure 4.4, the 60-bus 12.7/22kV three-phase three-wire network is supplied by a 132/22kV substation transformer. As the 25 loads are unevenly allocated among the three phases, the network is unbalanced, making it suitable for

this study. The total peak demands are 6.34MW, 5.46MW and 6.05MW for phases A, B and C respectively. The network serves a mixture of residential, commercial and industrial loads which are all modeled as constant PQ in this study. Additionally, due to the small feeder length, no voltage regulators are connected in this network. A full description of the simulated Forrestfield MV network is given in Appendix C.

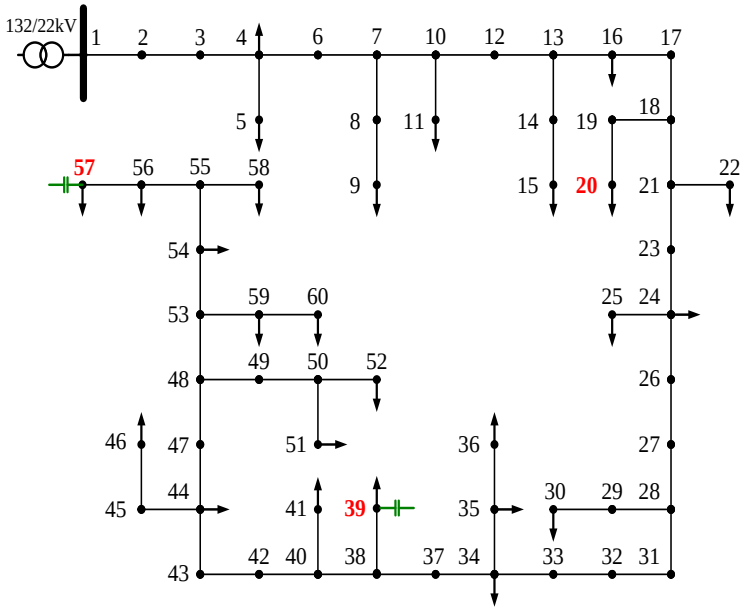

Figure 4.4 Real unbalanced MV distribution network in Western Australia.

4.5.2 Optimization Parameters Setting

Parameters used in this study are listed in tables 4.2 and 4.3. Particularly, the load levels identified by the load factor and the corresponding duration time are specified in the table 4.2 for the calculation of energy loss reduction SER and network capacity release SCR in Section 4.2. In addition, as shown in table 4.3, for the global optimal solution by PSO, the particle size is set to 10 000, which is large, to increase the diversity. A linearly decreasing inertia weight ω from 0.9 to 0.4 is also employed to ensure both the exploration and exploitation capabilities of PSO at the beginning and end of optimization respectively. Furthermore, as the multiple objectives of the optimization problem in equations (4.10-4.18) are mutually conflicting (e.g. emphasis on the voltage magnitude J_2 which requires a huge amount of capacitor injection may lead to a higher network loss J_1 due to the local overcompensation.), in

this study, to keep consistency with the placement model the priority is given to J_1 with $w_1 = 0.5$ while a smaller weight ($w_2 = 0.3$) is allocated to J_2 to reduce the risk of overcompensation. Additionally, the objective function threshold of capacitor control FC_{max} is set to be 0.28. That is, when $FC \geq 0.28$, optimal switching will be triggered.

Table 4.2 Load levels and duration time.

Load Levels	Peak (1.0)	Medium	Light (0.5)
Duration (h)	1000	6760	1000

Table 4.3 Parameters setting in calculation.

PSO		**Weighted sum method**	
Particle size	10,000	w_1	0.5
Iteration no.	15	w_2	0.3
C_1, C_2	2	w_3	0.2
ω	[0.9→0.4]	**Control threshold**: FC_{max}=0.28	

4.5.3 Results Analysis

A. Sequential Comprehensive Capacitor Placement

Based on the proposed sequential strategy and comprehensive optimization model, the placement problem of delta-connected switched capacitors is studied on the real test network of figure 4.4. In this study, three capacitors are assumed to be installed. To demonstrate the advantages of the proposed sequential strategy over the widely used clustered strategy [165, 169, 181], capacitor placement based on both strategies is carried out and results are compared in tables 4.4 and 4.5.

Specifically, according to table 4.4, in the proposed sequential strategy, when placing the first capacitor C1, the average loss sensitivity of all buses are initially calculated based on equation (4.9) and then ordered. Bus 57, which is located at the furthest end of feeder, is identified as the highest benefit bus with the highest loss sensitivity. Then, the comprehensive optimization problem defined by equations (4.1-4.8) is solved by the improved BSFS based PSO for the optimal capacitor size. As shown in table 4.4, a maximum annual net saving of $17,536 can be achieved with the optimal

size of 7/4/7 units (i.e. 1050/600/1050kVAr) for the bridges AB, BC and CA respectively at bus 57. As commercially available delta-connected switched capacitors all have the equal bridges, the final size installed is set as 1050/1050/1050kVAr, i.e. 7 capacitor units of 150kVAr on each bridge. With the optimal capacitor installed at bus 57, the second capacitor C2 is sequentially placed in a similar manner. Based on the second sensitivity analysis, bus 39 now has the highest loss sensitivity. This is because the network sensitivity profile has significantly changed after the capacitor placement at bus 57. The comprehensive optimization by PSO shows that the annual net saving can be further improved to $17,886 with the optimal capacitor size of 3/0/2 units (450/0/300kVAr) at bus 39. Finally, with the optimal capacitors placed at buses 57 and 39, bus 20 is found to be the most loss-sensitive bus for the placement of the 3rd capacitor C3. After optimization, interestingly the annual net saving still remains at $17,886 with zero capacitor reactive injection required, indicating capacitor placement at bus 20 is economically unfeasible. In contrast, when placing the three capacitors in the clustered strategy, unlike the sequential strategy, all three potential buses 57, 56 and 58 are identified simultaneously by doing the network sensitivity analysis only once. As illustrated in table 4.4, the corresponding annual net saving is only $17,687 after the placement of all three capacitors with C1, C2 and C3 at 0/0/0, 4/3/6, 4/1/1 (i.e. 0/0/0, 600/450/900, 600/150/150 kVAr), respectively.

Table 4.4 Comparison of sequential and clustered capacitor placement.

Placement strategy	Sequential			Clustered
Placement order	C1	C2	C3	(C1, C2, C3)
Highest benefit bus(es)	57	39	20	(57, 56, 58)
Annual net saving/$	-17,536	-17,886	-17,886	-17,687
Optimal size required (AB/BC/CA)/units	7/4/7	3/0/2	0/0/0	(0/0/0, 4/3/6, 4/1/1)
Optimal size installed (AB/BC/CA)/units	7/7/7	3/3/3	0/0/0	(0/0/0, 6/6/6, 4/4/4)

Table 4.5 Network loss and minimal voltage before and after capacitor placement.

Network Performance	Load Level	Without Capacitor	Sequential Placement			Clustered Placement
			C1	C2	C3	
Power Loss/MW	Peak	0.6889	0.6467	0.6417	0.6417	0.6449
	Medium	0.3952	0.3648	0.3636	0.3636	0.3639
	Light	0.2004	0.1805	0.1825	0.1825	0.1804
Minimal Voltage/kV	Peak	12.10	12.24	12.27	12.27	12.24
	Medium	12.21	12.35	12.38	12.38	12.35
	Light	12.33	12.46	12.49	12.49	12.46

Additionally, as described in table 4.5, after the sequential capacitor placement, network performance in terms of both power loss and minimal voltage has been more significantly improved under all three load levels compared to the clustered placement strategy. More exactly, after the sequential placement, the power losses under the peak and medium load levels have been declined from the original (without capacitors) 0.6889MW and 0.3952MW to 0.6417MW and 0.3636MW compared to the corresponding values of 0.6449MW and 0.3639MW by clustered placement. Besides, the network minimal voltages under all three load levels have also been improved after the sequential capacitor placement at 12.27kV, 12.38kV and 12.49kV comparing with the original values (without capacitors) of 12.10kV, 12.21kV and 12.33kV and the values by clustered placement of 12.24kV 12.35kV and 12.46kV respectively. Even though the power loss is slightly higher after the second capacitor C2 placement by sequential strategy under the light load condition (due to over-compensation), both the peak and medium load levels have experienced obvious reduction in loss with a better overall network performance obtained.

Based on the analysis and comparison above, it is evident that the proposed sequential strategy can generate a better economic and operational performance with a more reasonable capacitor placement than the widely used clustered strategy.

B. Real-Time Multi-Objective Capacitor Control

As demonstrated in table 4.6 and figures 4.5 and 4.7, without capacitor support, originally the network was heavily loaded, especially during the peak-load period between 17:00 and 22:00, causing a poor network performance with serious power loss and voltage drop. Besides, as loads were unevenly allocated among the three phases, the network was unbalanced with phase A had the most load connections while phase B had the least.

To improve the network performance in terms of network loss, voltage deviation and voltage balance, according to the proposed multi-objective strategy in Section 4.3.2, the delta-connected switched capacitors installed at buses 39 and 57 are controlled. Specifically, as shown in table 4.6, at 00:00 the original network performance was poor with an objective function of 0.2852, exceeding the given threshold 0.28. Thus the capacitors are optimally switched by solving the multi-objective optimization problem defined in Section 4.3.1 using the improved BSFS based PSO method. After control, the network performance is significantly improved with the objective function reduced to only 0.1611. Then the optimal settings of capacitors are passed down to the next hour. As shown in table 4.6 and figure 4.7, with the settings from last hour 00:00, the objective function values are all under the threshold ($FC_{max} = 0.28$) and significantly decreased between 01:00 and 16:00 comparing with the corresponding original values without capacitors. Although higher network loss and worse balance profile are found at a few points (e.g. hours 05:00-08:00, in red words) due to overcompensation as a result of lighter loads (figure 4.6), the overall network performance is still acceptable with $FC < 0.28$ and no capacitor switching is required. Then for the peak-load period from 17:00 to 22:00, the last-hour settings of capacitors become insufficient to support the desired network performance with the objective functions above the given threshold (table 4.6) and so multi-objective optimization is conducted for the corresponding optimal capacitor settings at all these hours. With the optimal capacitor injection, the network performance is significantly improved with smaller objective functions comparing against the values without capacitors and with last-hour capacitors. After that, with the optimal capacitor

settings of hour 22:00, satisfactory network performance is obtained at both hours 23:00 and 24:00 with no capacitor adjustments. Additionally, it is found that the objective function of the optimal capacitor settings is only slightly better than that of the last-hour settings. Even so, optimal capacitor control is still necessary and well-timed as it usually happens over the heavy-load period when slight improvement represents more benefits than during the off-peak hours.

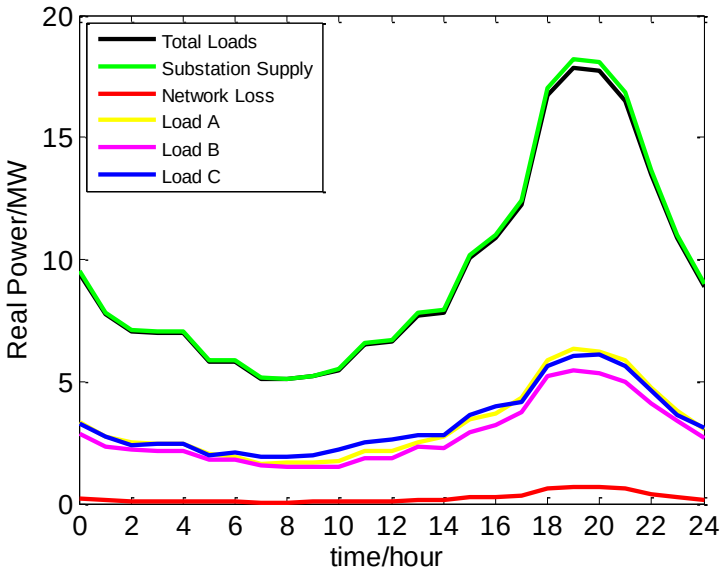

Figure 4.5 Network real power profile.

In this study, the weighted sum method is used to reflect the preferences on the control objectives and achieve the desired network performance. As shown in tables 4.3 and 4.6, network loss reduction J_1 is given the highest priority with $w_1 = 0.5$. Consequently, a reduced J_1 can always be observed after the optimal capacitor control comparing with the corresponding values without capacitors and with last-hour capacitors. In contrast, as the objective are mutually conflicting, therefore, as shown in table 4.6, objectives with lower priority, such as voltage magnitude profile $w_2 = 0.3$ and voltage unbalance profile $w_3 = 0.2$, may be sacrificed at some periods (e.g. 17:00-22:00, in red words) to ensure the reduction of network loss and the improvement of overall network performance.

Frequent switching of capacitors will shorten the lifetime and increase the operating

cost. Therefore, the total number of switching allowed each day should be limited. In this study, with the objective function threshold of 0.28, capacitor at bus 57 is switched 6 times while capacitor at bus 39 only 2 times. By increasing or decreasing the threshold, we can decrease or increase the switching number flexibly for various control purposes.

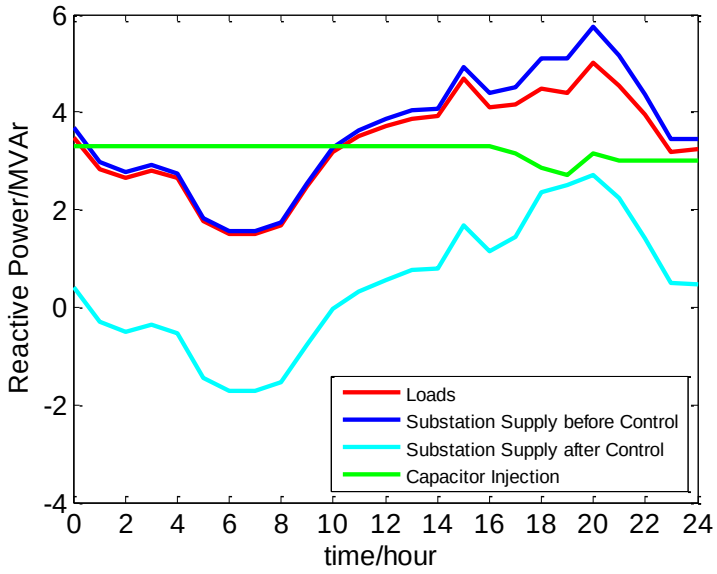

Figure 4.6 Reactive profiles for substation and load before and after capacitor control.

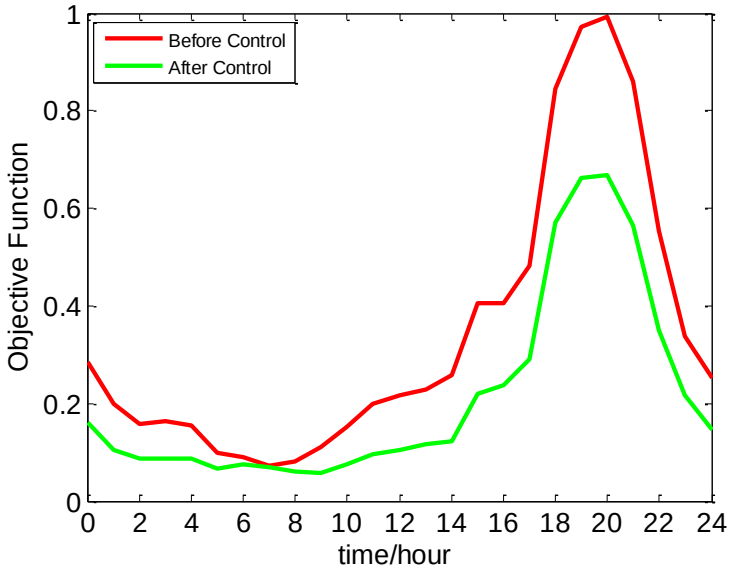

Figure 4.7 Objective functions before and after control.

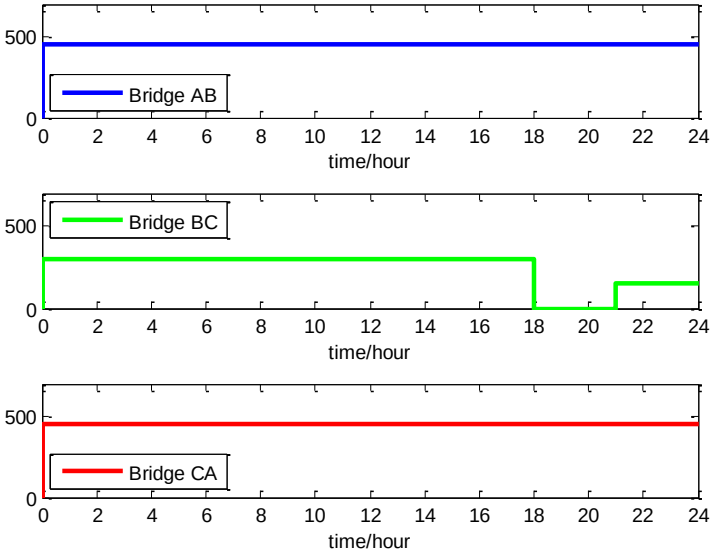

Figure 4.8 Capacitor switching (in kVAr) at bus 39 for AB, BC and CA bridges.

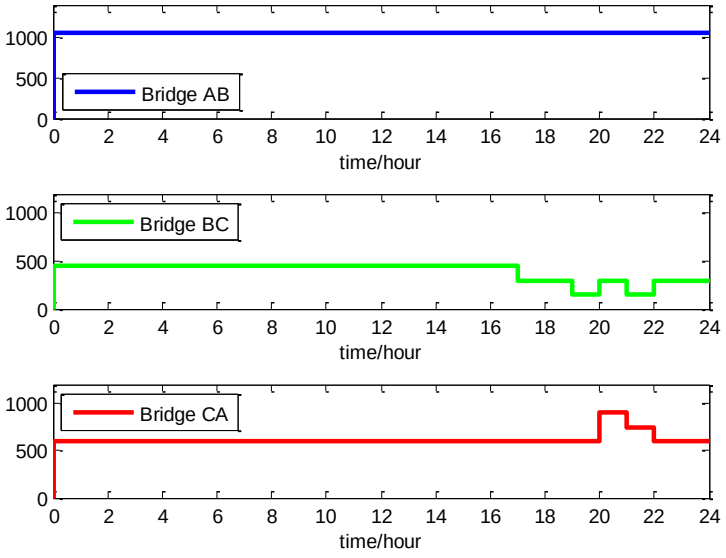

Figure 4.9 Capacitor switching (in kVAr) at bus 57 for AB, BC and CA bridges.

Table 4.6 Network performance after the proposed capacitor control over 24 hours. The highlighted yellow cells indicate an undesired network performance with $FC > 0.28$ while the green cells represent decrease of the value compared with the pervious case.

Time	Without Capacitor (ORIGINAL)				With Last-hour Capacitor				With Optimal Capacitor			
	FC	$J_1/0.5$	$J_2/0.3$	$J_3/0.2$	FC	$J_1/0.5$	$J_2/0.3$	$J_3/0.2$	FC	$J_1/0.5$	$J_2/0.3$	$J_3/0.2$
00:00	0.2852	2.004E5	9.001E6	4.190E-4	0.2852	2.004E5	9.001E6	4.190E-4	0.1611	1.796E5	2.805E6	1.210E-5
01:00	0.1991	1.340E5	5.914E6	3.733E-4	0.1045	1.249E5	1.269E6	7.497E-6	------	------	------	------
02:00	0.1586	1.114E5	4.922E6	2.423E-4	0.0871	1.060E5	7.350E5	2.651E-5	------	------	------	------
03:00	0.1641	1.118E5	5.177E6	2.661E-4	0.0858	1.043E5	9.089E5	8.471E-6	------	------	------	------
04:00	0.1552	1.101E5	4.875E6	2.228E-4	0.0859	1.053E5	7.751E5	1.587E-5	------	------	------	------
05:00	0.0999	7.211E4	2.832E6	1.675E-4	0.0664	8.280E4	2.071E5	4.397E-5	------	------	------	------
06:00	0.0897	7.066E4	2.634E6	9.921E-5	0.0740	8.651E4	3.928E5	7.266E-5	------	------	------	------
07:00	0.0718	5.583E4	2.258E6	6.801E-5	0.0681	7.205E4	3.758E5	1.181E-4	------	------	------	------
08:00	0.0812	5.651E4	2.422E6	1.379E-4	0.0592	6.906E4	3.843E5	5.186E-5	------	------	------	------
09:00	0.1098	6.528E4	3.347E6	2.578E-4	0.0565	6.433E4	4.496E5	5.136E-5	------	------	------	------
10:00	0.1510	8.059E4	4.854E6	3.920E-4	0.0760	6.769E4	1.237E6	1.345E-4	------	------	------	------
11:00	0.1988	1.101E5	6.162E6	5.119E-4	0.0963	9.087E4	1.566E6	1.350E-4	------	------	------	------
12:00	0.2178	1.163E5	6.819E6	5.846E-4	0.1059	9.306E4	2.032E6	1.641E-4	------	------	------	------
13:00	0.2295	1.478E5	7.765E6	3.770E-4	0.1177	1.220E5	2.136E6	6.456E-5	------	------	------	------
14:00	0.2590	1.526E5	8.247E6	5.799E-4	0.1228	1.249E5	2.448E6	6.005E-5	------	------	------	------
15:00	0.4046	2.468E5	1.274E7	8.614E-4	0.2185	2.042E5	5.082E6	1.581E-4	------	------	------	------
16:00	0.4055	2.703E5	1.233E7	7.486E-4	0.2361	2.374E5	4.856E6	1.205E-4	------	------	------	------
17:00	0.4832	3.344E5	1.435E7	8.418E-4	0.2919	2.983E5	5.830E6	1.327E-4	0.2903	2.983E5	6.088E6	8.952E-5
18:00	0.8449	6.067E5	2.296E7	1.544E-3	0.5735	5.616E5	1.195E7	3.934E-4	0.5705	5.598E5	1.265E7	2.771E-4
19:00	0.9718	6.889E5	2.532E7	1.955E-3	0.6643	6.437E5	1.452E7	4.246E-4	0.6636	6.426E5	1.493E7	3.671E-4
20:00	**0.9934**	**6.944E5**	**2.755E7**	**1.890E-3**	**0.6713**	**6.405E5**	**1.697E7**	**2.471E-4**	**0.6681**	**6.365E5**	**1.517E7**	4.357E-4
21:00	0.8588	5.958E5	2.341E7	1.708E-3	0.5667	5.481E5	1.198E7	4.085E-4	0.5649	5.478E5	1.260E7	3.231E-4
22:00	0.5529	3.952E5	1.576E7	9.443E-4	0.3541	3.623E5	7.268E6	1.375E-4	0.3501	3.619E5	7.418E6	8.563E-5
23:00	0.3374	2.539E5	9.876E6	4.595E-4	0.2174	2.362E5	3.552E6	8.407E-5	------	------	------	------
24:00	0.2519	1.765E5	7.703E6	3.999E-4	0.1449	1.587E5	2.478E6	3.480E-5	------	------	------	------

Table 4.7 Performance comparison of the proposed multi-objective control and existing single-objective control. The red/green fonts indicate increase/decrease after single-objective control comparing with the corresponding value after multi-objective control.

Time	Multi-objective				Single-objective					
	FC	$J_1/0.5$	$J_2/0.3$	$J_3/0.2$	FC_1	J_1	FC_2	J_2	FC_3	J_3
00:00	0.1611	1.796E5	2.805E6	1.210E-5	0.1901	1.761E5	0.1870	1.532E6	0.1765	5.462E-6
17:00	0.2903	2.983E5	6.088E6	8.952E-5	0.3190	2.975E5	0.3368	4.044E6	0.3032	1.063E-5
18:00	0.5705	5.598E5	1.265E7	2.771E-4	0.5777	5.589E5	0.6481	9.107E6	0.5838	7.251E-5
19:00	0.6636	6.426E5	1.493E7	3.671E-4	0.6804	6.402E5	0.7619	1.069E7	0.6740	1.712E-4
20:00	0.6681	6.365E5	1.517E7	4.357E-4	0.6790	6.336E5	0.7547	1.214E7	0.6856	1.473E-4
21:00	0.5649	5.478E5	1.260E7	3.231E-4	0.5758	5.463E5	0.6504	9.510E6	0.5763	1.067E-4
22:00	0.3501	3.619E5	7.418E6	8.563E-5	0.3809	3.606E5	0.4002	4.841E6	0.3732	1.434E-5

To show the advantages of the proposed multi-objective optimization strategy over the existing single-objective control strategies, three separate optimizations with a single objective are conducted to reduce the network loss J_1 [176, 177], mitigate the voltage magnitude deviation J_2 [178] and improve the balance profile J_3. To compare on the same basis, single-objective optimization is only performed at the hours when the multi-objective optimization took place. As shown in table 4.7, although the single-objective optimization can generate better values compared with the multi-objective strategy for the above-mentioned three single objectives, it also causes a worse overall network performance with a bigger objective function. This is because capacitor control involves multiple conflicting objectives and overemphasis on one single objective will aggravate the other objectives. For instance, as demonstrated in table 4.7, focus on only the voltage magnitude deviation J_2 requires more significant reactive power injection, i.e. local overcompensation. As a result, a worse objective function FC_2 marked by higher network loss and more serious network unbalance results.

Moreover, while the proposed approach of this paper is capable of balancing multiple objectives according to a specified control preference, it can also fulfill all the functions of single-objective optimization by simply allocating weights of 1 and 0 to the desired objective and remaining objectives, respectively.

C. Computation Efficiency Analysis

The proposed optimization solver based on the improved BSFS and PSO is

computationally efficient. Specifically, although the particle size is set as large as 10 000 to ensure the global optimality of solution, the average computing time of the capacitor control problem at each time point is only 135 seconds on a machine with Intel Core i5 processor at 3.2 GHz, which makes it possible for the efficient application of the proposed placement and control strategies of delta-connected switched capacitors in large-scale unbalanced distribution networks with a 1-15 minute iteration time.

D. Robustness Analysis

To show the robustness of the proposed improved BSFS based PSO method, three typical load levels (peak, medium and light, as given in table 4.2) have been included for the capacitor placement problem while 24 hours real system data has been used for the capacitor control problem. According to the results of tables 4.4-4.7, the proposed method is very robust with stable convergence for all the simulated cases.

Table 4.8 Statistical data of the annual net saving FP for the sequential placement.

	Worst	**Best**	**Mean**	**Deviation/%**
C1	-17536	-17536	-17536	0.000
C2	-17886	-17886	-17886	0.000
C3	-17886	-17886	-17886	0.000

Table 4.9 Statistical data of the objective function FC for the multi-objective control.

Time	**Worst**	**Best**	**Mean**	**Deviation/‰**
00:00	0.16110	0.16110	0.16110	0.000
17:00	0.29051	0.29026	0.29036	0.874
18:00	0.57081	0.57054	0.57067	0.472
19:00	0.66428	0.66364	0.66395	0.960
20:00	0.66890	0.66807	0.66847	1.249
21:00	0.56524	0.56493	0.56521	0.538
22:00	0.35010	0.35006	0.35002	0.138

Besides, to further verify the robustness of the proposed method, 30 independent runs were performed for the sequential capacitor placement and the 7 time points (i.e. 00:00, 17:00-22:00, as shown in table 4.6) of the multi-objective capacitor control to

measure the possibility of reaching the optimal or near optimal solution with all the related parameters in table 4.3 maintained. For the quantification of the robustness, the worst, best and mean values are given and a deviation is also calculated with a definition of $(worst - best)/best$. As described in table 4.8, for the sequential capacitor placement, the method shows a strong robustness with a stable annual net saving FP and an ideal deviation of 0% after the placement of each capacitor within 30 runs. Additionally, for the multi-objective capacitor control, in all 30 runs for each time point (table 4.9), the maximum deviation between the worst and the best values of the objective function is only 1.249‰, which marks an acceptable robustness of the proposed method.

4.6 CONCLUSION AND CONSIDERATIONS ON APPLICATION

To form the MV controller for the proposed hierarchical control, both the placement and control problems of delta-connected switched capacitors are studied in this chapter. Specifically, based on the unbalanced model of radial MV distribution networks, a comprehensive optimization based sequential strategy is firstly proposed for the capacitor placement with the maximization of annual net saving which both involves the savings from energy loss reduction and network capacity release and the costs of capacitor purchase, installation, operation and maintenance. To improve the computation efficiency, high benefit buses are selected based on the network loss sensitivity analysis for a sequential capacitor placement. On this basis, a multi-objective optimization based real-time control strategy for delta-connected switched capacitors is also proposed to simultaneously minimize network loss, voltage magnitude and VUF deviations. Additionally, to reflect our preferences on the mutually conflicting control objectives, the weighted sum method is utilized. For the MINLP problems of both capacitor placement and control, the improved BSFS based PSO is used for both the optimal and fast solution which allows the real-time applications. Finally, all the work above is tested by comparing against some existing popular schemes through detailed simulations over 24 hours on a real unbalanced radial Australian MV distribution network. The results indicate the proposed models

and strategies are feasible, effective and robust for the placement and control of delta-connected switched capacitors in unbalanced radial MV distribution networks.

When applying the work presented in this study to real applications, attention should be paid to the following aspects:

1) As the delta-connected and ungrounded star-connected configurations can be converted from one form to the other, the proposed placement and control models and strategies of delta-connected capacitors in this study can also be used for the star-connected (both grounded and ungrounded) switched capacitors with the detailed explanations and derivations presented in Appendix A;
2) Although the constant PQ model is used for all the loads and no voltage regulators are included in the network, the proposed problem model and solution algorithm are generalized and able to accommodate different load models and network components.

Chapter 5. Proposed Three-Step Hierarchical Control Strategy and Coordination Interface

5.1 INTRODUCTION

Based on the proposed LV controller in Chapter 3 and the MV controller in Chapter 4 as well as a careful study on the physical structure of distribution systems, a complete three-step hierarchical control strategy is proposed in this chapter to efficiently optimize the operation of the whole network by coordinating the control of both conventional and emerging devices (PVs in LV and delta switched capacitors in MV in this thesis). Besides, coordination interface plays an critical role in the hierarchical control as it is responsible for connecting and coordinating controllers on different levels [21, 32]. How the interface is formulated will directly impact the performance of the proposed hierarchical control in terms of both accuracy and efficiency. In this chapter, by carefully analysing the voltages, currents and power relationships between the MV and LV sides of a most common delta-grounded wye (Dyn11) distriution trasformer, an effective coordination interface is also built up to support the proposed three-step hierarchical control strategy. The work of this chapter has been included in our recently submitted paper [184] .

Specifically, this chapter will be organized as follows. Firstly, introduction of the chapter is presented in Section 5.1. Then, based on the LV and MV controllers in Chapters 3 and 4 and by examining the physical structure of distribution networks, a complete three-step hierarchical control strategy is proposed in Section 5.2. After that, based on detailed analyses on the voltages, currents and power of a most common delta-grounded wye distribution transformer, Section 5.3 proposes a effective interface to connect and coordinate the control actions on the MV and LV

levels and support the proposed three-step hierarchical control. Finally, Section 5.4 presents a brief remark on this chapter.

5.2 PROPOSED THREE-STEP HIERARCHICAL CONTROL STRATEGY

As analysed in Chapter 1, distribution networks typically starts with the distribution substation which serves one or more MV feeders. To supply the residential loads connected to the LV feeders, distribution transformers are utilized between the MV and the LV feeders to regulate the voltages [183, 185]. Thus, distribution networks have a natural two-level (i.e. MV and LV) decomposition isolated by the distribution transformer. Besides, with the increasing penetrations of renewable generations, the loading capability (both real and reactive) of distribution transformers can be actively regulated by the control of renewable units. This also provides us a chance to perform a hierarchical control on the whole distribution network. In this study, based on the two-level hierarchy of distribution networks, a complete three-step hierarchical control strategy is proposed to improve both the operational and computational performances by coordinating the LV and MV controllers.

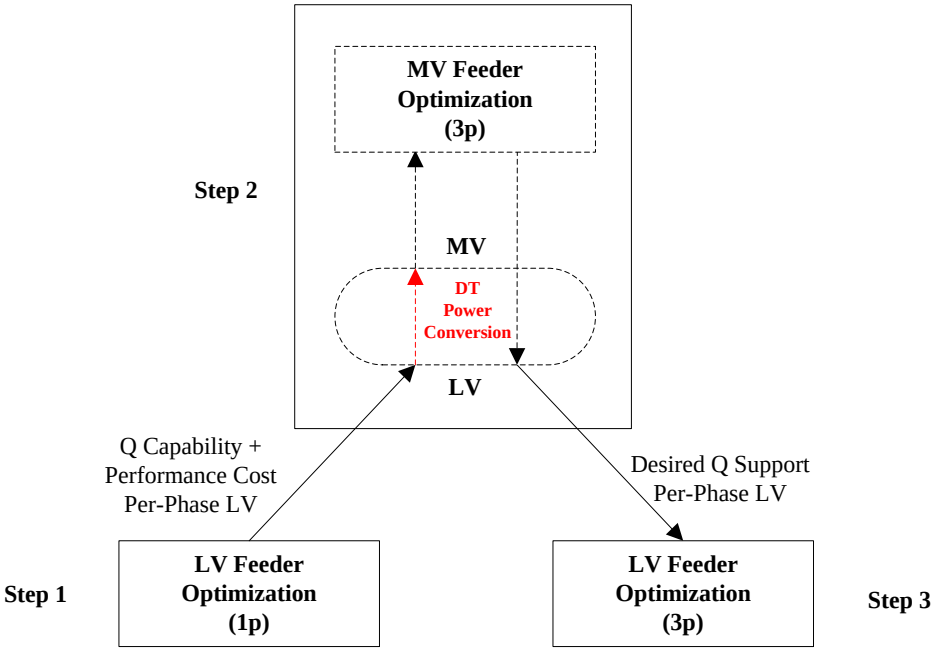

Figure 5.1 Proposed three-step hierarchical control strategy.

As shown in figure 5.1, the proposed hierarchical control strategy consists of three main steps as follows:

Step 1: *Single-phase optimization for the per-phase reactive capability and performance cost of LV feeders;*

As discussed in Section 1.4, to perform the proposed hierarchical control, we must first know the per-phase reactive capability and its corresponding performance cost of unbalanced LV feeders. Therefore, similarly as the study of Chapter 3, LV optimization is conducted on each phase to determine its reactive capability and performance cost by controlling the outputs of PV inverters.

Step 2: *Three-phase optimization to improve MV network operational performance with the desired per-phase reactive support of LV feeders generated;*

With the per-phase reactive capability and performance cost known, LV feeders can be treated as aggregated nodes in the MV network. Similar as the work of Chapter 4, a more comprehensive operation optimization of the three-phase MV network is conducted by controlling both the aggregated LV feeders and the existing MV delta switched capacitors.

To reduce the complexity of the problem as well as to improve the control accuracy, the reactive injections of LV feeders which are connected at the LV side of distribution transformer are selected as the control variables in the MV optimization. By doing so, the desired reactive support by LV feeders is directly generated after the MV optimization. However, as shown in figure 5.1 (red colour), to perform the MV network load flow by the improved BSFS method in the MV optimization, the reactive and real injections of LV feeders must be transformed from the LV side to the MV side of distribution transformer. This is the most critical of the proposed hierarchical control strategy, namely coordination interface, which will be carefully studied in the following Section 5.3.

Step 3: *Three-phase optimization to enhance LV network operational performance and meet the reactive request by MV optimization;*

With the desired per-phase reactive support of LV feeders decided by the MV optimization in step 2 as the equality constraints, as well as based on the LV optimization of Chapter 3, a more comprehensive optimization is also conducted on the three-phase LV feeder by controlling PV inverters to improve the operational performance and meet the reactive requests from the MV control.

5.3 PROPOSED HIERARCHICAL COORDINATION INTERFACE

In distribution networks, LV feeders are supplied by distribution transformers, which means the MV network and the LV feeders are not directly connected. Consequently, as analysed in Section 5.2, a real challenge of the proposed hierarchical control is how to pass the reactive and real injections of LV feeders from the LV side to the MV side of distribution transformers. In this section, we will firstly study on the voltages and currents relationships between the MV and LV sides of the most common delta-grounded wye distribution transformer. On this basis, a novel hierarchical coordination interface is proposed based on the detailed derivations of power relationships of the distribution transformer.

5.3.1 Voltages and Currents Analyses of Delta-Grounded Wye Distribution Transformer

Delta-grounded wye distribution transformer (Dyn11 in this discussion) is the most widely used in industrial, commercial and residential distribution networks because of the following advantages over other connections [183, 185, 186]:

1) The delta winding allows zero sequence fundamental or triple harmonic currents to circulate within the transformer and thus prevents it from flowing into power lines;
2) It allows both three- and single-phase load connections with the neutral wire.

However, a noticeable point of delta-wye (either grounded or ungrounded) transformers is that a 30 degree phase shift exists between the MV and LV voltages [183, 185, 186]. Specifically, positive-sequence voltage on the MV side leads the LV voltage by 30 degree while negative-sequence voltage on the MV side lags the LV

voltage by 30 degree. Therefore, careful attention must be paid to include this phase shift when modelling the delta-wye distribution transformer. Additionally, polarity of the distribution transformer windings also must be observed to identify the phasor relationships for both voltages and currents.

A. Voltages of Delta-Grounded Wye Distribution Transformer

The magnitude changes between the voltages can be defined in terms of the actual winding turns ratio (n_t). With reference to figure 5.2, this ratio is defined as follows:

$$n_t = \frac{VLL_{ratedMV}}{VLN_{ratedLV}} \tag{5.1}$$

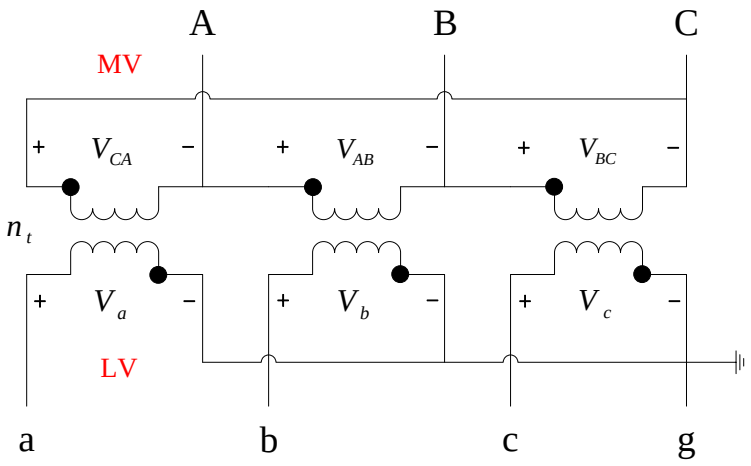

Figure 5.2 Standard delta-grounded wye connection with voltages.

In this research, the Forrestfield distribution network simulated is featured by $VLL_{ratedMV}$=22kV and $VLN_{ratedLV}$=240V, respectively.

1) Voltages Transformation from LV to MV

As shown in figure 5.2, the line to line voltages on the MV side as a function of the line to neutral/ground voltages on the LV side are given by:

$$\begin{bmatrix} V_{AB} \\ V_{BC} \\ V_{CA} \end{bmatrix} = n_t \begin{bmatrix} 0 & -1 & 0 \\ 0 & 0 & -1 \\ -1 & 0 & 0 \end{bmatrix} \begin{bmatrix} V_a \\ V_b \\ V_c \end{bmatrix} \tag{5.2}$$

However, in this study, we need the relationship of the line-to-neutral voltages on the MV and LV sides to support the final power relationship analysis. Therefore, 'euqivalent' MV line-to-neutral voltages are defined and determined from the existing MV line-to-line voltages by symmetrical components.

Specifically, the line to line voltages are firstly transformed to their sequence voltages by:

$$\begin{bmatrix} VLL_0 \\ VLL_1 \\ VLL_2 \end{bmatrix} = \frac{1}{3}\begin{bmatrix} 1 & 1 & 1 \\ 1 & \alpha & \alpha^2 \\ 1 & \alpha^2 & \alpha \end{bmatrix}\begin{bmatrix} V_{AB} \\ V_{BC} \\ V_{CA} \end{bmatrix} \tag{5.3}$$

where $\alpha = 1\angle 120^\circ$. By definition, the zero sequence line-to-line voltage is always zero due to the delta connection. Besides, the relationship between the positive and negative sequence line-to-neutral and line-to-line voltages is known [183], given by:

$$\begin{bmatrix} VLN_0 \\ VLN_1 \\ VLN_2 \end{bmatrix} = \begin{bmatrix} 1 & 0 & 0 \\ 0 & t_s^* & 0 \\ 0 & 0 & t_s \end{bmatrix}\begin{bmatrix} VLL_0 \\ VLL_1 \\ VLL_2 \end{bmatrix} \tag{5.4}$$

where $t_s = \frac{1}{3}\angle 30^\circ$ and it exactly models the 30 degree phase shift of voltages. Since the zero sequence line-to-line voltage is always zero, the (1,1) element of the coefficient matrix in equation (5.4) can be any value. For simplification, it is chosen to have a value of 1 in this research.

Knowing the sequence line-to-neutral voltages, the equivalent MV line to neutral voltages can be determined as follows:

$$\begin{bmatrix} V_A \\ V_B \\ V_C \end{bmatrix} = \begin{bmatrix} 1 & 1 & 1 \\ 1 & \alpha^2 & \alpha \\ 1 & \alpha & \alpha^2 \end{bmatrix}\begin{bmatrix} VLN_0 \\ VLN_1 \\ VLN_2 \end{bmatrix} \tag{5.5}$$

By substitution and rearrangement of the equations (5.2-5.5) above, equivalent MV line-to-neutral voltages as a function of the LV line-to-neutral voltages are derived by:

$$\begin{bmatrix} V_A \\ V_B \\ V_C \end{bmatrix} = \frac{-n_t}{3} \begin{bmatrix} 0 & 2 & 1 \\ 1 & 0 & 2 \\ 2 & 1 & 0 \end{bmatrix} \begin{bmatrix} V_a \\ V_b \\ V_c \end{bmatrix} \tag{5.6}$$

2) Voltages Transformation from MV to LV

When transforming the equivalent MV line-to-neutral voltages to the LV side, we cannot simply do it by the inversion of equation (5.6) due to the singularity of the coefficient matrix. Therefore, a reverse derivation is required to transform the equivalent MV line-to-neutral voltages to the LV line-to-neutral voltages.

Specifically, according to equation (5.2), the relationship between the LV line-to-neutral voltages and the MV line-to-line voltages is given by:

$$\begin{bmatrix} V_a \\ V_b \\ V_c \end{bmatrix} = \left(n_t \begin{bmatrix} 0 & -1 & 0 \\ 0 & 0 & -1 \\ -1 & 0 & 0 \end{bmatrix} \right)^{-1} \begin{bmatrix} V_{AB} \\ V_{BC} \\ V_{CA} \end{bmatrix} \tag{5.7}$$

The MV line-to-line voltages can be represented as a function of the equivalent MV line-to-neutral voltages by:

$$\begin{bmatrix} V_{AB} \\ V_{BC} \\ V_{CA} \end{bmatrix} = \begin{bmatrix} 1 & -1 & 0 \\ 0 & 1 & -1 \\ -1 & 0 & 1 \end{bmatrix} \begin{bmatrix} V_A \\ V_B \\ V_C \end{bmatrix} \tag{5.8}$$

By substitution and rearrangement of the equations (5.7-5.8), we can get the LV line-to-neutral voltages from the equivalent MV line to neutral voltages by:

$$\begin{bmatrix} V_a \\ V_b \\ V_c \end{bmatrix} = \frac{1}{n_t} \begin{bmatrix} 1 & 0 & -1 \\ -1 & 1 & 0 \\ 0 & -1 & 1 \end{bmatrix} \begin{bmatrix} V_A \\ V_B \\ V_C \end{bmatrix} \tag{5.9}$$

B. Currents of Delta-Grounded Wye Distribution Transformer

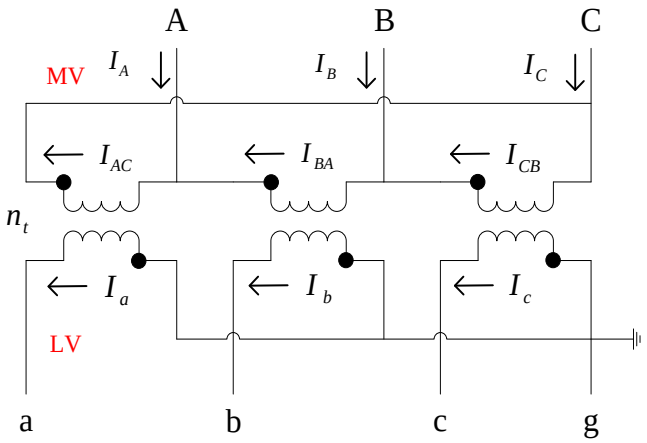

Figure 5.3 Standard delta-grounded wye connection with currents.

1) Currents Transformation from LV to MV

As illustrated in figure 5.3, according to Kirchhoff's current law (KCL), at the MV side, the line currents can be determined as a function of the Delta currents by:

$$\begin{bmatrix} I_A \\ I_B \\ I_C \end{bmatrix} = \begin{bmatrix} 1 & -1 & 0 \\ 0 & 1 & -1 \\ -1 & 0 & 1 \end{bmatrix} \begin{bmatrix} I_{AC} \\ I_{BA} \\ I_{CB} \end{bmatrix} \tag{5.10}$$

The matrix equation relating the MV delta currents to the LV line currents is given by:

$$\begin{bmatrix} I_{AC} \\ I_{BA} \\ I_{CB} \end{bmatrix} = \frac{1}{n_t} \begin{bmatrix} 1 & 0 & 0 \\ 0 & 1 & 0 \\ 0 & 0 & 1 \end{bmatrix} \begin{bmatrix} I_a \\ I_b \\ I_c \end{bmatrix} \tag{5.11}$$

After substitution and rearrangement of the equations (5.10-5.11), the relationship between the MV line currents and LV line currents can be obtained as:

$$\begin{bmatrix} I_A \\ I_B \\ I_C \end{bmatrix} = \frac{1}{n_t} \begin{bmatrix} 1 & -1 & 0 \\ 0 & 1 & -1 \\ -1 & 0 & 1 \end{bmatrix} \begin{bmatrix} I_a \\ I_b \\ I_c \end{bmatrix} \tag{5.12}$$

2) Currents Transformation from MV to LV

Similarly, the coefficient matrix in equation (5.12) is aslo sigular and invertible and the LV line currents cannot be got from the MV line currents simply by equation inversion. According to equation (5.11), LV line currents can be obtained from the MV delta currents by:

$$\begin{bmatrix} I_a \\ I_b \\ I_c \end{bmatrix} = n_t \begin{bmatrix} 1 & 0 & 0 \\ 0 & 1 & 0 \\ 0 & 0 & 1 \end{bmatrix} \begin{bmatrix} I_{AC} \\ I_{BA} \\ I_{CB} \end{bmatrix} \tag{5.13}$$

Then according to equation (5.10) and figure 5.3, MV delta currents can be represented by the related MV line currents by:

$$\begin{bmatrix} I_{AC} \\ I_{BA} \\ I_{CB} \end{bmatrix} = \begin{bmatrix} 1 & 0 & -1 \\ -1 & 1 & 0 \\ 0 & -1 & 1 \end{bmatrix} \begin{bmatrix} I_A \\ I_B \\ I_C \end{bmatrix} \tag{5.14}$$

Finally, by substituting and rearranging the equations (5.13-5.14), LV line currents can be formulated as a function of the MV line currents by:

$$\begin{bmatrix} I_a \\ I_b \\ I_c \end{bmatrix} = n_t \begin{bmatrix} 1 & 0 & -1 \\ -1 & 1 & 0 \\ 0 & -1 & 1 \end{bmatrix} \begin{bmatrix} I_A \\ I_B \\ I_C \end{bmatrix} \tag{5.15}$$

5.3.2 Power Coordination Interface of the Proposed Hierarchical Control

A. LV Voltages, Currents and Power

In this study, considering the real power control devices are currently non-existent on the MV level, only reactive power is managed in the proposed hierarchical control while the real power is constant with the assumption of neglegible network loss variation. Therefore, on the LV side, reactive power control can be equivalently considered as apparent power control according to equation (5.16):

$$\begin{aligned} S_a &= P_a + jQ_a \\ S_b &= P_b + jQ_b \end{aligned} \tag{5.16}$$

$$S_c = P_c + jQ_c$$

Where P_i is the real power injection of each phase of LV feeders and can be obtained from the LV load flow calculation.

Besides, the three-phase voltages at the LV side of distribution transformer are known and easily accessible from the SCADA system. In practice, they can be any real values while in this study the balanced rated values of 240V are used for the rated case simulation.

$$V_a = 240\angle 0^\circ = 240$$
$$V_b = 240\angle -120^\circ = -120 - j207.85 \quad (5.17)$$
$$V_c = 240\angle 120^\circ = -120 + j207.85$$

Therefore, current injection of each phase of LV feeders can be represented as a function of the real and reactive injections by the following equation (5.18):

$$I_a = \left(\frac{S_a}{V_a}\right)^* = \left(\frac{P_a + jQ_a}{240}\right)^* = \frac{P_a}{240} - j\frac{Q_a}{240}$$
$$I_b = \left(\frac{S_b}{V_b}\right)^* = \left(\frac{P_b + jQ_b}{-120 - j207.85}\right)^* = \frac{-120P_b - 207.85Q_b}{57602} + j\frac{-207.85P_b + 120Q_b}{57602} \quad (5.18)$$
$$I_c = \left(\frac{S_c}{V_c}\right)^* = \left(\frac{P_c + jQ_c}{-120 + j207.85}\right)^* = \frac{-120P_c + 207.85Q_c}{57602} + j\frac{207.85P_c + 120Q_c}{57602}$$

B. Proposed Voltages and Currents Transformation from LV to MV

According to equation (5.6) above, the equivalent MV line-to-neutral voltages can be determined from the LV line-to-netural voltages as follows:

$$\begin{bmatrix} V_A \\ V_B \\ V_C \end{bmatrix} = \frac{-n_t}{3}\begin{bmatrix} 0 & 2 & 1 \\ 1 & 0 & 2 \\ 2 & 1 & 0 \end{bmatrix}\begin{bmatrix} V_a \\ V_b \\ V_c \end{bmatrix} \quad (5.19)$$

In the simualted network of this study (Section 6.3.1), $n_t = \frac{22000V}{240V} = 91.6667$, therefore the equivalent MV line-to-neutral voltages are calculated as:

$$V_A = \frac{-n_t}{3}(2V_b + V_c) = 11000 + j6351 = 12702\angle 30.0001^\circ \approx 12700\angle 30^\circ\, V$$

$$= 1.0999e4 + j6.35e3\ V \tag{5.20}$$

$$V_B = \frac{-n_t}{3}(2V_c + V_a) = -j12702 = 12702\angle -90^\circ \approx 12700\angle -90^\circ\ V$$

$$= -j1.27e4\ V \tag{5.21}$$

$$V_C = \frac{-n_t}{3}(2V_a + V_b) = -11000 + j6351 = 12702\angle 150.0004^\circ \approx 12700\angle 150^\circ\ V$$

$$= -1.0999e4 + j6.35e3\ V \tag{5.22}$$

Similarly, according to equation (5.12), the MV line currents can be represented by the LV line currents as:

$$\begin{bmatrix} I_A \\ I_B \\ I_C \end{bmatrix} = \frac{1}{n_t}\begin{bmatrix} 1 & -1 & 0 \\ 0 & 1 & -1 \\ -1 & 0 & 1 \end{bmatrix}\begin{bmatrix} I_a \\ I_b \\ I_c \end{bmatrix} \tag{5.23}$$

Based on the LV line current injections in equation (5.18), the corresponding MV line currents can be calculated as a function of the LV real and reactive injections as follows:

$$I_A = \frac{1}{n_t}(I_a - I_b) = (4.5455e-5P_a + 2.2726e-5P_b + 3.9364e-5Q_b)$$

$$+j(3.9364e-5P_b - 2.2726e-5Q_b - 4.5455e-5Q_a) \tag{5.24}$$

$$I_B = \frac{1}{n_t}(I_b - I_c) = [2.2726e-5(P_c - P_b) - 3.9364e-5(Q_b + Q_c)]$$

$$+j[2.2726e-5(Q_b - Q_c) - 3.9364e-5(P_b + P_c)] \tag{5.25}$$

$$I_C = \frac{1}{n_t}(I_c - I_a) = (3.9364e-5Q_c - 2.2726e-5P_c - 4.5455e-5P_a)$$

$$+j(3.9364e-5P_c + 2.2726e-5Q_c + 4.5455e-5Q_a) \tag{5.26}$$

C. Proposed Power Transformation from LV to MV

With the equivalent MV line-to-neutral voltages and MV line currents obtained in equations (5.20-5.22) and (5.24-5.26), the corresponding MV apparent power can also be calculated for each phase.

Specifically, MV apparent power for phase A:

$$S_A = V_A {I_A}^*$$

$$= (1.0999e4 + j6.35e3)$$

$$\times \begin{bmatrix} (4.5455e-5P_a + 2.2726e-5P_b + 3.9364e-5Q_b) \\ -j(3.9364e-5P_b - 2.2726e-5Q_b - 4.5455e-5Q_a) \end{bmatrix} \quad (5.27)$$

By separateing the real elements of apparent power, MV real power for phase A is obtained:

$$P_A = 1.0999e4 \times (4.5455e-5P_a + 2.2726e-5P_b + 3.9364e-5Q_b)$$

$$+6.35e3 \times (3.9364e-5P_b - 2.2726e-5Q_b - 4.5455e-5Q_a)$$

$$= 0.5P_a + 0.5P_b + 0.2887Q_b - 0.2886Q_a$$

$$\approx 0.5(P_a + P_b) + 0.2886(Q_b - Q_a) \quad (5.28)$$

Likewise, MV reactive power for phase A can also be calculated by separating the imaginary elements:

$$Q_A = 6.35e3 \times (4.5455e-5P_a + 2.2726e-5P_b + 3.9364e-5Q_b)$$

$$-1.0999e4 \times (3.9364e-5P_b - 2.2726e-5Q_b - 4.5455e-5Q_a)$$

$$= 0.5(Q_a + Q_b) + 0.2886P_a - 0.2887P_b$$

$$\approx 0.5(Q_a + Q_b) + 0.2886(P_a - P_b) \quad (5.29)$$

Similarly, apparent power for phase B at the MV side equals:

$$S_B = V_B {I_B}^*$$

$$= -j1.27e4$$

$$\times \begin{Bmatrix} [2.2726e-5(P_c - P_b) - 3.9364e-5(Q_b + Q_c)] \\ -j[2.2726e-5(Q_b - Q_c) - 3.9364e-5(P_b + P_c)] \end{Bmatrix} \quad (5.30)$$

Real power for phase B on the MV side:

$$P_B = -1.27e4 \times [2.2726e-5(Q_b - Q_c) - 3.9364e-5(P_b + P_c)]$$

$$= 0.4999(P_b + P_c) + 0.2886(Q_c - Q_b)$$

$$\approx 0.5(P_b + P_c) + 0.2886(Q_c - Q_b) \tag{5.31}$$

Reactive power for phase B on the MV side:

$$Q_B = -1.27e4 \times [2.2726e-5(P_c - P_b) - 3.9364e-5(Q_b + Q_c)]$$
$$= 0.4999(Q_b + Q_c) + 0.2886(P_b - P_c)$$
$$\approx 0.5(Q_b + Q_c) + 0.2886(P_b - P_c) \tag{5.32}$$

Repeating the process above, apparent power for phase C at the MV side can be got:

$$S_C = V_C I_C{}^*$$
$$= (-1.0999e4 + j6.35e3)$$
$$\times \begin{bmatrix} (3.9364e-5Q_c - 2.2726e-5P_c - 4.5455e-5P_a) \\ -j(3.9364e-5P_c + 2.2726e-5Q_c + 4.5455e-5Q_a) \end{bmatrix} \tag{5.33}$$

Real power for phase C on the MV side:

$$P_C = -1.0999e4 \times (3.9364e-5Q_c - 2.2726e-5P_c - 4.5455e-5P_a)$$
$$+6.35e3 \times (3.9364e-5P_c + 2.2726e-5Q_c + 4.5455e-5Q_a)$$
$$= 0.5P_c + 0.5P_a + 0.2886Q_a - 0.2887Q_c$$
$$\approx 0.5(P_c + P_a) + 0.2886(Q_a - Q_c) \tag{5.34}$$

Reactive power for phase C on the MV side:

$$Q_C = 1.0999e4 \times (3.9364e-5P_c + 2.2726e-5Q_c + 4.5455e-5Q_a)$$
$$+6.35e3 \times (3.9364e-5Q_c - 2.2726e-5P_c - 4.5455e-5P_a)$$
$$= 0.5(Q_c + Q_a) + 0.2887P_c - 0.2886P_a$$
$$\approx 0.5(Q_c + Q_a) + 0.2886(P_c - P_a) \tag{5.35}$$

Equations (5.27-5.35) show that both the MV real and reactive power are a function of the related LV real and reactive power on each phase. In other words, real power is no longer constant after transformation from LV to MV due to the contribution of variable reactive power. To reduce the complexity of problem, MV real power is roughly treated constant in this study considering the following system situations:

1) In distribution networks, real power is always much bigger that reactive power;
2) In practical systems, unbalance is often limited within an acceptable range and the reactive power difference between any two phases is not significant.

Accordingly, MV real power equations (5.28, 5.31 and 5.34) can be reduced as:

$$\begin{aligned} P_A &= 0.5(P_a + P_b); \\ P_B &= 0.5(P_b + P_c); \\ P_C &= 0.5(P_c + P_a); \end{aligned} \tag{5.36}$$

Meanwhile, the original MV reactive power equations are kept for the accuracy of the control model.

$$\begin{aligned} Q_A &= 0.5(Q_a + Q_b) + 0.2886(P_a - P_b); \\ Q_B &= 0.5(Q_b + Q_c) + 0.2886(P_b - P_c); \\ Q_C &= 0.5(Q_c + Q_a) + 0.2886(P_c - P_a); \end{aligned} \tag{5.37}$$

Eeuqations (5.36-5.37) finally forms the coordination interface of the hierarchical control proposed in section 5.2 by transforming both reactive and real power from LV to MV to support the MV optimization of step 2.

5.4 CONCLUSION

This chapter is dedicated to present the complete hierarchical control strategy for distribution networks of high complexity. Specifically, based on the MV and LV level decomposition of distribution systems, a three-step hierarchical control strategy is proposed to coordinate the LV and MV controllers of Chapters 3 and 4. Then coordination interface, the most critical of the proposed hierarchical control, is studied based on the most common delta-grounded wye distribution transformer. Through detailed analyses on the voltages and currents relationships, power transformation relationship from LV to MV is finally formulated as the coordination interface to support the proposed three-step hierarchical control strategy.

Chapter 6. Proposed Three-Step Hierarchical Optimization Models and Simulations

6.1 INTRODUCTION

This chapter proposes and implements a complete three-step hierarchical optimization model for real-time optimal voltage, VAr and real power control of both MV and LV levels of distribution networks of high complexity by coordinating the control of MV delta switched capacitors and LV PV inverters. The approach is based on the findings and controllers of Chapters 3-5 and is also the main contribution of our submitted paper [184].

Specifically, in chapter 3, based on the latent reactive power capability and real power curtailment of PV inverters, a multi-objective optimization based LV controller is proposed to improve the operational performance of unbalanced four-wire LV distribution feeders. Then, in chapter 4, the optimal placement and control of delta-connected switched capacitors in unbalanced MV distribution networks is performed by a comprehensive optimization based sequential strategy and a multi-objective optimization based real-time strategy, which forms the MV controller. After that, a detailed derivation of the coordination interface in terms of voltages, currents and power is conducted on the most common delta-ground wye distribution transformer in chapter 5 and the complete three-step hierarchical control strategy is finally presented to coordinate the LV and MV controllers. On the basis of the studies of chapters 3, 4 and 5, this chapter will build up the detailed optimization models for each stage of the proposed three-step hierarchical control and then a series of simulations on a real Western Australian distribution network of complexity are conducted to verify the feasibility, effectiveness and efficiency of the proposed hierarchical optimization in this thesis.

In order to achieve the aforementioned objectives, this chapter is constructed in the following direction. Particularly, in Section 6.2, the LV and MV controllers presented in Chapters 3 and 4 will be slightly modified to provide the optimization models for each stage of the proposed three-step hierarchical control strategy of Chapter 5. Then, detailed simulations and analyses will be conducted in Section 6.3 to verify the superior performance of the hierarchical optimization developed in this thesis in terms of both optimality and efficiency. Finally, Section 6.4 concludes the whole content of the chapter.

6.2 HIERARCHICAL OPTIMIZATION MODELS

To apply the three-step hierarchical control strategy of unbalanced distribution networks proposed in Chapter 5, complete multi-objective optimization models for each step are constructed in this section based on the LV and MV controllers presented in Chapters 3 and 4. As an interface is introduced to coordinate the LV and MV controllers, the hierarchical optimization requires slight modifications on the existing LV and MV optimization models.

6.2.1 Single-Phase Optimization of LV Distribution Feeders for Step 1

According to Section 5.2, step 1 is employed to decide the reactive capability and the corresponding performance cost of each phase of unbalanced LV feeders. In this study, data fitting technique is used to decide the functional relationship between the performance cost and the reactive capability. Therefore, a number of optimizations need to be performed for each phase of LV feeders by controlling PV inverters to locate some typical points on the function curve. Besides, to maintain the consistency and accuracy of the proposed three-step hierarchical control, same optimization objectives of LV feeders should be defined for both steps 1 and 3 with the only difference that step 1 is on a single-phase basis while step 3 on three-phase. Both steps 1 and 3 obtain their optimization models from the LV controller presented in Chapter 3.

Specifically, step 1 performs optimization on a single-phase basis, thus the objective of voltage balance profile J_3 , defined in equation (3.3), should not be included. Besides, considering the current unavailability of real power control devices (e.g. solar and wind generators) in the MV distribution networks, this simulation now only focuses on the hierarchical voltage and reactive power optimization with the objective of PV real power curtailment J_5 in equation (3.5) also excluded. It should be noted that the proposed control strategy and optimization models are generalized and hierarchical real power optimization on the whole network scale can be easily integrated when necessary. In view of the above-mentioned differences, the optimization objectives of step 1 will consist of network losses J_1 in equation (3.1), voltage magnitude profile J_2 in equation (3.2) and PV generation cost J_4 in equation (3.4). All the variables of the optimization models below have the same definitions as described in Section 3.3.1 but on a single-phase basis.

A. Per-Phase LV Feeder Performance Cost

1) Network Losses:

$$J_1 = \sum_{i=1}^{n-1} \sum_{j=i+1}^{n} {I_{ij}}^2 R_{ij} \tag{6.1}$$

2) Voltage Magnitude Profile:

$$J_2 = \sum_{i=1}^{n} {\Delta V_{idb}}^2 \tag{6.2}$$

3) PV Generation Cost:

$$J_4 = \sum_{i \in \delta} \left(k_{i1} {S_{PVi}}^2 + k_{i2} S_{PVi} + k_{i3} \right) \tag{6.3}$$

Similarly, for this multi-objective optimization problem, the performance cost of each phase of LV distribution feeders can be defined by the weighted-sum method as:

$$F_{PC} = w_1 J_1/sf_1 + w_2 J_2/sf_2 + w_4 J_4/sf_4 \tag{6.4}$$

B. Per-Phase LV Feeder Reactive Capability

In this study, the per-phase reactive capability of LV feeders is defined as the reactive injection from the LV side of distribution transformer into the feeder and can be calculated as follows:

$$Q_{DTLV} = V_1 \sum_{j=1}^{n} \left(G_{1j} \sin \theta_{1j} - B_{1j} \cos \theta_{1j}\right) V_j \tag{6.5}$$

where V_1 and V_j are the voltage magnitudes of bus 1 and bus j while θ_{1j} is the voltage phase angle difference between them. In addition, G_{1j} and B_{1j} are the conductance and susceptance of the branch between buses 1 and j, respectively.

A noticeable point is that the LV feeder reactive injection is positive in most cases, which marks an inductive capability. On the other hand, it can also be a negative value representing a capacitive capability in some cases such as with significant capacitive reactive support by PV inverters.

C. Per-Phase LV Feeder Integrated Multi-Objective Optimization

To decide both the reactive capability and the corresponding performance cost of each phase of the LV feeders, an integrated multi-objective optimization model is defined below for step 1 by incorporating both the performance cost of equation (6.4) and the reactive capability of equation (6.5) using the weighted sum method.

$$F = \lambda_{PC} F_{PC} + \lambda_{DTLV} Q_{DTLV} / sf_{DTLV} \tag{6.6}$$

subject to:

$$P_{PVi} - P_{Li} - P_i = 0; \quad Q_{PVi} - Q_{Li} - Q_i = 0 \tag{6.7}$$

$$P_{PVi}{}^2 + Q_{PVi}{}^2 \leq S_i{}^2 \tag{6.8}$$

$$V_{ilb} \leq V_i \leq V_{iub} \tag{6.9}$$

where F is the integrated objective function involving both the performance cost F_{PC} and the reactive capability Q_{DTLV} on each phase while sf_{DTLV} is the scaling factor for Q_{DTLV}. According to the weighted-sum method, by adjusting the weights λ_{PC} and

λ_{DTLV}, we can change our preferences on the network performance and the reactive capability of LV feeders.

D. Reactive Capability and Performance Cost Function by Data-Fitting

The target of step 1 is to decide the reactive capability and its corresponding performance cost function of each phase of LV feeders. To achieve this goal, the popular data fitting technique is utilized in this study. Specifically, through adjusting the values of λ_{PC} and λ_{DTLV}, a number of optimizations based on the integrated single-phase model of equations (6.6-6.9) are firstly performed to obtain a set of typical points on the function curve. Then, by using the data fitting, the functional relationship between the performance cost and the reactive capability can be finally determined.

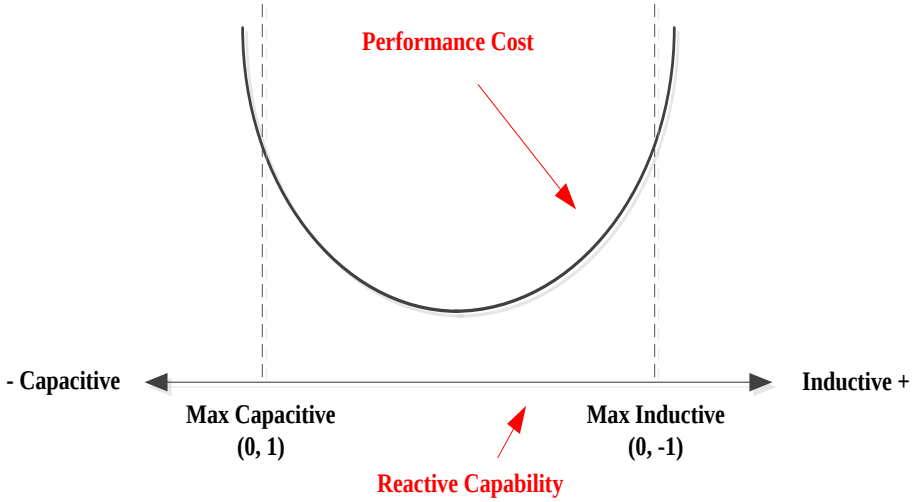

Figure 6.1 LV feeder performance cost and reactive capability.

As shown in figure 6.1, in this study, the reactive capability of LV feeders is defined by the maximum inductive (positive) reactive injection and the maximum capacitive (negative) injection by reactive control of PV inverters with the voltages maintained within the acceptable range specified by equation (6.9). Therefore, to decide the lower capacitive and the upper inductive bounds of the per-phase LV feeder reactive capability, we could simply do the single-phase optimization of equations (6.6-6.9) twice by setting the weights (λ_{PC}, λ_{DTLV}) as (0, 1) and (0, -1) respectively. Besides, the performance cost of LV feeders is defined as a quadratic function of the

corresponding reactive capability in this research. As demonstrated in figure 6.1 above, when too much inductive reactive power is injected into the LV feeder (i.e. strong inductive reactive capability), the performance cost is usually high as a result of a serious voltage drop. On the other hand, when a significant capacitive reactive power is exported from LV feeder (i.e. strong capacitive reactive capability), the performance cost is also often expensive due to a potential voltage rise. Accordingly, the performance cost is defined as a quadratic function of the LV feeder reactive capability as follows:

$$F_{PC} = r_1 {Q_{DTLV}}^2 + r_2 Q_{DTLV} + r_3 \tag{6.10}$$

where r_1, r_2 and r_3 are the coefficients of the quadratic function. To decide these coefficients, the most popular data-fitting technique is employed. Firstly, by randomly generating the weights λ_{PC} and λ_{DTLV} within the range of [0, 1] with $\lambda_{PC} + \lambda_{DTLV} = 1$, a number of single-phase optimizations defined in equations (6.6-6.9) are conducted to locate some typical points on the performance cost function of equation (6.10) and figure 6.1. Then, through data-fitting of these typical points, the coefficients r_1, r_2 and r_3 are determined. Obviously, the more typical points we could find by optimization, the more accurate the performance cost function would be.

6.2.2 Three-Phase Optimization of MV Distribution Network for Step 2

Step 2 of the proposed hierarchical control strategy in Chapter 5 is dedicated to optimize the operation of the MV distribution network by controlling both the MV delta-connected switched capacitors and the reactive injections of LV feeders. Specifically, with the reactive capability and the corresponding performance cost function obtained in step 1, LV feeders can be treated as aggregated buses with single-phase reactive capability in the MV network. Then, by controlling these aggregated LV-feeder buses as well as the MV delta-connected switched capacitors installed after the optimal placement of Section 4.2, a more comprehensive multi-objective optimization, which is similar as the MV controller of Section 4.3, is defined as follows to improve the operational performance of the MV network.

A. Three-Phase MV Optimization Objectives

Similar as the optimization model defined in Section 4.3, the objectives of network power losses J_1, voltage magnitude profile J_2 and voltage unbalance profile J_3 are retained with the same definitions of variables as follows:

1) Network Power Losses:

$$J_1 = \sum_{l=1}^{N-1} \sum_{p=1}^{3} BLoss_l^p \tag{6.11}$$

2) Voltage Magnitude Profile:

$$J_2 = \sum_{i=1}^{N} \sum_{p=1}^{3} \left(V_i^p - V_N\right)^2 \tag{6.12}$$

3) Voltage Balance Profile:

$$J_3 = \sum_{i=1}^{N} (VUF_i - VUF_{desired})^2 \tag{6.13}$$

4) Performance Cost of LV Feeder Reactive Power:

The reactive control of each phase of LV feeders will cause a related performance cost, which can be decided according to the performance cost function of equation (6.10). The overall performance cost of reactive control of LV feeders is modeled and included by equation (6.14) below.

$$J_4 = \sum_{i \in \varphi} \sum_{p=1}^{3} F_{PCi}^p \tag{6.14}$$

where φ is the set of distribution transformer buses in the MV network and F_{PCi}^p is the per-phase performance cost of LV feeders located at phase p and distribution transformer bus i, which is calculated by equation (6.10).

B. Three-Phase MV Multi-Objective Optimization by Weighted-Sum Method

By integrating the above-defined objectives of equations (6.11-6.14) based on the weight-sum method, the multi-objective optimization model of MV distribution network can be formulated below with the same variables' definitions of Chapter 4.

$$F = \sum_{i=1}^{4} w_i J_i / sf_i \tag{6.15}$$

subject to:

$$V_{min} \leq V_i^p \leq V_{max} \tag{6.16}$$

$$0 \leq Q_{Ci}^k \leq Q_{Cmaxi}^k \tag{6.17}$$

$$Q_{DTLVmini}^p \leq Q_{DTLVi}^p \leq Q_{DTLVmaxi}^p \tag{6.18}$$

$$\sqrt{\left(\sum_{p=1}^{3} P_{DTLVi}^p\right)^2 + \left(\sum_{p=1}^{3} Q_{DTLVi}^p\right)^2} \leq S_{DTi} \tag{6.19}$$

where the inequality constraints in equations (6.16-6.17) are the boundary limits on the voltage magnitude and the capacitor reactive capability decided by the capacitor size from the optimal placement of Section 4.2. Besides, the per-phase reactive capability of LV feeders obtained from step 1 is given in equation (6.18). In addition, when controlling the reactive injections of LV feeders, the overall three-phase outputs of real power P_{DTLVi}^p and reactive power Q_{DTLVi}^p must be within the limit of the distribution transformer rating S_{DTi}, which is presented in equation (6.19).

In this study, there is not cost associated with the MV capacitor control. This is primarily because comparing with capacitor control, the management of LV feeders' reactive injections is more expensive. Besides, MV capacitors have very high quality factors or very low loss angles and negligible losses. Therefore, imposing a lower or zero cost on the capacitor control will enable this more affordable technique to be applied firstly with a more reasonable overall performance achieved. In addition, as an alternative, the real-time capacitor control strategy proposed in Section 4.3 can be employed, when the capacitor switching cost is really a big concern.

C. Power Transformation from LV to MV of Distribution Transformer

As analyzed in the hierarchical control strategy of Chapter 5, in the MV optimization of equations (6.15-6.19) above, the reactive injections of LV feeders are selected as the control variables directly. By doing so, we could significantly reduce the complexity of the problem as well as keep control accuracy. However, to perform the MV optimization by PSO and improved BSFS method as presented in Chapter 4, the real and reactive injections of LV feeders must be transformed from the LV side to the MV side of the distribution transformer.

According to the coordination interface derived in Section 5.3, for the most common delta-grounded wye distribution transformer, the real and reactive power at the LV side can be transformed to the MV side by equations (6.20-6.21) as follows:

$$\begin{aligned} P_{DTMVi}^{A} &= 0.5\left(P_{DTLVi}^{a} + P_{DTLVi}^{b}\right); \\ P_{DTMVi}^{B} &= 0.5\left(P_{DTLVi}^{b} + P_{DTLVi}^{c}\right); \\ P_{DTMVi}^{C} &= 0.5(P_{DTLVi}^{c} + P_{DTLVi}^{a}); \end{aligned} \tag{6.20}$$

$$\begin{aligned} Q_{DTMVi}^{A} &= 0.5\left(Q_{DTLVi}^{a} + Q_{DTLVi}^{b}\right) + 0.2886\left(P_{DTLVi}^{a} - P_{DTLVi}^{b}\right); \\ Q_{DTMVi}^{B} &= 0.5\left(Q_{DTLVi}^{b} + Q_{DTLVi}^{c}\right) + 0.2886\left(P_{DTLVi}^{b} - P_{DTLVi}^{c}\right); \\ Q_{DTMVi}^{C} &= 0.5(Q_{DTLVi}^{c} + Q_{DTLVi}^{a}) + 0.2886(P_{DTLVi}^{c} - P_{DTLVi}^{a}); \end{aligned} \tag{6.21}$$

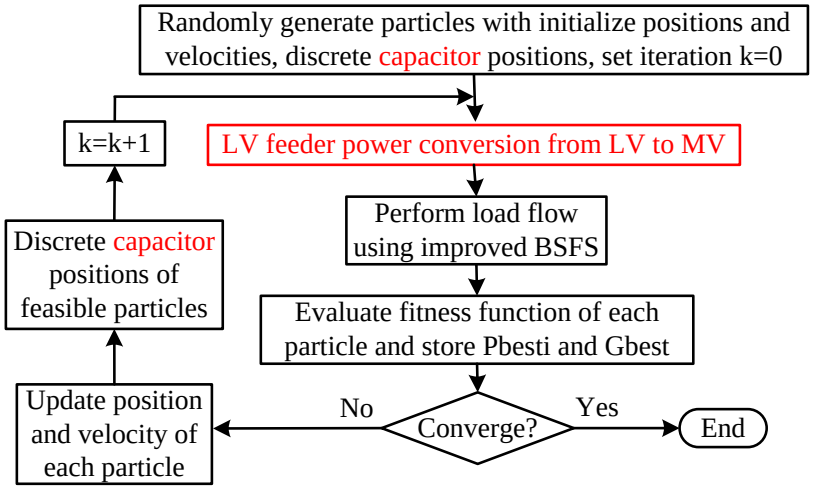

Figure 6.2 Modified flowchart of MV controller for both MV capacitors and LV feeders.

With the integration of the reactive control of LV feeders, the original flowchart of MV optimization presented by figure 4.3 should be modified to accurately describe the process of the more comprehensive optimization defined in equations (6.11-6.19), which involves the control of both MV capacitors and LV feeders. Specifically, as shown in figure 6.2, there are mainly two modifications:

1) At the initialization and update stage, discretion is only performed for capacitors as the LV feeders have a continuous reactive capability;

2) After initialization or update, both the real and reactive injections of LV feeders should be transformed from LV to MV through the distribution transformer based on equations (6.20-6.21) for the MV load flow calculation by improved BSFS method.

6.2.3 Three-Phase Optimization of LV Distribution Feeders for Step 3

As presented in Chapter 5, step 3 of the proposed hierarchical control strategy is to perform a three-phase multi-objective optimization on the LV feeder to improve the operational performance as well as to meet the reactive requests generated by the MV optimization in step 2. Specifically, as the reactive injections of LV feeders are selected as the control variables, the reactive requests on the LV feeders can be directly determined by solving the MV optimization problem of equations (6.11-6.19) in step 2. Then, adding these reactive requirements on LV feeders as the equality constraints, a comprehensive optimization, similar as that of Chapter 3, is formulated and conducted on the three-phase LV feeders by reactive control of PV inverters, to improve the operation of LV feeders and meet the MV reactive requests.

A. Three-Phase LV Optimization Objectives

Similar as the optimization model of Section 3.3, the objectives of three-phase LV feeder optimization at step 3 include network losses J_1, voltage magnitude profile J_2 and voltage balance profile J_3 as well as PV generation cost J_4 with the same variables' definitions.

1) Network Losses:

$$J_1 = \sum_{p=1}^{4} \sum_{i=1}^{n-1} \sum_{j=i+1}^{n} {I_{ij}^p}^2 R_{ij}^p \tag{6.22}$$

2) Voltage Magnitude Profile:

$$J_2 = \sum_{p=1}^{3} \sum_{i=1}^{n} {\Delta V_{idb}^p}^2 \tag{6.23}$$

3) Voltage Balance Profile:

$$J_3 = \sum_{i\in\lambda} \Delta VUF_{idb}{}^2 \tag{6.24}$$

4) PV Generation Cost:

$$J_4 = \sum_{p=1}^{3} \sum_{i\epsilon\delta} \left(k_{i1}^p S_{PVi}^p{}^2 + k_{i2}^p S_{PVi}^p + k_{i3}^p \right) \tag{6.25}$$

B. Three-Phase LV Optimization by Weighted-Sum Method

By using the weighted-sum method, the multi-objective optimization of LV feeder at step 3 can be formulated as follows with all the objectives of equations (6.22-6.25) above integrated:

$$\min \ F = \sum_{i=1}^{4} w_i J_i / sf_i \tag{6.26}$$

subject to:

$$P_{PVi}^p - P_{Li}^p - P_i^p = 0; \quad Q_{PVi}^p - Q_{Li}^p - Q_i^p = 0 \tag{6.27}$$

$$Q_{DTLVi}^p - Q_{DTLVi_{required}}^p = 0 \tag{6.28}$$

$$P_{PVi}^p{}^2 + Q_{PVi}^p{}^2 \le S_i^{p\,2} \tag{6.29}$$

$$V_{ilb}^p \le V_i^p \le V_{iub}^p \tag{6.30}$$

Comparing with the optimization model of Section 3.3, the only difference is the addition of equation (6.28). $Q_{DTLVi_{required}}^p$ is the required per-phase LV reactive support by MV network while Q_{DTLVi}^p is the actual reactive injection of LV feeders and can be calculated as follows:

$$Q_{DTLVi}^p = \sum_{j=1}^{n} \left(G_{ij}^p \sin\theta_{ij}^p - B_{ij}^p \cos\theta_{ij}^p \right) V_j^p \tag{6.31}$$

The addition of equation (6.28) can ensure the reactive requirements of MV network satisfied when optimizing the operational performance of LV feeders by reactive control of PV inverters.

6.3 SIMULATION RESULTS AND ANALYSIS

6.3.1 Selected Network for Simulations

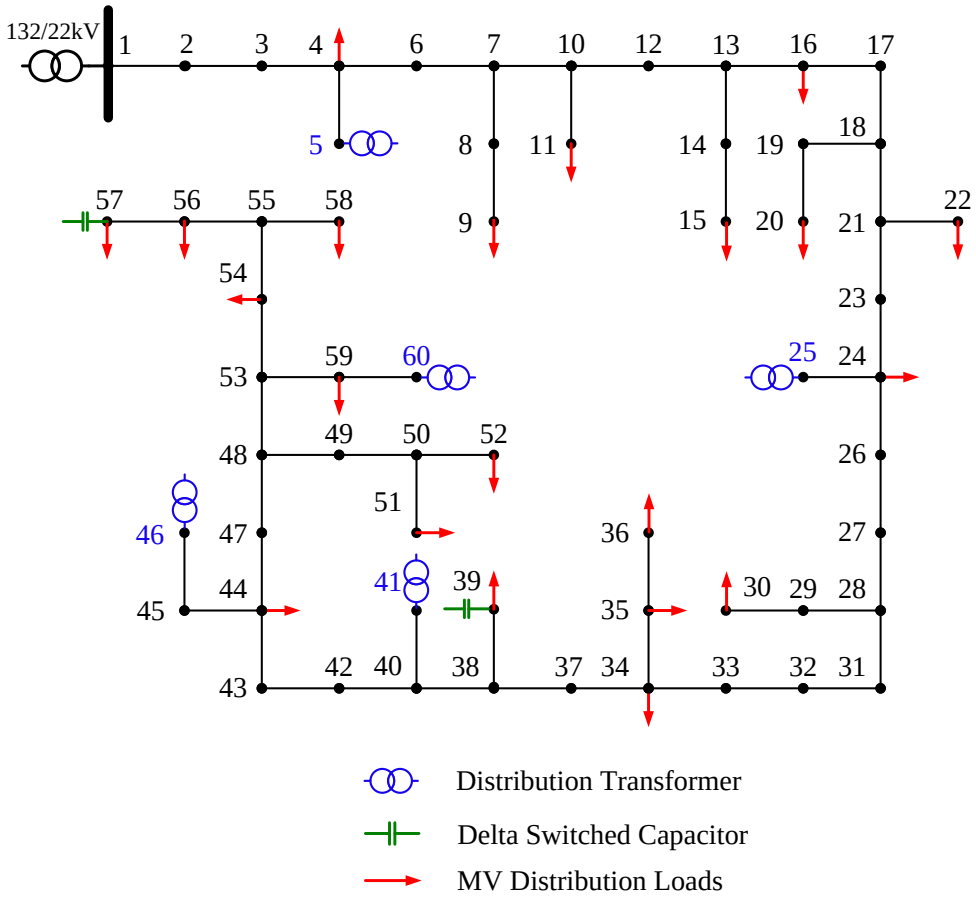

Figure 6.3 Forrestfield MV distribution network.

To verify the feasibility, effectiveness and efficiency of the proposed hierarchical control strategy in Chapter 5 and the proposed optimization models in Section 6.2, a real Western Australian distribution network with coverage from the substation to the LV feeders is simulated. As shown in figures 6.3 and 6.4, the whole distribution system consists of the Forrestfield MV network and five LV feeders with a total number of 560 buses. Specifically, the 22kV Forrestfield MV network is an extension of the one simulated in Chapter 4 (figure 4.4 and Appendix C) with the same physical structure and loading but five of the original loads at buses 5, 25, 41, 46 and 60 replaced with distribution transformers. All the distribution transformers have a rated 22kV/415V voltage and a delta-grounded wye connection. Among them,

the Pavetta1 LV distribution feeder simulated in Chapter 3 (figure 3.3 and Appendix B) is supplied by the distribution transformer at bus 41 with a capacity of 200 kVA. In this study, due to the unavailability of physical data, the other four LV feeders at MV buses 5, 25, 46 and 60 are modelled by copying the Pavetta1 LV feeder at MV bus 41. Additionally, according to the optimal placement of Section 4.2, the two delta-connected switched capacitors placed at the MV buses 39 and 57 have a capacity of 450kVAr and 1050kVAr respectively with a tap size of 150kVAr.

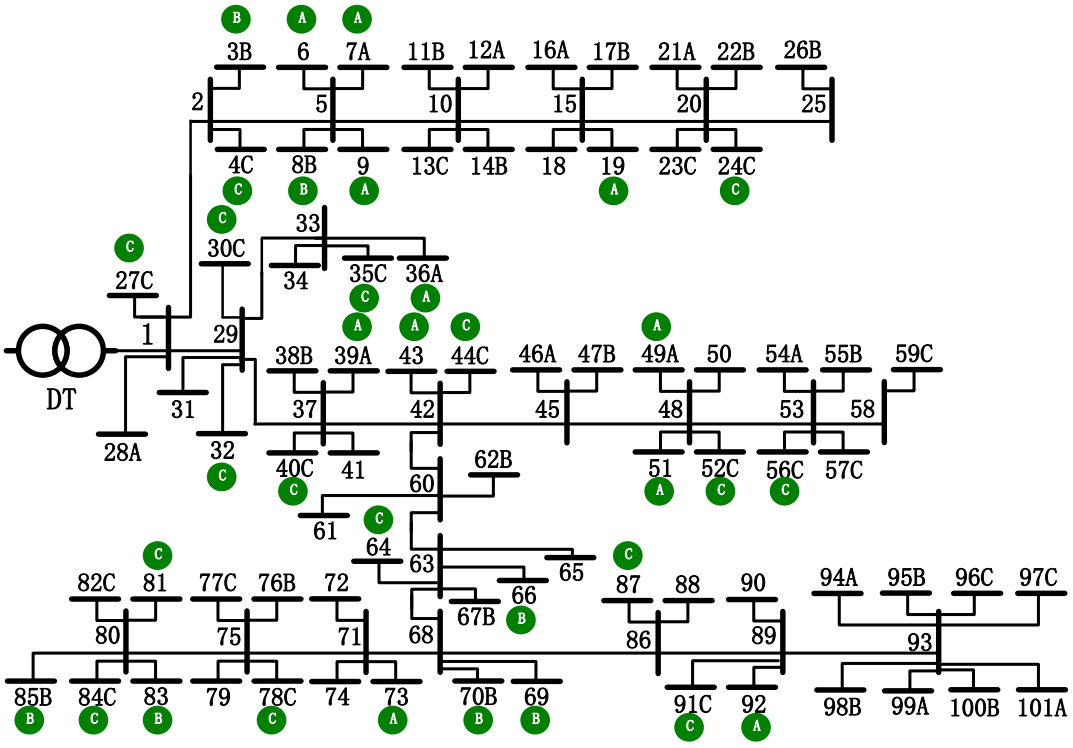

Figure 6.4 Pavetta1 LV distribution feeder at MV bus 41.

6.3.2 Simulated Cases and Optimization Parameters Setting

To verify the performance of the proposed hierarchical optimization, the high load low generation scenario described in Section 3.4.2 is simulated on the whole network scale. Specifically, this scenario features a high load demand but low PV generations, causing a significant load peak as well as a serious voltage drop in summer (25/01/2012). To improve the network operational performance, the proposed three-

step hierarchical optimization is applied based on coordinating the control of the MV switched capacitors and LV PV inverters. For comparison purpose, a reference case (ORIGINAL) is also simulated based on the original network status without any control. Additionally, simulations are performed and analysed over 24 hours for each stage of the proposed three-step hierarchical optimization and the reference case.

For the simulated scenario of peak load above, serious voltage drop is the foremost concern. Therefore, for the LV optimization in both steps 1 and 3 and the MV optimization in step 2 of the hierarchical control, the highest priority is given to the objective of voltage magnitude profile J_2 with the biggest weight $w_2 = 0.5$. This is followed by network losses J_1 and voltage balance profile J_3 with $w_1 = w_3 = 0.2$. Besides, to prove the effectiveness of the proposed hierarchical control, a lowest cost is imposed on the PV generation cost J_4 at steps 1 and 3 and the performance cost of LV feeders J_4 at step 2 with the smallest weight $w_4 = 0.1$. Additionally, for the objectives of voltage magnitude profile J_2 and voltage balance profile J_3 in LV optimization, dead band function is kept to encourage a more significant reactive capability of LV feeders.

Except the modifications above, all the other parameters of LV and MV optimization used in Chapters 3 and 4 are maintained. A brief summary of the optimization parameters utilized in the proposed hierarchical control is presented in table 6.1.

Table 6.1 Optimization parameters of the proposed hierarchical control.

LV Optimization (Steps 1 and 3)			**MV Optimization (Step 2)**			
Weighted-sum		Objectives	Weighted-sum		PSO	
w_1	0.2	Voltage dead band	w_1	0.2	Particle size	10,000
w_2	0.5	[-3%/232.8, +3%/247.2]	w_2	0.5	Iteration No	15
w_3	0.2	VUF dead band	w_3	0.2	w	[0.9→0.4]
w_4	0.1	[0, 1%]	w_4	0.1	C_1, C_2	2

6.3.3 Simulation Results Analysis

A. Single-Phase Optimization of LV Distribution Feeders for Step 1

As discussed in section 6.2.1, the single-phase LV optimization defined in equations (6.6-6.9) is iteratively performed by adjusting weights λ_{PC} and λ_{DTLV} within the range of [0, 1] to generate a group of typical points on the function curve, which are then used for determining the per-phase reactive capability and its corresponding performance cost function of LV feeders by data fitting. In this study, to ensure both the computation accuracy and efficiency, a total number of 18 sampling points are calculated for each phase simulation. Besides, as described in section 6.3.1, the other four LV feeders at MV buses 5, 25, 46 and 60 are copied exactly from the Pavetta1 LV feeder at MV bus 41. Thus, a detailed analysis will be only conducted for the Pavetta1 LV feeder with the same findings applicable to the other four LV feeders.

As shown in table 6.2 and figures 6.5-6.6, among the three phases of Pavetta1 LV feeder, phase C has the most load and PV connections and therefore gains more attention for analysis. As can be seen from figure 6.9 and table 6.5, the reactive capability and performance cost of phase C varies significantly at different hours due to different loading and generation conditions. Specifically, at the early morning of 06:00, the inductive reactive demand is the lowest (figure 6.5), which means it is the easiest to compensate. Therefore, with the capacitive injections of PV inverters, a strongest capacitive reactive capability of phase C can be obtained at this time point (green colour in figure 6.9 and table 6.5). Besides, hour 06:00 also has the lightest real and reactive load simultaneously (figures 6.5-6.6) and thus phase C is the healthiest at this time point with a lowest performance cost of reactive capability as shown in figure 6.9. With the increase of load demand, the operational performance of phase C deteriorates with a higher performance cost of reactive management. Therefore, at the reactive load peak of hour 21:00 when phase C has the worst operational performance according to the study of Chapter 3, the performance cost of reactive capability of phase C reaches the highest (figure 6.9 and table 6.5). Additionally, we can also find in figure 6.9 that the capacitive reactive capability at

hour 21:00 is rather limited. This is because the inductive reactive load peaks at this time, absorbing the capacitive contributions of PV inverters.

Table 6.2 Load and PV connections of Pavetta1 LV feeder at MV bus 41.

Phase	Consumers	PV Connection	PV Capacity	Penetration
A	13	11	21.31kW	10.7%
B	18	7	13.07kW	6.5%
C	20	16	29.43kW	14.7%
3 Phase	26	---	---	---
Total	77	34	63.81kW	31.9%

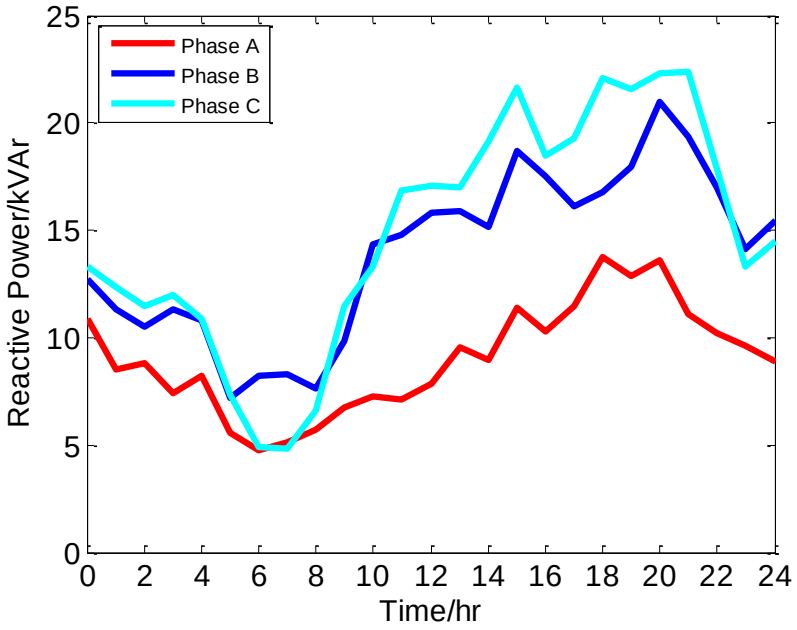

Figure 6.5 Reactive power profile of Pavetta1 LV feeder at MV bus 41.

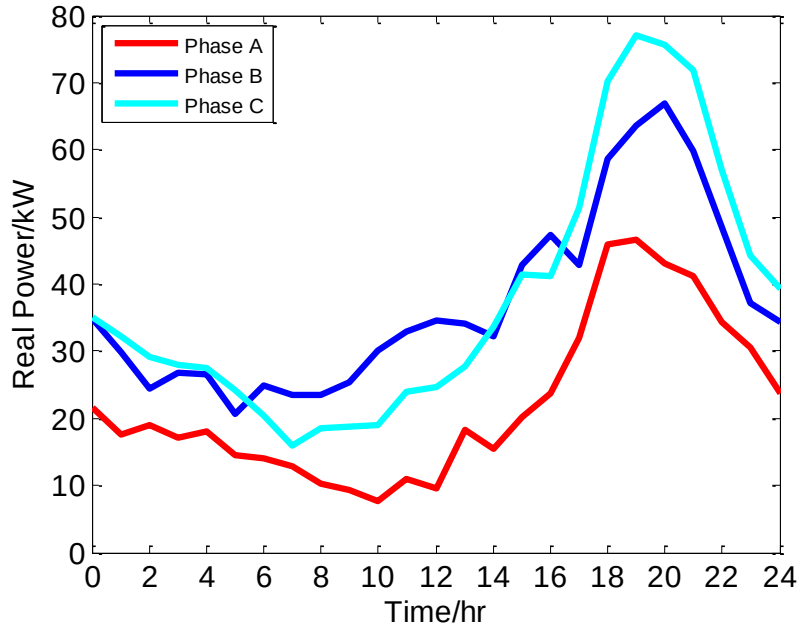

Figure 6.6 Real power profile of Pavetta1 LV feeder at MV bus 41.

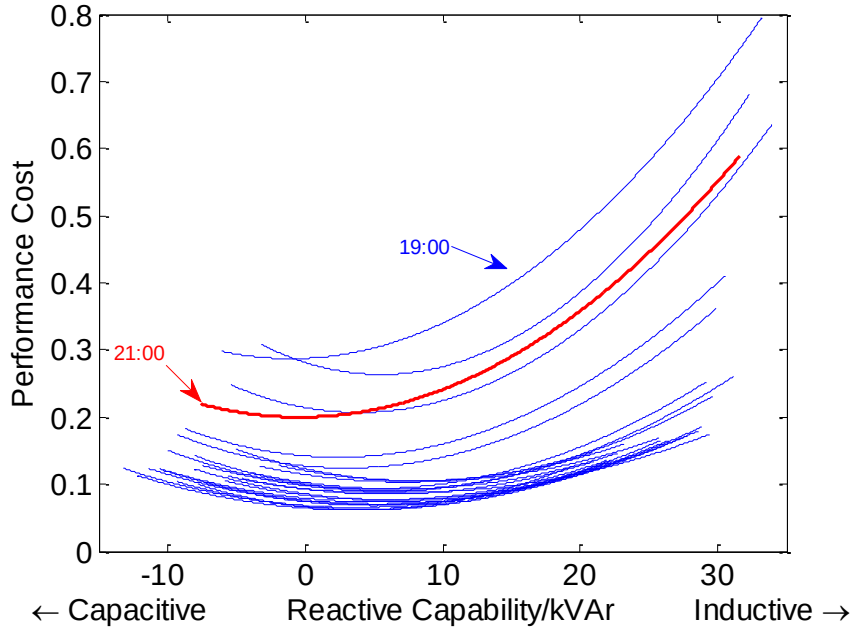

Figure 6.7 Reactive capability and performance cost of phase A of Pavetta1 over 24 hours.

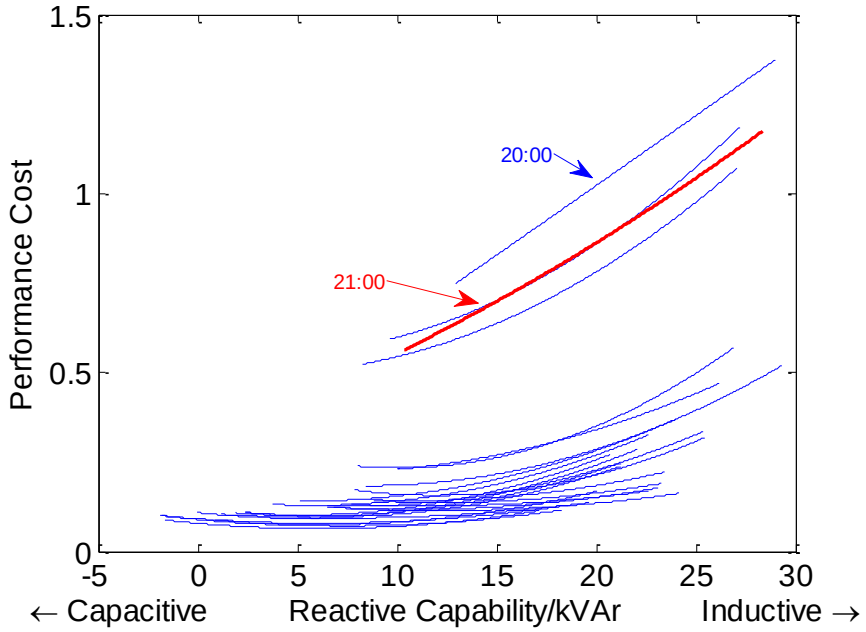

Figure 6.8 Reactive capability and performance cost of phase B of Pavetta1 over 24 hours.

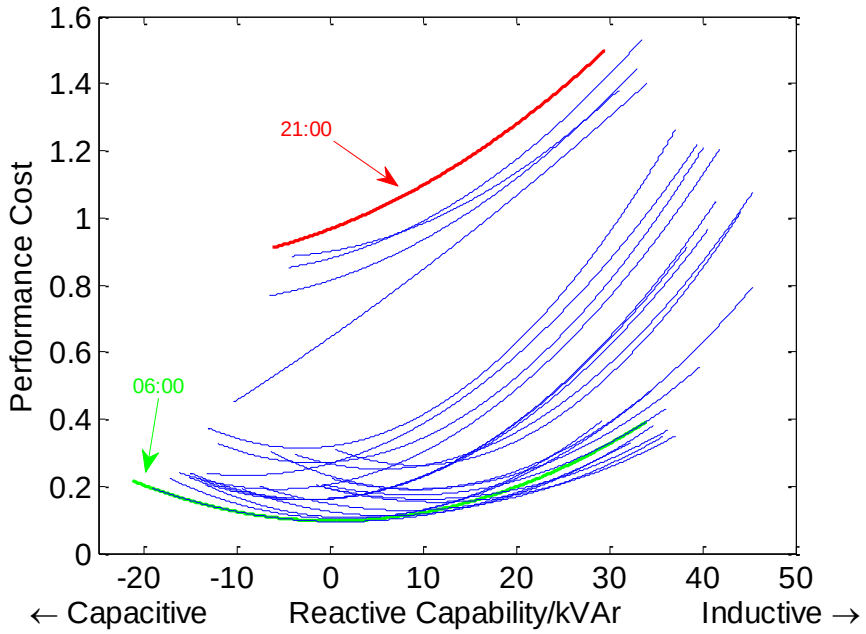

Figure 6.9 Reactive capability and performance cost of phase C of Pavetta1 over 24 hours.

Regarding phases A and B, as shown in figures 6.7-6.9 and tables 6.3-6.5, their performance costs at each hour e.g. hour 21:00 is generally lower than the corresponding value of phase C. This is because the performance cost is mainly determined by the load demand of each phase. From figure 6.6 and table 6.2 we can find that phases A and B generally have a lower load demand than phase C, and thus a lower performance cost as well. Additionally, for the same reason, the performance costs of phases A and B at hour 21:00 do not dominate over the 24 hours (red colour in figures 6.7-6.8 and tables 6.3-6.4) as their loads peak at hours 19:00 and 20:00 respectively (figure 6.6).

Generally, the reactive capability and performance cost of each phase of the LV feeders are determined by both the load and PV connections. For example, phase B has the weakest capacitive reactive capability, which is because it has the second highest inductive load but the least PV capacity (table 6.2 and figures 6.5-6.6). On the other hand, although phase C has the highest inductive load, it still has the strongest capacitive reactive capability as a result of the most PV connections. Another noticeable point is that the reactive capabilities of phases A, B and C are not necessarily proportional to their reactive load profiles. This is because, due to different sensitivities, the same reactive injection by PV inverters has a different impact on the LV feeders' reactive capabilities.

Table 6.3 Reactive capability and performance cost function of phase A of Pavetta1.

Time	$Q_{DTLVmin}$/kVAr	$Q_{DTLVmax}$/kVAr	r_1	r_2	r_3
00:00	-8.07	31.16	2.66E-10	-3.16E-06	0.10
01:00	-10.35	28.80	2.07E-10	-2.20E-06	0.08
02:00	-8.03	26.41	2.21E-10	-2.84E-06	0.09
03:00	-11.36	27.76	1.98E-10	-2.02E-06	0.08
04:00	-10.59	28.57	1.96E-10	-2.10E-06	0.08
05:00	-13.22	25.84	2.04E-10	-1.53E-06	0.07
06:00	-12.23	23.58	2.02E-10	-1.55E-06	0.06
07:00	-7.80	19.50	2.71E-10	-2.18E-06	0.07
08:00	-9.26	22.20	2.25E-10	-1.93E-06	0.07
09:00	-7.30	22.30	2.21E-10	-2.25E-06	0.07
10:00	-5.85	21.90	2.18E-10	-2.44E-06	0.08
11:00	-5.57	20.84	2.27E-10	-2.14E-06	0.09
12:00	-4.52	20.99	2.13E-10	-2.54E-06	0.09
13:00	-3.29	23.16	2.18E-10	-3.12E-06	0.11
14:00	-4.00	22.77	2.10E-10	-2.89E-06	0.10
15:00	-1.90	25.74	2.16E-10	-3.67E-06	0.12
16:00	-7.48	29.44	1.80E-10	-2.71E-06	0.10
17:00	-5.08	29.60	2.73E-10	-4.48E-06	0.12
18:00	-3.19	32.25	5.86E-10	-6.57E-06	0.28
19:00	-6.08	33.19	4.35E-10	8.45E-07	0.29
20:00	-5.40	33.91	4.77E-10	-3.77E-06	0.21
21:00	**-7.62**	**31.64**	**3.80E-10**	**2.60E-07**	**0.20**
22:00	-8.66	30.53	3.42E-10	-1.68E-06	0.14
23:00	-9.28	29.92	3.29E-10	-2.02E-06	0.13
24:00	-9.96	29.20	2.67E-10	-2.54E-06	0.10

Table 6.4 Reactive capability and performance cost function of phase B of Pavetta1.

Time	$Q_{DTLVmin}$/kVAr	$Q_{DTLVmax}$/kVAr	r_1	r_2	r_3
00:00	3.76	22.59	6.94E-10	-8.05E-06	0.15
01:00	2.41	21.23	6.40E-10	-7.83E-06	0.12
02:00	-0.03	22.03	6.52E-10	-6.46E-06	0.11
03:00	2.40	21.22	6.69E-10	-8.98E-06	0.13
04:00	1.90	20.72	6.91E-10	-6.97E-06	0.12
05:00	-1.61	17.10	4.10E-10	-4.98E-06	0.08
06:00	-1.87	20.03	4.66E-10	-5.43E-06	0.09
07:00	0.82	18.25	3.87E-10	-5.84E-06	0.09
08:00	-1.83	18.62	3.27E-10	-4.06E-06	0.09
09:00	1.18	19.65	2.80E-10	-4.11E-06	0.11
10:00	6.85	23.11	3.93E-10	-8.41E-06	0.16
11:00	7.70	22.59	3.45E-10	-8.02E-06	0.17
12:00	8.87	23.27	4.27E-10	-1.04E-05	0.20
13:00	8.67	23.40	5.08E-10	-1.11E-05	0.20
14:00	6.51	24.12	3.32E-10	-8.10E-06	0.16
15:00	8.41	29.30	7.79E-10	-1.34E-05	0.24
16:00	10.02	26.18	6.04E-10	-7.04E-06	0.24
17:00	7.88	25.46	8.92E-10	-2.14E-05	0.29
18:00	8.26	27.06	1.02E-09	-6.88E-06	0.51
19:00	9.66	27.23	1.12E-09	-7.57E-06	0.56
20:00	12.96	28.95	2.36E-11	3.80E-05	0.25
21:00	**10.36**	**28.38**	**3.50E-10**	**2.04E-05**	**0.31**
22:00	8.02	26.93	1.19E-09	-2.40E-05	0.35
23:00	5.15	24.02	6.59E-10	-7.10E-06	0.16
24:00	6.52	25.40	6.61E-10	-1.01E-05	0.16

Table 6.5 Reactive capability and performance cost function of phase C of Pavetta1.

Time	$Q_{DTLVmin}$/kVAr	$Q_{DTLVmax}$/kVAr	r_1	r_2	r_3
00:00	-13.37	39.40	4.16E-10	7.71E-06	0.27
01:00	-16.20	41.85	4.48E-10	5.11E-06	0.21
02:00	-15.18	40.60	4.31E-10	2.26E-06	0.16
03:00	-15.03	41.44	4.69E-10	1.94E-06	0.16
04:00	-14.22	38.35	4.53E-10	2.17E-06	0.16
05:00	-17.28	34.57	3.46E-10	-9.57E-07	0.10
06:00	**-21.27**	**34.05**	**2.59E-10**	**-1.37E-07**	**0.10**
07:00	-19.27	32.27	2.42E-10	-5.73E-07	0.09
08:00	-13.45	29.26	3.98E-10	-1.87E-06	0.11
09:00	-9.52	34.69	3.27E-10	-4.02E-06	0.12
10:00	-7.64	35.75	2.88E-10	-4.74E-06	0.15
11:00	-1.66	37.07	2.99E-10	-6.85E-06	0.19
12:00	-0.65	36.20	3.01E-10	-6.16E-06	0.19
13:00	-0.78	36.14	3.47E-10	-6.20E-06	0.20
14:00	0.21	39.69	3.90E-10	-7.19E-06	0.22
15:00	0.55	44.09	6.22E-10	-1.15E-05	0.32
16:00	-6.48	45.40	4.60E-10	-8.49E-06	0.23
17:00	-3.78	45.35	5.17E-10	-5.66E-06	0.27
18:00	-4.22	31.01	3.43E-10	4.85E-06	0.90
19:00	-6.54	33.06	3.07E-10	8.99E-06	0.81
20:00	-4.54	33.51	3.54E-10	7.60E-06	0.88
21:00	**-6.23**	**29.59**	**2.53E-10**	**1.05E-05**	**0.97**
22:00	-10.46	34.08	8.02E-11	1.95E-05	0.64
23:00	-13.24	37.12	5.90E-10	3.54E-06	0.32
24:00	-12.08	40.08	5.38E-10	1.83E-06	0.27

B. Three-Phase Optimization of MV Distribution Network for Step 2

According to both table 6.6 and figure 4.5 of Chapter 4, due to heavy load demand, the MV Forrestfield network had a poor operational performance, especially during the peak load hours between 15:00 and 22:00. The worst performance occurred at hour 20:00 with the maximum objective function of 0.864, including serious network losses J_1, significant voltage magnitude deviation J_2 and VUF deviation J_3 at 507 kW, 2.66E7 and 6.70E-4 respectively. Besides the heavy MV loads, another contributing factor for the poor MV network performance is the significant inductive reactive injections of LV feeders (figure 6.5), which can be proved by the highest performance cost of LV feeders' reactive injections J_4 of 11.90 at hour 20:00 as shown in table 6.6.

Based on the step 2 of the proposed hierarchical control strategy in section 5.2 and the optimization models in section 6.2.2, MV network performance can be significantly improved by optimally controlling both the MV delta-connected switched capacitors and the reactive injections of LV feeders. As can be seen in table 6.6, the objective function over 24 hours has all significantly reduced with the maximum value at hour 20:00 decreased to only 0.563 which includes the reductions of network losses J_1, voltage magnitude deviation J_2 and VUF deviation J_3 to 467kW, 1.43E7 and 2.12E-4 respectively. Additionally, as demonstrated in tables 6.6 and 6.8, after the MV optimization the overall inductive reactive demand of LV feeders is also reduced with a lower performance cost of LV feeders' reactive injections J_4 at 10.90.

As analysed in section 6.2.2, in this study, no cost is imposed on the capacitor switching which is more affordable comparing with the reactive regulation of LV feeders. Therefore, a more significant reactive injection of delta-connected capacitors can be found in table 6.7. Moreover, as shown in figures 6.7-6.9, in comparison of phases A and C of LV feeders, phase B mainly has an inductive reactive capability with almost no capacitive ability. Consequently, the corresponding bridge BC of delta-connected capacitors at both buses 39 and 57 is almost fully used (table 6.7).

Table 6.6 Forrestfield MV network optimization results over 24 hours. The highlighted green/red cells indicate decrease/increase of the value compared with the pervious case.

Time	ORIGINAL					OPTIMAL				
	F	$J_1/0.2$	$J_2/0.5$	$J_3/0.2$	$J_4/0.1$	F	$J_1/0.2$	$J_2/0.5$	$J_3/0.2$	$J_4/0.1$
00:00	0.222	1.33E5	6.91E6	1.13E-4	3.50	0.107	1.28E5	1.68E6	4.19E-5	2.65
01:00	0.182	9.86E4	5.64E6	1.71E-4	2.63	0.089	1.04E5	1.43E6	9.27E-5	2.03
02:00	0.135	8.03E4	4.06E6	1.01E-4	2.10	0.061	8.90E4	5.07E5	5.83E-5	1.86
03:00	0.147	8.16E4	4.65E6	8.36E-5	2.13	0.067	8.44E4	8.23E5	8.00E-5	1.93
04:00	0.135	7.96E4	4.24E6	4.29E-5	2.14	0.064	8.71E4	6.13E5	8.01E-5	1.93
05:00	0.087	5.25E4	2.63E6	6.14E-5	1.38	0.048	6.28E4	4.71E5	8.49E-5	1.24
06:00	0.097	5.23E4	3.25E6	3.15E-5	1.26	0.063	6.18E4	8.77E5	2.35E-4	1.20
07:00	0.086	4.17E4	2.83E6	6.88E-5	1.20	0.057	4.95E4	7.32E5	2.81E-4	1.16
08:00	0.092	4.28E4	2.99E6	9.05E-5	1.40	0.061	5.14E4	8.42E5	2.78E-4	1.29
09:00	0.116	5.05E4	3.40E6	3.15E-4	1.46	0.058	4.92E4	8.06E5	2.48E-4	1.43
10:00	0.202	6.62E4	6.25E6	6.92E-4	1.69	0.104	5.16E4	2.76E6	3.16E-4	1.67
11:00	0.223	8.72E4	6.62E6	7.80E-4	1.92	0.104	6.88E4	2.52E6	2.34E-4	1.90
12:00	0.267	9.41E4	8.16E6	9.44E-4	2.04	0.135	7.18E4	3.82E6	2.83E-4	1.97
13:00	0.216	1.10E5	6.91E6	2.87E-4	2.25	0.094	9.22E4	1.95E6	5.73E-5	2.23
14:00	0.252	1.15E5	8.15E6	4.74E-4	2.14	0.113	9.71E4	2.87E6	2.74E-5	2.13
15:00	0.392	1.86E5	1.26E7	6.68E-4	3.54	0.202	1.53E5	5.64E6	8.36E-5	3.03
16:00	0.385	2.02E5	1.24E7	5.25E-4	3.07	0.213	1.81E5	5.36E6	2.30E-4	2.87
17:00	0.387	2.42E5	1.23E7	3.00E-4	3.02	0.200	2.27E5	4.23E6	5.47E-5	2.92
18:00	0.653	4.36E5	1.86E7	5.70E-4	10.18	0.390	4.10E5	7.50E6	1.77E-4	9.65
19:00	0.773	5.00E5	2.24E7	8.28E-4	10.72	0.488	4.69E5	1.09E7	2.72E-4	9.54
20:00	**0.864**	**5.07E5**	**2.66E7**	**6.70E-4**	**11.90**	**0.563**	**4.67E5**	**1.43E7**	**2.12E-4**	**10.90**
21:00	0.739	4.36E5	2.22E7	6.88E-4	11.21	0.456	4.03E5	1.08E7	2.05E-4	9.64
22:00	0.478	2.87E5	1.47E7	2.58E-4	7.07	0.273	2.77E5	5.88E6	5.71E-5	5.97
23:00	0.277	1.82E5	8.44E6	1.14E-4	3.79	0.145	1.91E5	2.05E6	3.92E-5	3.75
24:00	0.263	1.46E5	8.71E6	7.79E-5	3.21	0.135	1.45E5	2.78E6	1.45E-5	3.02

Table 6.7 Capacitors switching of bridges AB, BC and CA after MV optimization.

Time	Bus 39/kVAr						Bus 57/kVAr					
	Q_{AB}		Q_{BC}		Q_{CA}		Q_{AB}		Q_{BC}		Q_{CA}	
	kVAr	Taps	kVAr	Taps	kVAr	Taps	kVAr	Taps	kVAr	Taps	kVAr	Taps
00:00	450	3	450	3	450	3	900	6	1050	7	900	6
01:00	450	3	450	3	300	2	600	4	1050	7	900	6
02:00	450	3	450	3	450	3	750	5	900	6	750	5
03:00	150	1	450	3	300	2	750	5	1050	7	750	5
04:00	300	2	450	3	300	2	750	5	1050	7	750	5
05:00	300	2	450	3	300	2	600	4	750	5	600	4
06:00	450	3	300	2	150	1	450	3	1050	7	150	1
07:00	450	3	300	2	150	1	600	4	900	6	0	0
08:00	300	2	450	3	300	2	600	4	900	6	150	1
09:00	450	3	450	3	150	1	300	2	1050	7	450	3
10:00	300	2	450	3	150	1	300	2	1050	7	300	2
11:00	150	1	450	3	300	2	450	3	1050	7	450	3
12:00	450	3	450	3	150	1	150	1	1050	7	600	4
13:00	150	1	450	3	450	3	750	5	1050	7	600	4
14:00	450	3	450	3	300	2	300	2	1050	7	1050	7
15:00	150	1	450	3	300	2	600	4	1050	7	1050	7
16:00	300	2	450	3	450	3	750	5	1050	7	750	5
17:00	450	3	300	2	450	3	900	6	1050	7	1050	7
18:00	300	2	300	2	450	3	1050	7	1050	7	1050	7
19:00	450	3	450	3	450	3	750	5	900	6	1050	7
20:00	300	2	450	3	450	3	900	6	1050	7	1050	7
21:00	300	2	450	3	450	3	750	5	1050	7	1050	7
22:00	300	2	450	3	450	3	1050	7	1050	7	1050	7
23:00	450	3	450	3	300	2	1050	7	1050	7	1050	7
24:00	150	1	450	3	450	3	1050	7	1050	7	900	6

In this research, the weighted sum method is employed to reflect our preferences on the control objectives and achieve a desired network performance. As seen in table 6.1, voltage magnitude profile J_2 is given the highest priority with $w_2 = 0.5$. Therefore, a significantly reduced J_2 can always be found over 24 hours in table 6.6 after the reactive control of both MV capacitors and LV feeders. Meanwhile, since

the objectives are mutually conflicting, as shown in table 6.6, objectives with lower priority, such as network losses J_1 with $w_1 = 0.2$ and voltage balance profile J_3 with $w_3 = 0.2$, may be sacrificed at some time points (red colour in table 6.6) to ensure the improvement of voltage magnitude profile as well as the optimization of overall network performance.

Table 6.8 Reactive request on each phase of the LV feeders by MV optimization.

Time	Bus 5/kVAr			Bus 25/kVAr			Bus 41/kVAr			Bus 46/kVAr			Bus 60/kVAr		
	A	B	C	A	B	C	A	B	C	A	B	C	A	B	C
00:00	19.2	17.8	12.9	20.4	13.1	3.4	9.6	8.4	1.6	6.9	10.7	12.6	19.7	4.0	10.0
01:00	8.5	4.3	5.8	6.5	7.1	15.5	19.4	15.4	7.9	9.1	3.8	12.6	5.8	6.4	15.4
02:00	10.9	7.3	3.9	13.7	7.5	0.7	19.1	0.9	8.4	5.9	1.4	10.3	26.1	5.0	5.2
03:00	9.8	7.8	3.7	16.6	4.9	11.0	21.4	2.6	10.8	22.4	9.9	5.6	14.4	7.5	9.0
04:00	7.0	7.5	5.0	14.1	6.8	4.3	25.2	2.4	3.4	15.6	2.0	6.8	28.1	2.9	0.8
05:00	9.0	7.1	1.5	18.0	1.8	1.4	13.4	6.3	1.0	23.3	3.5	0.1	18.5	6.0	3.9
06:00	5.6	6.5	0.1	10.2	0.3	2.6	10.0	0.7	1.5	10.9	2.2	2.2	12.7	0.2	1.2
07:00	7.4	6.8	2.5	5.8	8.4	5.1	9.0	4.9	3.5	10.1	2.5	6.2	6.8	3.1	5.2
08:00	6.3	6.3	2.7	13.1	1.3	4.0	14.8	0.8	6.3	14.1	0.1	4.1	14.0	0.0	5.9
09:00	9.6	6.1	6.4	6.6	1.9	4.5	19.4	5.4	6.0	14.2	5.3	8.1	7.3	11.7	8.4
10:00	8.2	12.0	7.1	12.6	10.8	3.7	13.0	10.9	9.2	14.4	8.1	3.9	10.0	13.1	6.1
11:00	6.7	14.7	11.2	6.5	11.2	6.7	13.3	8.5	8.2	10.6	7.9	3.7	12.1	7.9	9.9
12:00	10.2	10.8	6.7	10.1	12.2	2.8	8.2	9.0	11.0	11.0	9.6	8.0	4.2	10.2	7.5
13:00	3.9	9.1	5.6	12.7	9.2	6.8	17.9	10.8	4.9	19.8	13.2	8.9	21.0	13.1	7.0
14:00	15.8	17.0	15.8	4.5	8.6	11.3	12.4	9.4	16.1	5.0	22.1	6.6	18.7	7.2	7.3
15:00	8.8	14.2	10.3	18.0	8.7	1.0	3.5	9.8	21.1	1.6	12.9	8.5	17.4	16.8	11.7
16:00	21.8	17.3	13.3	19.6	13.1	4.3	14.1	15.5	4.1	21.2	12.6	6.8	19.7	11.4	5.5
17:00	11.3	13.3	3.4	4.6	8.6	3.5	5.1	21.6	1.5	22.9	23.1	4.7	16.0	17.6	1.7
18:00	7.7	15.5	2.2	10.3	8.5	1.9	14.0	20.2	11.8	17.0	19.2	3.1	12.2	18.1	12.3
19:00	0.0	19.0	6.1	8.4	14.7	7.1	15.7	11.3	5.4	4.2	11.1	21.3	3.1	16.2	4.8
20:00	15.7	20.2	4.0	15.4	17.3	2.0	11.1	19.3	5.4	3.3	24.4	10.9	4.2	14.5	16.0
21:00	15.3	16.5	5.9	4.3	12.5	5.6	12.0	17.8	5.7	10.1	10.6	4.1	17.3	13.0	6.8
22:00	8.4	21.5	2.0	8.4	10.9	16.0	20.9	10.2	8.3	1.0	23.4	4.4	15.0	14.9	1.7
23:00	2.7	17.3	5.9	25.9	14.8	11.2	18.5	9.4	2.8	4.7	7.8	6.5	19.1	12.0	12.0
24:00	12.3	21.0	2.1	16.0	16.2	5.1	25.5	14.4	4.0	27.1	6.7	10.2	0.7	7.1	6.8

C. Three-Phase Optimization of LV Distribution Feeders for Step 3

As presented in sections 5.2 and 6.2.3, step 3 of the proposed hierarchical control is to meet the per-phase reactive request on LV feeders in table 6.8 as well as to improve the feeder operational performance by optimal reactive control of PV inverters. Optimization results for all the LV feeders at MV buses 5, 25, 41, 46 and 60 are given in tables 6.10-6.14 respectively. Considering the other four LV feeders are copied from the Pavetta1 LV feeder at MV bus 41, only detailed analysis on the Pavetta1 LV feeder is performed here with the same findings applicable to the other LV feeders.

As shown in tables 6.9 and 6.12, after the optimization of step 3 defined in section 6.2.3, the operational performance of Pavetta1 LV feeder is significantly improved with the MV reactive requests exactly satisfied as well. Specifically, in this study, the MV reactive requests decided by the step 2 optimization are added as the constraints in the LV optimization of step 3. Therefore, the solving of step 3 optimization automatically ensures the satisfaction of the MV reactive requests on LV feeders, which has been proved by tables 6.8 and 6.9. Meanwhile, by optimally controlling reactive outputs of PV inverters, the operational performance of Pavetta1 LV feeder is also obviously improved over 24 hours. As can be found in table 6.12, after optimization, the maximum objective function at hour 21:00 is reduced dramatically from the original 1.335 to 0.608 with the objectives of network losses J_1, voltage magnitude profile J_2 and voltage balance profile J_3 decreased from 8.198kW, 36675 and 9.03E-4 to 7.635kW, 19721, 3.86E-5 respectively at the cost of a higher PV generation cost J_4.

Similar as the step 2 optimization, weighted sum method is also employed in the step 3 optimization to reflect our control preferences. As shown in table 6.1, the highest priority is given to the voltage magnitude profile J_2 with $w_2 = 0.5$. Thus, a continuously decreasing J_2 can be found after optimization at all the 24 hours (table 6.12). Additionally, as the objectives are mutually conflicting, objectives with lower weights (e.g. network losses $w_1 = 0.2$ and voltage balance profile $w_3 = 0.2$) may be sacrificed at some points (red colour in table 6.12) to ensure the improvement of

voltage magnitude profile and the minimization of the overall objective function. Besides, to meet the MV reactive requests, at some time points more significant reactive injections of PV inverters are needed, which may also cause a local reactive overcompensation with a worse network losses and voltage balance profile.

Table 6.9 Reactive support by each phase of LV feeders over 24 hours.

Time	Bus 5/kVAr			Bus 25/kVAr			Bus 41/kVAr			Bus 46/kVAr			Bus 60/kVAr		
	A	B	C	A	B	C	A	B	C	A	B	C	A	B	C
00:00	19.2	17.8	12.9	20.4	13.1	3.4	9.6	8.4	1.6	6.9	10.7	12.6	19.7	4.0	10.0
01:00	8.5	4.3	5.8	6.5	7.1	15.5	19.4	15.4	7.9	9.1	3.8	12.6	5.8	6.4	15.4
02:00	10.9	7.3	3.9	13.7	7.5	0.7	19.1	0.9	8.4	5.9	1.4	10.3	26.1	5.0	5.2
03:00	9.8	7.8	3.7	16.6	4.9	11.0	21.4	2.6	10.8	22.4	9.9	5.6	14.4	7.5	9.0
04:00	7.0	7.5	5.0	14.1	6.8	4.3	25.2	2.4	3.4	15.6	2.0	6.8	28.1	2.9	0.8
05:00	9.0	7.1	1.5	18.0	1.8	1.4	13.4	6.3	1.0	23.3	3.5	0.1	18.5	6.0	3.9
06:00	5.6	6.5	0.1	10.2	0.3	2.6	10.0	0.7	1.5	10.9	2.2	2.2	12.7	0.2	1.2
07:00	7.4	6.8	2.5	5.8	8.4	5.1	9.0	4.9	3.5	10.1	2.5	6.2	6.8	3.1	5.2
08:00	6.3	6.3	2.7	13.1	1.3	4.0	14.8	0.8	6.3	14.1	0.1	4.1	14.0	0.0	5.9
09:00	9.6	6.1	6.4	6.6	1.9	4.5	19.4	5.4	6.0	14.2	5.3	8.1	7.3	11.7	8.4
10:00	8.2	12.0	7.1	12.6	10.8	3.7	13.0	10.9	9.2	14.4	8.1	3.9	10.0	13.1	6.1
11:00	6.7	14.7	11.2	6.5	11.2	6.7	13.3	8.5	8.2	10.6	7.9	3.7	12.1	7.9	9.9
12:00	10.2	10.8	6.7	10.1	12.2	2.8	8.2	9.0	11.0	11.0	9.6	8.0	4.2	10.2	7.5
13:00	3.9	9.1	5.6	12.7	9.2	6.8	17.9	10.8	4.9	19.8	13.2	8.9	21.0	13.1	7.0
14:00	15.8	17.0	15.8	4.5	8.6	11.3	12.4	9.4	16.1	5.0	22.1	6.6	18.7	7.2	7.3
15:00	8.8	14.2	10.3	18.0	8.7	1.0	3.5	9.8	21.1	1.6	12.9	8.5	17.4	16.8	11.7
16:00	21.8	17.3	13.3	19.6	13.1	4.3	14.1	15.5	4.1	21.2	12.6	6.8	19.7	11.4	5.5
17:00	11.3	13.3	3.4	4.6	8.6	3.5	5.1	21.6	1.5	22.9	23.1	4.7	16.0	17.6	1.7
18:00	7.7	15.5	2.2	10.3	8.5	1.9	14.0	20.2	11.8	17.0	19.2	3.1	12.2	18.1	12.3
19:00	0.0	19.0	6.1	8.4	14.7	7.1	15.7	11.3	5.4	4.2	11.1	21.3	3.1	16.2	4.8
20:00	15.7	20.2	4.0	15.4	17.3	2.0	11.1	19.3	5.4	3.3	24.4	10.9	4.2	14.5	16.0
21:00	15.3	16.5	5.9	4.3	12.5	5.6	12.0	17.8	5.7	10.1	10.6	4.1	17.3	13.0	6.8
22:00	8.4	21.5	2.0	8.4	10.9	16.0	20.9	10.2	8.3	1.0	23.4	4.4	15.0	14.9	1.7
23:00	2.7	17.3	5.9	25.9	14.8	11.2	18.5	9.4	2.8	4.7	7.8	6.5	19.1	12.0	12.0
24:00	12.3	21.0	2.1	16.0	16.2	5.1	25.5	14.4	4.0	27.1	6.7	10.2	0.7	7.1	6.8

Additionally, as shown in tables 6.11 and 6.13, at some points (red colour of F), the LV operational performance gets worse with the objective function increased rather than decreased comparing with the original value. It is reasonable as in some cases,

to improve the performance of the overall distribution network by providing the desired reactive supports, the performance of a few LV feeders could be sacrificed.

Table 6.10 Optimization of the LV feeder at MV bus 5 over 24 hours. The highlighted green/red cells indicate decrease/increase of the value compared with the pervious case.

Time	ORIGINAL					OPTIMAL				
	F	$J_1/0.2$	$J_2/0.5$	$J_3/0.2$	$J_4/0.1$	F	$J_1/0.2$	$J_2/0.5$	$J_3/0.2$	$J_4/0.1$
00:00	0.151	2746	1763	1.29E-7	1016	0.098	3011	1620	0	1182
01:00	0.103	2094	1069	1.43E-6	1016	0.069	1853	286	5.00E-7	1211
02:00	0.096	1870	711	0	1016	0.056	1719	211	0	1162
03:00	0.096	1850	774	0	1015	0.057	1685	216	0	1178
04:00	0.096	1890	737	0	1015	0.057	1723	262	0	1137
05:00	0.076	1097	33	0	1016	0.024	1075	0	0	1116
06:00	0.074	1039	31	0	1027	0.023	1000	3	0	1103
07:00	0.071	824	0	0	1080	0.017	812	0	0	1122
08:00	0.078	1025	10	0	1156	0.022	987	0	0	1193
09:00	0.087	1079	2	0	1304	0.023	1016	0	0	1370
10:00	0.097	1296	43	0	1457	0.028	1190	10	0	1498
11:00	0.108	1642	30	1.81E-7	1537	0.035	1555	9	0	1566
12:00	0.114	1743	87	1.22E-7	1574	0.039	1571	9	0	1684
13:00	0.122	2076	178	0	1559	0.048	1839	6	0	1735
14:00	0.121	1999	262	0	1518	0.048	2062	96	0	1584
15:00	0.152	3315	1951	7.12E-8	1412	0.114	2988	779	0	1554
16:00	0.153	3150	1282	0	1266	0.096	3265	860	0	1419
17:00	0.142	3504	1391	0	1163	0.106	3323	306	0	1377
18:00	0.397	7635	10164	1.58E-5	1056	0.330	7261	5779	5.82E-8	1426
19:00	0.489	8772	13402	2.28E-6	1027	0.429	8467	9656	0	1433
20:00	0.462	8224	12243	3.19E-5	1015	0.382	7926	8067	0	1321
21:00	0.466	7711	11751	1.03E-4	1020	0.374	7394	7462	3.75E-5	1325
22:00	0.239	5112	5717	6.49E-6	1019	0.233	4969	3454	0	1315
23:00	0.161	3463	2614	0	1017	0.132	3349	1652	0	1227
24:00	0.147	2924	2034	0	1017	0.108	2959	1245	0	1280

Table 6.11 Optimization of the LV feeder at MV bus 25 over 24 hours. The highlighted green/red cells indicate decrease/increase of the value compared with the pervious case.

Time	ORIGINAL					OPTIMAL				
	F	$J_1/0.2$	$J_2/0.5$	$J_3/0.2$	$J_4/0.1$	F	$J_1/0.2$	$J_2/0.5$	$J_3/0.2$	$J_4/0.1$
00:00	0.194	2805	4509	4.14E-6	1016	0.147	2765	1489	0	1263
01:00	0.157	2135	2948	2.23E-5	1016	0.116	1998	890	1.98E-8	1190
02:00	0.129	1904	2117	0	1016	0.102	1743	312	0	1240
03:00	0.133	1885	2347	2.42E-7	1015	0.133	1881	534	6.60E-5	1225
04:00	0.130	1924	2152	0	1015	0.103	1800	393	0	1206
05:00	0.077	1111	287	0	1016	0.090	1200	0	2.25E-6	1324
06:00	0.080	1053	474	0	1027	0.080	1040	4	0	1221
07:00	0.070	834	51	0	1079	0.069	831	1	0	1080
08:00	0.121	1036	147	9.85E-5	1156	0.080	1068	0	0	1305
09:00	0.088	1095	154	0	1304	0.095	989	0	1.46E-5	1429
10:00	0.120	1323	1121	4.00E-6	1457	0.105	1226	222	0	1566
11:00	0.134	1679	1128	1.09E-5	1537	0.113	1502	211	3.90E-7	1623
12:00	0.164	1786	1843	4.28E-5	1574	0.126	1604	537	6.31E-8	1722
13:00	0.151	2124	1700	0	1559	0.126	1940	218	0	1696
14:00	0.157	2049	2073	4.54E-6	1518	0.121	1806	223	1.15E-6	1643
15:00	0.310	3422	7482	8.05E-5	1412	0.207	3123	2220	3.31E-5	1816
16:00	0.260	3255	6293	3.31E-5	1266	0.192	3184	2750	0	1531
17:00	0.253	3619	6409	0	1163	0.168	3286	1417	0	1513
18:00	0.723	7961	24204	1.33E-4	1056	0.439	7370	10911	3.40E-6	1595
19:00	0.877	9197	31620	1.04E-4	1027	0.599	8628	18813	0	1322
20:00	0.944	8629	31575	3.22E-4	1015	0.577	8088	17763	1.44E-5	1397
21:00	0.967	8060	28230	5.86E-4	1020	0.533	7369	14372	1.02E-4	1439
22:00	0.458	5284	14365	2.14E-4	1019	0.374	4972	7206	7.33E-5	1140
23:00	0.250	3550	6730	0	1017	0.206	3786	3367	2.33E-6	1284
24:00	0.220	2996	5734	0	1017	0.162	2908	2230	0	1221

Table 6.12 Optimization of the LV feeder at MV bus 41 over 24 hours. The highlighted green/red cells indicate decrease/increase of the value compared with the pervious case.

Time	ORIGINAL					OPTIMAL				
	F	$J_1/0.2$	$J_2/0.5$	$J_3/0.2$	$J_4/0.1$	F	$J_1/0.2$	$J_2/0.5$	$J_3/0.2$	$J_4/0.1$
00:00	0.201	2828	6110	9.99E-6	1016	0.134	2475	1191	8.87E-8	1235
01:00	0.153	2150	4058	4.30E-5	1016	0.135	2280	1415	0	1253
02:00	0.148	1917	2894	1.01E-4	1016	0.106	1898	349	0	1326
03:00	0.219	1981	3226	2.79E-4	1015	0.113	1898	511	1.04E-6	1350
04:00	0.154	1937	2943	0	1015	0.107	2005	283	9.59E-5	1484
05:00	0.081	1127	515	0	1016	0.035	1117	13	0	1192
06:00	0.081	1058	791	0	1027	0.040	1033	12	1.53E-9	1224
07:00	0.073	838	147	0	1080	0.021	830	0	0	1150
08:00	0.125	1086	326	1.03E-4	1156	0.029	1040	1	0	1337
09:00	0.127	1101	384	7.10E-10	1304	0.032	1179	1	8.13E-5	1500
10:00	0.107	1333	1950	2.94E-5	1457	0.083	1272	396	0	1520
11:00	0.119	1692	2025	2.82E-5	1537	0.092	1570	296	2.31E-7	1670
12:00	0.159	1802	3110	1.38E-4	1574	0.127	1567	699	1.47E-6	1684
13:00	0.135	2142	2757	2.37E-8	1559	0.107	2048	442	0	1751
14:00	0.136	2068	3394	2.41E-5	1518	0.129	1939	521	2.43E-5	1584
15:00	0.382	3462	10592	1.88E-4	1412	0.224	3060	3727	2.85E-5	1643
16:00	0.310	3294	9175	9.12E-5	1266	0.215	3141	4236	2.38E-7	1450
17:00	0.290	3663	9432	3.62E-7	1163	0.216	3560	3687	0	1501
18:00	0.969	8090	31513	2.34E-4	1056	0.546	7746	16926	0	1335
19:00	1.205	9366	40862	2.31E-4	1027	0.668	8743	21995	1.08E-5	1379
20:00	1.328	8791	41484	5.57E-4	1015	0.680	8150	23618	1.02E-6	1318
21:00	**1.335**	**8198**	**36675**	**9.03E-4**	**1020**	**0.608**	**7635**	**19721**	**3.86E-5**	**1282**
22:00	0.590	5353	19040	5.40E-4	1019	0.518	5059	7720	1.27E-4	1371
23:00	0.280	3584	9033	1.25E-5	1017	0.185	3385	2455	0	1319
24:00	0.241	3024	7837	0	1017	0.182	3094	2491	6.87E-6	1411

Table 6.13 Optimization of the LV feeder at MV bus 46 over 24 hours. The highlighted green/red cells indicate decrease/increase of the value compared with the pervious case.

Time	ORIGINAL					OPTIMAL				
	F	$J_1/0.2$	$J_2/0.5$	$J_3/0.2$	$J_4/0.1$	F	$J_1/0.2$	$J_2/0.5$	$J_3/0.2$	$J_4/0.1$
00:00	0.233	2831	6397	1.12E-5	1016	0.144	2648	1821	5.68E-6	1090
01:00	0.192	2153	4262	4.70E-5	1016	0.115	1922	724	4.34E-6	1247
02:00	0.146	1919	3033	0	1016	0.110	1737	415	2.29E-5	1197
03:00	0.153	1900	3388	1.24E-6	1015	0.118	1977	684	2.98E-7	1319
04:00	0.148	1939	3087	5.09E-5	1015	0.125	1836	322	0	1275
05:00	0.103	1118	559	2.00E-5	1016	0.083	0.088	2	0	1421
06:00	0.088	1059	855	0	1027	0.080	1043	26	0	1201
07:00	0.073	838	170	0	1080	0.076	834	0	1.28E-13	1219
08:00	0.190	1041	365	2.78E-4	1156	0.084	1092	0	0	1339
09:00	0.094	1102	435	2.41E-8	1304	0.106	1095	1	4.07E-5	1408
10:00	0.152	1335	2122	3.73E-5	1457	0.109	1241	306	5.11E-7	1609
11:00	0.163	1694	2208	3.30E-5	1537	0.120	1528	306	2.74E-7	1708
12:00	0.236	1804	3366	1.61E-4	1574	0.131	1605	819	2.44E-6	1688
13:00	0.176	2145	2963	6.42E-8	1559	0.138	2124	599	0	1708
14:00	0.196	2071	3654	3.02E-5	1518	0.150	2046	1343	0	1694
15:00	0.429	3469	11174	2.12E-4	1412	0.222	2987	4184	3.57E-7	1670
16:00	0.352	3301	9716	1.05E-4	1266	0.215	3224	3953	5.75E-8	1522
17:00	0.321	3856	9984	5.30E-7	1163	0.233	3670	4190	0	1530
18:00	0.932	8110	32760	2.55E-4	1056	0.552	7744	16925	1.21E-5	1365
19:00	1.140	9393	42450	2.55E-4	1027	0.675	8768	22096	2.97E-6	1529
20:00	1.270	8816	43222	6.00E-4	1015	0.720	8212	25266	1.17E-5	1397
21:00	1.296	8219	38144	9.62E-4	1020	0.599	7478	17955	8.90E-5	1475
22:00	0.586	5363	19861	1.38E-4	1019	0.362	5134	9915	0	1404
23:00	0.302	3589	9437	0	1017	0.174	3216	2467	0	1241
24:00	0.324	3111	8222	0	1017	0.267	3028	2092	3.99E-4	1477

Table 6.14 Optimization of the LV feeder at MV bus 60 over 24 hours. The highlighted green/red cells indicate decrease/increase of the value compared with the pervious case.

Time	ORIGINAL					OPTIMAL				
	F	$J_1/0.2$	$J_2/0.5$	$J_3/0.2$	$J_4/0.1$	F	$J_1/0.2$	$J_2/0.5$	$J_3/0.2$	$J_4/0.1$
00:00	0.247	2839	7033	1.45E-5	1016	0.241	2749	1318	4.28E-4	1290
01:00	0.204	2158	4704	5.65E-5	1016	0.067	1994	1056	2.43E-6	1191
02:00	0.152	1923	3337	3.33E-5	1016	0.065	2045	400	0	1423
03:00	0.160	1905	3730	1.75E-6	1015	0.056	1826	684	4.49E-6	1173
04:00	0.154	1944	3400	1.91E-4	1015	0.122	2100	287	0	1574
05:00	0.085	1120	658	0	1016	0.026	1234	16	0	1245
06:00	0.090	1061	980	2.67E-11	1027	0.023	1103	1	0	1428
07:00	0.074	839	220	0	1080	0.017	808	0	4.17E-13	1166
08:00	0.164	1043	446	3.80E-4	1156	0.086	1105	0	0	1325
09:00	0.096	1104	539	1.94E-7	1304	0.023	1063	7	2.07E-7	1361
10:00	0.164	1338	2430	5.44E-5	1457	0.040	1235	606	0	1510
11:00	0.174	1699	2553	4.44E-5	1537	0.041	1563	357	7.30E-7	1650
12:00	0.263	1809	3831	2.09E-4	1574	0.055	1549	966	1.81E-6	1693
13:00	0.184	2151	3377	2.38E-7	1559	0.060	2147	665	0	1747
14:00	0.210	2077	4165	4.15E-5	1518	0.094	1979	437	1.15E-4	1762
15:00	0.470	3482	12314	2.62E-4	1412	0.189	3257	5325	0	1537
16:00	0.384	3315	10792	1.37E-4	1266	0.160	3188	4117	3.51E-7	1535
17:00	0.344	3685	11177	9.64E-7	1163	0.155	3562	3547	0	1427
18:00	1.004	8157	35641	3.00E-4	1056	0.502	7722	15000	3.25E-8	1692
19:00	1.235	9453	46019	3.26E-4	1027	0.717	8704	23523	5.60E-6	1537
20:00	1.382	8874	46971	7.09E-4	1015	0.933	8105	25836	4.83E-4	1323
21:00	1.406	8269	41367	1.09E-3	1020	0.835	7650	20520	5.66E-4	1389
22:00	0.630	5388	21670	1.61E-4	1019	0.307	4975	8506	2.58E-5	1322
23:00	0.319	3602	10354	1.79E-6	1017	0.159	3574	3667	0	1173
24:00	0.282	3038	9022	8.29E-7	1017	0.101	2639	2009	0	1340

D. Overall Performance Summary

1) Operational Performance Summary

Table 6.15 Overall comparison of optimization objectives. The highlighted green/red cells indicate decrease/increase of the value compared with the pervious case.

Time	ORIGINAL					OPTIMAL				
	F_s	$J_{1s}/0.2$	$J_{2s}/0.5$	$J_{3s}/0.2$	$J_{4s}/0.1$	F_s	$J_{1s}/0.2$	$J_{2s}/0.5$	$J_{3s}/0.2$	$J_{4s}/0.1$
00:00	1.248	1.47E5	6.94E6	1.53E-4	5.08E3	0.871	1.42E5	1.69E6	4.76E-4	6.06E3
01:00	0.991	1.09E5	5.66E6	3.41E-4	5.08E3	0.591	1.14E5	1.43E6	1.00E-4	6.09E3
02:00	0.806	8.98E4	4.07E6	2.35E-4	5.08E3	0.5	9.81E4	5.09E5	8.12E-5	6.35E3
03:00	0.908	9.11E4	4.66E6	3.66E-4	5.08E3	0.544	9.37E4	8.26E5	1.52E-4	6.25E3
04:00	0.817	8.92E4	4.25E6	2.85E-4	5.08E3	0.578	9.66E4	6.15E5	1.76E-4	6.68E3
05:00	0.509	5.81E4	2.63E6	8.14E-5	5.08E3	0.306	6.74E4	4.71E5	8.72E-5	6.30E3
06:00	0.51	5.76E4	3.25E6	3.15E-5	5.14E3	0.309	6.70E4	8.77E5	2.35E-4	6.18E3
07:00	0.447	4.59E4	2.83E6	6.88E-5	5.40E3	0.257	5.36E4	7.32E5	2.81E-4	5.74E3
08:00	0.77	4.80E4	2.99E6	9.50E-4	5.78E3	0.362	5.67E4	8.42E5	2.78E-4	6.50E3
09:00	0.608	5.60E4	3.40E6	3.15E-4	6.52E3	0.337	5.45E4	8.06E5	3.85E-4	7.07E3
10:00	0.842	7.28E4	6.26E6	8.17E-4	7.29E3	0.469	5.78E4	2.76E6	3.17E-4	7.70E3
11:00	0.921	9.56E4	6.63E6	8.97E-4	7.69E3	0.505	7.65E4	2.52E6	2.36E-4	8.22E3
12:00	1.203	1.03E5	8.17E6	1.49E-3	7.87E3	0.613	7.97E4	3.82E6	2.89E-4	8.47E3
13:00	0.984	1.21E5	6.92E6	2.87E-4	7.80E3	0.573	1.02E5	1.95E6	5.73E-5	8.64E3
14:00	1.072	1.25E5	8.16E6	5.74E-4	7.59E3	0.655	1.07E5	2.87E6	1.68E-4	8.27E3
15:00	2.135	2.03E5	1.26E7	1.41E-3	7.06E3	1.158	1.68E5	5.66E6	1.46E-4	8.22E3
16:00	1.844	2.18E5	1.24E7	8.91E-4	6.33E3	1.091	1.97E5	5.38E6	2.31E-4	7.46E3
17:00	1.737	2.60E5	1.23E7	3.02E-4	5.82E3	1.078	2.44E5	4.24E6	5.47E-5	7.35E3
18:00	4.678	4.76E5	1.87E7	1.51E-3	5.29E3	2.759	4.48E5	7.57E6	1.93E-4	7.42E3
19:00	5.719	5.46E5	2.26E7	1.75E-3	5.15E3	3.576	5.12E5	1.10E7	2.91E-4	7.21E3
20:00	6.25	5.50E5	2.68E7	2.89E-3	5.09E3	3.855	5.07E5	1.44E7	7.22E-4	6.77E3
21:00	6.209	4.76E5	2.24E7	4.33E-3	5.11E3	3.405	4.41E5	1.09E7	1.04E-3	6.92E3
22:00	2.981	3.14E5	1.48E7	1.32E-3	5.10E3	2.067	3.02E5	5.92E6	2.83E-4	6.56E3
23:00	1.589	2.00E5	8.48E6	1.28E-4	5.09E3	1.001	2.08E5	2.06E6	4.15E-5	6.25E3
24:00	1.477	1.61E5	8.74E6	7.87E-5	5.09E3	0.955	1.60E5	2.79E6	4.20E-4	6.73E3

As analysed in the sections A-C above, the proposed three-step hierarchical control strategy and optimization models have been proved to be feasible and effective on both the MV network and the LV feeders simulated. To demonstrate the performance of the proposed hierarchical strategy and optimization models on the whole distribution network scale, the corresponding values of each objective defined for both the step 2 optimization of the Forrestfield MV network and the step 3 optimization of all five LV feeders are summed up as follows:

$$F_s = F_{MV} + \sum_{j\in\tau} F_{LV}^{j}; \qquad J_{is} = J_{MVi} + \sum_{j\in\tau} J_{LVi}^{j} \tag{6.32}$$

where $i = 1,2,3,4$ is the number of the optimization objectives while τ is the set of distribution transformer buses, i.e. $j = 5, 25, 41, 46, 60$.

We can see from table 6.15 that after the proposed three-step hierarchical optimization, the distribution network has an improved overall operational performance comparing with the original case. Besides, the hierarchical optimization generates a similar control effect as that by directly applying the proposed weighted sum method based multi-objective optimization on the whole network scale. However, as analysed in section 1.1, direct optimization on the whole distribution network scale is unfeasible due to the extremely large problem dimension, especially when the network is unbalanced. By contrast, the proposed hierarchical optimization can ensure not only a better operational performance but also a superior computational performance which is proved in the following section.

2) Computational performance summary

The proposed three-step hierarchical optimization is simulated over 24 hours on a machine with an Intel Core i5 processor at 3.2 GHz. The average computation time for each simulation is around 443 s/7.38 min which includes 135 s/2.25 min for the MV optimization of step 2 (as analysed in chapter 3) and 308 s/5.13 min for the LV optimization at step 3 (as analysed in chapter 4) with the support of parallel computation. It is less than the 15 min data collection interval of smart meters

installed on the simulated distribution network and therefore the proposed hierarchical optimization can support real-time applications.

It should be noted that the computation time of step 1 optimization is not included in the total time of the proposed hierarchical optimization. This is firstly because, as discussed in section 6.2.1, the computation time is inversely proportional to the computation accuracy. Therefore, the computation time depends on the accuracy requirement of a practical problem. Most importantly, in practice, before applying the proposed hierarchical optimization, the calculation of step 1 is recommended to be performed in advance in an offline manner based on the historical data. For more details, see the discussion in the future work in the next Chapter 7.

6.4 CONCLUSIONS

Based on the work of chapters 3, 4 and 5, this chapter builds up the complete optimization models for each stage of the proposed three-step hierarchical control strategy. Then, detailed simulations on a real Western Australian distribution network of complexity are carried out. The simulation results at all the three steps confirm that the proposed hierarchical control strategy and optimization models are feasible and effective. Comparing with the direct optimization on the whole distribution network scale which is computationally unfeasible in practice, the proposed hierarchical optimization can generate a similar overall operational performance as well as have a superior computational performance for the real-time applications.

Chapter 7. Conclusions

This PhD thesis proposes a novel three-step hierarchical voltage, VAr and real power control strategy for the real-time optimal operation of both MV and LV networks with high complexity which is based on coordinated control of MV delta switched capacitors and LV PV inverters.

Chapter 1 reviews the latest changes within distribution networks, particularly in smart grid era, and their impacts on system control. Then, the advanced hierarchical control theory which can effectively handle system complexity is introduced with a brief review on its applications in power systems. On this basis, the knowledge gap is identified to set the direction of this thesis. Finally, by studying the physical structure of smart distribution networks, a novel hierarchical control strategy based on the coordination of MV and LV controllers is proposed to efficiently optimize the operation of distribution networks of high complexity.

Chapter 2 presents a comprehensive review on some most popular algorithms for solving the optimization problems of power systems which generally fall into two categories: constrained nonlinear programming problem (CNLP) and mixed integer nonlinear programming problem (MINLP). Based on careful comparison, two most promising methods (i.e. SQP and PSO) are selected to support the proposed hierarchical optimization. Besides, optimization of distribution networks often involves multiple mutually conflicting objectives. Thus, a review on the strategies which can effectively handle multi-objective optimization problems is also presented.

Chapter 3 focuses on the formulation of LV controller of the proposed hierarchical control. Specifically, based on the reactive capability and real power curtailment of inverters, a comprehensive PV control strategy as well as a multi-objective

optimization model are proposed to improve the operation of unbalanced three-phase four-wire LV distribution networks with high residential PV penetrations.

Chapter 4 builds up the MV controller of the proposed hierarchical control. Specifically, a comprehensive optimization based sequential strategy and a multi-objective optimization based real-time strategy are presented for the first time for the optimal placement and control of delta switched capacitors in unbalanced MV distribution networks.

In Chapter 5, an effective coordination interface for the LV and MV controllers is formulated based on the detailed analyses of the most common delta-grounded wye distribution transformer. Then, by combining this interface with the LV and MV controllers of Chapters 3 and 4, a complete three-step hierarchical control strategy is proposed to coordinate the control on LV and MV levels and optimize the operation of the whole distribution network at an affordable computational cost.

Chapter 6 of the thesis presents the detailed optimization models for each stage of the proposed three-step hierarchical control based on the studies of Chapters 3, 4 and 5. Then detailed simulations on a real unbalanced Western Australian distribution network of high complexity are performed over 24 hours. The analysis and comparison on the results in terms of both optimality and efficiency demonstrate the feasibility and effectiveness of the proposed hierarchical optimization with a superior computational performance for real-time applications.

Finally, this Chapter concludes the whole contents of the thesis by summarizing and highlighting main contributions and possible future research directions.

7.1 THESIS CONTRIBUTIONS

The main results of this thesis have been published in seven research papers [132-136, 161, 184]. The primary contributions are summarized as follow.

1) A comprehensive review on the most popular optimization methods for both CNLP and MINLP problems of power systems is presented providing a general reference for the optimization algorithms selection.

2) Based on the reactive and real control of inverters, a novel PV control strategy and a multi-objective optimization model are proposed for the operation improvement of unbalanced three-phase four-wire LV distribution feeders. Simulations on both HLLG and HGLL scenarios have verified the feasibility, effectiveness and accuracy of the proposed LV controller.
3) For the first time, a comprehensive optimization based sequential strategy and a multi-objective optimization based real-time strategy are presented for the optimal placement and control of delta switched capacitors in unbalanced MV distribution networks. By comparing with some existing popular schemes, the feasibility, validity and robustness of the proposed MV controller are verified.
4) Based on the detailed analyses of the most common delta-grounded wye distribution transformer, an effective interface in terms of voltages, currents and power is presented to connect and coordinate the control on MV and LV levels of distribution networks.
5) By combining the PV inverters control of LV feeders and the delta switched capacitors control of MV network as well as the coordination interface, a complete three-step hierarchical control strategy with detailed optimization models for each step is proposed to support the efficient operation optimization of unbalanced distribution networks of high complexity. Simulations on a real Western Australian distribution network have demonstrated the feasibility and effectiveness of the proposed hierarchical optimization with a superior computational performance for real-time applications.
6) The proposed hierarchical control not only generates a similar optimization effect as that by centralized control which, however, is computationally unfeasible in complex distribution networks, but also has a superior computational performance for real-time applications.
7) The proposed hierarchical strategy can support different groups of objectives as well as optimization algorithms on the MV and LV levels within one complete control, which significantly improves the control flexibility and capability.

7.2 FUTURE WORK

The following topics are suggested for future research in continuation of this work.

1) In step 1 of the proposed hierarchical control, a number of single-phase LV optimizations are performed at each hour to decide the reactive capability and the corresponding performance cost function of LV feeders by data fitting. However, in practice it is very time-consuming as well as unfeasible. Instead, based on the historical data, typical daily models of different periods of time (e.g. weekdays and weekends of four seasons) can be formed in advance and made ready for use.

2) A more comprehensive hierarchical coordination strategy and optimization model is needed to effectively and efficiently control all the related traditional and emerging devices within distribution networks. For example, in LV feeders, battery storage units can be added to operate in conjunction with PV systems while in MV networks, capacitors could cooperate with online tap changer equipped transformers, DSTATCOMs, voltage regulators and even wind turbines. By doing so, the capabilities of all the control devices could be fully exploited to further expand network load capacity and accommodate more renewable connections.

3) The proposed hierarchical coordination interface is based on the model analysis of the most common delta-grounded wye distribution transformer. To make the proposed hierarchical strategy more capable and applicable, similar analyses on other distribution transformers of different winding connections should be performed.

4) Currently, due to the unavailability of real power management devices in the MV network, the proposed hierarchical optimization only performs real power control in the LV feeders (Chapter 3). With the connections of batteries on both LV and MV levels, a complete hierarchical real power optimization can be performed on the whole distribution network scale.

5) In addition, the application of the proposed hierarchical control can be well supported by the use of the multi-agent system. In a multi-agent system, both the

MV controller and the LV controllers are treated as agents who sense the network changes and work actively on the network to achieve the defined control objectives on each level. The introduction of the multi-agent system could further increase computation speed and decrease communication cost.

References

Every reasonable effort has been made to acknowledge the owners of copyright material. I would be pleased to hear from any copyright owner who has been omitted or incorrectly acknowledged.

[1] Australian Energy Regulator (AER) (2012). State of the energy market 2012 [Online]. Available at http://www.aer.gov.au/node/18959.

[2] Department of Resources Energy and Tourism (DRET) (2012). Energy white paper 2012 Australia's energy transformation [Online]. Available at http:// www.ret.gov.au/energy/facts/white_paper/Pages/energy_white_paper.aspx.

[3] M. J. E. Alam, K. M. Muttaqi, and D. Sutanto, "Mitigation of rooftop solar PV impacts and evening peak support by managing available capacity of distributed energy storage systems," *IEEE Trans. Power Systems,* vol. 28, pp. 3874-3884, 2013.

[4] M. J. E. Alam, K. M. Muttaqi, and D. Sutanto, "An approach for online assessment of rooftop solar PV impacts on low-voltage distribution networks," *IEEE Trans. Sustainable Energy,* vol. 5, pp. 663-672, 2014.

[5] H. Pezeshki, P. J. Wolfs, and G. Ledwich, "Impact of high PV penetration on distribution transformer insulation life," *IEEE Trans. Power Delivery,* vol. 29, pp. 1212-1220, 2014.

[6] M. Thomson and D. G. Infield, "Impact of widespread photovoltaics generation on distribution systems," *IET Renewable Power Generation,* vol. 1, pp. 33-40, 2007.

[7] J. Kabouris and F. D. Kanellos, "Impacts of large-scale wind penetration on designing and operation of electric power systems," *IEEE Trans. Sustainable Energy,* vol. 1, pp. 107-114, 2010.

[8] F. Vallee, J. Lobry, and O. Deblecker, "System reliability assessment method for wind power integration," *IEEE Trans. Power Systems,* vol. 23, pp. 1288-1297, 2008.

[9] P. Siano and G. Mokryani, "Probabilistic assessment of the impact of wind energy integration into distribution networks," *IEEE Trans. Power Systems,* vol. 28, pp. 4209-4217, 2013.

[10] E. Sortomme, M. M. Hindi, S. D. J. MacPherson, and S. S. Venkata, "Coordinated charging of plug-in hybrid electric vehicles to minimize distribution system losses," *IEEE Trans. Smart Grid,* vol. 2, pp. 198-205, 2011.

[11] F. Pieltain, X, L. Ndez, Roma, X, T. G. S. N, *et al.*, "Assessment of the impact of plug-in electric vehicles on distribution networks," *IEEE Trans. Power Systems*, vol. 26, pp. 206-213, 2011.

[12] P. Richardson, D. Flynn, and A. Keane, "Optimal charging of electric vehicles in low-voltage distribution systems," *IEEE Trans. Power Systems*, vol. 27, pp. 268-279, 2012.

[13] S. Deilami, A. S. Masoum, P. S. Moses, and M. A. S. Masoum, "Real-time coordination of plug-in electric vehicle charging in smart grids to minimize power losses and improve voltage profile," *IEEE Trans. Smart Grid*, vol. 2, pp. 456-467, 2011.

[14] X. Yixing and C. Singh, "Adequacy and economy analysis of distribution systems integrated with electric energy storage and renewable energy resources," *IEEE Trans. Power Systems*, vol. 27, pp. 2332-2341, 2012.

[15] S. Grillo, M. Marinelli, S. Massucco, and F. Silvestro, "Optimal management strategy of a battery-based storage system to improve renewable energy integration in distribution networks," *IEEE Trans. Smart Grid*, vol. 3, pp. 950-958, 2012.

[16] K. Worthmann, C. M. Kellett, P. Braun, L. Grune, and S. R. Weller, "Distributed and decentralized control of residential energy systems incorporating battery storage," *IEEE Trans. Smart Grid*, vol. PP, pp. 1-10, 2015.

[17] *Statement of Policy on Modernization of Electricity Grid*, Energy Independence & Security Act ’07, 2007.

[18] K. S. Reddy, M. Kumar, T. K. Mallick, H. Sharon, and S. Lokeswaran, "A review of integration, control, communication and metering (ICCM) of renewable energy based smart grid," *Renewable and Sustainable Energy Reviews*, vol. 38, pp. 180-192, 2014.

[19] M. D. Mesarovic, D. Macko, and Y. Takahara, *Theory of Hierarchical Multilevel Systems*, New York: Academic, 1970.

[20] W. Findeisen, M. Brdys, K. Malinowski, P. Tatjewski, and A. Wozniak, "On-line hierarchical control for steady-state systems," *IEEE Trans. Automatic Control*, vol. 23, pp. 189-209, 1978.

[21] W. Findeisen, F. N. Bailey, M. Bryds, K. Malinowski, P. Tatjewski, and A. Wozniak, *Control and Coordination in Hierarchical Systems*, John Wiley & Sons Ltd, 1980.

[22] S. K. Mitter and F. C. Schwepe, "Hierarchical system theory and electric power systems," in *Proc. the Symposium on Real-time Control of Electric Power Systems*, 1972, pp. 259-277.

[23] G. Ruipeng, C. Hsiao-Dong, W. Hao, L. Kewen, and D. Yong, "A two-level system-wide automatic voltage control system," in *Proc. 2012 IEEE Power and Energy Society General Meeting*, 2012, pp. 1-6.

[24] Q. Guo, H. Sun, B. Wang, B. Zhang, W. Wu, and L. Tang, "Hierarchical automatic voltage control for integration of large-scale wind power: design and implementation," *Electric Power Systems Research*, vol. 120, pp. 234-241, 2015.

[25] C. Xingong, Z. Yong, C. Lixia, L. Jiwen, S. Tao, and Z. Sheng, "A real-time hierarchical and distributed control scheme for reactive power optimization in multi-area power systems," in *Proc. 2005 IEEE/PES Transmission and Distribution Conference and Exhibition: Asia and Pacific*, 2005, pp. 1-6.

[26] M. Rahmani and N. Sadati, "Hierarchical optimal robust load-frequency control for power systems," *IET Generation, Transmission & Distribution*, vol. 6, pp. 303-312, 2012.

[27] S. Corsi, M. Pozzi, C. Sabelli, and A. Serrani, "The coordinated automatic voltage control of the Italian transmission grid - part I: reasons of the choice and overview of the consolidated hierarchical system," *IEEE Trans. Power Systems*, vol. 19, pp. 1723-1732, 2004.

[28] F. Katiraei and M. R. Iravani, "Power management strategies for a microgrid with multiple distributed generation units," *IEEE Trans. Power Systems*, vol. 21, pp. 1821-1831, 2006.

[29] Y. A. R. I. Mohamed and A. A. Radwan, "Hierarchical control system for robust microgrid operation and seamless mode transfer in active distribution systems," *IEEE Trans. Smart Grid*, vol. 2, pp. 352-362, 2011.

[30] J. M. Guerrero, M. Chandorkar, T. Lee, and P. C. Loh, "Advanced control architectures for intelligent microgrids - part I: decentralized and hierarchical control," *IEEE Trans. Industrial Electronics*, vol. 60, pp. 1254-1262, 2013.

[31] T. L. Vandoorn, J. C. Vasquez, J. De Kooning, J. M. Guerrero, and L. Vandevelde, "Microgrids: hierarchical control and an overview of the control and reserve management strategies," *IEEE Industrial Electronics Magazine*, vol. 7, pp. 42-55, 2013.

[32] A. Bidram and A. Davoudi, "Hierarchical structure of microgrids control system," *IEEE Trans. Smart Grid*, vol. 3, pp. 1963-1976, 2012.

[33] L. Lin, L. Junyong, and W. Jiajia, "A distributed hierarchical structure optimization algorithm based poly-particle swarm for reconfiguration of distribution network," in *Proc. 2009 International Conference on Sustainable Power Generation and Supply*, 2009, pp. 1-5.

[34] F. Ding and K. A. Loparo, "Hierarchical decentralized network reconfiguration for smart distribution systems - part I: problem formulation and algorithm development," *IEEE Trans. Power Systems*, vol. 30, pp. 734-743, 2015.

[35] Y. Qudaih and T. Hiyama, "Reconfiguration of power distribution system using multi agent and hierarchical based load following operation with energy capacitor system," in *Proc. 2007 International Power Engineering Conference*, 2007, pp. 223-227.

[36] M. Baran and T. E. McDermott, "Distribution system state estimation using AMI data," in *Proc. 2009 IEEE/PES Power Systems Conference and Exposition*, 2009, pp. 1-3.

[37] M. Braun, G. Arnold, and H. Laukamp, "Plugging into the zeitgeist," *IEEE Power and Energy Magazine*, vol. 7, pp. 63-76, 2009.

[38] P. Wolfs, "An economic assessment of second-use lithium-ion batteries for grid support," in *Proc. 2010 20th Australasian Universities Power Engineering Conference (AUPEC)*, 2010, pp. 1-6.

[39] X. Liang, C. Hsiao-Dong, and L. Shao-Hua, "Optimal power flow calculation of power system with wind farms," in *proc. 2011 IEEE Power and Energy Society General Meeting*, 2011, pp. 1-6.

[40] L. Mingbo, S. K. Tso, and C. Ying, "An extended nonlinear primal-dual interior-point algorithm for reactive-power optimization of large-scale power systems with discrete control variables," *IEEE Trans. Power Systems*, vol. 17, pp. 982-991, 2002.

[41] L. Duehee, K. Joonhyun, and R. Baldick, "Stochastic optimal control of the storage system to limit ramp rates of wind power output," *IEEE Trans. Smart Grid*, vol. 4, pp. 2256-2265, 2013.

[42] T. Ding, R. Bo, F. Li, Y. Gu, Q. Guo, and H. Sun, "Exact penalty function based constraint relaxation method for optimal power flow considering wind generation uncertainty," *IEEE Trans. Power Systems*, vol. 30, pp. 1546-1547, 2014.

[43] A. P. Mazzini and E. N. Asada, "A penalty function for reactive power optimization with discrete variables," in *Proc. 2014 IEEE PES General Meeting|Conference & Exposition*, 2014, pp. 1-5.

[44] H. Ambriz-Perez, E. Acha, C. R. Fuerte-Esquivel, and A. De La Torre, "Incorporation of a UPFC model in an optimal power flow using Newton's method," *IEE Proceedings-Generation, Transmission and Distribution*, vol. 145, pp. 336-344, 1998.

[45] A. Pazderin and S. Yuferev, "Power flow calculation by combination of Newton-Raphson method and Newton's method in optimization," in *Proc. 35th Annual Conference of IEEE Industrial Electronics*, 2009, pp. 1693-1696.

[46] A. V. Pazderin and S. V. Yuferev, "Steady-state calculation of electrical power system by the Newton's method in optimization," in *Proc. 2009 IEEE Bucharest PowerTech*, 2009, pp. 1-6.

[47] D. I. Sun, B. Ashley, B. Brewer, A. Hughes, and W. F. Tinney, "Optimal power flow by Newton approach," *IEEE Trans. Power Apparatus and Systems*, vol. PAS-103, pp. 2864-2880, 1984.

[48] D. I. Sun, T. I. Hu, G.-S. Lin, C.-J. Lin, and C.-M. Chen, "Experiences with implementing optimal power flow for reactive scheduling in the Taiwan power system," *IEEE Trans. Power Systems*, vol. 3, pp. 1193-1120, 1988.

[49] M. Hestenes and E. Stiefel, "Methods of conjugate gradients for solving linear systems," *Journal of Research of the National Bureau of Standards*, vol. 49, pp. 409-436, 1952.

[50] R. Fletcher and C. M. Reeves, "Function minimization by conjugate gradients," *The Computer Journal*, vol. 7, pp. 149-154, 1964.

[51] S. Kilyeni, P. Andea, M. Groza, and C. Barbulescu, "Optimal compensation of radial networks part II: optimisation problem's solution," in *Proc. The International Conference on Computer as a Tool*, 2005, pp. 1517-1520.

[52] S. Kilyeni, P. Andea, M. Groza, and C. Barbulescu, "Optimal compensation of radial networks part I: the calculation of state variables," in *Proc. The International Conference on Computer as a Tool,* 2005, pp. 1513-1516.

[53] S. Q. Yuan and D. Z. Fang, "Robust PSS parameters design using a trajectory sensitivity approach," *IEEE Trans. Power Systems,* vol. 24, pp. 1011-1018, 2009.

[54] T. S. Halliburton and H. R. Sirisena, "Long-term optimal operation of a power system," *IEE Proceedings-Generation, Transmission and Distribution,* vol. 129, pp. 185-191, 1982.

[55] C. R. Gagnon and J. F. Bolton, "Optimal hydro scheduling at the Bonneville power administration," *IEEE Trans. Power Apparatus and Systems,* vol. PAS-97, pp. 772-776, 1978.

[56] W. Sun, *Optimization Theory and Methods : Nonlinear Programming,* Boston, MA : Springer US, 2006.

[57] M. Bartholomew-Biggs, *Nonlinear Optimization with Engineering Applications,* Boston, MA : Springer US, 2008.

[58] H. K. Alaei, A. Yazdizadeh, and A. Aliabadi, "Nonlinear predictive controller design for load frequency control in power system using quasi Newton optimization approach," in *Proc. 2013 IEEE International Conference on Control Applications*, 2013, pp. 679-684.

[59] C. J. Rehn, J. A. Bubenko, and D. Sjelvgren, "Voltage optimization using augmented Lagrangian functions and quasi-Newton techniques," *IEEE Trans. Power Systems,* vol. 4, pp. 1470-1483, 1989.

[60] S. Bruno, S. Lamonaca, G. Rotondo, U. Stecchi, and M. La Scala, "Unbalanced three-phase optimal power flow for smart grids," *IEEE Trans. Industrial Electronics,* vol. 58, pp. 4504-4513, 2011.

[61] F. Liu, Y. H. Song, J. Ma, S. Mei, and Q. Lu, "Optimal load-frequency control in restructured power systems," *IEE Proceedings-Generation, Transmission and Distribution,* vol. 150, pp. 87-95, 2003.

[62] X.-M. Mao, Y. Zhang, L. Guan, and X. Wu, "Researches on coordinated control strategy for inter-area oscillations in AC/DC hybrid grid with multi-infeed HVDC," in *Proc. 2005 IEEE/PES Transmission and Distribution Conference and Exhibition: Asia and Pacific,* 2005, pp. 1-6.

[63] R. Frisch and U. I. O. Economics, "The logarithmic potential method of convex programming with particular application to the dynamics of planning for national development", In *Proc. the International Colloquium of Econometrics*, 1955, pp. 337-371.

[64] A. V. Fiacco and G. P. McCormick, *Nonlinear programming: sequential unconstrained minimization techniques*: Wiley, 1968.

[65] N. Karmarkar, "A new polynomial-time algorithm for linear programming," *Combinatorica,* vol. 4, pp. 373-395, 1984.

[66] V. H. Quintana, G. L. Torres, and J. Medina-Palomo, "Interior-point methods and their applications to power systems: a classification of publications and software codes," *IEEE Trans. Power Systems,* vol. 15, pp. 170-176, 2000.

[67] I. A. Farhat and M. E. El-hawary, "Interior point methods application in optimum operational scheduling of electric power systems," *IET Generation, Transmission & Distribution*, vol. 3, pp. 1020-1029, 2009.

[68] G. D. Irisarri, X. Wang, J. Tong, and S. Mokhtari, "Maximum loadability of power systems using interior point nonlinear optimization method," *IEEE Trans. Power Systems*, vol. 12, pp. 162-172, 1997.

[69] Y. Wang and Q. Jiang, "Reactive power optimizatin of distribution network based on primal-dual interior point method and simplified branch and bound method," in *Proc. 2014 IEEE PES T&D Conference and Exposition*, 2014, pp. 1-4.

[70] K. Xie and Y. H. Song, "Power market oriented optimal power flow via an interior point method," *IEE Proceedings-Generation, Transmission and Distribution*, vol. 148, pp. 549-556, 2001.

[71] R. A. Jabr, "Radial distribution load flow using conic programming," *IEEE Trans. Power Systems*, vol. 21, pp. 1458-1459, 2006.

[72] R. Singh, B. C. Pal, R. A. Jabr, and P. D. Lang, "Distribution system load flow using primal dual interior point method," in *Proc. 2008 Joint International Conference on Power System Technology and IEEE Power India Conference*, 2008, pp. 1-5.

[73] M. B. Liu, C. A. Canizares, and W. Huang, "Reactive power and voltage control in distribution systems with limited switching operations," *IEEE Trans. Power Systems*, vol. 24, pp. 889-899, 2009.

[74] X. Kai and Y. H. Song, "Optimal power flow with time-related constraints by a nonlinear interior point method," in *Proc. 2000 IEEE Power Engineering Society Winter Meeting*, 2000, pp. 1751-1759.

[75] J. A. Momoh, L. G. Dias, S. X. Guo, and R. Adapa, "Economic operation and planning of multi-area interconnected power systems," *IEEE Trans. Power Systems*, vol. 10, pp. 1044-1053, 1995.

[76] H. Jin-Lin, W. Zhipeng, H. McCann, L. E. Davis, and X. Cheng-Gang, "Sequential quadratic programming method for solution of electromagnetic inverse problems," *IEEE Trans. Antennas and Propagation*, vol. 53, pp. 2680-2687, 2005.

[77] Z. Renjun, Z. Yanping, and L. Jianhua, "Reactive power optimization algorithm based on trust-region global SQP," in *Proc. IEEE 2006 Power Engineering Society General Meeting*, 2006, pp. 1-5.

[78] R. B. Wilson, "A simplicial algorithm for concave programming," P.h.D. dissertation, Graduate School of Business Administration, George F. Baker Foundation, Harvard University, 1963.

[79] W. Hock and K. Schittkowski, *Test Examples for Nonlinear Programming Codes*, Springer-Verlag, 1981.

[80] I. M. Nejdawi, K. A. Clements, and P. W. Davis, "An efficient interior point method for sequential quadratic programming based optimal power flow," *IEEE Trans. Power Systems*, vol. 15, pp. 1179-1183, 2000.

[81] C. Lehmkoster, "Security constrained optimal power flow for an economical operation of FACTS-devices in liberalized energy markets," *IEEE Trans. Power Delivery*, vol. 17, pp. 603-608, 2002.

[82] S. Wanxing, L. Ke-yan, and C. Sheng, "Optimal power flow algorithm and analysis in distribution system considering distributed generation," *IET Generation, Transmission & Distribution*, vol. 8, pp. 261-272, 2014.

[83] V. Calderaro, V. Galdi, F. Lamberti, and A. Piccolo, "A smart strategy for voltage control ancillary service in distribution networks," *IEEE Trans. Power Systems*, vol. 30, pp. 494-502, 2015.

[84] W. Sheng, K. Y. Liu, S. Cheng, X. Meng, and W. Dai, "A trust region SQP method for coordinated voltage control in smart distribution grid," *IEEE Trans. Smart Grid*, vol. PP, pp. 1-11, 2015.

[85] M. F. AlHajri and M. E. El-Hawary, "Optimal distribution generation sizing via fast sequential quadratic programming," in *Proc. 2007 Large Engineering Systems Conference on Power Engineering*, 2007, pp. 63-66.

[86] Q. H. Wu and J. T. Ma, "Power system optimal reactive power dispatch using evolutionary programming," *IEEE Trans. Power Systems*, vol. 10, pp. 1243-1249, 1995.

[87] T. Bäck, *Evolutionary Algorithms in Theory and Practice: Evolution Strategies, Evolutionary Programming, Genetic Algorithms*, New York : Oxford University Press, 1996.

[88] V. Gopalakrishnan, P. Thirunavukkarasu, and R. Prasanna, "Reactive power planning using hybrid evolutionary programming method," in *Proc. IEEE PES 2004 Power Systems Conference and Exposition*, 2004, pp. 1319-1323 .

[89] K. Y. Lee and F. F. Yang, "Optimal reactive power planning using evolutionary algorithms: a comparative study for evolutionary programming, evolutionary strategy, genetic algorithm, and linear programming," *IEEE Trans. Power Systems*, vol. 13, pp. 101-108, 1998.

[90] L. L. Lai and J. T. Ma, "Application of evolutionary programming to reactive power planning - comparison with nonlinear programming approach," *IEEE Trans. Power Systems*, vol. 12, pp. 198-206, 1997.

[91] S. Kirkpatrick, "Optimization by simulated annealing: quantitative studies," *Journal of Statistical Physics*, vol. 34, pp. 975-986, 1984.

[92] V. Černý, "Thermodynamical approach to the traveling salesman problem: an efficient simulation algorithm," *Journal of Optimization Theory and Applications*, vol. 45, pp. 41-51, 1985.

[93] M. Eslami, H. Shareef, and A. Mohamed, "Power system stabilizer design based on optimization techniques," in *Proc. 2011 4th International Conf. on Modeling, Simulation and Applied Optimization*, 2011, pp. 1-7.

[94] L. H. Hassan, M. Moghavvemi, and H. A. F. Mohamed, "Power system stabilization based on artificial intelligent techniques: a review," in *Proc. 2009 International Conference for Technical Postgraduates*, 2009, pp. 1-6.

[95] M. A. Abido, "Robust design of multimachine power system stabilizers using simulated annealing," *IEEE Trans. Energy Conversion*, vol. 15, pp. 297-304, 2000.

[96] Z. Jinxiang, G. Bilbro, and C. Mo-Yuen, "Phase balancing using simulated annealing," *IEEE Trans. Power Systems*, vol. 14, pp. 1508-1513, 1999.
[97] W. Yurong, L. Fangxing, W. Qiulan, and C. Hao, "Reactive power planning based on fuzzy clustering, gray code, and simulated annealing," *IEEE Trans. Power Systems*, vol. 26, pp. 2246-2255, 2011.
[98] J. P. F. Trovao, V. D. N. Santos, P. G. Pereirinha, H. M. Jorge, and C. H. Antunes, "A simulated annealing approach for optimal power source management in a small EV," *IEEE Trans. Sustainable Energy*, vol. 4, pp. 867-876, 2013.
[99] A. P. Alves da Silva and P. J. Abrao, "Applications of evolutionary computation in electric power systems," in *Proc. the 2002 Congress on Evolutionary Computation*, 2002, pp. 1057-1062.
[100] Z. Wenjuan, L. Fangxing, and L. M. Tolbert, "Review of reactive power planning: objectives, constraints, and algorithms," *IEEE Trans. Power Systems*, vol. 22, pp. 2177-2186, 2007.
[101] D. P. Kothari, "Power system optimization," in *Proc. 2012 2nd National Conference on Computational Intelligence and Signal Processing*, 2012, pp. 18-21.
[102] Y. L. Abdel-Magid, M. A. Abido, and A. H. Mantaway, "Robust tuning of power system stabilizers in multimachine power systems," *IEEE Trans. Power Systems*, vol. 15, pp. 735-740, 2000.
[103] L. Whei-Min, C. Fu-Sheng, and T. Ming-Tong, "An improved tabu search for economic dispatch with multiple minima," *IEEE Trans. Power Systems*, vol. 17, pp. 108-112, 2002.
[104] H. Mori and Y. Iimura, "Dual tabu search for capacitor control in distribution systems," in *Porc. 2004 IEEE PES Power Systems Conference and Exposition*, 2004, pp. 1434-1439.
[105] Y. Nakachi, A. Kato, and H. Ukai, "Voltage/reactive power control optimization with economy and security using tabu search," in *Porc. IEEE 22nd International Symposium on Intelligent Control*, 2007, pp. 634-639.
[106] Y. Zou, "Optimal reactive power planning based on improved tabu search algorithm," in *Proc. 2010 International Conference on Electrical and Control Engineering*, 2010, pp. 3945-3948.
[107] G. Granelli, M. Montagna, F. Zanellini, P. Bresesti, and R. Vailati, "A genetic algorithm-based procedure to optimize system topology against parallel flows," *IEEE Trans. Power Systems*, vol. 21, pp. 333-340, 2006.
[108] A. R. Jordehi and J. Jasni, "Heuristic methods for solution of FACTS optimization problem in power systems," in *Proc. 2011 IEEE Student Conference on Research and Development*, 2011, pp. 30-35.
[109] L. Furong, J. D. Pilgrim, C. Dabeedin, A. Chebbo, and R. K. Aggarwal, "Genetic algorithms for optimal reactive power compensation on the national grid system," *IEEE Trans. Power Systems*, vol. 20, pp. 493-500, 2005.
[110] J. E. Mendoza, D. A. Morales, R. A. Lopez, E. A. Lopez, J. C. Vannier, and C. A. C. Coello, "Multiobjective location of automatic voltage regulators in a

radial distribution network using a micro genetic algorithm," *IEEE Trans. Power Systems*, vol. 22, pp. 404-412, 2007.

[111] L. M. O. Queiroz and C. Lyra, "Adaptive hybrid genetic algorithm for technical loss reduction in distribution networks under variable demands," *IEEE Trans. Power Systems*, vol. 24, pp. 445-453, 2009.

[112] J. Kennedy and R. Eberhart, "Particle swarm optimization," in *Proc. IEEE International Conference on Neural Networks*, 1995, pp. 1942-1948.

[113] W. Wu-Chang, T. Men-Shen, and H. Fu-Yuan, "A new binary coding particle swarm optimization for feeder reconfiguration," in *Proc. International Conf. on Intelligent Systems Applications to Power Systems*, 2007, pp. 1-6.

[114] R. C. Eberhart and S. Yuhui, "Particle swarm optimization: developments, applications and resources," in *Proc. the 2001 Congress on Evolutionary Computation*, 2001, pp. 81-86.

[115] Y. del Valle, G. K. Venayagamoorthy, S. Mohagheghi, J. C. Hernandez, and R. G. Harley, "Particle swarm optimization: basic concepts, variants and applications in power systems," *IEEE Trans. Evolutionary Computation,* vol. 12, pp. 171-195, 2008.

[116] D. Vijayakumar and R. K. Nema, "Superiority of PSO relay coordination algorithm over non-linear programming: a comparison, review and verification," in *Proc. Joint International Conference on Power System Technology and IEEE Power India Conference*, 2008, pp. 1-6.

[117] O. Chao and L. Weixing, "Comparison between PSO and GA for parameters optimization of PID controller," in *Proc. 2006 IEEE International Conference on Mechatronics and Automation*, 2006, pp. 2471-2475.

[118] O. Naing Win, "A comparison study on particle swarm and evolutionary particle swarm optimization using capacitor placement problem," in *Proc. IEEE 2nd International Power and Energy Conference*, 2008, pp. 1208-1211.

[119] R. Dubey, S. Dixit, and G. Agnihotri, "Optimal placement of shunt FACTs devices using heuristic optimization techniques: an overview," in *Proc. 2014 Fourth International Conference on Communication Systems and Network Technologies*, 2014, pp. 518-523.

[120] H. Yoshida, K. Kawata, Y. Fukuyama, S. Takayama, and Y. Nakanishi, "A particle swarm optimization for reactive power and voltage control considering voltage security assessment," *IEEE Trans. Power Systems*, vol. 15, pp. 1232-1239, 2000.

[121] A. A. A. Esmin, G. Lambert-Torres, and A. C. Z. de Souza, "A hybrid particle swarm optimization applied to loss power minimization," *IEEE Trans. Power Systems*, vol. 20, pp. 859-866, 2005.

[122] B. Zhao, C. X. Guo, and Y. J. Cao, "A multiagent-based particle swarm optimization approach for optimal reactive power dispatch," *IEEE Trans. Power Systems*, vol. 20, pp. 1070-1078, 2005.

[123] I. Ziari, G. Ledwich, A. Ghosh, and G. Platt, "Optimal control of distributed generators and capacitors by hybrid DPSO," in *Proc. 2011 21st Australasian Universities Power Engineering Conference*, 2011, pp. 1-6.

[124] Matlab Global Optimization Toolbox: Global Search and Multistart solvers. (2014). MathWorks, Inc. Natick, MA. [Online]. Available: http://www. mathworks.com.au/ products/globaloptimization/description3.html

[125] L. Thu Bui, *Multi-Objective Optimization in Computational Intelligence: Theory and Practice*, Information Science Reference, 2008.

[126] N. M. Pindoriya, S. N. Singh, and K. Y. Lee, "A comprehensive survey on multi-objective evolutionary optimization in power system applications," in *Proc. 2010 IEEE Power and Energy Society General Meeting*, 2010, pp. 1-8.

[127] J. H. Van Sickel and K. Y. Lee, "Pareto optimization with reverse normal-boundary intersection for power plant models," in *Proc. 2010 IEEE Power and Energy Society General Meeting*, 2010, pp. 1-6.

[128] M. O. W. Grond, N. H. Luong, J. Morren, and J. G. Slootweg, "Multi-objective optimization techniques and applications in electric power systems," in *Proc. 2012 47th International Universities Power Engineering Conference*, 2012, pp. 1-6.

[129] R. T. Marler and J. Arora, "The weighted sum method for multi-objective optimization: new insights," *Structural and Multidisciplinary Optimization*, vol. 41, pp. 853-862, 2010.

[130] I. Y. Kim and O. L. de Weck, "Adaptive weighted sum method for multiobjective optimization: a new method for Pareto front generation," *Structural and Multidisciplinary Optimization*, vol. 31, pp. 105-116, 2006.

[131] A. M. Jubril, O. A. Komolafe, and K. O. Alawode, "Solving multi-objective economic dispatch problem via semidefinite programming," *IEEE Trans. Power Systems*, vol. 28, pp. 2056-2064, 2013.

[132] X. Su, M. A. S. Masoum, and P. Wolfs, "PSO based multi-objective optimization of unbalanced lv distribution network by PV inverter control," in *Proc. 2014 China International Conference on Electricity Distribution (CICED)*, 2014, pp. 1744-1748.

[133] X. Su, M. A. S. Masoum, and P. Wolfs, "Comprehensive optimization of PV inverter reactive and real power flows in unbalanced four wire LV distribution network operations," in *Proc. 2013 IEEE Power and Energy Society General Meeting (PES)*, 2013, pp. 1-5.

[134] X. Su, P. Wolfs, and M. A. S. Masoum, "Optimal operation of multiple unbalanced distributed generation sources in three-phase four-wire LV distribution networks," in *Proc. 2012 22nd Australasian Universities Power Engineering Conference (AUPEC)*, 2012, pp. 1-6.

[135] X. Su, M. A. S. Masoum, and P. J. Wolfs, "Optimal PV inverter reactive power control and real power curtailment to improve performance of unbalanced four-wire LV distribution networks," *IEEE Trans. Sustainable Energy*, vol. 5, pp. 967-977, 2014.

[136] X. Su, M. A. S. Masoum, and P. Wolfs, "Comprehensive optimal photovoltaic inverter control strategy in unbalanced three-phase four-wire low voltage distribution networks," *IET Generation, Transmission & Distribution*, vol. 8, pp. 1848-1859, 2014.

[137] P. M. S. Carvalho, P. F. Correia, and L. A. F. Ferreira, "Distributed reactive power generation control for voltage rise mitigation in distribution networks," *IEEE Trans. Power Systems*, vol. 23, pp. 766-772, 2008.
[138] K. H. Chua, L. Yun Seng, P. Taylor, S. Morris, and W. Jianhui, "Energy storage system for mitigating voltage unbalance on low-voltage networks with photovoltaic systems," *IEEE Trans. Power Delivery*, vol. 27, pp. 1783-1790, 2012.
[139] K. Tanaka, M. Oshiro, S. Toma, A. Yona, T. Senjyu, T. Funabashi, *et al.*, "Decentralised control of voltage in distribution systems by distributed generators," *IET Generation, Transmission & Distribution*, vol. 4, pp. 1251-1260, 2010.
[140] Y. Hen-Geul, D. F. Gayme, and S. H. Low, "Adaptive VAR control for distribution circuits with photovoltaic generators," *IEEE Trans. Power Systems*, vol. 27, pp. 1656-1663, 2012.
[141] L. Xiaohu, A. Aichhorn, L. Liming, and L. Hui, "Coordinated control of distributed energy storage system with tap changer transformers for voltage rise mitigation under high photovoltaic penetration," *IEEE Trans. Smart Grid*, vol. 3, pp. 897-906, 2012.
[142] M. Farivar, R. Neal, C. Clarke, and S. Low, "Optimal inverter VAR control in distribution systems with high PV penetration," in *Proc. 2012 IEEE Power and Energy Society General Meeting*, 2012, pp. 1-7.
[143] E. Dall'Anese, S. V. Dhople, and G. B. Giannakis, "Optimal dispatch of photovoltaic inverters in residential distribution systems," *IEEE Trans. Sustainable Energy*, vol. 5, pp. 487-497, 2014.
[144] E. Dall'Anese, G. B. Giannakis, and B. F. Wollenberg, "Optimization of unbalanced power distribution networks via semidefinite relaxation," in *Proc. North American Power Symposium*, 2012, pp. 1-6.
[145] P. Sulc, S. Backhaus, and M. Chertkov, "Optimal distributed control of reactive power via the alternating direction method of multipliers," *IEEE Trans. Energy Conversion*, vol. 29, pp. 968-977, 2014.
[146] E. Demirok, G. Casado, x, P. lez, K. H. B. Frederiksen, D. Sera, *et al.*, "Local reactive power control methods for overvoltage prevention of distributed solar inverters in low-voltage grids," *IEEE Journal of Photovoltaics*, vol. 1, pp. 174-182, 2011.
[147] R. Aghatehrani and A. Golnas, "Reactive power control of photovoltaic systems based on the voltage sensitivity analysis," in *Proc. 2012 IEEE Power and Energy Society General Meeting*, 2012, pp. 1-5.
[148] P. Jahangiri and D. C. Aliprantis, "Distributed Volt/VAr control by PV inverters," *IEEE Trans. Power Systems*, vol. 28, pp. 3429-3439, 2013.
[149] J. Yuryevich and W. Kit Po, "Evolutionary programming based optimal power flow algorithm," *IEEE Trans. Power Systems*, vol. 14, pp. 1245-1250, 1999.
[150] D. Gan, R. J. Thomas, and R. D. Zimmerman, "Stability-constrained optimal power flow," *IEEE Trans. Power Systems*, vol. 15, pp. 535-540, 2000.

[151] K. Turitsyn, x030C, P. ulc, S. Backhaus, and M. Chertkov, "Distributed control of reactive power flow in a radial distribution circuit with high photovoltaic penetration," in *Proc. 2010 IEEE Power and Energy Society General Meeting*, 2010, pp. 1-6.

[152] R. Tonkoski, L. A. C. Lopes, and T. H. M. El-Fouly, "Coordinated active power curtailment of grid connected PV inverters for overvoltage prevention," *IEEE Trans. Sustainable Energy,* vol. 2, pp. 139-147, 2011.

[153] *Electromagnetic Compatibility (EMC) - Limits - Steady State Voltage Limits in Public Electricity Systems,* Australian Standard AS 61000.3.100-2011, Dec. 2011.

[154] P. Pillay and M. Manyage, "Definitions of voltage unbalance," *IEEE Power Engineering Review,* vol. 21, pp. 49-51, 2001.

[155] M. Braun, "Reactive power supplied by PV inverters - cost benefit analysis," in *Proc. 22nd European Photovoltaic Solar Energy Conference and Exhibition*, 2007, pp. 1-7.

[156] Z. Ugray, L. Lasdon, J. Plummer, F. Glover, J. Kelly, and R. Martí, "Scatter search and local NLP solvers: a multistart framework for global optimization," *INFORMS Journal on Computing,* vol. 19, pp. 328-340, 2007.

[157] Perth Solar City Annual Report. (2012, Dec.). Western Power, Perth, WA, Australia. [Online]. Available: http://www.westernpower.com.au/network-projects/smartGrid/ Perth_Solar_City.html.

[158] Rooftop PV information paper-national electricity forecasting. Australian Energy Market Operator. (2012, Jun). Australian Energy Market Operator. [Online]. Available: http://www.aemo.com.au/ Reports-and-Documents.

[159] Western Australian distribution connections manual. (2013, Jun). Western Power, Perth, WA, Australia. [Online]. Available: http://www. westernpower. com.au/ documents.

[160] B. A. Robbins, C. N. Hadjicostis, and A. D. Dominguez-Garcia, "A two-stage distributed architecture for voltage control in power distribution systems," *IEEE Trans. Power Systems,* vol. 28, pp. 1470-1482, 2013.

[161] X. Su, M. A. S. Masoum, and P. J. Wolfs, "PSO and improved BSFS based sequential comprehensive placement and real-time multi-objective control of delta-connected switched capacitors in unbalanced radial MV distribution networks," *IEEE Trans. on Power Systems,* vol. PP, pp. 1-11, 2015.

[162] C. Hsiao-Dong, W. Jin-Cheng, T. Jianzhong, and G. Darling, "Optimal capacitor placement, replacement and control in large-scale unbalanced distribution systems: system solution algorithms and numerical studies," *IEEE Trans. Power Systems,* vol. 10, pp. 363-369, 1995.

[163] X. Yan, D. Zhao Yang, W. Kit Po, E. Liu, and B. Yue, "Optimal capacitor placement to distribution transformers for power loss reduction in radial distribution systems," *IEEE Trans. Power Systems,* vol. 28, pp. 4072-4079, 2013.

[164] M. E. Baran and F. F. Wu, "Optimal capacitor placement on radial distribution systems,"*IEEE Trans. Power Delivery,* vol. 4, pp. 725-734, 1989.

[165] A. A. El-Fergany and A. Y. Abdelaziz, "Efficient heuristic-based approach for multi-objective capacitor allocation in radial distribution networks," *IET Generation, Transmission & Distribution,* vol. 8, pp. 70-80, 2014.

[166] M. Ladjavardi and M. A. S. Masoum, "Genetically optimized fuzzy placement and sizing of capacitor banks in distorted distribution networks," *IEEE Trans. Power Delivery,* vol. 23, pp. 449-456, 2008.

[167] M. A. S. Masoum, M. Ladjevardi, A. Jafarian, and E. F. Fuchs, "Optimal placement, replacement and sizing of capacitor Banks in distorted distribution networks by genetic algorithms," *IEEE Trans. Power Delivery,* vol. 19, pp. 1794-1801, 2004.

[168] C. S. Chen, C. T. Hsu, and Y. H. Yan, "Optimal distribution feeder capacitor placement considering mutual coupling effect of conductors," *IEEE Trans. Power Delivery,* vol. 10, pp. 987-994, 1995.

[169] V. Farahani, S. H. H. Sadeghi, H. A. Abyaneh, S. M. M. Agah, and K. Mazlumi, "Energy loss reduction by conductor replacement and capacitor placement in distribution systems," *IEEE Trans. Power Systems,* vol. 28, pp. 2077-2085, 2013.

[170] D. Das, "Optimal placement of capacitors in radial distribution system using a Fuzzy-GA method," *International Journal of Electrical Power & Energy Systems,* vol. 30, pp. 361-367, 2008.

[171] A. A. Eajal and M. E. El-Hawary, "Optimal capacitor placement and sizing in unbalanced distribution systems with harmonics consideration using particle swarm optimization," *IEEE Trans. Power Delivery,* vol. 25, pp. 1734-1741, 2010.

[172] T. L. Huang, Y. T. Hsiao, C. H. Chang, and J. A. Jiang, "Optimal placement of capacitors in distribution systems using an immune multi-objective algorithm," *International Journal of Electrical Power & Energy Systems,* vol. 30, pp. 184-192, 2008.

[173] M. Ponnavaikko and K. S. P. Rao, "Optimal choice of fixed and switched shunt capacitors on radial distributors by the method of local variations," *IEEE Power Engineering Review,* vol. PER-3, pp. 35-36, 1983.

[174] H. N. Ng, M. M. A. Salama, and A. Y. Chikhani, "Classification of capacitor allocation techniques," *IEEE Trans. Power Delivery,* vol. 15, pp. 387-392, 2000.

[175] R. Sirjani, A. Mohamed, and H. Sharff, "Heuristic optimization techniques to determine optimal capacitor placement and sizing in radial distribution networks: a comprehensive review," *PRZEGLĄD ELEKTROTECHNICZNY (Electrical Review),* vol. 88, pp. 1-7, July 2012.

[176] Y. Bo, J. Skliutas, L. Freeman, D. Guinn, and R. Cheney, "Optimal control of capacitors on distribution feeders," in *Proc. 2011 IEEE Power and Energy Society General Meeting*, 2011, pp. 1-7.

[177] K. N. Miu, C. Hsiao-Dong, and G. Darling, "Capacitor placement, replacement and control in large-scale distribution systems by a GA-based two-stage algorithm," *IEEE Trans. Power Systems,* vol. 12, pp. 1160-1166, 1997.

[178] M. R. Kleinberg, K. Miu, N. Segal, H. Lehmann, and T. R. Figura, "A partitioning method for distributed capacitor control of electric power distribution systems," *IEEE Trans. Power Systems*, vol.29, pp. 637-644, 2014.
[179] Power Capacitors and Harmonic Filters, Buyer's Guide. (2013, Sep.). ABB, Ludivika, Sweden. [Online]. Available: http://new.abb.com/high-voltage /capacitors/hv/ harmonic-filters.
[180] *Standard Voltages*, Australia Standard AS 60038-2012, 2012.
[181] R. A. Gallego, A. J. Monticelli, and R. Romero, "Optimal capacitor placement in radial distribution networks," *IEEE Trans. Power Systems*, vol. 16, pp. 630-637, 2001.
[182] S. Ghosh and D. Das, "Method for load-flow solution of radial distribution networks," *IEE Proceedings-Generation, Transmission and Distribution*, vol. 146, pp. 641-648, 1999.
[183] W. H. Kersting, *Distribution System Modeling and Analysis*, 3rd ed., CRC Press, 2011.
[184] X. Su, M. A. S. Masoum, and P. J. Wolfs, "Multi-Objective hierarchical control of unbalanced distribution networks to accommodate more renewable connections in the smart grid era," Submitted to *IEEE Trans. on Power Systems*, Manuscript ID: TPWRS-00665-2015, 2015.
[185] T. Short, *Electric Power Distribution Handbook*, CRC Press, 2004.
[186] *Power Transformers - Application Guide* , Australia Standards AS 2374.8-2009, 2009.

Appendix A. Application of the Proposed Delta Placement and Control Strategies and Models for Star Switched Capacitors

The proposed placement and control strategies, optimization models and solution methods of delta-connected switched capacitors in Chapter 4 are highly generalized and can be used for the related studies of both ungrounded and grounded star-connected switched capacitors with slight modifications.

A. Ungrounded Star-Connected Switched Capacitors

According to the well-known star-delta transformation (figure A.1), the impedances of the ungrounded star-connected branches can be converted to the corresponding values of delta-connected configuration:

$$\begin{aligned} Z_{ab} &= (Z_a Z_b + Z_b Z_c + Z_c Z_a)/Z_c \\ Z_{bc} &= (Z_a Z_b + Z_b Z_c + Z_c Z_a)/Z_a \\ Z_{ca} &= (Z_a Z_b + Z_b Z_c + Z_c Z_a)/Z_b \end{aligned} \tag{A.1}$$

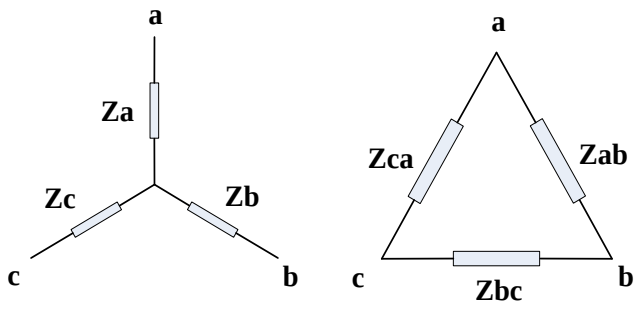

Figure A.1 Star-delta impedance transformation.

In Section 4.4.2, when performing the load flow of networks with ungrounded star-connected capacitors by the improved BSFS method, the following steps should be

added before the step 2:

1) Using an approach similar to equation (4.23), calculate the constant susceptance of the per phase capacitor branch of the star connection based on the rated capacity and rated phase voltage:

$$B = kVAr/(kV_p^2 \cdot 1000)\ \text{S} \qquad \text{(A.2)}$$

2) Based on the star-delta impedance transformation, obtain the corresponding susceptance of the phase-phase capacitor bridge of the delta connection.

Load flow can be carried out by continuing the steps in Section 4.4.2 from step 2 with the new susceptances.

Accordingly, the solution process of the delta-connected capacitor problems by the improved BSFS based PSO (figure 4.3) can be slightly modified for the studies of star-connected capacitors as shown in figure A.2.

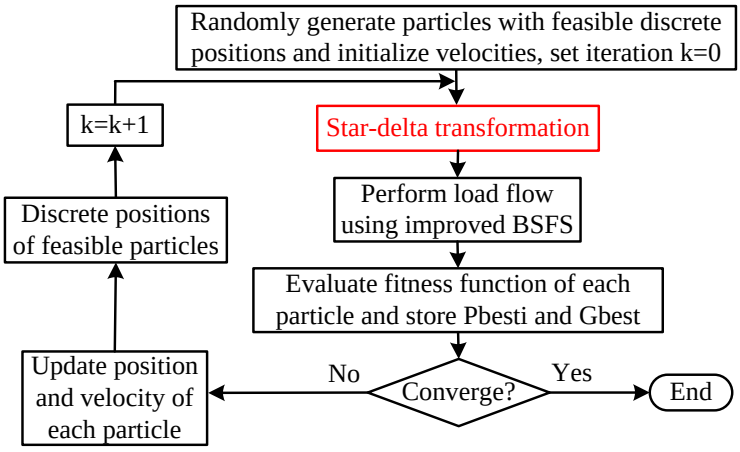

Figure A.2 Modified flowchart of optimization for the star-connected capacitors.

B. Grounded Star-Connected Switched Capacitors

With all the branches solidly grounded, the start-connected switched capacitors can be modeled as a negative reactive load with the current injection calculated as follows:

$$IC_n^p = jQC_n^p/V_n^{p*} \qquad p = a, b, c \qquad \text{(A.3)}$$

Appendix B. Pavetta1 LV Network Data

Table B.1 Branch data of Pavetta1 LV Network.

Bus i	Bus j	Phase	Branch Length (m)	R_{ij} (Ω/km)	X_{ij} (Ω/km)
1	2	Three Phase	46	0.453	0.304
1	27	C	24	3.700	0.369
1	28	A	16	3.700	0.369
1	29	Three Phase	44	0.453	0.304
2	3	B	15	3.700	0.369
2	4	C	15	3.700	0.369
2	5	Three Phase	45	0.453	0.304
5	6	Three Phase	12	3.700	0.369
5	7	A	11	3.700	0.369
5	8	B	26	3.700	0.369
5	9	Three Phase	27	3.700	0.369
5	10	Three Phase	42	0.453	0.304
10	11	B	15	3.700	0.369
10	12	A	15	3.700	0.369
10	13	C	35	3.700	0.369

10	14	B	25	3.700	0.369
10	15	Three Phase	42	0.453	0.304
15	16	A	15	3.700	0.369
15	17	B	15	3.700	0.369
15	18	Three Phase	27	3.700	0.369
15	19	Three Phase	26	3.700	0.369
15	20	Three Phase	42	0.453	0.304
20	21	A	15	3.700	0.369
20	22	B	15	3.700	0.369
20	23	C	24	3.700	0.369
20	24	C	26	3.700	0.369
20	25	Three Phase	39	0.453	0.304
25	26	B	15	3.700	0.369
29	30	C	32	3.700	0.369
29	31	Three Phase	36	3.700	0.369
29	32	Three Phase	15	3.700	0.369
29	33	Three Phase	45	0.453	0.304
29	37	Three Phase	44	0.453	0.304
33	34	Three Phase	33	3.700	0.369
33	35	C	36	3.700	0.369
33	36	A	11	3.700	0.369
37	38	B	14	3.700	0.369
37	39	A	12	3.700	0.369
37	40	C	34	3.700	0.369

37	41	Three Phase	29	3.700	0.369
37	42	Three Phase	46	0.453	0.304
42	43	Three Phase	18	3.700	0.369
42	44	C	9	3.700	0.369
42	45	Three Phase	44	0.453	0.304
42	60	Three Phase	30	0.316	0.292
45	46	A	15	3.700	0.369
45	47	B	12	3.700	0.369
45	48	Three Phase	45	0.453	0.304
48	49	A	15	3.700	0.369
48	50	Three Phase	14	3.700	0.369
48	51	Three Phase	35	3.700	0.369
48	52	C	30	3.700	0.369
48	53	Three Phase	45	0.453	0.304
53	54	A	17	3.700	0.369
53	55	B	12	3.700	0.369
53	56	C	32	3.700	0.369
53	57	C	37	3.700	0.369
53	58	Three Phase	49	0.453	0.304
58	59	C	15	3.700	0.369
60	61	Three Phase	24	3.700	0.369
60	62	B	10	3.700	0.369
60	63	Three Phase	35	0.316	0.292
63	64	Three Phase	24	3.700	0.369

63	65	Three Phase	29	3.700	0.369
63	66	Three Phase	15	3.700	0.369
63	67	B	11	3.700	0.369
63	68	Three Phase	35	0.316	0.292
68	69	Three Phase	12	3.700	0.369
68	70	B	15	3.700	0.369
68	71	Three Phase	45	0.316	0.292
68	86	Three Phase	43	0.316	0.292
71	72	Three Phase	10	3.700	0.369
71	73	Three Phase	15	3.700	0.369
71	74	Three Phase	30	3.700	0.369
71	75	Three Phase	45	0.316	0.292
75	76	B	12	3.700	0.369
75	77	C	10	3.700	0.369
75	78	C	25	3.700	0.369
75	79	Three Phase	25	3.700	0.369
75	80	Three Phase	45	0.316	0.292
80	81	Three Phase	11	3.700	0.369
80	82	C	14	3.700	0.369
80	83	Three Phase	26	3.700	0.369
80	84	C	33	3.700	0.369
80	85	B	32	3.700	0.369
86	87	Three Phase	14	3.700	0.369
86	88	Three Phase	12	3.700	0.369

86	89	Three Phase	25	0.316	0.292
89	90	Three Phase	25	3.700	0.369
89	91	C	25	3.700	0.369
89	92	Three Phase	18	3.700	0.369
89	93	Three Phase	23	0.316	0.292
93	94	A	21	3.700	0.369
93	95	B	21	3.700	0.369
93	96	C	21	3.700	0.369
93	97	C	21	3.700	0.369
93	98	B	21	3.700	0.369
93	99	A	21	3.700	0.369
93	100	B	21	3.700	0.369
93	101	A	21	3.700	0.369

Table B.2 PV connections of Pavetta1 LV network.

Bus	Phase	PV Size (kW)	Bus	Phase	PV Size (kW)
3	B	2.54	49	A	2.00
4	C	1.59	51	A	2.00
6	A	1.88	52	C	1.59
7	A	1.88	56	C	1.59
8	B	1.59	64	C	2.00
9	A	1.88	66	B	1.88
19	A	1.59	69	B	1.59
24	C	1.88	70	B	1.59
27	C	1.59	73	A	2.61
30	C	2.22	78	C	2.50
32	C	1.59	81	C	2.10
35	C	1.88	83	B	1.88
36	A	2.00	84	C	1.59
39	A	2.00	85	B	2.00
40	C	2.00	87	C	1.88
43	A	1.88	91	C	1.55
44	C	1.88	92	A	1.59

Table B.3 Loads and PV generations at single-phase buses of Pavetta1 LV network over 24 hours.

Time	Bus	Phase	P_L (kW)	Q_L(kVAr)	P_{PV} (kW)	Q_{PV}(kVAr)	Bus	Phase	P_L (kW)	Q_L(kVAr)	P_{PV} (kW)	Q_{PV}(kVAr)
00:00	3	B	2.92	1.60	0.00	0.00	49	A	2.44	1.32	0.00	0.00
01:00	3	B	1.88	1.24	0.00	0.00	49	A	0.88	0.44	0.00	0.00
02:00	3	B	0.56	0.32	0.00	0.00	49	A	0.24	0.12	0.00	0.00
03:00	3	B	1.96	1.24	0.00	0.00	49	A	0.24	0.12	0.00	0.00
04:00	3	B	0.80	0.68	0.00	0.00	49	A	0.20	0.16	0.00	0.00
05:00	3	B	0.48	0.24	0.00	0.00	49	A	0.20	0.16	0.00	0.00
06:00	3	B	0.56	0.32	0.00	0.00	49	A	0.20	0.04	0.00	0.00
07:00	3	B	2.56	2.32	0.16	0.00	49	A	0.04	0.08	0.00	0.00
08:00	3	B	0.64	0.40	0.44	0.00	49	A	0.00	0.16	0.20	0.00
09:00	3	B	0.44	0.32	1.04	0.00	49	A	0.00	0.20	0.60	0.00
10:00	3	B	4.52	3.08	1.48	0.00	49	A	0.00	0.20	1.00	0.00
11:00	3	B	4.48	2.64	1.80	0.00	49	A	0.00	0.24	1.20	0.00
12:00	3	B	4.56	2.64	2.00	0.00	49	A	0.00	0.24	1.28	0.00
13:00	3	B	4.60	2.64	2.08	0.00	49	A	0.00	0.28	1.32	0.00
14:00	3	B	4.80	2.68	2.00	0.00	49	A	0.00	0.24	1.12	0.00
15:00	3	B	4.72	2.56	1.88	0.00	49	A	0.00	0.24	1.16	0.00
16:00	3	B	4.72	2.68	1.36	0.00	49	A	0.00	0.20	0.80	0.00
17:00	3	B	3.72	2.20	1.20	0.00	49	A	0.00	0.20	0.68	0.00
18:00	3	B	0.48	0.48	0.12	0.00	49	A	0.00	0.12	0.24	0.00
19:00	3	B	0.60	0.64	0.00	0.00	49	A	0.20	0.08	0.00	0.00
20:00	3	B	5.48	3.08	0.00	0.00	49	A	0.28	0.16	0.00	0.00
21:00	3	B	4.16	2.08	0.00	0.00	49	A	0.32	0.16	0.00	0.00
22:00	3	B	4.36	2.52	0.00	0.00	49	A	0.32	0.08	0.00	0.00
23:00	3	B	4.20	2.28	0.00	0.00	49	A	0.24	0.12	0.00	0.00
24:00	3	B	4.08	2.64	0.00	0.00	49	A	0.24	0.08	0.00	0.00
00:00	4	C	1.20	0.16	0.00	0.00	52	C	2.00	1.28	0.00	0.00
01:00	4	C	1.12	0.12	0.00	0.00	52	C	1.60	0.92	0.00	0.00

02:00	4	C	1.12	0.12	0.00	0.00	52	C	1.32	0.80	0.00	0.00
03:00	4	C	1.00	0.04	0.00	0.00	52	C	1.32	0.84	0.00	0.00
04:00	4	C	0.96	0.00	0.00	0.00	52	C	1.16	0.68	0.00	0.00
05:00	4	C	1.92	0.04	0.00	0.00	52	C	1.24	0.60	0.00	0.00
06:00	4	C	1.24	0.04	0.00	0.00	52	C	0.68	0.52	0.00	0.00
07:00	4	C	0.84	0.12	0.00	0.00	52	C	0.80	0.60	0.08	0.00
08:00	4	C	0.28	0.12	0.00	0.00	52	C	0.68	0.52	0.24	0.00
09:00	4	C	0.12	0.12	0.00	0.00	52	C	1.28	1.04	0.60	0.00
10:00	4	C	0.16	0.24	0.00	0.00	52	C	1.32	1.08	0.92	0.00
11:00	4	C	0.28	0.36	0.04	0.00	52	C	1.80	1.28	1.12	0.00
12:00	4	C	0.40	0.40	0.00	0.00	52	C	1.52	1.08	1.24	0.00
13:00	4	C	0.52	0.40	0.00	0.00	52	C	1.56	1.12	1.28	0.00
14:00	4	C	0.68	0.36	0.00	0.00	52	C	3.16	1.36	1.24	0.00
15:00	4	C	0.88	0.36	0.00	0.00	52	C	3.80	1.28	1.16	0.00
16:00	4	C	1.28	0.28	0.00	0.00	52	C	2.36	1.20	0.84	0.00
17:00	4	C	1.28	0.04	0.00	0.00	52	C	3.84	1.48	0.72	0.00
18:00	4	C	1.96	0.20	0.00	0.00	52	C	3.68	1.40	0.24	0.00
19:00	4	C	2.20	0.08	0.00	0.00	52	C	3.64	1.24	0.00	0.00
20:00	4	C	2.08	0.16	0.00	0.00	52	C	3.52	1.40	0.00	0.00
21:00	4	C	2.00	0.24	0.00	0.00	52	C	3.40	1.24	0.00	0.00
22:00	4	C	1.84	0.12	0.00	0.00	52	C	2.72	1.16	0.00	0.00
23:00	4	C	2.80	0.04	0.00	0.00	52	C	1.68	1.12	0.00	0.00
24:00	4	C	0.92	0.04	0.00	0.00	52	C	1.00	0.96	0.00	0.00
00:00	7	A	0.44	0.28	0.00	0.00	54	A	0.44	0.36	0.00	0.00
01:00	7	A	0.44	0.28	0.00	0.00	54	A	0.32	0.16	0.00	0.00
02:00	7	A	0.48	0.36	0.00	0.00	54	A	0.84	0.40	0.00	0.00
03:00	7	A	0.52	0.16	0.00	0.00	54	A	0.84	0.48	0.00	0.00
04:00	7	A	0.52	0.24	0.00	0.00	54	A	0.80	0.40	0.00	0.00
05:00	7	A	0.32	0.12	0.00	0.00	54	A	0.76	0.32	0.00	0.00
06:00	7	A	0.40	0.32	0.00	0.00	54	A	0.76	0.32	0.00	0.00

07:00	7	A	0.20	0.12	0.00	0.00	54	A	0.88	0.44	0.00	0.00
08:00	7	A	0.60	0.16	0.00	0.00	54	A	0.28	0.28	0.00	0.00
09:00	7	A	0.44	0.16	0.00	0.00	54	A	0.28	0.28	0.00	0.00
10:00	7	A	0.40	0.16	0.00	0.00	54	A	0.24	0.20	0.00	0.00
11:00	7	A	0.36	0.16	0.00	0.00	54	A	0.20	0.12	0.00	0.00
12:00	7	A	1.48	0.40	0.00	0.00	54	A	0.24	0.16	0.00	0.00
13:00	7	A	1.68	0.36	0.00	0.00	54	A	0.28	0.24	0.00	0.00
14:00	7	A	1.72	0.40	0.00	0.00	54	A	0.40	0.20	0.00	0.00
15:00	7	A	2.44	0.80	0.00	0.00	54	A	0.40	0.32	0.00	0.00
16:00	7	A	2.28	1.08	0.00	0.00	54	A	0.32	0.20	0.00	0.00
17:00	7	A	2.24	1.08	0.00	0.00	54	A	0.36	0.28	0.00	0.00
18:00	7	A	3.16	0.96	0.00	0.00	54	A	0.52	0.32	0.00	0.00
19:00	7	A	3.04	1.00	0.00	0.00	54	A	0.76	0.36	0.00	0.00
20:00	7	A	2.68	1.00	0.00	0.00	54	A	0.92	0.40	0.00	0.00
21:00	7	A	2.72	0.68	0.00	0.00	54	A	1.36	0.44	0.00	0.00
22:00	7	A	0.92	0.48	0.00	0.00	54	A	1.48	0.40	0.00	0.00
23:00	7	A	0.52	0.40	0.00	0.00	54	A	1.64	0.36	0.00	0.00
24:00	7	A	0.40	0.28	0.00	0.00	54	A	1.64	0.40	0.00	0.00
00:00	8	B	2.12	0.54	0.00	0.00	55	B	3.60	0.00	0.00	0.00
01:00	8	B	1.85	0.45	0.00	0.00	55	B	2.00	0.00	0.00	0.00
02:00	8	B	0.42	0.10	0.00	0.00	55	B	2.40	0.00	0.00	0.00
03:00	8	B	0.50	0.13	0.00	0.00	55	B	1.60	0.00	0.00	0.00
04:00	8	B	0.48	0.12	0.00	0.00	55	B	1.60	0.00	0.00	0.00
05:00	8	B	0.48	0.12	0.00	0.00	55	B	1.20	0.00	0.00	0.00
06:00	8	B	0.49	0.13	0.01	0.00	55	B	1.20	0.00	0.00	0.00
07:00	8	B	0.54	0.21	0.10	0.00	55	B	1.60	0.00	0.00	0.00
08:00	8	B	0.72	0.36	0.27	0.00	55	B	2.00	0.07	0.00	0.00
09:00	8	B	0.64	0.17	0.64	0.00	55	B	2.80	0.00	0.00	0.00
10:00	8	B	0.62	0.18	0.92	0.00	55	B	2.80	0.00	0.00	0.00
11:00	8	B	0.62	0.20	1.12	0.00	55	B	3.20	0.00	0.00	0.00

12:00	8	B	0.70	0.31	1.22	0.00	55	B	2.80	0.03	0.00	0.00
13:00	8	B	0.69	0.31	1.27	0.00	55	B	3.20	0.02	0.00	0.00
14:00	8	B	0.61	0.23	1.23	0.00	55	B	3.20	0.00	0.00	0.00
15:00	8	B	1.45	0.25	1.15	0.00	55	B	3.20	0.00	0.00	0.00
16:00	8	B	1.38	0.47	0.86	0.00	55	B	3.20	0.00	0.00	0.00
17:00	8	B	1.13	0.45	0.63	0.00	55	B	1.60	0.00	0.00	0.00
18:00	8	B	1.10	0.44	0.06	0.00	55	B	2.00	0.00	0.00	0.00
19:00	8	B	1.37	0.41	0.01	0.00	55	B	3.20	0.00	0.00	0.00
20:00	8	B	1.08	0.43	0.00	0.00	55	B	4.00	0.00	0.00	0.00
21:00	8	B	1.15	0.43	0.00	0.00	55	B	3.20	0.00	0.00	0.00
22:00	8	B	0.57	0.18	0.00	0.00	55	B	2.80	0.00	0.00	0.00
23:00	8	B	0.46	0.17	0.00	0.00	55	B	1.60	0.00	0.00	0.00
24:00	8	B	0.46	0.17	0.00	0.00	55	B	2.00	0.00	0.00	0.00
00:00	11	B	2.80	0.52	0.00	0.00	56	C	1.04	0.01	0.00	0.00
01:00	11	B	2.40	0.52	0.00	0.00	56	C	0.76	0.02	0.00	0.00
02:00	11	B	1.60	0.52	0.00	0.00	56	C	0.04	0.01	0.00	0.00
03:00	11	B	2.00	0.56	0.00	0.00	56	C	0.72	0.01	0.00	0.00
04:00	11	B	2.00	0.56	0.00	0.00	56	C	0.72	0.03	0.00	0.00
05:00	11	B	2.00	0.60	0.00	0.00	56	C	1.20	0.01	0.00	0.00
06:00	11	B	3.20	0.72	0.00	0.00	56	C	0.76	0.00	0.04	0.00
07:00	11	B	4.00	0.96	0.00	0.00	56	C	0.80	0.00	0.12	0.00
08:00	11	B	3.20	0.72	0.00	0.00	56	C	0.12	0.01	0.24	0.00
09:00	11	B	4.80	0.64	0.00	0.00	56	C	0.12	0.01	0.64	0.00
10:00	11	B	3.20	0.60	0.00	0.00	56	C	0.12	0.02	0.96	0.00
11:00	11	B	5.20	0.68	0.00	0.00	56	C	0.08	0.00	1.12	0.00
12:00	11	B	4.80	0.56	0.00	0.00	56	C	0.12	0.00	1.24	0.00
13:00	11	B	5.60	0.56	0.00	0.00	56	C	0.12	0.00	1.28	0.00
14:00	11	B	4.80	0.60	0.00	0.00	56	C	0.08	0.00	1.24	0.00
15:00	11	B	5.60	0.52	0.00	0.00	56	C	0.16	0.00	1.16	0.00
16:00	11	B	6.00	0.68	0.00	0.00	56	C	0.20	0.01	0.84	0.00

17:00	11	B	5.60	0.56	0.00	0.00	56	C	0.28	0.00	0.72	0.00
18:00	11	B	6.00	0.52	0.00	0.00	56	C	0.40	0.00	0.40	0.00
19:00	11	B	5.20	0.36	0.00	0.00	56	C	0.40	0.00	0.04	0.00
20:00	11	B	5.20	0.32	0.00	0.00	56	C	1.16	0.00	0.00	0.00
21:00	11	B	4.40	0.28	0.00	0.00	56	C	1.16	0.00	0.00	0.00
22:00	11	B	4.40	0.36	0.00	0.00	56	C	2.12	0.00	0.00	0.00
23:00	11	B	3.60	0.44	0.00	0.00	56	C	1.68	0.00	0.00	0.00
24:00	11	B	3.20	0.56	0.00	0.00	56	C	0.92	0.01	0.00	0.00
00:00	12	A	0.20	0.12	0.00	0.00	57	C	0.36	0.20	0.00	0.00
01:00	12	A	0.16	0.08	0.00	0.00	57	C	0.36	0.24	0.00	0.00
02:00	12	A	0.20	0.08	0.00	0.00	57	C	0.40	0.20	0.00	0.00
03:00	12	A	0.20	0.08	0.00	0.00	57	C	0.32	0.20	0.00	0.00
04:00	12	A	0.20	0.12	0.00	0.00	57	C	0.32	0.12	0.00	0.00
05:00	12	A	0.20	0.08	0.00	0.00	57	C	0.36	0.24	0.00	0.00
06:00	12	A	0.16	0.04	0.00	0.00	57	C	0.44	0.12	0.00	0.00
07:00	12	A	0.48	0.08	0.00	0.00	57	C	0.60	0.20	0.00	0.00
08:00	12	A	0.24	0.08	0.00	0.00	57	C	0.28	0.16	0.00	0.00
09:00	12	A	0.32	0.08	0.00	0.00	57	C	0.24	0.12	0.00	0.00
10:00	12	A	0.16	0.08	0.00	0.00	57	C	0.24	0.16	0.00	0.00
11:00	12	A	0.16	0.08	0.00	0.00	57	C	0.40	0.24	0.00	0.00
12:00	12	A	0.12	0.04	0.00	0.00	57	C	0.44	0.28	0.00	0.00
13:00	12	A	0.24	0.16	0.00	0.00	57	C	0.36	0.24	0.00	0.00
14:00	12	A	0.16	0.08	0.00	0.00	57	C	0.36	0.24	0.00	0.00
15:00	12	A	0.12	0.08	0.00	0.00	57	C	0.40	0.24	0.00	0.00
16:00	12	A	0.16	0.12	0.00	0.00	57	C	0.56	0.16	0.00	0.00
17:00	12	A	0.72	0.56	0.00	0.00	57	C	1.32	0.24	0.00	0.00
18:00	12	A	0.68	0.52	0.00	0.00	57	C	0.36	0.12	0.00	0.00
19:00	12	A	0.68	0.48	0.00	0.00	57	C	0.48	0.20	0.00	0.00
20:00	12	A	0.72	0.56	0.00	0.00	57	C	0.48	0.16	0.00	0.00
21:00	12	A	0.72	0.56	0.00	0.00	57	C	1.16	0.12	0.00	0.00

22:00	12	A	0.52	0.40	0.00	0.00	57	C	0.44	0.28	0.00	0.00
23:00	12	A	0.20	0.12	0.00	0.00	57	C	0.44	0.16	0.00	0.00
24:00	12	A	0.20	0.12	0.00	0.00	57	C	0.32	0.12	0.00	0.00
00:00	13	C	0.40	0.24	0.00	0.00	59	C	0.24	0.28	0.00	0.00
01:00	13	C	0.80	0.28	0.00	0.00	59	C	0.12	0.12	0.00	0.00
02:00	13	C	1.20	0.52	0.00	0.00	59	C	0.20	0.16	0.00	0.00
03:00	13	C	1.20	0.68	0.00	0.00	59	C	0.24	0.24	0.00	0.00
04:00	13	C	1.20	0.52	0.00	0.00	59	C	0.20	0.24	0.00	0.00
05:00	13	C	1.20	0.48	0.00	0.00	59	C	0.24	0.24	0.00	0.00
06:00	13	C	1.20	0.52	0.00	0.00	59	C	0.12	0.08	0.00	0.00
07:00	13	C	0.40	0.28	0.00	0.00	59	C	0.24	0.24	0.00	0.00
08:00	13	C	0.80	0.48	0.00	0.00	59	C	0.24	0.24	0.00	0.00
09:00	13	C	0.80	0.52	0.00	0.00	59	C	0.20	0.24	0.00	0.00
10:00	13	C	1.20	0.84	0.00	0.00	59	C	0.12	0.04	0.00	0.00
11:00	13	C	1.60	1.04	0.00	0.00	59	C	0.24	0.24	0.00	0.00
12:00	13	C	1.20	0.72	0.00	0.00	59	C	0.24	0.24	0.00	0.00
13:00	13	C	1.60	0.80	0.00	0.00	59	C	0.24	0.24	0.00	0.00
14:00	13	C	1.60	1.16	0.00	0.00	59	C	0.20	0.24	0.00	0.00
15:00	13	C	4.00	2.16	0.00	0.00	59	C	0.24	0.24	0.00	0.00
16:00	13	C	4.00	2.20	0.00	0.00	59	C	0.24	0.24	0.00	0.00
17:00	13	C	3.60	1.80	0.00	0.00	59	C	0.28	0.40	0.00	0.00
18:00	13	C	4.40	1.96	0.00	0.00	59	C	0.28	0.36	0.00	0.00
19:00	13	C	4.00	1.72	0.00	0.00	59	C	0.36	0.36	0.00	0.00
20:00	13	C	4.40	1.76	0.00	0.00	59	C	0.32	0.36	0.00	0.00
21:00	13	C	4.00	1.84	0.00	0.00	59	C	0.32	0.32	0.00	0.00
22:00	13	C	3.60	1.96	0.00	0.00	59	C	0.32	0.36	0.00	0.00
23:00	13	C	0.40	0.08	0.00	0.00	59	C	0.32	0.40	0.00	0.00
24:00	13	C	0.40	0.16	0.00	0.00	59	C	0.24	0.28	0.00	0.00
00:00	14	B	0.08	0.00	0.00	0.00	62	B	1.20	0.84	0.00	0.00
01:00	14	B	0.08	0.00	0.00	0.00	62	B	1.20	0.64	0.00	0.00

02:00	14	B	0.04	0.00	0.00	0.00	62	B	1.20	1.00	0.00	0.00
03:00	14	B	0.08	0.00	0.00	0.00	62	B	1.20	0.72	0.00	0.00
04:00	14	B	0.08	0.00	0.00	0.00	62	B	1.20	0.68	0.00	0.00
05:00	14	B	0.04	0.00	0.00	0.00	62	B	0.80	0.32	0.00	0.00
06:00	14	B	0.00	0.00	0.00	0.00	62	B	0.40	0.04	0.00	0.00
07:00	14	B	0.32	0.00	0.00	0.00	62	B	0.80	0.20	0.00	0.00
08:00	14	B	0.20	0.04	0.00	0.00	62	B	0.40	0.04	0.00	0.00
09:00	14	B	0.24	0.04	0.00	0.00	62	B	0.40	0.32	0.00	0.00
10:00	14	B	0.12	0.00	0.00	0.00	62	B	0.80	0.28	0.00	0.00
11:00	14	B	0.12	0.00	0.00	0.00	62	B	0.80	0.24	0.00	0.00
12:00	14	B	2.04	0.64	0.00	0.00	62	B	0.80	0.28	0.00	0.00
13:00	14	B	0.28	0.08	0.00	0.00	62	B	0.40	0.24	0.00	0.00
14:00	14	B	0.12	0.00	0.00	0.00	62	B	0.80	0.28	0.00	0.00
15:00	14	B	1.88	0.56	0.00	0.00	62	B	0.80	0.24	0.00	0.00
16:00	14	B	1.80	0.68	0.00	0.00	62	B	0.40	0.28	0.00	0.00
17:00	14	B	1.96	0.64	0.00	0.00	62	B	0.80	0.28	0.00	0.00
18:00	14	B	3.04	0.64	0.00	0.00	62	B	1.20	0.20	0.00	0.00
19:00	14	B	2.20	0.60	0.00	0.00	62	B	0.80	0.24	0.00	0.00
20:00	14	B	1.88	0.56	0.00	0.00	62	B	1.20	1.04	0.00	0.00
21:00	14	B	1.96	0.60	0.00	0.00	62	B	1.60	0.96	0.00	0.00
22:00	14	B	2.56	0.52	0.00	0.00	62	B	1.20	0.76	0.00	0.00
23:00	14	B	0.12	0.00	0.00	0.00	62	B	1.20	0.84	0.00	0.00
24:00	14	B	0.12	0.00	0.00	0.00	62	B	1.20	0.96	0.00	0.00
00:00	16	A	0.52	0.48	0.00	0.00	67	B	1.60	0.52	0.00	0.00
01:00	16	A	0.48	0.48	0.00	0.00	67	B	1.20	0.20	0.00	0.00
02:00	16	A	0.48	0.48	0.00	0.00	67	B	1.20	0.52	0.00	0.00
03:00	16	A	0.52	0.52	0.00	0.00	67	B	1.20	0.20	0.00	0.00
04:00	16	A	0.56	0.48	0.00	0.00	67	B	1.20	0.48	0.00	0.00
05:00	16	A	0.76	0.04	0.00	0.00	67	B	1.20	0.12	0.00	0.00
06:00	16	A	1.08	0.04	0.00	0.00	67	B	1.20	0.60	0.00	0.00

07:00	16	A	1.08	0.04	0.00	0.00	67	B	0.40	0.00	0.00	0.00
08:00	16	A	0.48	0.04	0.00	0.00	67	B	0.40	0.12	0.00	0.00
09:00	16	A	0.08	0.00	0.00	0.00	67	B	0.40	0.12	0.00	0.00
10:00	16	A	0.12	0.04	0.00	0.00	67	B	0.40	0.08	0.00	0.00
11:00	16	A	0.72	0.04	0.00	0.00	67	B	0.40	0.24	0.00	0.00
12:00	16	A	1.08	0.04	0.00	0.00	67	B	0.40	0.24	0.00	0.00
13:00	16	A	1.08	0.04	0.00	0.00	67	B	0.40	0.16	0.00	0.00
14:00	16	A	0.60	0.04	0.00	0.00	67	B	0.40	0.24	0.00	0.00
15:00	16	A	0.12	0.04	0.00	0.00	67	B	0.40	0.20	0.00	0.00
16:00	16	A	0.12	0.04	0.00	0.00	67	B	0.40	0.24	0.00	0.00
17:00	16	A	0.64	0.04	0.00	0.00	67	B	0.80	0.24	0.00	0.00
18:00	16	A	1.60	0.48	0.00	0.00	67	B	6.40	1.00	0.00	0.00
19:00	16	A	1.56	0.48	0.00	0.00	67	B	6.00	0.76	0.00	0.00
20:00	16	A	1.52	0.44	0.00	0.00	67	B	3.20	0.48	0.00	0.00
21:00	16	A	0.76	0.52	0.00	0.00	67	B	0.40	0.00	0.00	0.00
22:00	16	A	0.56	0.52	0.00	0.00	67	B	0.40	0.32	0.00	0.00
23:00	16	A	0.52	0.52	0.00	0.00	67	B	0.40	0.08	0.00	0.00
24:00	16	A	0.52	0.52	0.00	0.00	67	B	0.80	0.36	0.00	0.00
00:00	17	B	1.20	0.36	0.00	0.00	70	B	0.48	0.03	0.00	0.00
01:00	17	B	1.20	0.36	0.00	0.00	70	B	0.32	0.04	0.00	0.00
02:00	17	B	0.80	0.32	0.00	0.00	70	B	0.52	0.20	0.00	0.00
03:00	17	B	1.20	0.36	0.00	0.00	70	B	0.40	0.10	0.00	0.00
04:00	17	B	1.20	0.36	0.00	0.00	70	B	0.28	0.03	0.00	0.00
05:00	17	B	0.40	0.04	0.00	0.00	70	B	0.32	0.07	0.00	0.00
06:00	17	B	0.40	0.04	0.00	0.00	70	B	0.36	0.15	0.00	0.00
07:00	17	B	0.00	0.12	0.00	0.00	70	B	0.32	0.07	0.12	0.00
08:00	17	B	1.60	0.36	0.00	0.00	70	B	0.48	0.07	0.04	0.00
09:00	17	B	1.60	0.44	0.00	0.00	70	B	0.72	0.17	0.68	0.00
10:00	17	B	1.60	0.48	0.00	0.00	70	B	0.88	0.17	0.92	0.00
11:00	17	B	2.00	0.68	0.00	0.00	70	B	1.20	0.01	1.12	0.00

12:00	17	B	2.40	0.56	0.00	0.00	70	B	1.24	0.09	1.20	0.00
13:00	17	B	2.40	0.68	0.00	0.00	70	B	2.48	0.22	1.28	0.00
14:00	17	B	2.00	0.72	0.00	0.00	70	B	1.88	0.10	1.24	0.00
15:00	17	B	1.60	0.76	0.00	0.00	70	B	1.56	0.11	1.16	0.00
16:00	17	B	2.40	0.76	0.00	0.00	70	B	1.36	0.02	0.84	0.00
17:00	17	B	3.20	1.28	0.00	0.00	70	B	1.84	0.27	0.76	0.00
18:00	17	B	3.20	1.24	0.00	0.00	70	B	1.64	0.12	0.40	0.00
19:00	17	B	2.40	1.24	0.00	0.00	70	B	1.80	0.00	0.00	0.00
20:00	17	B	3.20	1.12	0.00	0.00	70	B	2.32	0.30	0.00	0.00
21:00	17	B	2.40	0.64	0.00	0.00	70	B	1.76	0.19	0.00	0.00
22:00	17	B	2.40	0.60	0.00	0.00	70	B	0.72	0.08	0.00	0.00
23:00	17	B	2.00	0.68	0.00	0.00	70	B	0.44	0.08	0.00	0.00
24:00	17	B	1.60	0.44	0.00	0.00	70	B	0.48	0.23	0.00	0.00
00:00	21	A	0.44	0.16	0.00	0.00	76	B	1.20	0.56	0.00	0.00
01:00	21	A	0.44	0.12	0.00	0.00	76	B	1.60	0.60	0.00	0.00
02:00	21	A	0.40	0.08	0.00	0.00	76	B	1.60	0.64	0.00	0.00
03:00	21	A	0.36	0.04	0.00	0.00	76	B	1.20	0.60	0.00	0.00
04:00	21	A	0.96	0.16	0.00	0.00	76	B	1.20	0.52	0.00	0.00
05:00	21	A	0.36	0.04	0.00	0.00	76	B	1.60	0.68	0.00	0.00
06:00	21	A	0.32	0.04	0.00	0.00	76	B	1.20	0.36	0.00	0.00
07:00	21	A	0.40	0.08	0.00	0.00	76	B	1.60	0.60	0.00	0.00
08:00	21	A	0.28	0.00	0.00	0.00	76	B	1.60	0.48	0.00	0.00
09:00	21	A	0.88	0.20	0.00	0.00	76	B	1.60	0.44	0.00	0.00
10:00	21	A	0.68	0.08	0.00	0.00	76	B	1.60	0.60	0.00	0.00
11:00	21	A	0.28	0.12	0.00	0.00	76	B	1.60	0.72	0.00	0.00
12:00	21	A	0.32	0.24	0.00	0.00	76	B	1.60	0.72	0.00	0.00
13:00	21	A	2.72	0.80	0.00	0.00	76	B	2.00	0.72	0.00	0.00
14:00	21	A	2.08	0.68	0.00	0.00	76	B	1.60	0.76	0.00	0.00
15:00	21	A	1.64	0.68	0.00	0.00	76	B	2.00	0.68	0.00	0.00
16:00	21	A	1.92	0.68	0.00	0.00	76	B	2.00	0.72	0.00	0.00

17:00	21	A	1.96	0.64	0.00	0.00	76	B	2.00	0.72	0.00	0.00
18:00	21	A	2.24	0.72	0.00	0.00	76	B	2.00	0.64	0.00	0.00
19:00	21	A	2.04	0.60	0.00	0.00	76	B	2.40	0.64	0.00	0.00
20:00	21	A	1.84	0.68	0.00	0.00	76	B	2.40	0.72	0.00	0.00
21:00	21	A	0.72	0.20	0.00	0.00	76	B	2.40	0.84	0.00	0.00
22:00	21	A	0.56	0.04	0.00	0.00	76	B	2.00	0.80	0.00	0.00
23:00	21	A	0.60	0.08	0.00	0.00	76	B	1.60	0.68	0.00	0.00
24:00	21	A	0.52	0.16	0.00	0.00	76	B	1.60	0.60	0.00	0.00
00:00	22	B	0.48	0.44	0.00	0.00	77	C	2.40	0.44	0.00	0.00
01:00	22	B	0.48	0.40	0.00	0.00	77	C	1.60	0.52	0.00	0.00
02:00	22	B	0.32	0.20	0.00	0.00	77	C	1.60	0.56	0.00	0.00
03:00	22	B	0.44	0.44	0.00	0.00	77	C	1.60	0.36	0.00	0.00
04:00	22	B	0.40	0.24	0.00	0.00	77	C	2.00	0.56	0.00	0.00
05:00	22	B	0.44	0.36	0.00	0.00	77	C	2.40	0.64	0.00	0.00
06:00	22	B	0.28	0.20	0.00	0.00	77	C	2.40	0.68	0.00	0.00
07:00	22	B	0.28	0.20	0.00	0.00	77	C	2.80	0.48	0.00	0.00
08:00	22	B	0.40	0.32	0.00	0.00	77	C	3.20	0.72	0.00	0.00
09:00	22	B	0.44	0.36	0.00	0.00	77	C	2.40	0.56	0.00	0.00
10:00	22	B	0.36	0.20	0.00	0.00	77	C	2.80	0.92	0.00	0.00
11:00	22	B	0.48	0.44	0.00	0.00	77	C	2.80	0.64	0.00	0.00
12:00	22	B	0.40	0.28	0.00	0.00	77	C	2.80	0.60	0.00	0.00
13:00	22	B	0.48	0.44	0.00	0.00	77	C	2.80	0.52	0.00	0.00
14:00	22	B	0.48	0.44	0.00	0.00	77	C	2.80	0.60	0.00	0.00
15:00	22	B	0.40	0.36	0.00	0.00	77	C	2.40	0.56	0.00	0.00
16:00	22	B	0.48	0.44	0.00	0.00	77	C	1.60	0.64	0.00	0.00
17:00	22	B	0.48	0.44	0.00	0.00	77	C	1.60	0.56	0.00	0.00
18:00	22	B	0.44	0.40	0.00	0.00	77	C	1.60	0.52	0.00	0.00
19:00	22	B	0.52	0.44	0.00	0.00	77	C	1.60	0.56	0.00	0.00
20:00	22	B	1.60	0.84	0.00	0.00	77	C	1.60	0.44	0.00	0.00
21:00	22	B	1.52	0.60	0.00	0.00	77	C	2.00	0.40	0.00	0.00

22:00	22	B	1.32	1.20	0.00	0.00	77	C	2.00	0.48	0.00	0.00
23:00	22	B	1.08	0.88	0.00	0.00	77	C	1.60	0.52	0.00	0.00
24:00	22	B	1.20	1.12	0.00	0.00	77	C	1.60	0.52	0.00	0.00
00:00	23	C	1.00	0.00	0.00	0.00	78	C	0.76	0.54	0.00	0.00
01:00	23	C	0.96	0.00	0.00	0.00	78	C	0.80	0.55	0.00	0.00
02:00	23	C	0.96	0.00	0.00	0.00	78	C	0.60	0.42	0.00	0.00
03:00	23	C	0.24	0.00	0.00	0.00	78	C	0.68	0.52	0.00	0.00
04:00	23	C	0.68	0.00	0.00	0.00	78	C	0.52	0.36	0.00	0.00
05:00	23	C	0.76	0.00	0.00	0.00	78	C	0.68	0.55	0.00	0.00
06:00	23	C	0.64	0.00	0.00	0.00	78	C	0.60	0.51	0.04	0.00
07:00	23	C	0.68	0.00	0.00	0.00	78	C	0.44	0.34	0.16	0.00
08:00	23	C	0.68	0.00	0.00	0.00	78	C	0.76	0.56	0.44	0.00
09:00	23	C	0.72	0.00	0.00	0.00	78	C	1.00	0.33	1.00	0.00
10:00	23	C	1.08	0.00	0.00	0.00	78	C	0.76	0.58	1.36	0.00
11:00	23	C	0.96	0.00	0.00	0.00	78	C	0.84	0.61	1.56	0.00
12:00	23	C	0.96	0.00	0.00	0.00	78	C	1.16	0.53	1.96	0.00
13:00	23	C	0.96	0.00	0.00	0.00	78	C	1.28	0.61	2.00	0.00
14:00	23	C	1.28	0.00	0.00	0.00	78	C	1.04	0.44	1.92	0.00
15:00	23	C	1.08	0.00	0.00	0.00	78	C	1.24	0.60	1.84	0.00
16:00	23	C	1.32	0.00	0.00	0.00	78	C	1.20	0.56	1.28	0.00
17:00	23	C	3.16	0.00	0.00	0.00	78	C	1.24	0.64	1.16	0.00
18:00	23	C	1.52	0.00	0.00	0.00	78	C	2.24	0.74	0.56	0.00
19:00	23	C	1.24	0.00	0.00	0.00	78	C	1.16	0.50	0.00	0.00
20:00	23	C	1.32	0.00	0.00	0.00	78	C	1.28	0.77	0.00	0.00
21:00	23	C	1.20	0.00	0.00	0.00	78	C	0.88	0.42	0.00	0.00
22:00	23	C	1.48	0.00	0.00	0.00	78	C	0.76	0.48	0.00	0.00
23:00	23	C	1.52	0.00	0.00	0.00	78	C	0.48	0.32	0.00	0.00
24:00	23	C	1.04	0.00	0.00	0.00	78	C	0.60	0.48	0.00	0.00
00:00	24	C	1.28	0.40	0.00	0.00	82	C	0.16	0.04	0.00	0.00
01:00	24	C	1.20	0.36	0.00	0.00	82	C	0.32	0.20	0.00	0.00

02:00	24	C	1.24	0.40	0.00	0.00	82	C	0.20	0.08	0.00	0.00
03:00	24	C	1.28	0.44	0.00	0.00	82	C	0.36	0.24	0.00	0.00
04:00	24	C	1.36	0.48	0.00	0.00	82	C	0.16	0.04	0.00	0.00
05:00	24	C	1.36	0.52	0.00	0.00	82	C	0.36	0.24	0.00	0.00
06:00	24	C	0.88	0.20	0.00	0.00	82	C	0.20	0.08	0.00	0.00
07:00	24	C	0.40	0.16	0.00	0.00	82	C	0.32	0.20	0.00	0.00
08:00	24	C	0.00	0.24	0.12	0.00	82	C	0.56	0.28	0.00	0.00
09:00	24	C	0.00	0.28	0.17	0.00	82	C	1.20	0.68	0.00	0.00
10:00	24	C	0.00	0.36	0.35	0.00	82	C	1.60	0.84	0.00	0.00
11:00	24	C	0.00	0.36	0.40	0.00	82	C	1.16	0.28	0.00	0.00
12:00	24	C	0.00	0.40	0.30	0.00	82	C	1.08	0.16	0.00	0.00
13:00	24	C	0.00	0.40	0.25	0.00	82	C	1.20	0.36	0.00	0.00
14:00	24	C	0.00	0.36	0.22	0.00	82	C	1.08	0.24	0.00	0.00
15:00	24	C	0.00	0.32	0.08	0.00	82	C	1.20	0.40	0.00	0.00
16:00	24	C	0.16	0.28	0.00	0.00	82	C	1.16	0.44	0.00	0.00
17:00	24	C	0.36	0.32	0.00	0.00	82	C	1.20	0.32	0.00	0.00
18:00	24	C	1.96	0.76	0.00	0.00	82	C	2.20	0.28	0.00	0.00
19:00	24	C	2.64	0.72	0.00	0.00	82	C	1.72	0.36	0.00	0.00
20:00	24	C	3.00	0.68	0.00	0.00	82	C	1.44	0.24	0.00	0.00
21:00	24	C	3.48	0.68	0.00	0.00	82	C	1.04	0.16	0.00	0.00
22:00	24	C	2.48	0.60	0.00	0.00	82	C	1.04	0.36	0.00	0.00
23:00	24	C	2.92	0.76	0.00	0.00	82	C	0.44	0.08	0.00	0.00
24:00	24	C	1.72	0.40	0.00	0.00	82	C	0.40	0.20	0.00	0.00
00:00	26	B	1.60	1.04	0.00	0.00	84	C	0.80	0.84	0.00	0.00
01:00	26	B	1.20	1.04	0.00	0.00	84	C	0.88	0.88	0.00	0.00
02:00	26	B	1.20	1.08	0.00	0.00	84	C	0.76	0.76	0.00	0.00
03:00	26	B	0.80	1.08	0.00	0.00	84	C	0.72	0.64	0.00	0.00
04:00	26	B	1.20	1.12	0.00	0.00	84	C	0.88	0.84	0.00	0.00
05:00	26	B	0.80	1.08	0.00	0.00	84	C	0.84	0.84	0.00	0.00
06:00	26	B	1.20	1.00	0.00	0.00	84	C	0.72	0.68	0.02	0.00

07:00	26	B	1.20	1.04	0.00	0.00	84	C	1.08	0.84	0.10	0.00
08:00	26	B	1.60	1.00	0.00	0.00	84	C	1.16	0.92	0.06	0.00
09:00	26	B	2.00	1.16	0.00	0.00	84	C	1.20	0.76	0.09	0.00
10:00	26	B	2.00	1.08	0.00	0.00	84	C	1.08	0.72	1.16	0.00
11:00	26	B	2.00	1.08	0.00	0.00	84	C	0.96	0.84	1.31	0.00
12:00	26	B	2.00	1.12	0.00	0.00	84	C	0.88	0.96	1.31	0.00
13:00	26	B	1.60	1.16	0.00	0.00	84	C	0.72	0.68	1.26	0.00
14:00	26	B	2.00	1.24	0.00	0.00	84	C	0.88	0.92	1.11	0.00
15:00	26	B	1.60	1.20	0.00	0.00	84	C	0.88	0.96	0.91	0.00
16:00	26	B	2.00	1.20	0.00	0.00	84	C	0.92	0.96	0.53	0.00
17:00	26	B	1.60	1.04	0.00	0.00	84	C	0.92	0.92	0.26	0.00
18:00	26	B	3.20	0.92	0.00	0.00	84	C	1.88	0.88	0.04	0.00
19:00	26	B	1.60	1.04	0.00	0.00	84	C	1.40	1.08	0.01	0.00
20:00	26	B	1.60	0.96	0.00	0.00	84	C	1.16	0.76	0.00	0.00
21:00	26	B	1.60	1.00	0.00	0.00	84	C	1.48	0.80	0.00	0.00
22:00	26	B	1.20	0.96	0.00	0.00	84	C	1.28	0.84	0.00	0.00
23:00	26	B	1.20	0.96	0.00	0.00	84	C	1.20	0.76	0.00	0.00
24:00	26	B	0.80	0.92	0.00	0.00	84	C	1.08	0.64	0.00	0.00
00:00	27	C	0.56	0.60	0.00	0.00	85	B	0.72	0.40	0.00	0.00
01:00	27	C	0.32	0.35	0.00	0.00	85	B	0.56	0.28	0.00	0.00
02:00	27	C	0.32	0.35	0.00	0.00	85	B	0.72	0.40	0.00	0.00
03:00	27	C	0.42	0.45	0.00	0.00	85	B	0.56	0.24	0.00	0.00
04:00	27	C	0.51	0.38	0.00	0.00	85	B	1.92	0.68	0.00	0.00
05:00	27	C	0.45	0.51	0.00	0.00	85	B	0.84	0.24	0.00	0.00
06:00	27	C	0.32	0.35	0.00	0.00	85	B	0.96	0.48	0.04	0.00
07:00	27	C	0.35	0.42	0.11	0.00	85	B	0.36	0.20	0.40	0.00
08:00	27	C	0.38	0.29	0.36	0.00	85	B	0.56	0.24	0.84	0.00
09:00	27	C	0.22	0.16	0.77	0.00	85	B	0.60	0.40	1.20	0.00
10:00	27	C	0.42	0.42	1.10	0.00	85	B	0.36	0.12	1.48	0.00
11:00	27	C	0.48	0.51	1.35	0.00	85	B	0.68	0.28	1.60	0.00

12:00	27	C	0.35	0.35	1.49	0.00	85	B	1.36	1.12	1.60	0.00
13:00	27	C	1.89	1.25	1.54	0.00	85	B	1.28	0.88	1.60	0.00
14:00	27	C	3.62	2.24	1.47	0.00	85	B	2.72	0.96	1.48	0.00
15:00	27	C	3.68	2.24	1.33	0.00	85	B	2.76	1.00	1.32	0.00
16:00	27	C	3.81	2.37	0.96	0.00	85	B	1.28	1.12	0.84	0.00
17:00	27	C	3.87	2.24	0.72	0.00	85	B	2.04	1.20	0.48	0.00
18:00	27	C	4.03	1.95	0.34	0.00	85	B	1.36	0.96	0.08	0.00
19:00	27	C	3.84	1.89	0.01	0.00	85	B	2.88	1.40	0.00	0.00
20:00	27	C	3.87	1.95	0.00	0.00	85	B	1.40	0.88	0.00	0.00
21:00	27	C	2.56	1.70	0.00	0.00	85	B	1.64	0.88	0.00	0.00
22:00	27	C	2.72	1.76	0.00	0.00	85	B	1.52	0.92	0.00	0.00
23:00	27	C	2.56	1.66	0.00	0.00	85	B	1.56	1.00	0.00	0.00
24:00	27	C	0.35	0.22	0.00	0.00	85	B	1.60	1.00	0.00	0.00
00:00	28	A	1.60	0.48	0.00	0.00	91	C	1.24	0.92	0.00	0.00
01:00	28	A	1.20	0.52	0.00	0.00	91	C	1.20	0.88	0.00	0.00
02:00	28	A	1.20	0.52	0.00	0.00	91	C	1.24	0.92	0.00	0.00
03:00	28	A	1.20	0.52	0.00	0.00	91	C	1.12	0.84	0.00	0.00
04:00	28	A	1.20	0.44	0.00	0.00	91	C	1.16	0.84	0.00	0.00
05:00	28	A	0.80	0.40	0.00	0.00	91	C	1.40	0.96	0.00	0.00
06:00	28	A	1.20	0.28	0.00	0.00	91	C	0.80	0.32	0.00	0.00
07:00	28	A	0.40	0.20	0.00	0.00	91	C	0.44	0.16	0.00	0.00
08:00	28	A	0.00	0.08	0.00	0.00	91	C	0.36	0.24	0.02	0.00
09:00	28	A	0.40	0.12	0.00	0.00	91	C	0.20	0.20	0.10	0.00
10:00	28	A	0.00	0.28	0.00	0.00	91	C	0.16	0.20	0.25	0.00
11:00	28	A	0.40	0.28	0.00	0.00	91	C	0.12	0.24	0.36	0.00
12:00	28	A	0.40	0.20	0.00	0.00	91	C	0.08	0.24	0.38	0.00
13:00	28	A	0.00	0.20	0.00	0.00	91	C	1.04	0.24	0.00	0.00
14:00	28	A	0.40	0.24	0.00	0.00	91	C	1.04	0.56	0.00	0.00
15:00	28	A	2.40	0.76	0.00	0.00	91	C	0.44	0.84	0.00	0.00
16:00	28	A	2.80	0.84	0.00	0.00	91	C	0.60	0.68	0.00	0.00

17:00	28	A	2.80	0.84	0.00	0.00	91	C	0.64	0.76	0.00	0.00
18:00	28	A	2.40	0.80	0.00	0.00	91	C	1.40	0.68	0.00	0.00
19:00	28	A	2.40	0.48	0.00	0.00	91	C	1.96	0.24	0.00	0.00
20:00	28	A	0.80	0.24	0.00	0.00	91	C	2.36	0.48	0.00	0.00
21:00	28	A	0.80	0.24	0.00	0.00	91	C	1.76	0.84	0.00	0.00
22:00	28	A	2.80	0.76	0.00	0.00	91	C	0.88	0.68	0.00	0.00
23:00	28	A	3.20	0.72	0.00	0.00	91	C	0.88	0.64	0.00	0.00
24:00	28	A	2.00	0.48	0.00	0.00	91	C	0.80	0.56	0.00	0.00
00:00	30	C	0.80	0.04	0.00	0.00	94	A	0.16	0.24	0.00	0.00
01:00	30	C	0.68	0.14	0.00	0.00	94	A	0.12	0.16	0.00	0.00
02:00	30	C	0.52	0.03	0.00	0.00	94	A	0.16	0.16	0.00	0.00
03:00	30	C	0.56	0.06	0.00	0.00	94	A	0.08	0.08	0.00	0.00
04:00	30	C	0.56	0.09	0.00	0.00	94	A	0.20	0.20	0.00	0.00
05:00	30	C	0.68	0.13	0.00	0.00	94	A	0.12	0.12	0.00	0.00
06:00	30	C	0.40	0.00	0.08	0.00	94	A	0.16	0.20	0.00	0.00
07:00	30	C	0.48	0.06	0.76	0.00	94	A	0.08	0.04	0.00	0.00
08:00	30	C	0.48	0.13	1.20	0.00	94	A	0.20	0.24	0.00	0.00
09:00	30	C	0.52	0.15	1.56	0.00	94	A	1.44	0.60	0.00	0.00
10:00	30	C	0.44	0.04	1.76	0.00	94	A	3.04	0.56	0.00	0.00
11:00	30	C	0.44	0.10	1.88	0.00	94	A	1.60	0.56	0.00	0.00
12:00	30	C	0.44	0.05	1.88	0.00	94	A	1.52	0.60	0.00	0.00
13:00	30	C	0.60	0.16	1.76	0.00	94	A	1.48	0.60	0.00	0.00
14:00	30	C	0.80	0.18	1.56	0.00	94	A	1.52	0.60	0.00	0.00
15:00	30	C	0.88	0.24	1.24	0.00	94	A	1.52	0.60	0.00	0.00
16:00	30	C	0.64	0.16	0.72	0.00	94	A	1.52	0.64	0.00	0.00
17:00	30	C	0.64	0.13	0.12	0.00	94	A	1.64	0.52	0.00	0.00
18:00	30	C	0.60	0.13	0.08	0.00	94	A	1.60	0.48	0.00	0.00
19:00	30	C	0.68	0.16	0.00	0.00	94	A	1.56	0.44	0.00	0.00
20:00	30	C	0.60	0.14	0.00	0.00	94	A	0.32	0.20	0.00	0.00
21:00	30	C	0.72	0.12	0.00	0.00	94	A	0.24	0.16	0.00	0.00

22:00	30	C	0.72	0.13	0.00	0.00	94	A	0.20	0.20	0.00	0.00
23:00	30	C	0.64	0.10	0.00	0.00	94	A	0.16	0.24	0.00	0.00
24:00	30	C	0.72	0.14	0.00	0.00	94	A	0.16	0.24	0.00	0.00
00:00	35	C	1.04	0.00	0.00	0.00	95	B	2.00	0.38	0.00	0.00
01:00	35	C	1.00	0.00	0.00	0.00	95	B	2.40	0.40	0.00	0.00
02:00	35	C	0.88	0.00	0.00	0.00	95	B	2.00	0.38	0.00	0.00
03:00	35	C	0.80	0.00	0.00	0.00	95	B	2.00	0.38	0.00	0.00
04:00	35	C	0.76	0.00	0.00	0.00	95	B	2.00	0.40	0.00	0.00
05:00	35	C	0.52	0.00	0.00	0.00	95	B	2.40	0.50	0.00	0.00
06:00	35	C	0.40	0.00	0.00	0.00	95	B	2.00	0.40	0.00	0.00
07:00	35	C	0.16	0.00	0.00	0.00	95	B	3.60	0.42	0.00	0.00
08:00	35	C	0.00	0.00	0.04	0.00	95	B	2.40	0.40	0.00	0.00
09:00	35	C	0.00	0.00	0.40	0.00	95	B	2.40	0.39	0.00	0.00
10:00	35	C	0.00	0.00	0.64	0.00	95	B	2.00	0.33	0.00	0.00
11:00	35	C	0.00	0.00	0.80	0.00	95	B	2.40	0.40	0.00	0.00
12:00	35	C	0.00	0.00	0.92	0.00	95	B	2.80	0.26	0.00	0.00
13:00	35	C	0.00	0.00	0.96	0.00	95	B	2.80	0.37	0.00	0.00
14:00	35	C	0.00	0.00	0.96	0.00	95	B	2.00	0.46	0.00	0.00
15:00	35	C	0.00	0.00	0.84	0.00	95	B	2.40	0.32	0.00	0.00
16:00	35	C	0.00	0.00	0.52	0.00	95	B	3.20	0.33	0.00	0.00
17:00	35	C	0.00	0.00	0.36	0.00	95	B	2.40	0.38	0.00	0.00
18:00	35	C	0.08	0.00	0.04	0.00	95	B	2.80	0.31	0.00	0.00
19:00	35	C	2.72	0.00	0.00	0.00	95	B	5.20	0.14	0.00	0.00
20:00	35	C	2.80	0.00	0.00	0.00	95	B	2.80	0.15	0.00	0.00
21:00	35	C	2.68	0.00	0.00	0.00	95	B	2.40	0.17	0.00	0.00
22:00	35	C	1.64	0.00	0.00	0.00	95	B	2.80	0.27	0.00	0.00
23:00	35	C	1.32	0.00	0.00	0.00	95	B	3.20	0.31	0.00	0.00
24:00	35	C	1.08	0.00	0.00	0.00	95	B	2.80	0.37	0.00	0.00
00:00	36	A	1.20	0.16	0.00	0.00	96	C	1.20	0.12	0.00	0.00
01:00	36	A	1.08	0.12	0.00	0.00	96	C	0.92	0.12	0.00	0.00

02:00	36	A	0.96	0.16	0.00	0.00	96	C	0.88	0.04	0.00	0.00
03:00	36	A	0.88	0.12	0.00	0.00	96	C	0.84	0.08	0.00	0.00
04:00	36	A	0.84	0.16	0.00	0.00	96	C	0.88	0.20	0.00	0.00
05:00	36	A	0.64	0.12	0.00	0.00	96	C	0.84	0.12	0.00	0.00
06:00	36	A	0.64	0.04	0.00	0.00	96	C	0.80	0.08	0.00	0.00
07:00	36	A	0.72	0.08	0.00	0.00	96	C	0.84	0.16	0.00	0.00
08:00	36	A	0.40	0.12	0.03	0.00	96	C	1.32	0.16	0.00	0.00
09:00	36	A	1.40	0.40	0.00	0.00	96	C	0.88	0.12	0.00	0.00
10:00	36	A	0.72	0.00	0.10	0.00	96	C	0.88	0.08	0.00	0.00
11:00	36	A	2.08	0.00	0.00	0.00	96	C	1.16	0.04	0.00	0.00
12:00	36	A	2.04	0.00	0.00	0.00	96	C	1.28	0.12	0.00	0.00
13:00	36	A	3.08	0.24	0.00	0.00	96	C	1.12	0.16	0.00	0.00
14:00	36	A	3.16	0.28	0.00	0.00	96	C	1.20	0.08	0.00	0.00
15:00	36	A	2.64	0.00	0.00	0.00	96	C	1.24	0.12	0.00	0.00
16:00	36	A	3.08	0.00	0.00	0.00	96	C	1.20	0.12	0.00	0.00
17:00	36	A	3.96	0.24	0.00	0.00	96	C	1.16	0.08	0.00	0.00
18:00	36	A	3.76	0.08	0.00	0.00	96	C	1.12	0.04	0.00	0.00
19:00	36	A	4.00	0.24	0.00	0.00	96	C	1.28	0.04	0.00	0.00
20:00	36	A	4.72	0.00	0.00	0.00	96	C	1.16	0.08	0.00	0.00
21:00	36	A	3.60	0.00	0.00	0.00	96	C	1.08	0.04	0.00	0.00
22:00	36	A	2.40	0.12	0.00	0.00	96	C	1.08	0.04	0.00	0.00
23:00	36	A	1.24	0.16	0.00	0.00	96	C	1.08	0.04	0.00	0.00
24:00	36	A	1.12	0.08	0.00	0.00	96	C	1.28	0.12	0.00	0.00
00:00	38	B	0.20	0.12	0.00	0.00	97	C	1.20	0.00	0.00	0.00
01:00	38	B	0.16	0.12	0.00	0.00	97	C	1.20	0.00	0.00	0.00
02:00	38	B	0.12	0.04	0.00	0.00	97	C	1.20	0.00	0.00	0.00
03:00	38	B	0.16	0.16	0.00	0.00	97	C	1.20	0.00	0.00	0.00
04:00	38	B	0.12	0.04	0.00	0.00	97	C	1.20	0.00	0.00	0.00
05:00	38	B	0.20	0.16	0.00	0.00	97	C	1.20	0.00	0.00	0.00
06:00	38	B	0.44	0.16	0.00	0.00	97	C	1.20	0.00	0.00	0.00

07:00	38	B	0.12	0.04	0.00	0.00	97	C	1.20	0.00	0.00	0.00
08:00	38	B	0.16	0.16	0.00	0.00	97	C	3.60	0.00	0.00	0.00
09:00	38	B	0.08	0.00	0.00	0.00	97	C	2.00	0.00	0.00	0.00
10:00	38	B	0.16	0.16	0.00	0.00	97	C	2.40	0.00	0.00	0.00
11:00	38	B	0.04	0.00	0.00	0.00	97	C	2.00	0.00	0.00	0.00
12:00	38	B	0.16	0.16	0.00	0.00	97	C	2.00	0.00	0.00	0.00
13:00	38	B	0.12	0.08	0.00	0.00	97	C	4.00	0.02	0.00	0.00
14:00	38	B	0.16	0.16	0.00	0.00	97	C	3.20	0.00	0.00	0.00
15:00	38	B	0.20	0.16	0.00	0.00	97	C	3.20	0.00	0.00	0.00
16:00	38	B	0.28	0.16	0.00	0.00	97	C	4.80	0.00	0.00	0.00
17:00	38	B	0.28	0.04	0.00	0.00	97	C	2.80	0.00	0.00	0.00
18:00	38	B	2.24	0.52	0.00	0.00	97	C	4.00	0.00	0.00	0.00
19:00	38	B	2.00	0.48	0.00	0.00	97	C	2.40	0.00	0.00	0.00
20:00	38	B	1.88	0.44	0.00	0.00	97	C	2.80	0.00	0.00	0.00
21:00	38	B	1.88	0.48	0.00	0.00	97	C	2.80	0.00	0.00	0.00
22:00	38	B	1.84	0.36	0.00	0.00	97	C	3.60	0.00	0.00	0.00
23:00	38	B	1.92	0.52	0.00	0.00	97	C	3.60	0.00	0.00	0.00
24:00	38	B	1.96	0.56	0.00	0.00	97	C	3.60	0.00	0.00	0.00
00:00	39	A	1.08	1.00	0.00	0.00	98	B	1.20	0.24	0.00	0.00
01:00	39	A	1.28	0.79	0.00	0.00	98	B	0.40	0.16	0.00	0.00
02:00	39	A	1.12	0.99	0.00	0.00	98	B	0.40	0.24	0.00	0.00
03:00	39	A	1.08	1.01	0.00	0.00	98	B	0.80	0.28	0.00	0.00
04:00	39	A	1.12	1.03	0.00	0.00	98	B	0.40	0.20	0.00	0.00
05:00	39	A	1.36	1.07	0.00	0.00	98	B	0.40	0.20	0.00	0.00
06:00	39	A	1.08	1.03	0.04	0.00	98	B	0.40	0.24	0.00	0.00
07:00	39	A	1.12	1.02	0.12	0.00	98	B	0.40	0.20	0.00	0.00
08:00	39	A	1.16	1.06	0.08	0.00	98	B	2.00	0.48	0.00	0.00
09:00	39	A	1.20	1.12	0.72	0.00	98	B	1.20	0.40	0.00	0.00
10:00	39	A	1.20	1.14	1.16	0.00	98	B	2.80	0.88	0.00	0.00
11:00	39	A	1.20	1.11	1.40	0.00	98	B	1.20	0.52	0.00	0.00

12:00	39	A	1.12	1.17	1.44	0.00	98	B	1.60	0.44	0.00	0.00
13:00	39	A	1.12	1.12	1.44	0.00	98	B	0.80	0.48	0.00	0.00
14:00	39	A	1.24	1.17	1.36	0.00	98	B	1.20	0.76	0.00	0.00
15:00	39	A	1.32	1.13	1.48	0.00	98	B	0.80	0.56	0.00	0.00
16:00	39	A	1.32	1.15	1.08	0.00	98	B	1.20	0.68	0.00	0.00
17:00	39	A	1.28	1.12	0.92	0.00	98	B	1.20	0.76	0.00	0.00
18:00	39	A	1.40	1.06	0.12	0.00	98	B	1.20	0.56	0.00	0.00
19:00	39	A	1.40	0.82	0.00	0.00	98	B	0.80	0.44	0.00	0.00
20:00	39	A	1.24	0.56	0.00	0.00	98	B	1.60	0.56	0.00	0.00
21:00	39	A	2.60	0.46	0.00	0.00	98	B	2.00	0.56	0.00	0.00
22:00	39	A	1.00	0.39	0.00	0.00	98	B	0.80	0.36	0.00	0.00
23:00	39	A	1.08	0.43	0.00	0.00	98	B	0.40	0.32	0.00	0.00
24:00	39	A	1.12	0.98	0.00	0.00	98	B	0.40	0.28	0.00	0.00
00:00	40	C	0.64	0.30	0.00	0.00	99	A	0.20	0.20	0.00	0.00
01:00	40	C	0.56	0.28	0.00	0.00	99	A	0.20	0.20	0.00	0.00
02:00	40	C	0.32	0.21	0.00	0.00	99	A	0.20	0.20	0.00	0.00
03:00	40	C	0.28	0.20	0.00	0.00	99	A	0.16	0.16	0.00	0.00
04:00	40	C	0.28	0.22	0.00	0.00	99	A	0.12	0.12	0.00	0.00
05:00	40	C	0.28	0.22	0.00	0.00	99	A	0.12	0.08	0.00	0.00
06:00	40	C	0.28	0.23	0.04	0.00	99	A	0.24	0.12	0.00	0.00
07:00	40	C	0.32	0.23	0.12	0.00	99	A	0.24	0.20	0.00	0.00
08:00	40	C	0.44	0.27	0.20	0.00	99	A	0.52	0.20	0.00	0.00
09:00	40	C	0.32	0.23	0.08	0.00	99	A	0.12	0.20	0.00	0.00
10:00	40	C	1.28	0.02	1.16	0.00	99	A	0.12	0.20	0.00	0.00
11:00	40	C	0.56	0.33	1.40	0.00	99	A	0.16	0.20	0.00	0.00
12:00	40	C	0.60	0.33	1.48	0.00	99	A	0.12	0.16	0.00	0.00
13:00	40	C	1.44	0.00	1.52	0.00	99	A	0.08	0.12	0.00	0.00
14:00	40	C	1.36	0.11	1.44	0.00	99	A	0.12	0.24	0.00	0.00
15:00	40	C	1.52	0.01	1.48	0.00	99	A	0.12	0.00	0.00	0.00
16:00	40	C	1.76	0.00	1.04	0.00	99	A	0.16	0.20	0.00	0.00

17:00	40	C	1.56	0.00	0.92	0.00	99	A	0.12	0.20	0.00	0.00
18:00	40	C	1.56	0.00	0.40	0.00	99	A	0.80	0.20	0.00	0.00
19:00	40	C	1.52	0.00	0.04	0.00	99	A	0.12	0.16	0.00	0.00
20:00	40	C	1.04	0.03	0.00	0.00	99	A	0.16	0.16	0.00	0.00
21:00	40	C	1.20	0.05	0.00	0.00	99	A	0.12	0.20	0.00	0.00
22:00	40	C	0.84	0.37	0.00	0.00	99	A	0.12	0.16	0.00	0.00
23:00	40	C	0.80	0.35	0.00	0.00	99	A	0.28	0.20	0.00	0.00
24:00	40	C	1.04	0.37	0.00	0.00	99	A	0.36	0.16	0.00	0.00
00:00	44	C	0.72	0.40	0.00	0.00	100	B	0.72	0.08	0.00	0.00
01:00	44	C	0.76	0.40	0.00	0.00	100	B	0.72	0.08	0.00	0.00
02:00	44	C	0.48	0.16	0.00	0.00	100	B	0.80	0.08	0.00	0.00
03:00	44	C	0.64	0.36	0.00	0.00	100	B	0.60	0.12	0.00	0.00
04:00	44	C	1.08	0.16	0.00	0.00	100	B	0.52	0.08	0.00	0.00
05:00	44	C	0.68	0.36	0.00	0.00	100	B	0.48	0.12	0.00	0.00
06:00	44	C	0.52	0.20	0.00	0.00	100	B	0.24	0.04	0.00	0.00
07:00	44	C	0.16	0.20	0.00	0.00	100	B	0.12	0.00	0.00	0.00
08:00	44	C	0.00	0.00	0.08	0.00	100	B	0.16	0.00	0.00	0.00
09:00	44	C	0.00	0.20	0.28	0.00	100	B	0.16	0.00	0.00	0.00
10:00	44	C	0.00	0.24	0.60	0.00	100	B	0.16	0.00	0.00	0.00
11:00	44	C	0.00	0.24	0.80	0.00	100	B	0.16	0.00	0.00	0.00
12:00	44	C	0.00	0.24	0.84	0.00	100	B	0.16	0.00	0.00	0.00
13:00	44	C	0.00	0.24	0.92	0.00	100	B	0.16	0.00	0.00	0.00
14:00	44	C	0.00	0.28	0.84	0.00	100	B	0.12	0.00	0.00	0.00
15:00	44	C	0.00	0.28	0.72	0.00	100	B	0.16	0.04	0.00	0.00
16:00	44	C	0.08	0.32	0.44	0.00	100	B	0.20	0.00	0.00	0.00
17:00	44	C	0.00	0.28	0.32	0.00	100	B	0.72	0.04	0.00	0.00
18:00	44	C	0.28	0.24	0.00	0.00	100	B	1.40	0.00	0.00	0.00
19:00	44	C	0.16	0.04	0.00	0.00	100	B	0.24	0.00	0.00	0.00
20:00	44	C	1.28	0.64	0.00	0.00	100	B	0.20	0.00	0.00	0.00
21:00	44	C	1.36	0.60	0.00	0.00	100	B	0.08	0.00	0.00	0.00

22:00	44	C	1.08	0.44	0.00	0.00	100	B	0.16	0.04	0.00	0.00
23:00	44	C	0.92	0.40	0.00	0.00	100	B	0.20	0.00	0.00	0.00
24:00	44	C	0.52	0.16	0.00	0.00	100	B	0.28	0.04	0.00	0.00
00:00	46	A	0.80	0.48	0.00	0.00	101	A	0.56	0.02	0.00	0.00
01:00	46	A	0.80	0.44	0.00	0.00	101	A	0.52	0.01	0.00	0.00
02:00	46	A	2.80	0.40	0.00	0.00	101	A	0.52	0.01	0.00	0.00
03:00	46	A	2.40	0.36	0.00	0.00	101	A	0.52	0.01	0.00	0.00
04:00	46	A	2.80	0.44	0.00	0.00	101	A	0.52	0.01	0.00	0.00
05:00	46	A	0.80	0.28	0.00	0.00	101	A	0.60	0.04	0.00	0.00
06:00	46	A	0.40	0.28	0.00	0.00	101	A	0.12	0.00	0.00	0.00
07:00	46	A	0.40	0.32	0.00	0.00	101	A	0.20	0.00	0.00	0.00
08:00	46	A	0.80	0.20	0.00	0.00	101	A	0.24	0.00	0.00	0.00
09:00	46	A	0.40	0.28	0.00	0.00	101	A	0.20	0.00	0.00	0.00
10:00	46	A	0.40	0.52	0.00	0.00	101	A	0.20	0.00	0.00	0.00
11:00	46	A	0.40	0.56	0.00	0.00	101	A	0.68	0.00	0.00	0.00
12:00	46	A	0.80	0.52	0.00	0.00	101	A	0.44	0.00	0.00	0.00
13:00	46	A	0.40	0.52	0.00	0.00	101	A	0.64	0.00	0.00	0.00
14:00	46	A	0.40	0.48	0.00	0.00	101	A	0.64	0.00	0.00	0.00
15:00	46	A	0.40	0.52	0.00	0.00	101	A	0.44	0.00	0.00	0.00
16:00	46	A	4.00	0.92	0.00	0.00	101	A	0.20	0.00	0.00	0.00
17:00	46	A	3.60	0.80	0.00	0.00	101	A	0.80	0.02	0.00	0.00
18:00	46	A	3.60	0.76	0.00	0.00	101	A	1.52	0.01	0.00	0.00
19:00	46	A	3.60	0.80	0.00	0.00	101	A	1.60	0.00	0.00	0.00
20:00	46	A	4.00	0.72	0.00	0.00	101	A	1.52	0.01	0.00	0.00
21:00	46	A	3.60	0.40	0.00	0.00	101	A	1.44	0.00	0.00	0.00
22:00	46	A	3.20	0.76	0.00	0.00	101	A	1.44	0.02	0.00	0.00
23:00	46	A	2.80	0.52	0.00	0.00	101	A	0.68	0.00	0.00	0.00
24:00	46	A	2.00	0.32	0.00	0.00	101	A	0.60	0.04	0.00	0.00
00:00	47	B	0.40	0.44	0.00	0.00						
01:00	47	B	0.40	0.44	0.00	0.00						

02:00	47	B	0.80	0.40	0.00	0.00						
03:00	47	B	0.80	0.44	0.00	0.00						
04:00	47	B	0.80	0.48	0.00	0.00						
05:00	47	B	0.80	0.44	0.00	0.00						
06:00	47	B	0.80	0.48	0.00	0.00						
07:00	47	B	0.80	0.44	0.00	0.00						
08:00	47	B	0.80	0.48	0.00	0.00						
09:00	47	B	0.80	0.44	0.00	0.00						
10:00	47	B	0.80	0.40	0.00	0.00						
11:00	47	B	0.80	0.44	0.00	0.00						
12:00	47	B	0.80	0.40	0.00	0.00						
13:00	47	B	0.80	0.44	0.00	0.00						
14:00	47	B	0.80	0.56	0.00	0.00						
15:00	47	B	0.80	0.40	0.00	0.00						
16:00	47	B	0.80	0.52	0.00	0.00						
17:00	47	B	1.20	0.40	0.00	0.00						
18:00	47	B	1.60	0.44	0.00	0.00						
19:00	47	B	0.80	0.40	0.00	0.00						
20:00	47	B	0.80	0.40	0.00	0.00						
21:00	47	B	0.80	0.44	0.00	0.00						
22:00	47	B	0.80	0.44	0.00	0.00						
23:00	47	B	0.80	0.40	0.00	0.00						
24:00	47	B	0.80	0.48	0.00	0.00						

Table B.4 Loads and PV generations at three-phase buses of Pavetta1 LV network over 24 hours.

Time	Bus	P_{LA}(kW)	P_{LB}(kW)	P_{LC}(kW)	Q_{LA}(kVAr)	Q_{LB}(kVAr)	Q_{LC}(kVAr)	P_{PVA}(kW)	P_{PVB}(kW)	P_{PVC}(kW)	Q_{PVA}(kVAr)	Q_{PVB}(kVAr)	Q_{PVC}(kVAr)
00:00	6	0.52	0.00	0.00	0.24	0.02	0.00	0.00	0.00	0.00	0.00	0.00	0.00
01:00	6	0.40	0.00	0.00	0.16	0.02	0.00	0.00	0.00	0.00	0.00	0.00	0.00
02:00	6	0.28	0.00	0.00	0.12	0.02	0.00	0.00	0.00	0.00	0.00	0.00	0.00
03:00	6	0.28	0.00	0.00	0.20	0.02	0.00	0.00	0.00	0.00	0.00	0.00	0.00
04:00	6	0.24	0.00	0.00	0.12	0.02	0.00	0.00	0.00	0.00	0.00	0.00	0.00
05:00	6	0.28	0.00	0.00	0.20	0.02	0.00	0.00	0.00	0.00	0.00	0.00	0.00
06:00	6	0.12	0.04	0.00	0.08	0.02	0.00	0.06	0.00	0.00	0.00	0.00	0.00
07:00	6	0.00	0.00	0.00	0.04	0.01	0.00	0.34	0.00	0.00	0.00	0.00	0.00
08:00	6	0.00	0.00	0.00	0.16	0.02	0.00	0.95	0.00	0.00	0.00	0.00	0.00
09:00	6	0.00	0.68	0.00	0.08	0.50	0.00	1.40	0.00	0.00	0.00	0.00	0.00
10:00	6	0.00	0.68	0.00	0.04	0.49	0.00	1.68	0.00	0.00	0.00	0.00	0.00
11:00	6	0.00	1.04	0.00	0.08	0.66	0.00	1.68	0.00	0.00	0.00	0.00	0.00
12:00	6	0.04	1.04	0.04	0.08	0.66	0.00	1.62	0.00	0.00	0.00	0.00	0.00
13:00	6	0.12	1.08	0.00	0.12	0.66	0.00	1.01	0.00	0.00	0.00	0.00	0.00
14:00	6	0.04	0.92	0.00	0.12	0.63	0.00	1.23	0.00	0.00	0.00	0.00	0.00
15:00	6	0.00	0.44	0.00	0.08	0.34	0.00	1.06	0.00	0.00	0.00	0.00	0.00
16:00	6	0.04	0.56	0.00	0.12	0.36	0.00	0.45	0.00	0.00	0.00	0.00	0.00
17:00	6	0.12	0.44	0.04	0.08	0.30	0.00	0.00	0.00	0.00	0.00	0.00	0.00
18:00	6	0.44	0.88	0.04	0.20	0.54	0.00	0.00	0.00	0.00	0.00	0.00	0.00
19:00	6	0.72	0.00	3.76	0.32	0.01	0.76	0.00	0.00	0.00	0.00	0.00	0.00
20:00	6	1.64	0.00	0.96	0.16	0.02	0.19	0.00	0.00	0.00	0.00	0.00	0.00
21:00	6	1.88	0.00	0.00	0.12	0.02	0.00	0.00	0.00	0.00	0.00	0.00	0.00
22:00	6	1.00	0.00	0.00	0.28	0.01	0.00	0.00	0.00	0.00	0.00	0.00	0.00
23:00	6	0.36	0.00	0.00	0.12	0.02	0.00	0.00	0.00	0.00	0.00	0.00	0.00
24:00	6	0.40	0.00	0.00	0.20	0.02	0.00	0.00	0.00	0.00	0.00	0.00	0.00
00:00	9	1.20	0.08	0.00	0.16	0.12	0.00	0.00	0.00	0.00	0.00	0.00	0.00
01:00	9	1.20	0.08	0.04	0.32	0.08	0.00	0.00	0.00	0.00	0.00	0.00	0.00

02:00	9	1.20	0.12	0.00	0.32	0.08	0.00	0.00	0.00	0.00	0.00	0.00	0.00
03:00	9	0.80	0.12	0.00	0.12	0.12	0.00	0.00	0.00	0.00	0.00	0.00	0.00
04:00	9	0.40	0.12	0.00	0.24	0.08	0.00	0.00	0.00	0.00	0.00	0.00	0.00
05:00	9	0.00	0.12	0.00	0.04	0.12	0.00	0.00	0.00	0.00	0.00	0.00	0.00
06:00	9	0.40	0.44	0.04	0.28	0.12	0.00	0.00	0.00	0.00	0.00	0.00	0.00
07:00	9	0.80	0.16	0.00	0.48	0.16	0.00	0.00	0.00	0.00	0.00	0.00	0.00
08:00	9	2.00	0.28	0.00	0.48	0.16	0.00	0.00	0.00	0.00	0.00	0.00	0.00
09:00	9	2.40	0.08	0.04	0.36	0.16	0.00	0.00	0.00	0.00	0.00	0.00	0.00
10:00	9	2.40	0.08	0.00	0.32	0.16	0.00	0.00	0.00	0.00	0.00	0.00	0.00
11:00	9	2.00	0.08	3.32	0.20	0.12	3.12	0.00	0.00	0.00	0.00	0.00	0.00
12:00	9	1.60	0.08	3.44	0.20	0.16	3.08	0.00	0.00	0.00	0.00	0.00	0.00
13:00	9	2.00	0.08	3.44	0.16	0.16	3.00	0.00	0.00	0.00	0.00	0.00	0.00
14:00	9	1.60	0.08	3.56	0.24	0.16	3.08	0.00	0.00	0.00	0.00	0.00	0.00
15:00	9	1.60	0.08	3.56	0.16	0.16	3.00	0.00	0.00	0.00	0.00	0.00	0.00
16:00	9	2.00	0.08	3.52	0.20	0.20	3.04	0.00	0.00	0.00	0.00	0.00	0.00
17:00	9	2.00	0.08	3.48	0.36	0.16	3.00	0.00	0.00	0.00	0.00	0.00	0.00
18:00	9	2.40	0.04	3.48	0.48	0.16	2.96	0.00	0.00	0.00	0.00	0.00	0.00
19:00	9	2.00	0.08	3.32	0.32	0.12	2.76	0.00	0.00	0.00	0.00	0.00	0.00
20:00	9	2.00	0.08	3.20	0.56	0.12	2.80	0.00	0.00	0.00	0.00	0.00	0.00
21:00	9	2.00	0.08	3.08	0.44	0.12	2.80	0.00	0.00	0.00	0.00	0.00	0.00
22:00	9	3.20	0.08	0.00	0.60	0.12	0.00	0.00	0.00	0.00	0.00	0.00	0.00
23:00	9	3.20	0.08	0.00	0.60	0.12	0.00	0.00	0.00	0.00	0.00	0.00	0.00
24:00	9	1.60	0.08	3.16	0.48	0.12	3.12	0.00	0.00	0.00	0.00	0.00	0.00
00:00	18	0.00	0.04	0.20	0.00	0.00	0.00	0.00	0.00	0.00	0.00	0.00	0.00
01:00	18	0.00	0.04	0.16	0.00	0.00	0.00	0.00	0.00	0.00	0.00	0.00	0.00
02:00	18	0.00	0.00	0.20	0.00	0.00	0.00	0.00	0.00	0.00	0.00	0.00	0.00
03:00	18	0.00	0.00	0.28	0.00	0.00	0.00	0.00	0.00	0.00	0.00	0.00	0.00
04:00	18	0.00	0.00	0.24	0.00	0.04	0.00	0.00	0.00	0.00	0.00	0.00	0.00
05:00	18	0.00	0.04	0.24	0.00	0.04	0.00	0.00	0.00	0.00	0.00	0.00	0.00
06:00	18	0.00	0.00	0.28	0.00	0.04	0.00	0.00	0.00	0.00	0.00	0.00	0.00

07:00	18	0.04	0.00	0.36	0.00	0.04	0.04	0.00	0.00	0.00	0.00	0.00	0.00
08:00	18	0.20	0.00	0.32	0.00	0.04	0.04	0.00	0.00	0.00	0.00	0.00	0.00
09:00	18	0.88	0.68	1.44	0.64	0.68	0.80	0.00	0.00	0.00	0.00	0.00	0.00
10:00	18	1.36	1.04	2.08	1.00	1.08	1.16	0.00	0.00	0.00	0.00	0.00	0.00
11:00	18	1.44	1.08	2.08	1.00	1.08	1.16	0.00	0.00	0.00	0.00	0.00	0.00
12:00	18	1.48	1.12	2.08	1.04	1.08	1.08	0.00	0.00	0.00	0.00	0.00	0.00
13:00	18	1.48	1.20	2.08	0.96	1.04	1.12	0.00	0.00	0.00	0.00	0.00	0.00
14:00	18	1.52	1.20	2.04	0.96	1.12	1.16	0.00	0.00	0.00	0.00	0.00	0.00
15:00	18	1.48	1.24	2.00	0.96	1.12	1.08	0.00	0.00	0.00	0.00	0.00	0.00
16:00	18	1.52	1.20	2.12	0.96	1.12	1.12	0.00	0.00	0.00	0.00	0.00	0.00
17:00	18	1.48	1.24	2.08	0.92	1.16	1.12	0.00	0.00	0.00	0.00	0.00	0.00
18:00	18	1.40	1.16	2.04	0.84	1.12	1.04	0.00	0.00	0.00	0.00	0.00	0.00
19:00	18	1.36	1.12	1.92	0.84	1.12	1.00	0.00	0.00	0.00	0.00	0.00	0.00
20:00	18	1.36	1.04	1.96	0.84	1.08	0.96	0.00	0.00	0.00	0.00	0.00	0.00
21:00	18	1.24	1.00	1.88	0.84	1.08	0.88	0.00	0.00	0.00	0.00	0.00	0.00
22:00	18	0.32	0.28	0.64	0.20	0.28	0.24	0.00	0.00	0.00	0.00	0.00	0.00
23:00	18	0.04	0.04	0.16	0.00	0.04	0.00	0.00	0.00	0.00	0.00	0.00	0.00
24:00	18	0.00	0.00	0.24	0.00	0.04	0.00	0.00	0.00	0.00	0.00	0.00	0.00
00:00	19	0.00	0.80	0.00	0.00	0.20	0.00	0.00	0.00	0.00	0.00	0.00	0.00
01:00	19	0.00	0.40	0.00	0.00	0.08	0.00	0.00	0.00	0.00	0.00	0.00	0.00
02:00	19	0.00	0.80	0.00	0.00	0.28	0.00	0.00	0.00	0.00	0.00	0.00	0.00
03:00	19	0.00	0.80	0.00	0.00	0.24	0.00	0.00	0.00	0.00	0.00	0.00	0.00
04:00	19	0.00	0.80	0.00	0.00	0.24	0.00	0.00	0.00	0.00	0.00	0.00	0.00
05:00	19	0.00	1.60	0.00	0.00	0.32	0.00	0.00	0.00	0.00	0.00	0.00	0.00
06:00	19	0.00	1.60	0.00	0.00	0.24	0.00	0.00	0.00	0.00	0.00	0.00	0.00
07:00	19	0.00	1.60	0.00	0.00	0.28	0.00	0.00	0.00	0.00	0.00	0.00	0.00
08:00	19	0.00	1.60	0.60	0.00	0.28	0.64	0.00	0.00	0.00	0.00	0.00	0.00
09:00	19	0.00	2.40	2.48	0.00	0.68	2.28	0.00	0.00	0.00	0.00	0.00	0.00
10:00	19	0.00	2.40	2.60	0.00	0.48	2.28	0.00	0.00	0.00	0.00	0.00	0.00
11:00	19	0.00	2.80	2.72	0.00	0.60	2.20	0.00	0.00	0.00	0.00	0.00	0.00

12:00	19	0.00	2.40	2.76	0.00	0.60	2.24	0.00	0.00	0.00	0.00	0.00	0.00
13:00	19	0.00	2.40	2.88	0.00	0.72	2.16	0.00	0.00	0.00	0.00	0.00	0.00
14:00	19	0.00	2.40	2.88	0.00	0.84	2.20	0.00	0.00	0.00	0.00	0.00	0.00
15:00	19	0.00	2.40	2.96	0.00	0.72	2.12	0.00	0.00	0.00	0.00	0.00	0.00
16:00	19	0.00	2.40	2.92	0.00	0.68	2.16	0.00	0.00	0.00	0.00	0.00	0.00
17:00	19	0.00	2.40	2.92	0.00	0.72	2.12	0.00	0.00	0.00	0.00	0.00	0.00
18:00	19	0.00	1.20	2.80	0.00	0.32	2.08	0.00	0.00	0.00	0.00	0.00	0.00
19:00	19	0.00	2.40	2.68	0.00	0.48	2.00	0.00	0.00	0.00	0.00	0.00	0.00
20:00	19	0.00	3.20	2.44	0.00	0.52	2.04	0.00	0.00	0.00	0.00	0.00	0.00
21:00	19	0.00	2.80	2.32	0.00	0.52	1.96	0.00	0.00	0.00	0.00	0.00	0.00
22:00	19	0.00	2.80	1.08	0.00	0.52	0.96	0.00	0.00	0.00	0.00	0.00	0.00
23:00	19	0.00	0.80	0.00	0.00	0.24	0.00	0.00	0.00	0.00	0.00	0.00	0.00
24:00	19	0.00	0.80	0.00	0.00	0.24	0.00	0.00	0.00	0.00	0.00	0.00	0.00
00:00	31	0.00	1.20	1.36	0.00	0.72	0.48	0.00	0.00	0.00	0.00	0.00	0.00
01:00	31	0.00	2.00	1.44	0.00	0.88	0.50	0.00	0.00	0.00	0.00	0.00	0.00
02:00	31	0.00	0.40	1.32	0.00	0.48	0.48	0.00	0.00	0.00	0.00	0.00	0.00
03:00	31	0.00	0.40	1.28	0.00	0.40	0.47	0.00	0.00	0.00	0.00	0.00	0.00
04:00	31	0.00	0.80	0.00	0.00	0.44	0.00	0.00	0.00	0.00	0.00	0.00	0.00
05:00	31	0.00	0.80	0.08	0.00	0.44	0.00	0.00	0.00	0.00	0.00	0.00	0.00
06:00	31	0.00	0.80	0.08	0.00	0.32	0.00	0.00	0.00	0.00	0.00	0.00	0.00
07:00	31	0.00	0.40	0.08	0.00	0.48	0.00	0.00	0.00	0.00	0.00	0.00	0.00
08:00	31	0.00	0.80	0.04	0.00	0.40	0.00	0.00	0.00	0.00	0.00	0.00	0.00
09:00	31	0.00	0.80	0.04	0.00	0.40	0.00	0.00	0.00	0.00	0.00	0.00	0.00
10:00	31	0.00	0.80	2.68	0.00	0.40	0.10	0.00	0.00	0.00	0.00	0.00	0.00
11:00	31	0.58	2.40	2.80	0.13	0.80	0.12	0.00	0.00	0.00	0.00	0.00	0.00
12:00	31	0.00	0.80	2.84	0.00	0.36	0.11	0.00	0.00	0.00	0.00	0.00	0.00
13:00	31	0.00	0.40	0.28	0.00	0.48	0.01	0.00	0.00	0.00	0.00	0.00	0.00
14:00	31	0.00	0.40	0.00	0.00	0.36	0.00	0.00	0.00	0.00	0.00	0.00	0.00
15:00	31	0.00	0.40	0.04	0.00	0.48	0.00	0.00	0.00	0.00	0.00	0.00	0.00
16:00	31	0.00	0.40	0.08	0.00	0.36	0.00	0.00	0.00	0.00	0.00	0.00	0.00

17:00	31	0.05	0.80	2.92	0.00	0.44	0.10	0.00	0.00	0.00	0.00	0.00	0.00
18:00	31	0.19	0.80	2.92	0.07	0.36	0.08	0.00	0.00	0.00	0.00	0.00	0.00
19:00	31	0.00	1.20	4.24	0.00	0.44	0.37	0.00	0.00	0.00	0.00	0.00	0.00
20:00	31	0.00	0.80	4.44	0.00	0.36	0.39	0.00	0.00	0.00	0.00	0.00	0.00
21:00	31	0.00	0.80	1.44	0.00	0.44	0.39	0.00	0.00	0.00	0.00	0.00	0.00
22:00	31	0.00	0.40	1.44	0.00	0.44	0.42	0.00	0.00	0.00	0.00	0.00	0.00
23:00	31	0.00	0.40	1.24	0.00	0.40	0.40	0.00	0.00	0.00	0.00	0.00	0.00
24:00	31	0.00	1.20	1.32	0.00	0.68	0.44	0.00	0.00	0.00	0.00	0.00	0.00
00:00	32	0.20	0.00	1.60	0.12	0.00	0.00	0.00	0.00	0.00	0.00	0.00	0.00
01:00	32	0.12	0.00	1.40	0.04	0.00	0.00	0.00	0.00	0.00	0.00	0.00	0.00
02:00	32	0.20	0.00	1.04	0.12	0.00	0.00	0.00	0.00	0.00	0.00	0.00	0.00
03:00	32	0.28	0.00	0.00	0.20	0.00	0.00	0.00	0.00	0.00	0.00	0.00	0.00
04:00	32	0.20	0.00	0.00	0.16	0.00	0.00	0.00	0.00	0.00	0.00	0.00	0.00
05:00	32	0.16	0.00	0.00	0.04	0.00	0.00	0.00	0.00	0.00	0.00	0.00	0.00
06:00	32	0.16	0.00	0.04	0.08	0.00	0.00	0.00	0.00	0.00	0.00	0.00	0.00
07:00	32	0.44	0.00	0.00	0.20	0.00	0.00	0.00	0.00	0.08	0.00	0.00	0.00
08:00	32	0.40	0.00	0.00	0.24	0.00	0.00	0.00	0.00	0.32	0.00	0.00	0.00
09:00	32	0.80	0.00	0.00	0.24	0.00	0.00	0.00	0.00	0.64	0.00	0.00	0.00
10:00	32	0.44	0.00	0.00	0.20	0.00	0.00	0.00	0.00	0.92	0.00	0.00	0.00
11:00	32	0.44	0.00	0.56	0.12	0.00	0.00	0.00	0.00	0.36	0.00	0.00	0.00
12:00	32	0.24	0.00	1.04	0.08	0.00	0.00	0.00	0.00	0.00	0.00	0.00	0.00
13:00	32	0.40	0.00	1.00	0.12	0.00	0.00	0.00	0.00	0.00	0.00	0.00	0.00
14:00	32	0.20	0.00	1.00	0.08	0.00	0.00	0.00	0.00	0.00	0.00	0.00	0.00
15:00	32	0.24	0.00	1.12	0.16	0.00	0.00	0.00	0.00	0.00	0.00	0.00	0.00
16:00	32	0.20	0.00	1.44	0.20	0.00	0.00	0.00	0.00	0.00	0.00	0.00	0.00
17:00	32	0.20	0.00	1.56	0.24	0.00	0.00	0.00	0.00	0.00	0.00	0.00	0.00
18:00	32	0.40	0.00	2.24	0.20	0.00	0.00	0.00	0.00	0.00	0.00	0.00	0.00
19:00	32	0.44	0.00	2.24	0.12	0.00	0.00	0.00	0.00	0.00	0.00	0.00	0.00
20:00	32	0.36	0.00	1.68	0.16	0.00	0.00	0.00	0.00	0.00	0.00	0.00	0.00
21:00	32	0.32	0.00	1.60	0.16	0.00	0.00	0.00	0.00	0.00	0.00	0.00	0.00

22:00	32	0.20	0.00	1.60	0.12	0.00	0.00	0.00	0.00	0.00	0.00	0.00	0.00
23:00	32	0.28	0.00	1.64	0.16	0.00	0.00	0.00	0.00	0.00	0.00	0.00	0.00
24:00	32	0.28	0.00	1.32	0.24	0.00	0.00	0.00	0.00	0.00	0.00	0.00	0.00
00:00	34	0.00	0.08	0.40	0.00	0.00	0.12	0.00	0.00	0.00	0.00	0.00	0.00
01:00	34	0.00	0.00	0.80	0.00	0.00	0.12	0.00	0.00	0.00	0.00	0.00	0.00
02:00	34	0.00	0.00	0.80	0.00	0.00	0.12	0.00	0.00	0.00	0.00	0.00	0.00
03:00	34	0.00	0.04	0.40	0.00	0.00	0.16	0.00	0.00	0.00	0.00	0.00	0.00
04:00	34	0.00	0.00	0.80	0.00	0.00	0.12	0.00	0.00	0.00	0.00	0.00	0.00
05:00	34	0.00	0.04	0.40	0.00	0.00	0.12	0.00	0.00	0.00	0.00	0.00	0.00
06:00	34	0.00	1.00	0.40	0.00	0.03	0.20	0.00	0.00	0.00	0.00	0.00	0.00
07:00	34	0.00	1.08	0.40	0.00	0.00	0.16	0.00	0.00	0.00	0.00	0.00	0.00
08:00	34	0.00	0.68	1.60	0.00	0.00	0.36	0.00	0.00	0.00	0.00	0.00	0.00
09:00	34	0.00	0.72	1.60	0.00	0.00	0.40	0.00	0.00	0.00	0.00	0.00	0.00
10:00	34	0.00	0.88	1.60	0.00	0.00	0.36	0.00	0.00	0.00	0.00	0.00	0.00
11:00	34	0.00	1.12	0.80	0.00	0.00	0.08	0.00	0.00	0.00	0.00	0.00	0.00
12:00	34	0.00	2.28	0.80	0.00	0.23	0.08	0.00	0.00	0.00	0.00	0.00	0.00
13:00	34	0.00	1.32	0.40	0.00	0.12	0.20	0.00	0.00	0.00	0.00	0.00	0.00
14:00	34	0.00	2.40	0.80	0.00	0.28	0.24	0.00	0.00	0.00	0.00	0.00	0.00
15:00	34	0.00	2.40	1.60	0.00	0.36	0.40	0.00	0.00	0.00	0.00	0.00	0.00
16:00	34	0.00	2.36	1.20	0.00	0.33	0.52	0.00	0.00	0.00	0.00	0.00	0.00
17:00	34	1.22	2.24	2.00	0.07	0.22	0.52	0.00	0.00	0.00	0.00	0.00	0.00
18:00	34	0.70	2.36	2.00	0.04	0.30	0.36	0.00	0.00	0.00	0.00	0.00	0.00
19:00	34	0.00	2.36	1.60	0.00	0.34	0.36	0.00	0.00	0.00	0.00	0.00	0.00
20:00	34	0.00	2.28	2.00	0.00	0.36	0.24	0.00	0.00	0.00	0.00	0.00	0.00
21:00	34	0.00	2.20	0.80	0.00	0.24	0.04	0.00	0.00	0.00	0.00	0.00	0.00
22:00	34	0.00	2.08	1.20	0.00	0.11	0.04	0.00	0.00	0.00	0.00	0.00	0.00
23:00	34	0.00	1.24	0.80	0.00	0.00	0.08	0.00	0.00	0.00	0.00	0.00	0.00
24:00	34	0.00	0.12	0.80	0.00	0.00	0.20	0.00	0.00	0.00	0.00	0.00	0.00
00:00	41	0.00	0.00	0.12	0.00	0.00	0.16	0.00	0.00	0.00	0.00	0.00	0.00
01:00	41	0.00	0.00	0.12	0.00	0.00	0.12	0.00	0.00	0.00	0.00	0.00	0.00

02:00	41	0.00	0.00	0.12	0.00	0.00	0.20	0.00	0.00	0.00	0.00	0.00	0.00
03:00	41	0.00	0.00	0.12	0.00	0.00	0.16	0.00	0.00	0.00	0.00	0.00	0.00
04:00	41	0.00	0.00	0.12	0.00	0.00	0.16	0.00	0.00	0.00	0.00	0.00	0.00
05:00	41	0.00	0.00	0.16	0.00	0.00	0.16	0.00	0.00	0.00	0.00	0.00	0.00
06:00	41	0.00	0.00	0.12	0.00	0.00	0.12	0.00	0.00	0.00	0.00	0.00	0.00
07:00	41	0.00	0.00	0.16	0.00	0.00	0.16	0.00	0.00	0.00	0.00	0.00	0.00
08:00	41	0.00	0.00	0.16	0.00	0.00	0.16	0.00	0.00	0.00	0.00	0.00	0.00
09:00	41	0.00	0.00	0.12	0.00	0.00	0.08	0.00	0.00	0.00	0.00	0.00	0.00
10:00	41	0.00	0.00	0.16	0.00	0.00	0.12	0.00	0.00	0.00	0.00	0.00	0.00
11:00	41	0.00	0.00	0.12	0.00	0.00	0.16	0.00	0.00	0.00	0.00	0.00	0.00
12:00	41	0.04	0.00	0.12	0.00	0.00	0.12	0.00	0.00	0.00	0.00	0.00	0.00
13:00	41	0.00	0.00	0.08	0.00	0.00	0.08	0.00	0.00	0.00	0.00	0.00	0.00
14:00	41	0.00	0.00	0.16	0.00	0.00	0.16	0.00	0.00	0.00	0.00	0.00	0.00
15:00	41	0.00	0.00	0.12	0.00	0.00	0.12	0.00	0.00	0.00	0.00	0.00	0.00
16:00	41	0.00	0.00	0.12	0.00	0.00	0.12	0.00	0.00	0.00	0.00	0.00	0.00
17:00	41	0.04	0.00	0.12	0.00	0.00	0.12	0.00	0.00	0.00	0.00	0.00	0.00
18:00	41	0.00	0.00	0.12	0.00	0.00	0.12	0.00	0.00	0.00	0.00	0.00	0.00
19:00	41	0.00	0.00	0.20	0.00	0.00	0.20	0.00	0.00	0.00	0.00	0.00	0.00
20:00	41	0.00	0.00	0.16	0.00	0.00	0.16	0.00	0.00	0.00	0.00	0.00	0.00
21:00	41	0.00	0.00	0.16	0.00	0.00	0.16	0.00	0.00	0.00	0.00	0.00	0.00
22:00	41	0.00	0.00	0.16	0.00	0.00	0.16	0.00	0.00	0.00	0.00	0.00	0.00
23:00	41	0.00	0.00	0.16	0.00	0.00	0.16	0.00	0.00	0.00	0.00	0.00	0.00
24:00	41	0.04	0.00	0.24	0.00	0.00	0.08	0.00	0.00	0.00	0.00	0.00	0.00
00:00	43	0.03	0.16	0.00	0.00	0.04	0.00	0.00	0.00	0.00	0.00	0.00	0.00
01:00	43	0.03	0.12	0.00	0.00	0.00	0.00	0.00	0.00	0.00	0.00	0.00	0.00
02:00	43	0.03	0.16	0.00	0.00	0.00	0.00	0.00	0.00	0.00	0.00	0.00	0.00
03:00	43	0.03	0.16	0.00	0.00	0.04	0.00	0.00	0.00	0.00	0.00	0.00	0.00
04:00	43	0.03	0.16	0.00	0.00	0.00	0.00	0.00	0.00	0.00	0.00	0.00	0.00
05:00	43	0.03	0.20	0.00	0.00	0.04	0.00	0.00	0.00	0.00	0.00	0.00	0.00
06:00	43	0.02	0.16	0.00	0.00	0.00	0.00	0.00	0.00	0.00	0.00	0.00	0.00

07:00	43	0.00	0.20	0.00	0.00	0.00	0.00	0.04	0.00	0.00	0.00	0.00	0.00
08:00	43	0.00	0.36	0.00	0.00	0.04	0.00	0.08	0.00	0.00	0.00	0.00	0.00
09:00	43	0.00	1.72	0.00	0.00	0.36	0.00	0.48	0.00	0.00	0.00	0.00	0.00
10:00	43	0.00	0.72	0.00	0.00	0.24	0.00	0.72	0.00	0.00	0.00	0.00	0.00
11:00	43	0.00	0.08	0.00	0.00	0.04	0.00	1.00	0.00	0.00	0.00	0.00	0.00
12:00	43	0.00	0.16	0.00	0.00	0.04	0.00	1.08	0.00	0.00	0.00	0.00	0.00
13:00	43	0.00	0.32	0.00	0.00	0.16	0.00	1.16	0.00	0.00	0.00	0.00	0.00
14:00	43	0.00	0.68	0.00	0.00	0.32	0.00	1.12	0.00	0.00	0.00	0.00	0.00
15:00	43	0.00	0.28	0.00	0.00	0.04	0.00	1.04	0.00	0.00	0.00	0.00	0.00
16:00	43	0.24	0.32	0.00	0.00	0.08	0.00	0.68	0.00	0.00	0.00	0.00	0.00
17:00	43	0.00	0.36	0.00	0.00	0.04	0.00	0.60	0.00	0.00	0.00	0.00	0.00
18:00	43	0.00	0.24	0.00	0.00	0.00	0.00	0.28	0.00	0.00	0.00	0.00	0.00
19:00	43	0.02	0.20	0.00	0.00	0.04	0.00	0.00	0.00	0.00	0.00	0.00	0.00
20:00	43	0.03	0.84	0.00	0.00	0.36	0.00	0.00	0.00	0.00	0.00	0.00	0.00
21:00	43	0.03	0.84	0.00	0.00	0.40	0.00	0.00	0.00	0.00	0.00	0.00	0.00
22:00	43	0.03	0.84	0.00	0.00	0.44	0.00	0.00	0.00	0.00	0.00	0.00	0.00
23:00	43	0.03	0.32	0.00	0.00	0.00	0.00	0.00	0.00	0.00	0.00	0.00	0.00
24:00	43	0.03	0.28	0.00	0.00	0.08	0.00	0.00	0.00	0.00	0.00	0.00	0.00
00:00	50	0.92	0.00	0.01	0.60	0.01	0.00	0.00	0.00	0.00	0.00	0.00	0.00
01:00	50	0.84	0.00	0.00	0.44	0.00	0.00	0.00	0.00	0.00	0.00	0.00	0.00
02:00	50	0.88	0.00	0.01	0.56	0.01	0.00	0.00	0.00	0.00	0.00	0.00	0.00
03:00	50	0.52	0.00	0.00	0.40	0.01	0.00	0.00	0.00	0.00	0.00	0.00	0.00
04:00	50	0.20	0.00	0.01	0.12	0.01	0.00	0.00	0.00	0.00	0.00	0.00	0.00
05:00	50	0.24	0.00	0.01	0.16	0.01	0.00	0.00	0.00	0.00	0.00	0.00	0.00
06:00	50	0.72	0.00	0.00	0.20	0.00	0.00	0.00	0.00	0.00	0.00	0.00	0.00
07:00	50	0.32	0.00	0.01	0.28	0.01	0.00	0.00	0.00	0.00	0.00	0.00	0.00
08:00	50	0.44	0.00	0.01	0.28	0.01	0.00	0.00	0.00	0.00	0.00	0.00	0.00
09:00	50	0.32	0.19	1.52	0.24	0.01	0.41	0.00	0.00	0.00	0.00	0.00	0.00
10:00	50	0.48	0.56	0.77	0.36	0.02	0.31	0.00	0.00	0.00	0.00	0.00	0.00
11:00	50	0.32	0.00	0.84	0.32	0.00	0.29	0.00	0.00	0.00	0.00	0.00	0.00

12:00	50	0.32	0.00	0.88	0.36	0.01	0.29	0.00	0.00	0.00	0.00	0.00	0.00
13:00	50	0.56	0.00	0.88	0.32	0.01	0.26	0.00	0.00	0.00	0.00	0.00	0.00
14:00	50	0.36	0.00	0.99	0.36	0.01	0.27	0.00	0.00	0.00	0.00	0.00	0.00
15:00	50	0.44	0.01	1.03	0.36	0.01	0.27	0.00	0.00	0.00	0.00	0.00	0.00
16:00	50	0.64	0.51	1.06	0.36	0.03	0.28	0.00	0.00	0.00	0.00	0.00	0.00
17:00	50	0.52	0.00	1.06	0.32	0.01	0.21	0.00	0.00	0.00	0.00	0.00	0.00
18:00	50	0.44	0.00	0.88	0.32	0.01	0.14	0.00	0.00	0.00	0.00	0.00	0.00
19:00	50	0.64	0.00	0.80	0.36	0.01	0.12	0.00	0.00	0.00	0.00	0.00	0.00
20:00	50	1.24	0.00	0.74	0.64	0.00	0.09	0.00	0.00	0.00	0.00	0.00	0.00
21:00	50	1.40	0.00	0.58	0.60	0.01	0.07	0.00	0.00	0.00	0.00	0.00	0.00
22:00	50	1.12	0.00	0.26	0.64	0.01	0.03	0.00	0.00	0.00	0.00	0.00	0.00
23:00	50	0.96	0.00	0.01	0.56	0.01	0.00	0.00	0.00	0.00	0.00	0.00	0.00
24:00	50	0.88	0.00	0.01	0.44	0.01	0.00	0.00	0.00	0.00	0.00	0.00	0.00
00:00	51	0.36	0.00	0.00	0.44	0.00	0.00	0.00	0.00	0.00	0.00	0.00	0.00
01:00	51	0.36	0.04	0.00	0.40	0.00	0.00	0.00	0.00	0.00	0.00	0.00	0.00
02:00	51	0.24	0.04	0.00	0.28	0.00	0.00	0.00	0.00	0.00	0.00	0.00	0.00
03:00	51	0.16	0.00	0.00	0.08	0.00	0.00	0.00	0.00	0.00	0.00	0.00	0.00
04:00	51	0.36	0.00	0.00	0.36	0.00	0.00	0.00	0.00	0.00	0.00	0.00	0.00
05:00	51	0.84	0.08	0.00	0.40	0.12	0.00	0.00	0.00	0.00	0.00	0.00	0.00
06:00	51	0.28	0.00	0.00	0.24	0.00	0.00	0.00	0.00	0.00	0.00	0.00	0.00
07:00	51	0.08	0.00	0.00	0.08	0.00	0.00	0.00	0.00	0.00	0.00	0.00	0.00
08:00	51	0.00	0.00	0.00	0.28	0.00	0.00	0.16	0.00	0.00	0.00	0.00	0.00
09:00	51	0.00	0.00	0.00	0.32	0.00	0.00	0.76	0.00	0.00	0.00	0.00	0.00
10:00	51	0.00	0.04	0.00	0.40	0.00	0.00	0.88	0.00	0.00	0.00	0.00	0.00
11:00	51	0.00	0.04	0.00	0.40	0.00	0.00	1.04	0.00	0.00	0.00	0.00	0.00
12:00	51	0.00	0.04	0.00	0.52	0.00	0.00	1.36	0.00	0.00	0.00	0.00	0.00
13:00	51	0.00	0.04	0.00	0.56	0.00	0.00	1.44	0.00	0.00	0.00	0.00	0.00
14:00	51	0.00	0.00	0.00	0.56	0.00	0.00	1.28	0.00	0.00	0.00	0.00	0.00
15:00	51	0.00	0.00	0.00	0.56	0.00	0.00	1.20	0.00	0.00	0.00	0.00	0.00
16:00	51	0.40	0.04	0.36	0.44	0.00	0.12	0.72	0.00	0.00	0.00	0.00	0.00

17:00	51	0.48	0.08	1.76	0.40	0.00	0.45	0.00	0.00	0.00	0.00	0.00	0.00
18:00	51	0.48	0.08	1.48	0.28	0.00	0.35	0.00	0.00	0.00	0.00	0.00	0.00
19:00	51	0.60	0.08	1.71	0.36	0.01	0.39	0.00	0.00	0.00	0.00	0.00	0.00
20:00	51	1.32	0.84	2.14	0.84	0.65	0.73	0.00	0.00	0.00	0.00	0.00	0.00
21:00	51	0.96	0.12	1.62	0.36	0.15	0.35	0.00	0.00	0.00	0.00	0.00	0.00
22:00	51	0.56	0.12	1.57	0.28	0.16	0.38	0.00	0.00	0.00	0.00	0.00	0.00
23:00	51	0.36	0.04	0.00	0.44	0.02	0.00	0.00	0.00	0.00	0.00	0.00	0.00
24:00	51	0.32	0.04	0.00	0.32	0.00	0.00	0.00	0.00	0.00	0.00	0.00	0.00
00:00	61	0.00	1.72	0.52	0.00	0.18	0.00	0.00	0.00	0.00	0.00	0.00	0.00
01:00	61	0.00	1.64	0.32	0.00	0.16	0.00	0.00	0.00	0.00	0.00	0.00	0.00
02:00	61	0.00	0.00	0.28	0.00	0.00	0.00	0.00	0.00	0.00	0.00	0.00	0.00
03:00	61	0.00	1.52	0.28	0.00	0.13	0.00	0.00	0.00	0.00	0.00	0.00	0.00
04:00	61	0.00	1.04	0.28	0.00	0.02	0.00	0.00	0.00	0.00	0.00	0.00	0.00
05:00	61	0.00	0.00	0.20	0.00	0.00	0.00	0.00	0.00	0.00	0.00	0.00	0.00
06:00	61	0.00	0.00	0.64	0.00	0.00	0.02	0.00	0.00	0.00	0.00	0.00	0.00
07:00	61	0.00	0.00	0.32	0.00	0.00	0.02	0.00	0.00	0.00	0.00	0.00	0.00
08:00	61	0.00	0.00	0.28	0.00	0.00	0.02	0.00	0.00	0.00	0.00	0.00	0.00
09:00	61	0.32	0.00	0.96	0.00	0.00	0.04	0.00	0.00	0.00	0.00	0.00	0.00
10:00	61	0.00	0.00	0.44	0.00	0.00	0.02	0.00	0.00	0.00	0.00	0.00	0.00
11:00	61	0.00	0.00	0.32	0.00	0.00	0.00	0.00	0.00	0.00	0.00	0.00	0.00
12:00	61	0.00	0.00	0.36	0.00	0.00	0.00	0.00	0.00	0.00	0.00	0.00	0.00
13:00	61	0.00	0.00	0.36	0.00	0.00	0.00	0.00	0.00	0.00	0.00	0.00	0.00
14:00	61	0.00	0.00	0.36	0.00	0.00	0.00	0.00	0.00	0.00	0.00	0.00	0.00
15:00	61	0.00	0.52	0.32	0.00	0.02	0.00	0.00	0.00	0.00	0.00	0.00	0.00
16:00	61	0.00	2.04	0.32	0.00	0.24	0.00	0.00	0.00	0.00	0.00	0.00	0.00
17:00	61	0.00	0.84	0.48	0.00	0.10	0.00	0.00	0.00	0.00	0.00	0.00	0.00
18:00	61	0.59	1.84	0.56	0.00	0.18	0.00	0.00	0.00	0.00	0.00	0.00	0.00
19:00	61	0.00	1.20	0.40	0.00	0.10	0.00	0.00	0.00	0.00	0.00	0.00	0.00
20:00	61	0.00	1.92	0.40	0.00	0.14	0.00	0.00	0.00	0.00	0.00	0.00	0.00
21:00	61	0.00	2.08	0.52	0.00	0.19	0.00	0.00	0.00	0.00	0.00	0.00	0.00

22:00	61	0.00	1.76	0.48	0.00	0.17	0.00	0.00	0.00	0.00	0.00	0.00	0.00
23:00	61	0.00	0.88	0.52	0.00	0.11	0.00	0.00	0.00	0.00	0.00	0.00	0.00
24:00	61	0.00	0.00	0.28	0.00	0.00	0.02	0.00	0.00	0.00	0.00	0.00	0.00
00:00	64	0.40	0.00	1.16	0.40	0.00	0.88	0.00	0.00	0.00	0.00	0.00	0.00
01:00	64	0.44	0.00	1.00	0.48	0.00	0.84	0.00	0.00	0.00	0.00	0.00	0.00
02:00	64	0.56	0.00	1.12	0.60	0.00	0.88	0.00	0.00	0.00	0.00	0.00	0.00
03:00	64	0.36	0.00	1.08	0.28	0.00	0.88	0.00	0.00	0.00	0.00	0.00	0.00
04:00	64	0.48	0.00	1.04	0.48	0.00	0.88	0.00	0.00	0.00	0.00	0.00	0.00
05:00	64	0.92	0.02	0.28	0.60	0.01	0.04	0.00	0.00	0.00	0.00	0.00	0.00
06:00	64	0.64	0.12	0.20	0.36	0.08	0.04	0.00	0.00	0.04	0.00	0.00	0.00
07:00	64	1.12	0.00	0.08	0.64	0.00	0.00	0.00	0.00	0.44	0.00	0.00	0.00
08:00	64	0.64	0.00	0.12	0.52	0.02	0.00	0.00	0.00	0.76	0.00	0.00	0.00
09:00	64	0.60	0.00	1.20	0.48	0.03	0.80	0.00	0.00	1.04	0.00	0.00	0.00
10:00	64	0.56	0.00	1.44	0.64	0.04	0.96	0.00	0.00	1.16	0.00	0.00	0.00
11:00	64	0.40	0.00	1.44	0.36	0.04	0.92	0.00	0.00	1.24	0.00	0.00	0.00
12:00	64	0.56	0.00	1.44	0.52	0.04	0.92	0.00	0.00	1.24	0.00	0.00	0.00
13:00	64	0.72	0.00	1.60	0.72	0.04	0.88	0.00	0.00	1.20	0.00	0.00	0.00
14:00	64	0.48	0.00	1.40	0.56	0.03	0.92	0.00	0.00	1.04	0.00	0.00	0.00
15:00	64	0.56	0.00	0.04	0.64	0.02	0.00	0.00	0.00	0.80	0.00	0.00	0.00
16:00	64	0.60	0.00	0.16	0.72	0.00	0.00	0.00	0.00	0.28	0.00	0.00	0.00
17:00	64	0.44	0.00	0.04	0.48	0.00	0.00	0.00	0.00	0.04	0.00	0.00	0.00
18:00	64	0.52	0.00	0.16	0.56	0.00	0.00	0.00	0.00	0.00	0.00	0.00	0.00
19:00	64	0.40	0.00	0.04	0.36	0.00	0.00	0.00	0.00	0.00	0.00	0.00	0.00
20:00	64	0.52	0.00	0.08	0.60	0.00	0.00	0.00	0.00	0.00	0.00	0.00	0.00
21:00	64	0.72	0.00	1.24	0.32	0.00	0.76	0.00	0.00	0.00	0.00	0.00	0.00
22:00	64	0.72	0.00	1.16	0.44	0.00	0.84	0.00	0.00	0.00	0.00	0.00	0.00
23:00	64	0.72	0.00	1.04	0.40	0.00	0.84	0.00	0.00	0.00	0.00	0.00	0.00
24:00	64	0.36	0.00	1.08	0.24	0.00	0.80	0.00	0.00	0.00	0.00	0.00	0.00
00:00	65	0.56	0.20	0.00	0.33	0.04	0.00	0.00	0.00	0.00	0.00	0.00	0.00
01:00	65	0.56	0.24	0.00	0.34	0.08	0.00	0.00	0.00	0.00	0.00	0.00	0.00

02:00	65	0.55	0.20	0.00	0.34	0.04	0.00	0.00	0.00	0.00	0.00	0.00	0.00
03:00	65	0.56	0.16	0.00	0.34	0.00	0.00	0.00	0.00	0.00	0.00	0.00	0.00
04:00	65	0.56	0.24	0.00	0.33	0.08	0.00	0.00	0.00	0.00	0.00	0.00	0.00
05:00	65	0.56	0.28	0.00	0.34	0.08	0.00	0.00	0.00	0.00	0.00	0.00	0.00
06:00	65	0.56	0.24	0.00	0.34	0.08	0.00	0.00	0.00	0.00	0.00	0.00	0.00
07:00	65	0.52	0.24	0.00	0.36	0.08	0.00	0.00	0.00	0.00	0.00	0.00	0.00
08:00	65	0.53	0.60	0.00	0.36	0.00	0.00	0.00	0.00	0.00	0.00	0.00	0.00
09:00	65	0.52	0.16	0.00	0.36	0.04	0.00	0.00	0.00	0.00	0.00	0.00	0.00
10:00	65	0.52	0.24	0.00	0.35	0.12	0.00	0.00	0.00	0.00	0.00	0.00	0.00
11:00	65	0.44	0.20	0.00	0.36	0.04	0.00	0.00	0.00	0.00	0.00	0.00	0.00
12:00	65	0.45	0.12	0.00	0.36	0.04	0.00	0.00	0.00	0.00	0.00	0.00	0.00
13:00	65	0.45	0.20	0.00	0.36	0.08	0.00	0.00	0.00	0.00	0.00	0.00	0.00
14:00	65	0.48	0.28	0.00	0.36	0.04	0.00	0.00	0.00	0.00	0.00	0.00	0.00
15:00	65	0.68	0.84	0.00	0.40	0.00	0.00	0.00	0.00	0.00	0.00	0.00	0.00
16:00	65	0.68	0.92	0.00	0.40	0.12	0.00	0.00	0.00	0.00	0.00	0.00	0.00
17:00	65	0.67	1.04	0.00	0.38	0.20	0.00	0.00	0.00	0.00	0.00	0.00	0.00
18:00	65	0.66	0.88	0.00	0.37	0.24	0.00	0.00	0.00	0.00	0.00	0.00	0.00
19:00	65	0.66	0.84	0.00	0.36	0.20	0.00	0.00	0.00	0.00	0.00	0.00	0.00
20:00	65	0.66	0.92	0.00	0.37	0.24	0.00	0.00	0.00	0.00	0.00	0.00	0.00
21:00	65	0.66	1.52	0.00	0.36	0.36	0.00	0.00	0.00	0.00	0.00	0.00	0.00
22:00	65	0.67	0.60	0.00	0.37	0.32	0.00	0.00	0.00	0.00	0.00	0.00	0.00
23:00	65	0.66	0.40	0.00	0.37	0.24	0.00	0.00	0.00	0.00	0.00	0.00	0.00
24:00	65	0.67	0.52	0.00	0.38	0.32	0.00	0.00	0.00	0.00	0.00	0.00	0.00
00:00	66	0.40	0.00	1.16	0.40	0.00	0.88	0.00	0.00	0.00	0.00	0.00	0.00
01:00	66	0.44	0.00	1.00	0.48	0.00	0.84	0.00	0.00	0.00	0.00	0.00	0.00
02:00	66	0.56	0.00	1.12	0.60	0.00	0.88	0.00	0.00	0.00	0.00	0.00	0.00
03:00	66	0.36	0.00	1.08	0.28	0.00	0.88	0.00	0.00	0.00	0.00	0.00	0.00
04:00	66	0.48	0.00	1.04	0.48	0.00	0.88	0.00	0.00	0.00	0.00	0.00	0.00
05:00	66	0.92	0.02	0.28	0.60	0.01	0.04	0.00	0.00	0.00	0.00	0.00	0.00
06:00	66	0.64	0.12	0.20	0.36	0.08	0.04	0.00	0.04	0.00	0.00	0.00	0.00

07:00	66	1.12	0.00	0.08	0.64	0.00	0.00	0.00	0.44	0.00	0.00	0.00	0.00
08:00	66	0.64	0.00	0.12	0.52	0.02	0.00	0.00	0.76	0.00	0.00	0.00	0.00
09:00	66	0.60	0.00	1.20	0.48	0.03	0.80	0.00	1.04	0.00	0.00	0.00	0.00
10:00	66	0.56	0.00	1.44	0.64	0.04	0.96	0.00	1.16	0.00	0.00	0.00	0.00
11:00	66	0.40	0.00	1.44	0.36	0.04	0.92	0.00	1.24	0.00	0.00	0.00	0.00
12:00	66	0.56	0.00	1.44	0.52	0.04	0.92	0.00	1.24	0.00	0.00	0.00	0.00
13:00	66	0.72	0.00	1.60	0.72	0.04	0.88	0.00	1.20	0.00	0.00	0.00	0.00
14:00	66	0.48	0.00	1.40	0.56	0.03	0.92	0.00	1.04	0.00	0.00	0.00	0.00
15:00	66	0.56	0.00	0.04	0.64	0.02	0.00	0.00	0.80	0.00	0.00	0.00	0.00
16:00	66	0.60	0.00	0.16	0.72	0.00	0.00	0.00	0.28	0.00	0.00	0.00	0.00
17:00	66	0.44	0.00	0.04	0.48	0.00	0.00	0.00	0.04	0.00	0.00	0.00	0.00
18:00	66	0.52	0.00	0.16	0.56	0.00	0.00	0.00	0.00	0.00	0.00	0.00	0.00
19:00	66	0.40	0.00	0.04	0.36	0.00	0.00	0.00	0.00	0.00	0.00	0.00	0.00
20:00	66	0.52	0.00	0.08	0.60	0.00	0.00	0.00	0.00	0.00	0.00	0.00	0.00
21:00	66	0.72	0.00	1.24	0.32	0.00	0.76	0.00	0.00	0.00	0.00	0.00	0.00
22:00	66	0.72	0.00	1.16	0.44	0.00	0.84	0.00	0.00	0.00	0.00	0.00	0.00
23:00	66	0.72	0.00	1.04	0.40	0.00	0.84	0.00	0.00	0.00	0.00	0.00	0.00
24:00	66	0.36	0.00	1.08	0.24	0.00	0.80	0.00	0.00	0.00	0.00	0.00	0.00
00:00	69	0.16	0.00	2.00	0.00	0.00	0.80	0.00	0.00	0.00	0.00	0.00	0.00
01:00	69	0.20	0.00	0.80	0.00	0.00	0.48	0.00	0.00	0.00	0.00	0.00	0.00
02:00	69	0.16	0.04	1.20	0.00	0.00	0.56	0.00	0.00	0.00	0.00	0.00	0.00
03:00	69	0.16	0.00	0.80	0.00	0.00	0.48	0.00	0.00	0.00	0.00	0.00	0.00
04:00	69	0.20	0.00	1.20	0.00	0.00	0.44	0.00	0.00	0.00	0.00	0.00	0.00
05:00	69	0.20	0.00	1.60	0.00	0.00	0.44	0.00	0.00	0.00	0.00	0.00	0.00
06:00	69	0.28	0.36	2.00	0.00	0.00	0.44	0.00	0.00	0.00	0.00	0.00	0.00
07:00	69	0.12	0.04	1.60	0.00	0.02	0.32	0.00	0.36	0.00	0.00	0.00	0.00
08:00	69	0.04	0.00	1.60	0.00	0.05	0.36	0.00	0.84	0.00	0.00	0.00	0.00
09:00	69	0.04	0.00	1.20	0.00	0.07	0.32	0.00	1.08	0.00	0.00	0.00	0.00
10:00	69	0.04	0.00	0.40	0.00	0.08	0.32	0.00	1.20	0.00	0.00	0.00	0.00
11:00	69	0.04	0.00	0.40	0.00	0.10	0.32	0.00	1.32	0.00	0.00	0.00	0.00

12:00	69	0.04	0.00	0.40	0.00	0.10	0.32	0.00	1.28	0.00	0.00	0.00	0.00
13:00	69	2.76	0.00	0.80	0.00	0.09	0.32	0.00	0.96	0.00	0.00	0.00	0.00
14:00	69	3.32	0.00	2.00	0.00	0.08	0.36	0.00	1.08	0.00	0.00	0.00	0.00
15:00	69	2.16	0.00	0.80	0.00	0.07	0.36	0.00	0.88	0.00	0.00	0.00	0.00
16:00	69	0.04	0.00	0.40	0.00	0.04	0.32	0.00	0.48	0.00	0.00	0.00	0.00
17:00	69	0.04	0.00	0.40	0.00	0.00	0.32	0.00	0.24	0.00	0.00	0.00	0.00
18:00	69	0.04	0.00	0.80	0.00	0.00	0.20	0.00	0.04	0.00	0.00	0.00	0.00
19:00	69	0.04	0.00	1.20	0.00	0.00	0.20	0.00	0.00	0.00	0.00	0.00	0.00
20:00	69	0.04	0.00	1.60	0.00	0.00	0.24	0.00	0.00	0.00	0.00	0.00	0.00
21:00	69	0.08	0.00	1.20	0.00	0.00	0.20	0.00	0.00	0.00	0.00	0.00	0.00
22:00	69	0.08	0.00	0.00	0.00	0.00	0.24	0.00	0.00	0.00	0.00	0.00	0.00
23:00	69	0.04	0.00	0.40	0.00	0.00	0.28	0.00	0.00	0.00	0.00	0.00	0.00
24:00	69	0.04	0.00	0.40	0.00	0.00	0.32	0.00	0.00	0.00	0.00	0.00	0.00
00:00	72	0.01	0.00	0.12	0.00	0.00	0.01	0.00	0.00	0.00	0.00	0.00	0.00
01:00	72	0.00	0.00	0.24	0.00	0.00	0.12	0.00	0.00	0.00	0.00	0.00	0.00
02:00	72	0.00	0.00	0.08	0.00	0.00	0.00	0.00	0.00	0.00	0.00	0.00	0.00
03:00	72	0.00	0.00	0.20	0.00	0.00	0.12	0.00	0.00	0.00	0.00	0.00	0.00
04:00	72	0.01	0.00	0.12	0.00	0.00	0.00	0.00	0.00	0.00	0.00	0.00	0.00
05:00	72	0.01	0.00	0.20	0.00	0.00	0.12	0.00	0.00	0.00	0.00	0.00	0.00
06:00	72	0.00	0.00	0.12	0.00	0.00	0.10	0.00	0.00	0.00	0.00	0.00	0.00
07:00	72	0.00	0.00	0.04	0.00	0.00	0.01	0.00	0.00	0.00	0.00	0.00	0.00
08:00	72	0.01	0.00	0.16	0.00	0.00	0.13	0.00	0.00	0.00	0.00	0.00	0.00
09:00	72	0.01	0.00	0.12	0.00	0.00	0.08	0.00	0.00	0.00	0.00	0.00	0.00
10:00	72	0.00	0.00	0.04	0.00	0.00	0.00	0.00	0.00	0.00	0.00	0.00	0.00
11:00	72	0.01	0.00	0.12	0.00	0.00	0.10	0.00	0.00	0.00	0.00	0.00	0.00
12:00	72	0.00	0.00	0.16	0.00	0.00	0.11	0.00	0.00	0.00	0.00	0.00	0.00
13:00	72	0.01	0.00	0.04	0.00	0.00	0.00	0.00	0.00	0.00	0.00	0.00	0.00
14:00	72	0.00	0.00	0.16	0.00	0.00	0.10	0.00	0.00	0.00	0.00	0.00	0.00
15:00	72	0.00	0.00	0.16	0.00	0.00	0.10	0.00	0.00	0.00	0.00	0.00	0.00
16:00	72	0.00	0.00	0.08	0.00	0.00	0.00	0.00	0.00	0.00	0.00	0.00	0.00

17:00	72	0.53	0.00	0.16	0.35	0.00	0.13	0.00	0.00	0.00	0.00	0.00	0.00
18:00	72	0.91	0.00	0.52	0.61	0.00	0.09	0.00	0.00	0.00	0.00	0.00	0.00
19:00	72	0.89	0.00	0.64	0.61	0.00	0.06	0.00	0.00	0.00	0.00	0.00	0.00
20:00	72	0.72	0.00	0.64	0.69	0.00	0.09	0.00	0.00	0.00	0.00	0.00	0.00
21:00	72	0.71	0.00	0.60	0.69	0.00	0.07	0.00	0.00	0.00	0.00	0.00	0.00
22:00	72	0.01	0.00	0.20	0.00	0.00	0.11	0.00	0.00	0.00	0.00	0.00	0.00
23:00	72	0.00	0.00	0.20	0.00	0.00	0.12	0.00	0.00	0.00	0.00	0.00	0.00
24:00	72	0.01	0.00	0.20	0.00	0.00	0.12	0.00	0.00	0.00	0.00	0.00	0.00
00:00	73	0.12	0.20	0.60	0.30	0.06	0.37	0.00	0.00	0.00	0.00	0.00	0.00
01:00	73	0.12	0.16	0.60	0.15	0.02	0.37	0.00	0.00	0.00	0.00	0.00	0.00
02:00	73	0.00	0.20	0.16	0.00	0.06	0.02	0.00	0.00	0.00	0.00	0.00	0.00
03:00	73	0.04	0.28	0.12	0.04	0.09	0.00	0.00	0.00	0.00	0.00	0.00	0.00
04:00	73	0.04	0.24	0.12	0.02	0.10	0.00	0.00	0.00	0.00	0.00	0.00	0.00
05:00	73	0.04	0.28	0.12	0.02	0.12	0.00	0.00	0.00	0.00	0.00	0.00	0.00
06:00	73	0.08	0.20	0.12	0.10	0.07	0.00	0.00	0.00	0.00	0.00	0.00	0.00
07:00	73	0.00	0.20	0.52	0.00	0.08	0.36	0.08	0.00	0.00	0.00	0.00	0.00
08:00	73	0.00	0.28	0.04	0.20	0.10	0.04	0.32	0.00	0.00	0.00	0.00	0.00
09:00	73	0.00	0.20	0.04	0.12	0.08	0.04	1.00	0.00	0.00	0.00	0.00	0.00
10:00	73	0.00	0.32	0.04	0.21	0.04	0.04	1.44	0.00	0.00	0.00	0.00	0.00
11:00	73	0.00	0.24	0.04	0.18	0.03	0.04	1.84	0.00	0.00	0.00	0.00	0.00
12:00	73	0.00	0.28	0.08	0.15	0.12	0.04	2.04	0.00	0.00	0.00	0.00	0.00
13:00	73	0.00	0.24	0.04	0.23	0.08	0.04	2.08	0.00	0.00	0.00	0.00	0.00
14:00	73	0.00	0.28	0.04	0.14	0.13	0.04	2.12	0.00	0.00	0.00	0.00	0.00
15:00	73	0.00	0.28	0.04	0.24	0.11	0.04	1.84	0.00	0.00	0.00	0.00	0.00
16:00	73	0.00	0.28	0.04	0.11	0.12	0.04	1.32	0.00	0.00	0.00	0.00	0.00
17:00	73	0.00	0.28	0.04	0.07	0.13	0.04	0.24	0.00	0.00	0.00	0.00	0.00
18:00	73	0.04	0.32	0.68	0.05	0.09	0.33	0.00	0.00	0.00	0.00	0.00	0.00
19:00	73	0.08	0.60	0.72	0.03	0.06	0.50	0.04	0.00	0.00	0.00	0.00	0.00
20:00	73	0.12	0.52	0.76	0.08	0.04	0.46	0.00	0.00	0.00	0.00	0.00	0.00
21:00	73	0.08	0.64	0.72	0.02	0.04	0.48	0.00	0.00	0.00	0.00	0.00	0.00

22:00	73	0.12	0.68	0.68	0.10	0.02	0.44	0.00	0.00	0.00	0.00	0.00	0.00
23:00	73	0.04	0.72	0.64	0.00	0.06	0.43	0.00	0.00	0.00	0.00	0.00	0.00
24:00	73	0.12	0.60	0.76	0.08	0.08	0.49	0.00	0.00	0.00	0.00	0.00	0.00
00:00	74	0.32	0.52	0.00	0.04	0.28	0.00	0.00	0.00	0.00	0.00	0.00	0.00
01:00	74	0.16	0.44	0.00	0.00	0.16	0.00	0.00	0.00	0.00	0.00	0.00	0.00
02:00	74	0.16	0.48	0.00	0.00	0.20	0.00	0.00	0.00	0.00	0.00	0.00	0.00
03:00	74	0.16	0.44	0.00	0.00	0.20	0.00	0.00	0.00	0.00	0.00	0.00	0.00
04:00	74	0.16	0.40	0.00	0.00	0.16	0.00	0.00	0.00	0.00	0.00	0.00	0.00
05:00	74	1.44	0.48	0.00	0.28	0.16	0.00	0.00	0.00	0.00	0.00	0.00	0.00
06:00	74	1.12	0.92	0.00	0.16	0.32	0.00	0.00	0.00	0.00	0.00	0.00	0.00
07:00	74	0.76	0.48	0.00	0.08	0.24	0.00	0.00	0.00	0.00	0.00	0.00	0.00
08:00	74	0.16	0.48	0.00	0.00	0.28	0.00	0.00	0.00	0.00	0.00	0.00	0.00
09:00	74	0.16	0.44	0.00	0.00	0.24	0.00	0.00	0.00	0.00	0.00	0.00	0.00
10:00	74	0.16	0.52	0.00	0.00	0.36	0.00	0.00	0.00	0.00	0.00	0.00	0.00
11:00	74	0.20	0.52	0.00	0.00	0.36	0.00	0.00	0.00	0.00	0.00	0.00	0.00
12:00	74	0.16	0.48	0.00	0.00	0.24	0.00	0.00	0.00	0.00	0.00	0.00	0.00
13:00	74	0.16	0.60	0.00	0.00	0.36	0.00	0.00	0.00	0.00	0.00	0.00	0.00
14:00	74	0.16	0.56	0.00	0.00	0.36	0.00	0.00	0.00	0.00	0.00	0.00	0.00
15:00	74	0.16	0.60	0.00	0.00	0.32	0.00	0.00	0.00	0.00	0.00	0.00	0.00
16:00	74	0.16	0.56	0.00	0.00	0.32	0.00	0.00	0.00	0.00	0.00	0.00	0.00
17:00	74	0.64	0.64	0.04	0.16	0.36	0.01	0.00	0.00	0.00	0.00	0.00	0.00
18:00	74	2.96	0.68	2.76	0.00	0.40	0.38	0.00	0.00	0.00	0.00	0.00	0.00
19:00	74	2.72	0.68	2.72	0.00	0.36	0.37	0.00	0.00	0.00	0.00	0.00	0.00
20:00	74	0.52	0.72	2.72	0.00	0.28	0.36	0.00	0.00	0.00	0.00	0.00	0.00
21:00	74	1.16	1.16	2.72	0.12	0.36	0.36	0.00	0.00	0.00	0.00	0.00	0.00
22:00	74	1.12	0.76	0.52	0.12	0.28	0.07	0.00	0.00	0.00	0.00	0.00	0.00
23:00	74	1.12	0.56	0.00	0.12	0.32	0.00	0.00	0.00	0.00	0.00	0.00	0.00
24:00	74	0.32	0.60	0.00	0.00	0.32	0.00	0.00	0.00	0.00	0.00	0.00	0.00
00:00	79	2.40	0.00	0.00	0.54	0.00	0.00	0.00	0.00	0.00	0.00	0.00	0.00
01:00	79	0.80	0.00	0.00	0.09	0.00	0.00	0.00	0.00	0.00	0.00	0.00	0.00

02:00	79	0.80	0.00	0.04	0.00	0.00	0.00	0.00	0.00	0.00	0.00	0.00	0.00
03:00	79	0.80	0.00	0.00	0.04	0.00	0.00	0.00	0.00	0.00	0.00	0.00	0.00
04:00	79	0.80	0.00	0.00	0.00	0.00	0.00	0.00	0.00	0.00	0.00	0.00	0.00
05:00	79	0.80	0.00	0.00	0.03	0.00	0.00	0.00	0.00	0.00	0.00	0.00	0.00
06:00	79	0.80	0.00	0.00	0.01	0.00	0.00	0.00	0.00	0.00	0.00	0.00	0.00
07:00	79	0.80	0.00	0.00	0.00	0.00	0.00	0.00	0.00	0.00	0.00	0.00	0.00
08:00	79	1.60	0.00	0.04	0.12	0.00	0.00	0.00	0.00	0.00	0.00	0.00	0.00
09:00	79	1.20	0.00	0.04	0.00	0.00	0.00	0.00	0.00	0.00	0.00	0.00	0.00
10:00	79	1.20	0.00	0.04	0.00	0.00	0.00	0.00	0.00	0.00	0.00	0.00	0.00
11:00	79	4.00	0.00	3.40	0.22	0.00	0.00	0.00	0.00	0.00	0.00	0.00	0.00
12:00	79	3.60	0.00	2.60	0.24	0.00	0.00	0.00	0.00	0.00	0.00	0.00	0.00
13:00	79	4.00	0.00	2.80	0.12	0.00	0.00	0.00	0.00	0.00	0.00	0.00	0.00
14:00	79	2.80	0.00	2.88	0.00	0.00	0.00	0.00	0.00	0.00	0.00	0.00	0.00
15:00	79	2.80	0.00	2.92	0.00	0.00	0.00	0.00	0.00	0.00	0.00	0.00	0.00
16:00	79	2.80	0.00	2.84	0.00	0.00	0.00	0.00	0.00	0.00	0.00	0.00	0.00
17:00	79	0.80	0.00	2.88	0.01	0.00	0.00	0.00	0.00	0.00	0.00	0.00	0.00
18:00	79	3.20	0.00	2.80	0.28	0.00	0.00	0.00	0.00	0.00	0.00	0.00	0.00
19:00	79	4.80	0.00	2.48	0.10	0.00	0.00	0.00	0.00	0.00	0.00	0.00	0.00
20:00	79	2.80	0.00	2.52	0.32	0.00	0.00	0.00	0.00	0.00	0.00	0.00	0.00
21:00	79	2.80	0.00	2.16	0.30	0.00	0.00	0.00	0.00	0.00	0.00	0.00	0.00
22:00	79	3.20	0.00	1.84	0.39	0.00	0.00	0.00	0.00	0.00	0.00	0.00	0.00
23:00	79	3.60	0.00	1.84	0.64	0.00	0.00	0.00	0.00	0.00	0.00	0.00	0.00
24:00	79	3.60	0.00	1.80	0.52	0.00	0.00	0.00	0.00	0.00	0.00	0.00	0.00
00:00	81	1.44	1.36	2.36	0.88	1.12	1.32	0.00	0.00	0.00	0.00	0.00	0.00
01:00	81	1.44	1.32	2.20	0.88	1.16	1.28	0.00	0.00	0.00	0.00	0.00	0.00
02:00	81	1.32	1.24	2.32	0.92	1.08	1.36	0.00	0.00	0.00	0.00	0.00	0.00
03:00	81	1.28	1.20	2.24	0.88	1.08	1.32	0.00	0.00	0.00	0.00	0.00	0.00
04:00	81	1.32	1.16	2.24	0.92	1.08	1.36	0.00	0.00	0.00	0.00	0.00	0.00
05:00	81	0.04	0.00	0.40	0.00	0.00	0.00	0.00	0.00	0.00	0.00	0.00	0.00
06:00	81	0.04	0.00	0.40	0.00	0.00	0.04	0.00	0.00	0.00	0.00	0.00	0.00

07:00	81	0.00	0.00	0.32	0.00	0.00	0.04	0.00	0.00	0.44	0.00	0.00	0.00
08:00	81	0.04	0.00	0.96	0.00	0.00	0.00	0.00	0.00	0.84	0.00	0.00	0.00
09:00	81	0.00	0.00	0.28	0.00	0.00	0.04	0.00	0.00	1.28	0.00	0.00	0.00
10:00	81	0.00	0.00	0.24	0.00	0.00	0.00	0.00	0.00	1.60	0.00	0.00	0.00
11:00	81	0.56	0.00	0.60	0.00	0.00	0.00	0.00	0.00	1.76	0.00	0.00	0.00
12:00	81	0.00	0.00	1.32	0.00	0.00	0.48	0.00	0.00	1.80	0.00	0.00	0.00
13:00	81	0.00	0.00	0.64	0.00	0.00	0.24	0.00	0.00	1.76	0.00	0.00	0.00
14:00	81	0.04	0.04	0.76	0.04	0.04	0.04	0.00	0.00	1.56	0.00	0.00	0.00
15:00	81	1.80	0.20	3.00	1.04	1.16	1.32	0.00	0.00	0.00	0.00	0.00	0.00
16:00	81	0.04	0.00	0.52	0.00	0.00	0.00	0.00	0.00	0.88	0.00	0.00	0.00
17:00	81	0.72	0.36	1.00	0.20	0.32	0.36	0.00	0.00	0.36	0.00	0.00	0.00
18:00	81	1.68	1.52	2.68	0.80	1.16	1.24	0.00	0.00	0.00	0.00	0.00	0.00
19:00	81	1.64	1.40	2.76	0.92	1.04	1.12	0.00	0.00	0.00	0.00	0.00	0.00
20:00	81	1.84	1.28	2.56	0.84	1.08	0.96	0.00	0.00	0.00	0.00	0.00	0.00
21:00	81	1.56	1.28	2.60	0.76	1.12	0.96	0.00	0.00	0.00	0.00	0.00	0.00
22:00	81	1.52	1.40	2.56	0.72	1.16	1.16	0.00	0.00	0.00	0.00	0.00	0.00
23:00	81	1.44	1.44	2.64	0.76	1.12	1.24	0.00	0.00	0.00	0.00	0.00	0.00
24:00	81	1.40	1.32	2.32	0.80	1.12	1.28	0.00	0.00	0.00	0.00	0.00	0.00
00:00	83	1.44	1.36	2.36	0.88	1.12	1.32	0.00	0.00	0.00	0.00	0.00	0.00
01:00	83	1.44	1.32	2.20	0.88	1.16	1.28	0.00	0.00	0.00	0.00	0.00	0.00
02:00	83	1.32	1.24	2.32	0.92	1.08	1.36	0.00	0.00	0.00	0.00	0.00	0.00
03:00	83	1.28	1.20	2.24	0.88	1.08	1.32	0.00	0.00	0.00	0.00	0.00	0.00
04:00	83	1.32	1.16	2.24	0.92	1.08	1.36	0.00	0.00	0.00	0.00	0.00	0.00
05:00	83	0.04	0.00	0.40	0.00	0.00	0.00	0.00	0.00	0.00	0.00	0.00	0.00
06:00	83	0.04	0.00	0.40	0.00	0.00	0.04	0.00	0.00	0.00	0.00	0.00	0.00
07:00	83	0.00	0.00	0.32	0.00	0.00	0.04	0.00	0.44	0.00	0.00	0.00	0.00
08:00	83	0.04	0.00	0.96	0.00	0.00	0.00	0.00	0.84	0.00	0.00	0.00	0.00
09:00	83	0.00	0.00	0.28	0.00	0.00	0.04	0.00	1.28	0.00	0.00	0.00	0.00
10:00	83	0.00	0.00	0.24	0.00	0.00	0.00	0.00	1.60	0.00	0.00	0.00	0.00
11:00	83	0.56	0.00	0.60	0.00	0.00	0.00	0.00	1.76	0.00	0.00	0.00	0.00

12:00	83	0.00	0.00	1.32	0.00	0.00	0.48	0.00	1.80	0.00	0.00	0.00	0.00
13:00	83	0.00	0.00	0.64	0.00	0.00	0.24	0.00	1.76	0.00	0.00	0.00	0.00
14:00	83	0.04	0.04	0.76	0.04	0.04	0.04	0.00	1.56	0.00	0.00	0.00	0.00
15:00	83	1.80	0.20	3.00	1.04	1.16	1.32	0.00	0.00	0.00	0.00	0.00	0.00
16:00	83	0.04	0.00	0.52	0.00	0.00	0.00	0.00	0.88	0.00	0.00	0.00	0.00
17:00	83	0.72	0.36	1.00	0.20	0.32	0.36	0.00	0.36	0.00	0.00	0.00	0.00
18:00	83	1.68	1.52	2.68	0.80	1.16	1.24	0.00	0.00	0.00	0.00	0.00	0.00
19:00	83	1.64	1.40	2.76	0.92	1.04	1.12	0.00	0.00	0.00	0.00	0.00	0.00
20:00	83	1.84	1.28	2.56	0.84	1.08	0.96	0.00	0.00	0.00	0.00	0.00	0.00
21:00	83	1.56	1.28	2.60	0.76	1.12	0.96	0.00	0.00	0.00	0.00	0.00	0.00
22:00	83	1.52	1.40	2.56	0.72	1.16	1.16	0.00	0.00	0.00	0.00	0.00	0.00
23:00	83	1.44	1.44	2.64	0.76	1.12	1.24	0.00	0.00	0.00	0.00	0.00	0.00
24:00	83	1.40	1.32	2.32	0.80	1.12	1.28	0.00	0.00	0.00	0.00	0.00	0.00
00:00	87	0.16	0.08	0.00	0.08	0.00	0.00	0.00	0.00	0.00	0.00	0.00	0.00
01:00	87	0.24	0.04	0.96	0.08	0.00	0.00	0.00	0.00	0.00	0.00	0.00	0.00
02:00	87	0.16	0.96	0.00	0.04	0.20	0.00	0.00	0.00	0.00	0.00	0.00	0.00
03:00	87	0.20	1.12	0.80	0.12	0.24	0.00	0.00	0.00	0.00	0.00	0.00	0.00
04:00	87	0.24	1.12	0.00	0.16	0.24	0.00	0.00	0.00	0.00	0.00	0.00	0.00
05:00	87	0.20	0.28	0.00	0.08	0.08	0.00	0.00	0.00	0.00	0.00	0.00	0.00
06:00	87	0.60	2.04	0.00	0.12	1.32	0.00	0.00	0.00	0.00	0.00	0.00	0.00
07:00	87	0.20	0.04	0.00	0.08	0.00	0.00	0.00	0.00	0.00	0.00	0.00	0.00
08:00	87	0.20	0.72	0.00	0.12	0.20	0.00	0.00	0.00	0.00	0.00	0.00	0.00
09:00	87	0.12	1.12	0.00	0.00	0.28	0.00	0.00	0.00	0.00	0.00	0.00	0.00
10:00	87	0.44	3.04	1.12	0.00	1.68	0.00	0.00	0.00	0.00	0.00	0.00	0.00
11:00	87	0.48	3.04	0.00	0.08	1.84	0.00	0.00	0.00	0.00	0.00	0.00	0.00
12:00	87	0.52	3.04	0.00	0.12	1.68	0.00	0.00	0.00	0.00	0.00	0.00	0.00
13:00	87	1.28	3.08	0.00	0.44	1.72	0.00	0.00	0.00	0.00	0.00	0.00	0.00
14:00	87	0.48	0.04	0.00	0.36	0.00	0.00	0.00	0.00	0.00	0.00	0.00	0.00
15:00	87	0.44	4.20	0.00	0.00	1.72	0.00	0.00	0.00	0.00	0.00	0.00	0.00
16:00	87	0.60	4.20	1.40	0.08	1.76	0.00	0.00	0.00	0.00	0.00	0.00	0.00

17:00	87	0.20	0.04	0.00	0.08	0.00	0.00	0.00	0.00	0.00	0.00	0.00	0.00
18:00	87	0.16	0.04	0.00	0.04	0.00	0.00	0.00	0.00	0.00	0.00	0.00	0.00
19:00	87	0.52	4.12	0.96	0.04	1.20	0.04	0.00	0.00	0.00	0.00	0.00	0.00
20:00	87	1.32	4.12	0.00	0.08	1.20	0.00	0.00	0.00	0.00	0.00	0.00	0.00
21:00	87	0.84	4.00	2.04	0.44	1.40	0.00	0.00	0.00	0.00	0.00	0.00	0.00
22:00	87	0.52	0.32	2.08	0.00	0.08	0.00	0.00	0.00	0.00	0.00	0.00	0.00
23:00	87	0.36	0.04	0.00	0.04	0.00	0.00	0.00	0.00	0.00	0.00	0.00	0.00
24:00	87	0.28	0.04	0.00	0.12	0.00	0.00	0.00	0.00	0.00	0.00	0.00	0.00
00:00	88	0.44	0.32	0.00	0.04	0.00	0.00	0.00	0.00	0.00	0.00	0.00	0.00
01:00	88	0.44	0.00	0.00	0.04	0.00	0.00	0.00	0.00	0.00	0.00	0.00	0.00
02:00	88	0.56	0.00	0.00	0.08	0.00	0.00	0.00	0.00	0.00	0.00	0.00	0.00
03:00	88	0.52	0.04	0.00	0.08	0.00	0.00	0.00	0.00	0.00	0.00	0.00	0.00
04:00	88	0.56	0.00	0.00	0.08	0.00	0.00	0.00	0.00	0.00	0.00	0.00	0.00
05:00	88	0.56	0.00	0.00	0.08	0.00	0.00	0.00	0.00	0.00	0.00	0.00	0.00
06:00	88	0.68	0.40	0.00	0.08	0.00	0.00	0.00	0.00	0.00	0.00	0.00	0.00
07:00	88	1.04	0.00	0.00	0.12	0.00	0.00	0.00	0.00	0.00	0.00	0.00	0.00
08:00	88	0.60	0.28	0.00	0.12	0.00	0.00	0.00	0.00	0.00	0.00	0.00	0.00
09:00	88	0.20	0.00	0.00	0.08	0.00	0.00	0.00	0.00	0.00	0.00	0.00	0.00
10:00	88	0.20	0.00	0.00	0.12	0.00	0.00	0.00	0.00	0.00	0.00	0.00	0.00
11:00	88	0.20	0.00	0.00	0.12	0.00	0.00	0.00	0.00	0.00	0.00	0.00	0.00
12:00	88	0.12	0.00	0.00	0.08	0.00	0.00	0.00	0.00	0.00	0.00	0.00	0.00
13:00	88	0.12	0.00	0.00	0.08	0.00	0.00	0.00	0.00	0.00	0.00	0.00	0.00
14:00	88	0.16	0.00	0.00	0.08	0.00	0.00	0.00	0.00	0.00	0.00	0.00	0.00
15:00	88	0.20	0.28	0.00	0.12	0.00	0.00	0.00	0.00	0.00	0.00	0.00	0.00
16:00	88	0.16	0.00	0.00	0.08	0.00	0.00	0.00	0.00	0.00	0.00	0.00	0.00
17:00	88	0.12	0.00	0.00	0.08	0.00	0.00	0.00	0.00	0.00	0.00	0.00	0.00
18:00	88	0.16	0.00	0.00	0.08	0.00	0.00	0.00	0.00	0.00	0.00	0.00	0.00
19:00	88	0.20	0.60	0.00	0.08	0.00	0.00	0.00	0.00	0.00	0.00	0.00	0.00
20:00	88	0.20	0.00	0.00	0.12	0.00	0.00	0.00	0.00	0.00	0.00	0.00	0.00
21:00	88	0.16	0.00	0.00	0.08	0.00	0.00	0.00	0.00	0.00	0.00	0.00	0.00

22:00	88	0.16	0.00	0.00	0.12	0.00	0.00	0.00	0.00	0.00	0.00	0.00	0.00
23:00	88	0.20	0.24	0.00	0.12	0.00	0.00	0.00	0.00	0.00	0.00	0.00	0.00
24:00	88	0.16	0.00	0.00	0.12	0.00	0.00	0.00	0.00	0.00	0.00	0.00	0.00
00:00	90	0.00	1.20	0.39	0.00	0.17	0.00	0.00	0.00	0.00	0.00	0.00	0.00
01:00	90	0.00	1.20	0.39	0.00	0.21	0.00	0.00	0.00	0.00	0.00	0.00	0.00
02:00	90	0.00	1.20	0.39	0.00	0.16	0.00	0.00	0.00	0.00	0.00	0.00	0.00
03:00	90	0.00	1.20	0.39	0.00	0.28	0.00	0.00	0.00	0.00	0.00	0.00	0.00
04:00	90	0.00	1.20	0.39	0.00	0.18	0.00	0.00	0.00	0.00	0.00	0.00	0.00
05:00	90	0.00	1.20	0.39	0.00	0.27	0.00	0.00	0.00	0.00	0.00	0.00	0.00
06:00	90	0.00	0.80	0.40	0.00	0.24	0.00	0.00	0.00	0.00	0.00	0.00	0.00
07:00	90	0.00	1.60	0.39	0.00	0.25	0.00	0.00	0.00	0.00	0.00	0.00	0.00
08:00	90	0.00	1.60	0.39	0.00	0.30	0.00	0.00	0.00	0.00	0.00	0.00	0.00
09:00	90	0.00	1.20	0.39	0.00	0.28	0.00	0.00	0.00	0.00	0.00	0.00	0.00
10:00	90	0.00	1.60	0.40	0.00	0.11	0.00	0.00	0.00	0.00	0.00	0.00	0.00
11:00	90	0.00	2.00	0.39	0.00	0.09	0.00	0.00	0.00	0.00	0.00	0.00	0.00
12:00	90	0.00	1.60	0.42	0.00	0.13	0.00	0.00	0.00	0.00	0.00	0.00	0.00
13:00	90	0.00	2.40	0.52	0.00	0.13	0.00	0.00	0.00	0.00	0.00	0.00	0.00
14:00	90	0.00	2.00	0.52	0.00	0.15	0.00	0.00	0.00	0.00	0.00	0.00	0.00
15:00	90	0.00	2.00	0.52	0.00	0.04	0.00	0.00	0.00	0.00	0.00	0.00	0.00
16:00	90	0.00	2.00	0.52	0.00	0.04	0.00	0.00	0.00	0.00	0.00	0.00	0.00
17:00	90	0.00	1.60	0.52	0.00	0.14	0.00	0.00	0.00	0.00	0.00	0.00	0.00
18:00	90	0.00	2.00	0.53	0.00	0.18	0.00	0.00	0.00	0.00	0.00	0.00	0.00
19:00	90	0.00	2.00	0.53	0.00	0.24	0.00	0.00	0.00	0.00	0.00	0.00	0.00
20:00	90	0.00	2.00	0.53	0.00	0.17	0.00	0.00	0.00	0.00	0.00	0.00	0.00
21:00	90	0.00	2.00	0.53	0.00	0.00	0.00	0.00	0.00	0.00	0.00	0.00	0.00
22:00	90	0.00	1.60	0.29	0.00	0.09	0.00	0.00	0.00	0.00	0.00	0.00	0.00
23:00	90	0.00	1.60	0.22	0.00	0.07	0.00	0.00	0.00	0.00	0.00	0.00	0.00
24:00	90	0.00	1.20	0.22	0.00	0.08	0.00	0.00	0.00	0.00	0.00	0.00	0.00
00:00	92	0.04	0.00	0.36	0.00	0.00	0.04	0.00	0.00	0.00	0.00	0.00	0.00
01:00	92	0.04	0.00	0.36	0.00	0.00	0.02	0.00	0.00	0.00	0.00	0.00	0.00

02:00	92	0.04	0.00	0.24	0.00	0.00	0.04	0.00	0.00	0.00	0.00	0.00	0.00
03:00	92	0.04	0.00	0.28	0.00	0.00	0.04	0.00	0.00	0.00	0.00	0.00	0.00
04:00	92	0.04	0.00	0.28	0.00	0.00	0.04	0.00	0.00	0.00	0.00	0.00	0.00
05:00	92	0.04	0.00	0.28	0.00	0.00	0.04	0.00	0.00	0.00	0.00	0.00	0.00
06:00	92	0.00	0.00	0.24	0.00	0.00	0.04	0.00	0.00	0.00	0.00	0.00	0.00
07:00	92	0.00	0.00	0.04	0.00	0.00	0.00	0.40	0.00	0.00	0.00	0.00	0.00
08:00	92	0.00	0.00	0.04	0.00	0.00	0.00	0.72	0.00	0.00	0.00	0.00	0.00
09:00	92	0.00	0.00	0.16	0.00	0.00	0.00	1.04	0.00	0.00	0.00	0.00	0.00
10:00	92	0.00	0.00	0.12	0.00	0.00	0.00	1.20	0.00	0.00	0.00	0.00	0.00
11:00	92	0.00	0.00	0.08	0.00	0.00	0.00	1.28	0.00	0.00	0.00	0.00	0.00
12:00	92	0.00	0.00	0.12	0.00	0.00	0.00	1.24	0.00	0.00	0.00	0.00	0.00
13:00	92	0.00	0.00	0.16	0.00	0.00	0.00	1.20	0.00	0.00	0.00	0.00	0.00
14:00	92	0.00	0.00	0.16	0.00	0.00	0.00	1.08	0.00	0.00	0.00	0.00	0.00
15:00	92	0.00	0.00	0.16	0.00	0.00	0.00	0.84	0.00	0.00	0.00	0.00	0.00
16:00	92	0.04	0.44	0.16	0.00	0.04	0.00	0.36	0.00	0.00	0.00	0.00	0.00
17:00	92	2.20	0.04	0.84	0.06	0.00	0.05	0.00	0.00	0.00	0.00	0.00	0.00
18:00	92	2.32	0.00	0.76	0.01	0.00	0.00	0.00	0.00	0.00	0.00	0.00	0.00
19:00	92	2.36	0.00	0.32	0.00	0.00	0.00	0.00	0.00	0.00	0.00	0.00	0.00
20:00	92	1.92	0.00	0.12	0.06	0.00	0.00	0.00	0.00	0.00	0.00	0.00	0.00
21:00	92	2.00	0.00	0.12	0.04	0.00	0.00	0.00	0.00	0.00	0.00	0.00	0.00
22:00	92	1.16	0.00	0.16	0.03	0.00	0.00	0.00	0.00	0.00	0.00	0.00	0.00
23:00	92	1.12	0.00	0.20	0.02	0.00	0.01	0.00	0.00	0.00	0.00	0.00	0.00
24:00	92	0.04	0.00	0.56	0.00	0.00	0.04	0.00	0.00	0.00	0.00	0.00	0.00

Appendix C. Forrestfield MV Network Data

Table C.1 Branch data of Forrestfield MV network.

Bus i	Bus j	Length(m)	R_{PP}(Ω/km)	X_{PP}(Ω/km)	R_{AB}(Ω/km)	X_{AB}(Ω/km)	R_{BC}(Ω/km)	X_{BC}(Ω/km)	R_{CA}(Ω/km)	X_{CA}(Ω/km)
1	2	828	0.143	0.726	0.049	0.434	0.049	0.434	0.049	0.393
2	3	77	0.143	0.726	0.049	0.434	0.049	0.434	0.049	0.393
3	4	11	0.143	0.726	0.049	0.434	0.049	0.434	0.049	0.393
4	5	58	0.882	0.796	0.049	0.434	0.049	0.434	0.049	0.393
4	6	11	0.143	0.726	0.049	0.434	0.049	0.434	0.049	0.393
6	7	769	0.143	0.726	0.049	0.434	0.049	0.434	0.049	0.393
7	8	111	0.281	0.756	0.049	0.434	0.049	0.434	0.049	0.393
8	9	16	0.882	0.796	0.049	0.434	0.049	0.434	0.049	0.393
7	10	254	0.281	0.756	0.049	0.434	0.049	0.434	0.049	0.393
10	11	42	0.882	0.796	0.049	0.434	0.049	0.434	0.049	0.393
10	12	233	0.281	0.756	0.049	0.434	0.049	0.434	0.049	0.393
12	13	66	0.281	0.756	0.049	0.434	0.049	0.434	0.049	0.393
13	14	35	0.281	0.756	0.049	0.434	0.049	0.434	0.049	0.393
14	15	423	0.419	0.771	0.049	0.434	0.049	0.434	0.049	0.393
13	16	46	0.281	0.756	0.049	0.434	0.049	0.434	0.049	0.393

16	17	479	0.281	0.756	0.049	0.434	0.049	0.434	0.049	0.393
17	18	134	0.281	0.756	0.049	0.434	0.049	0.434	0.049	0.393
18	19	242	0.738	0.790	0.049	0.434	0.049	0.434	0.049	0.393
19	20	92	0.419	0.771	0.049	0.434	0.049	0.434	0.049	0.393
18	21	267	0.281	0.756	0.049	0.434	0.049	0.434	0.049	0.393
21	22	19	0.307	0.759	0.049	0.434	0.049	0.434	0.049	0.393
21	23	50	0.307	0.759	0.049	0.434	0.049	0.434	0.049	0.393
23	24	192	0.281	0.756	0.049	0.434	0.049	0.434	0.049	0.393
24	25	16	0.738	0.790	0.049	0.434	0.049	0.434	0.049	0.393
24	26	87	0.281	0.756	0.049	0.434	0.049	0.434	0.049	0.393
26	27	87	0.281	0.756	0.049	0.434	0.049	0.434	0.049	0.393
27	28	38	0.281	0.756	0.049	0.434	0.049	0.434	0.049	0.393
28	29	27	0.882	0.796	0.049	0.434	0.049	0.434	0.049	0.393
29	30	127	0.882	0.796	0.049	0.434	0.049	0.434	0.049	0.393
28	31	187	0.281	0.756	0.049	0.434	0.049	0.434	0.049	0.393
31	32	51	0.281	0.756	0.049	0.434	0.049	0.434	0.049	0.393
32	33	329	0.419	0.771	0.049	0.434	0.049	0.434	0.049	0.393
33	34	32	0.281	0.756	0.049	0.434	0.049	0.434	0.049	0.393
34	35	59	0.281	0.756	0.049	0.434	0.049	0.434	0.049	0.393
35	36	14	0.882	0.796	0.049	0.434	0.049	0.434	0.049	0.393
34	37	36	0.281	0.756	0.049	0.434	0.049	0.434	0.049	0.393
37	38	80	0.281	0.756	0.049	0.434	0.049	0.434	0.049	0.393
38	39	284	0.882	0.796	0.049	0.434	0.049	0.434	0.049	0.393
38	40	142	0.281	0.756	0.049	0.434	0.049	0.434	0.049	0.393

40	41	48	0.882	0.796	0.049	0.434	0.049	0.434	0.049	0.393
40	42	73	0.281	0.756	0.049	0.434	0.049	0.434	0.049	0.393
42	43	114	0.143	0.726	0.049	0.434	0.049	0.434	0.049	0.393
43	44	131	0.281	0.756	0.049	0.434	0.049	0.434	0.049	0.393
44	45	46	0.628	0.785	0.049	0.434	0.049	0.434	0.049	0.393
45	46	104	0.882	0.796	0.049	0.434	0.049	0.434	0.049	0.393
44	47	238	0.628	0.785	0.049	0.434	0.049	0.434	0.049	0.393
47	48	37	0.628	0.785	0.049	0.434	0.049	0.434	0.049	0.393
48	49	85	0.628	0.785	0.049	0.434	0.049	0.434	0.049	0.393
49	50	71	0.628	0.785	0.049	0.434	0.049	0.434	0.049	0.393
50	51	143	0.882	0.796	0.049	0.434	0.049	0.434	0.049	0.393
50	52	32	0.628	0.785	0.049	0.434	0.049	0.434	0.049	0.393
48	53	131	0.628	0.785	0.049	0.434	0.049	0.434	0.049	0.393
53	54	73	0.628	0.785	0.049	0.434	0.049	0.434	0.049	0.393
54	55	109	0.628	0.785	0.049	0.434	0.049	0.434	0.049	0.393
55	56	43	0.628	0.785	0.049	0.434	0.049	0.434	0.049	0.393
56	57	188	0.281	0.756	0.049	0.434	0.049	0.434	0.049	0.393
55	58	210	0.628	0.785	0.049	0.434	0.049	0.434	0.049	0.393
53	59	58	0.281	0.756	0.049	0.434	0.049	0.434	0.049	0.393
59	60	13	0.882	0.796	0.049	0.434	0.049	0.434	0.049	0.393

Table C.2 LV-side loads at distribution transformer buses of Forrestfield MV network over 24 hours.

Time	Bus(es)	P_{LA} (kW)	P_{LB} (kW)	P_{LC} (kW)	Q_{LA} (kVAr)	Q_{LB} (kVAr)	Q_{LC} (kVAr)
00:00	5/25/41/46/60	21.19	33.85	33.76	9.86	11.81	10.91
01:00	5/25/41/46/60	17.19	29.09	31.20	7.67	10.45	10.24
02:00	5/25/41/46/60	18.63	23.78	28.24	7.82	9.47	9.32
03:00	5/25/41/46/60	16.84	26.18	27.13	6.61	10.62	10.72
04:00	5/25/41/46/60	17.68	25.84	26.72	7.13	10.03	9.26
05:00	5/25/41/46/60	14.36	20.31	23.64	4.85	6.76	5.95
06:00	5/25/41/46/60	13.85	24.48	20.02	3.82	7.54	3.58
07:00	5/25/41/46/60	12.63	23.05	15.66	4.12	7.39	3.61
08:00	5/25/41/46/60	10.19	22.98	17.86	4.86	7.00	5.00
09:00	5/25/41/46/60	9.33	24.74	17.88	5.77	8.87	10.02
10:00	5/25/41/46/60	7.46	29.34	17.96	6.34	13.40	12.01
11:00	5/25/41/46/60	10.88	32.07	22.44	6.27	13.73	15.01
12:00	5/25/41/46/60	9.35	33.72	23.13	7.01	15.08	15.18
13:00	5/25/41/46/60	17.93	33.30	25.96	8.59	15.05	15.11
14:00	5/25/41/46/60	15.29	31.38	31.65	7.91	14.43	16.75
15:00	5/25/41/46/60	19.86	41.51	39.11	10.18	17.61	18.97
16:00	5/25/41/46/60	23.28	45.88	39.50	8.96	16.28	15.82
17:00	5/25/41/46/60	31.30	41.70	49.42	10.40	14.97	16.35
18:00	5/25/41/46/60	44.53	56.16	66.54	11.98	14.83	17.97
19:00	5/25/41/46/60	45.04	60.28	73.35	11.04	15.41	17.47
20:00	5/25/41/46/60	41.68	63.68	71.97	12.15	19.66	18.46
21:00	5/25/41/46/60	39.88	57.16	68.05	9.87	17.20	18.35
22:00	5/25/41/46/60	33.47	46.98	54.28	9.12	15.70	14.63
23:00	5/25/41/46/60	29.86	36.22	42.67	8.52	12.79	10.51
24:00	5/25/41/46/60	23.19	33.50	37.74	7.97	14.60	12.10

Table C.3 Loads of Forrestfield MV network over 24 hours.

Time	Bus	P_{LA} (kW)	P_{LB} (kW)	P_{LC} (kW)	Q_{LA}(kVAr)	Q_{LB}(kVAr)	Q_{LC}(kVAr)	Bus	P_{LA} (kW)	P_{LB} (kW)	P_{LC} (kW)	Q_{LA}(kVAr)	Q_{LB}(kVAr)	Q_{LC}(kVAr)
00:00	4	38.28	61.15	61.00	17.80	21.34	19.71	36	16.95	27.08	27.01	7.88	9.45	8.73
01:00	4	31.06	52.56	56.36	13.85	18.87	18.49	36	13.75	23.27	24.96	6.13	8.36	8.19
02:00	4	33.65	42.96	51.02	14.12	17.11	16.83	36	14.90	19.02	22.59	6.25	7.58	7.45
03:00	4	30.41	47.29	49.01	11.95	19.19	19.37	36	13.47	20.94	21.71	5.29	8.50	8.58
04:00	4	31.95	46.69	48.26	12.87	18.12	16.72	36	14.15	20.68	21.37	5.70	8.03	7.40
05:00	4	25.94	36.69	42.71	8.76	12.21	10.74	36	11.49	16.25	18.92	3.88	5.41	4.76
06:00	4	25.02	44.22	36.16	6.91	13.62	6.47	36	11.08	19.58	16.01	3.06	6.03	2.86
07:00	4	22.82	41.64	28.29	7.44	13.35	6.52	36	10.11	18.44	12.53	3.29	5.91	2.89
08:00	4	18.41	41.51	32.27	8.77	12.64	9.03	36	8.15	18.38	14.29	3.88	5.60	4.00
09:00	4	16.85	44.70	32.31	10.43	16.03	18.10	36	7.46	19.80	14.31	4.62	7.10	8.02
10:00	4	13.48	53.00	32.45	11.46	24.21	21.70	36	5.97	23.47	14.37	5.08	10.72	9.61
11:00	4	19.65	57.94	40.54	11.33	24.81	27.12	36	8.70	25.66	17.95	5.02	10.99	12.01
12:00	4	16.89	60.92	41.79	12.66	27.24	27.42	36	7.48	26.98	18.50	5.61	12.06	12.14
13:00	4	32.39	60.16	46.90	15.53	27.19	27.30	36	14.34	26.64	20.77	6.88	12.04	12.09
14:00	4	27.63	56.70	57.17	14.29	26.06	30.27	36	12.23	25.11	25.32	6.33	11.54	13.40
15:00	4	35.87	74.98	70.65	18.39	31.81	34.27	36	15.88	33.21	31.29	8.15	14.09	15.18
16:00	4	42.05	82.88	71.36	16.19	29.42	28.58	36	18.62	36.70	31.60	7.17	13.03	12.65
17:00	4	56.55	75.34	89.28	18.78	27.04	29.53	36	25.04	33.36	39.54	8.32	11.97	13.08
18:00	4	80.44	101.45	120.20	21.64	26.79	32.46	36	35.62	44.93	53.23	9.58	11.86	14.38
19:00	4	81.37	108.90	132.50	19.95	27.84	31.57	36	36.04	48.22	58.68	8.83	12.33	13.98
20:00	4	75.30	115.03	130.01	21.94	35.51	33.35	36	33.35	50.94	57.57	9.72	15.72	14.77
21:00	4	72.05	103.25	122.93	17.82	31.07	33.14	36	31.91	45.72	54.44	7.89	13.76	14.68
22:00	4	60.46	84.86	98.06	16.48	28.36	26.43	36	26.77	37.58	43.42	7.30	12.56	11.70
23:00	4	53.94	65.43	77.08	15.40	23.10	18.98	36	23.89	28.98	34.13	6.82	10.23	8.41
24:00	4	41.90	60.52	68.18	14.40	26.37	21.86	36	18.55	26.80	30.20	6.38	11.68	9.68
00:00	9	10.60	16.92	16.88	4.93	5.91	5.46	39	71.66	114.46	114.17	33.33	39.95	36.90
01:00	9	8.60	14.55	15.60	3.83	5.22	5.12	39	58.13	98.37	105.49	25.92	35.32	34.61

02:00	9	9.31	11.89	14.12	3.91	4.74	4.66	39	62.99	80.41	95.49	26.43	32.03	31.50
03:00	9	8.42	13.09	13.57	3.31	5.31	5.36	39	56.93	88.53	91.75	22.36	35.91	36.26
04:00	9	8.84	12.92	13.36	3.56	5.02	4.63	39	59.80	87.39	90.34	24.10	33.93	31.30
05:00	9	7.18	10.16	11.82	2.42	3.38	2.97	39	48.56	68.69	79.95	16.40	22.86	20.11
06:00	9	6.92	12.24	10.01	1.91	3.77	1.79	39	46.83	82.78	67.68	12.93	25.50	12.11
07:00	9	6.32	11.52	7.83	2.06	3.69	1.80	39	42.72	77.94	52.96	13.92	24.98	12.20
08:00	9	5.10	11.49	8.93	2.43	3.50	2.50	39	34.46	77.69	60.40	16.42	23.66	16.90
09:00	9	4.66	12.37	8.94	2.89	4.44	5.01	39	31.54	83.67	60.47	19.52	30.01	33.88
10:00	9	3.73	14.67	8.98	3.17	6.70	6.01	39	25.24	99.21	60.75	21.46	45.31	40.62
11:00	9	5.44	16.04	11.22	3.14	6.87	7.51	39	36.78	108.45	75.89	21.21	46.44	50.76
12:00	9	4.68	16.86	11.57	3.50	7.54	7.59	39	31.62	114.04	78.22	23.69	50.99	51.32
13:00	9	8.96	16.65	12.98	4.30	7.53	7.56	39	60.62	112.62	87.79	29.06	50.90	51.11
14:00	9	7.65	15.69	15.82	3.96	7.21	8.38	39	51.71	106.13	107.02	26.75	48.78	56.66
15:00	9	9.93	20.75	19.55	5.09	8.80	9.49	39	67.14	140.36	132.24	34.43	59.54	64.15
16:00	9	11.64	22.94	19.75	4.48	8.14	7.91	39	78.71	155.13	133.58	30.30	55.06	53.49
17:00	9	15.65	20.85	24.71	5.20	7.48	8.17	39	105.85	141.02	167.11	35.15	50.61	55.28
18:00	9	22.26	28.08	33.27	5.99	7.41	8.98	39	150.57	189.91	224.99	40.51	50.15	60.76
19:00	9	22.52	30.14	36.67	5.52	7.70	8.74	39	152.32	203.84	248.02	37.34	52.11	59.09
20:00	9	20.84	31.84	35.98	6.07	9.83	9.23	39	140.95	215.32	243.36	41.08	66.47	62.42
21:00	9	19.94	28.58	34.02	4.93	8.60	9.17	39	134.87	193.27	230.11	33.36	58.16	62.04
22:00	9	16.73	23.49	27.14	4.56	7.85	7.32	39	113.17	158.85	183.55	30.85	53.08	49.48
23:00	9	14.93	18.11	21.33	4.26	6.39	5.25	39	100.97	122.48	144.28	28.83	43.24	35.53
24:00	9	11.60	16.75	18.87	3.99	7.30	6.05	39	78.42	113.28	127.63	26.96	49.36	40.92
00:00	11	55.24	88.23	88.01	25.69	30.79	28.44	44	38.28	61.15	61.00	17.80	21.34	19.71
01:00	11	44.81	75.83	81.31	19.98	27.23	26.68	44	31.06	52.56	56.36	13.85	18.87	18.49
02:00	11	48.55	61.98	73.61	20.37	24.69	24.28	44	33.65	42.96	51.02	14.12	17.11	16.83
03:00	11	43.88	68.24	70.72	17.24	27.68	27.95	44	30.41	47.29	49.01	11.95	19.19	19.37
04:00	11	46.09	67.36	69.64	18.57	26.15	24.12	44	31.95	46.69	48.26	12.87	18.12	16.72
05:00	11	37.43	52.94	61.63	12.64	17.62	15.50	44	25.94	36.69	42.71	8.76	12.21	10.74
06:00	11	36.09	63.81	52.17	9.97	19.65	9.33	44	25.02	44.22	36.16	6.91	13.62	6.47

07:00	11	32.93	60.07	40.82	10.73	19.25	9.40	44	22.82	41.64	28.29	7.44	13.35	6.52
08:00	11	26.57	59.89	46.55	12.66	18.24	13.03	44	18.41	41.51	32.27	8.77	12.64	9.03
09:00	11	24.31	64.50	46.61	15.05	23.13	26.11	44	16.85	44.70	32.31	10.43	16.03	18.10
10:00	11	19.46	76.48	46.82	16.54	34.93	31.31	44	13.48	53.00	32.45	11.46	24.21	21.70
11:00	11	28.35	83.60	58.50	16.35	35.79	39.13	44	19.65	57.94	40.54	11.33	24.81	27.12
12:00	11	24.38	87.90	60.29	18.26	39.30	39.56	44	16.89	60.92	41.79	12.66	27.24	27.42
13:00	11	46.73	86.81	67.67	22.40	39.23	39.39	44	32.39	60.16	46.90	15.53	27.19	27.30
14:00	11	39.86	81.80	82.49	20.62	37.60	43.67	44	27.63	56.70	57.17	14.29	26.06	30.27
15:00	11	51.75	108.19	101.93	26.54	45.90	49.45	44	35.87	74.98	70.65	18.39	31.81	34.27
16:00	11	60.67	119.58	102.97	23.35	42.44	41.23	44	42.05	82.88	71.36	16.19	29.42	28.58
17:00	11	81.59	108.70	128.81	27.10	39.01	42.61	44	56.55	75.34	89.28	18.78	27.04	29.53
18:00	11	116.06	146.38	173.42	31.23	38.65	46.84	44	80.44	101.45	120.20	21.64	26.79	32.46
19:00	11	117.41	157.12	191.18	28.78	40.16	45.55	44	81.37	108.90	132.50	19.95	27.84	31.57
20:00	11	108.65	165.97	187.59	31.66	51.23	48.11	44	75.30	115.03	130.01	21.94	35.51	33.35
21:00	11	103.96	148.98	177.37	25.71	44.83	47.82	44	72.05	103.25	122.93	17.82	31.07	33.14
22:00	11	87.23	122.44	141.48	23.78	40.92	38.14	44	60.46	84.86	98.06	16.48	28.36	26.43
23:00	11	77.83	94.41	111.21	22.22	33.33	27.39	44	53.94	65.43	77.08	15.40	23.10	18.98
24:00	11	60.45	87.32	98.38	20.78	38.05	31.54	44	41.90	60.52	68.18	14.40	26.37	21.86
00:00	15	10.60	16.92	16.88	4.93	5.91	5.46	51	59.48	94.99	94.76	27.66	33.16	30.62
01:00	15	8.60	14.55	15.60	3.83	5.22	5.12	51	48.25	81.65	87.55	21.51	29.32	28.73
02:00	15	9.31	11.89	14.12	3.91	4.74	4.66	51	52.28	66.74	79.26	21.94	26.58	26.15
03:00	15	8.42	13.09	13.57	3.31	5.31	5.36	51	47.25	73.47	76.15	18.56	29.81	30.10
04:00	15	8.84	12.92	13.36	3.56	5.02	4.63	51	49.63	72.53	74.98	20.00	28.16	25.98
05:00	15	7.18	10.16	11.82	2.42	3.38	2.97	51	40.30	57.01	66.36	13.61	18.97	16.69
06:00	15	6.92	12.24	10.01	1.91	3.77	1.79	51	38.86	68.70	56.18	10.73	21.16	10.05
07:00	15	6.32	11.52	7.83	2.06	3.69	1.80	51	35.45	64.68	43.95	11.55	20.73	10.12
08:00	15	5.10	11.49	8.93	2.43	3.50	2.50	51	28.60	64.48	50.13	13.63	19.64	14.03
09:00	15	4.66	12.37	8.94	2.89	4.44	5.01	51	26.18	69.44	50.19	16.20	24.90	28.12
10:00	15	3.73	14.67	8.98	3.17	6.70	6.01	51	20.95	82.34	50.42	17.81	37.61	33.72
11:00	15	5.44	16.04	11.22	3.14	6.87	7.51	51	30.52	90.01	62.98	17.61	38.54	42.13

12:00	15	4.68	16.86	11.57	3.50	7.54	7.59	51	26.25	94.65	64.92	19.66	42.32	42.59
13:00	15	8.96	16.65	12.98	4.30	7.53	7.56	51	50.32	93.47	72.87	24.12	42.24	42.42
14:00	15	7.65	15.69	15.82	3.96	7.21	8.38	51	42.92	88.08	88.82	22.20	40.49	47.02
15:00	15	9.93	20.75	19.55	5.09	8.80	9.49	51	55.73	116.49	109.75	28.58	49.42	53.24
16:00	15	11.64	22.94	19.75	4.48	8.14	7.91	51	65.32	128.75	110.87	25.14	45.70	44.39
17:00	15	15.65	20.85	24.71	5.20	7.48	8.17	51	87.86	117.04	138.70	29.18	42.00	45.88
18:00	15	22.26	28.08	33.27	5.99	7.41	8.98	51	124.97	157.61	186.73	33.62	41.62	50.43
19:00	15	22.52	30.14	36.67	5.52	7.70	8.74	51	126.42	169.18	205.85	30.99	43.25	49.04
20:00	15	20.84	31.84	35.98	6.07	9.83	9.23	51	116.99	178.71	201.98	34.09	55.16	51.80
21:00	15	19.94	28.58	34.02	4.93	8.60	9.17	51	111.93	160.41	190.98	27.69	48.27	51.49
22:00	15	16.73	23.49	27.14	4.56	7.85	7.32	51	93.93	131.84	152.34	25.61	44.06	41.06
23:00	15	14.93	18.11	21.33	4.26	6.39	5.25	51	83.80	101.65	119.75	23.92	35.88	29.49
24:00	15	11.60	16.75	18.87	3.99	7.30	6.05	51	65.09	94.02	105.93	22.37	40.97	33.96
00:00	16	38.28	61.15	61.00	17.80	21.34	19.71	52	38.28	61.15	61.00	17.80	21.34	19.71
01:00	16	31.06	52.56	56.36	13.85	18.87	18.49	52	31.06	52.56	56.36	13.85	18.87	18.49
02:00	16	33.65	42.96	51.02	14.12	17.11	16.83	52	33.65	42.96	51.02	14.12	17.11	16.83
03:00	16	30.41	47.29	49.01	11.95	19.19	19.37	52	30.41	47.29	49.01	11.95	19.19	19.37
04:00	16	31.95	46.69	48.26	12.87	18.12	16.72	52	31.95	46.69	48.26	12.87	18.12	16.72
05:00	16	25.94	36.69	42.71	8.76	12.21	10.74	52	25.94	36.69	42.71	8.76	12.21	10.74
06:00	16	25.02	44.22	36.16	6.91	13.62	6.47	52	25.02	44.22	36.16	6.91	13.62	6.47
07:00	16	22.82	41.64	28.29	7.44	13.35	6.52	52	22.82	41.64	28.29	7.44	13.35	6.52
08:00	16	18.41	41.51	32.27	8.77	12.64	9.03	52	18.41	41.51	32.27	8.77	12.64	9.03
09:00	16	16.85	44.70	32.31	10.43	16.03	18.10	52	16.85	44.70	32.31	10.43	16.03	18.10
10:00	16	13.48	53.00	32.45	11.46	24.21	21.70	52	13.48	53.00	32.45	11.46	24.21	21.70
11:00	16	19.65	57.94	40.54	11.33	24.81	27.12	52	19.65	57.94	40.54	11.33	24.81	27.12
12:00	16	16.89	60.92	41.79	12.66	27.24	27.42	52	16.89	60.92	41.79	12.66	27.24	27.42
13:00	16	32.39	60.16	46.90	15.53	27.19	27.30	52	32.39	60.16	46.90	15.53	27.19	27.30
14:00	16	27.63	56.70	57.17	14.29	26.06	30.27	52	27.63	56.70	57.17	14.29	26.06	30.27
15:00	16	35.87	74.98	70.65	18.39	31.81	34.27	52	35.87	74.98	70.65	18.39	31.81	34.27
16:00	16	42.05	82.88	71.36	16.19	29.42	28.58	52	42.05	82.88	71.36	16.19	29.42	28.58

17:00	16	56.55	75.34	89.28	18.78	27.04	29.53	52	56.55	75.34	89.28	18.78	27.04	29.53
18:00	16	80.44	101.45	120.20	21.64	26.79	32.46	52	80.44	101.45	120.20	21.64	26.79	32.46
19:00	16	81.37	108.90	132.50	19.95	27.84	31.57	52	81.37	108.90	132.50	19.95	27.84	31.57
20:00	16	75.30	115.03	130.01	21.94	35.51	33.35	52	75.30	115.03	130.01	21.94	35.51	33.35
21:00	16	72.05	103.25	122.93	17.82	31.07	33.14	52	72.05	103.25	122.93	17.82	31.07	33.14
22:00	16	60.46	84.86	98.06	16.48	28.36	26.43	52	60.46	84.86	98.06	16.48	28.36	26.43
23:00	16	53.94	65.43	77.08	15.40	23.10	18.98	52	53.94	65.43	77.08	15.40	23.10	18.98
24:00	16	41.90	60.52	68.18	14.40	26.37	21.86	52	41.90	60.52	68.18	14.40	26.37	21.86
00:00	20	59.48	94.99	94.76	27.66	33.16	30.62	54	10.60	16.92	16.88	4.93	5.91	5.46
01:00	20	48.25	81.65	87.55	21.51	29.32	28.73	54	8.60	14.55	15.60	3.83	5.22	5.12
02:00	20	52.28	66.74	79.26	21.94	26.58	26.15	54	9.31	11.89	14.12	3.91	4.74	4.66
03:00	20	47.25	73.47	76.15	18.56	29.81	30.10	54	8.42	13.09	13.57	3.31	5.31	5.36
04:00	20	49.63	72.53	74.98	20.00	28.16	25.98	54	8.84	12.92	13.36	3.56	5.02	4.63
05:00	20	40.30	57.01	66.36	13.61	18.97	16.69	54	7.18	10.16	11.82	2.42	3.38	2.97
06:00	20	38.86	68.70	56.18	10.73	21.16	10.05	54	6.92	12.24	10.01	1.91	3.77	1.79
07:00	20	35.45	64.68	43.95	11.55	20.73	10.12	54	6.32	11.52	7.83	2.06	3.69	1.80
08:00	20	28.60	64.48	50.13	13.63	19.64	14.03	54	5.10	11.49	8.93	2.43	3.50	2.50
09:00	20	26.18	69.44	50.19	16.20	24.90	28.12	54	4.66	12.37	8.94	2.89	4.44	5.01
10:00	20	20.95	82.34	50.42	17.81	37.61	33.72	54	3.73	14.67	8.98	3.17	6.70	6.01
11:00	20	30.52	90.01	62.98	17.61	38.54	42.13	54	5.44	16.04	11.22	3.14	6.87	7.51
12:00	20	26.25	94.65	64.92	19.66	42.32	42.59	54	4.68	16.86	11.57	3.50	7.54	7.59
13:00	20	50.32	93.47	72.87	24.12	42.24	42.42	54	8.96	16.65	12.98	4.30	7.53	7.56
14:00	20	42.92	88.08	88.82	22.20	40.49	47.02	54	7.65	15.69	15.82	3.96	7.21	8.38
15:00	20	55.73	116.49	109.75	28.58	49.42	53.24	54	9.93	20.75	19.55	5.09	8.80	9.49
16:00	20	65.32	128.75	110.87	25.14	45.70	44.39	54	11.64	22.94	19.75	4.48	8.14	7.91
17:00	20	87.86	117.04	138.70	29.18	42.00	45.88	54	15.65	20.85	24.71	5.20	7.48	8.17
18:00	20	124.97	157.61	186.73	33.62	41.62	50.43	54	22.26	28.08	33.27	5.99	7.41	8.98
19:00	20	126.42	169.18	205.85	30.99	43.25	49.04	54	22.52	30.14	36.67	5.52	7.70	8.74
20:00	20	116.99	178.71	201.98	34.09	55.16	51.80	54	20.84	31.84	35.98	6.07	9.83	9.23
21:00	20	111.93	160.41	190.98	27.69	48.27	51.49	54	19.94	28.58	34.02	4.93	8.60	9.17

22:00	20	93.93	131.84	152.34	25.61	44.06	41.06	54	16.73	23.49	27.14	4.56	7.85	7.32
23:00	20	83.80	101.65	119.75	23.92	35.88	29.49	54	14.93	18.11	21.33	4.26	6.39	5.25
24:00	20	65.09	94.02	105.93	22.37	40.97	33.96	54	11.60	16.75	18.87	3.99	7.30	6.05
00:00	22	38.28	61.15	61.00	17.80	21.34	19.71	56	38.28	61.15	61.00	17.80	21.34	19.71
01:00	22	31.06	52.56	56.36	13.85	18.87	18.49	56	31.06	52.56	56.36	13.85	18.87	18.49
02:00	22	33.65	42.96	51.02	14.12	17.11	16.83	56	33.65	42.96	51.02	14.12	17.11	16.83
03:00	22	30.41	47.29	49.01	11.95	19.19	19.37	56	30.41	47.29	49.01	11.95	19.19	19.37
04:00	22	31.95	46.69	48.26	12.87	18.12	16.72	56	31.95	46.69	48.26	12.87	18.12	16.72
05:00	22	25.94	36.69	42.71	8.76	12.21	10.74	56	25.94	36.69	42.71	8.76	12.21	10.74
06:00	22	25.02	44.22	36.16	6.91	13.62	6.47	56	25.02	44.22	36.16	6.91	13.62	6.47
07:00	22	22.82	41.64	28.29	7.44	13.35	6.52	56	22.82	41.64	28.29	7.44	13.35	6.52
08:00	22	18.41	41.51	32.27	8.77	12.64	9.03	56	18.41	41.51	32.27	8.77	12.64	9.03
09:00	22	16.85	44.70	32.31	10.43	16.03	18.10	56	16.85	44.70	32.31	10.43	16.03	18.10
10:00	22	13.48	53.00	32.45	11.46	24.21	21.70	56	13.48	53.00	32.45	11.46	24.21	21.70
11:00	22	19.65	57.94	40.54	11.33	24.81	27.12	56	19.65	57.94	40.54	11.33	24.81	27.12
12:00	22	16.89	60.92	41.79	12.66	27.24	27.42	56	16.89	60.92	41.79	12.66	27.24	27.42
13:00	22	32.39	60.16	46.90	15.53	27.19	27.30	56	32.39	60.16	46.90	15.53	27.19	27.30
14:00	22	27.63	56.70	57.17	14.29	26.06	30.27	56	27.63	56.70	57.17	14.29	26.06	30.27
15:00	22	35.87	74.98	70.65	18.39	31.81	34.27	56	35.87	74.98	70.65	18.39	31.81	34.27
16:00	22	42.05	82.88	71.36	16.19	29.42	28.58	56	42.05	82.88	71.36	16.19	29.42	28.58
17:00	22	56.55	75.34	89.28	18.78	27.04	29.53	56	56.55	75.34	89.28	18.78	27.04	29.53
18:00	22	80.44	101.45	120.20	21.64	26.79	32.46	56	80.44	101.45	120.20	21.64	26.79	32.46
19:00	22	81.37	108.90	132.50	19.95	27.84	31.57	56	81.37	108.90	132.50	19.95	27.84	31.57
20:00	22	75.30	115.03	130.01	21.94	35.51	33.35	56	75.30	115.03	130.01	21.94	35.51	33.35
21:00	22	72.05	103.25	122.93	17.82	31.07	33.14	56	72.05	103.25	122.93	17.82	31.07	33.14
22:00	22	60.46	84.86	98.06	16.48	28.36	26.43	56	60.46	84.86	98.06	16.48	28.36	26.43
23:00	22	53.94	65.43	77.08	15.40	23.10	18.98	56	53.94	65.43	77.08	15.40	23.10	18.98
24:00	22	41.90	60.52	68.18	14.40	26.37	21.86	56	41.90	60.52	68.18	14.40	26.37	21.86
00:00	24	38.28	61.15	61.00	17.80	21.34	19.71	57	38.28	61.15	61.00	17.80	21.34	19.71
01:00	24	31.06	52.56	56.36	13.85	18.87	18.49	57	31.06	52.56	56.36	13.85	18.87	18.49

02:00	24	33.65	42.96	51.02	14.12	17.11	16.83	57	33.65	42.96	51.02	14.12	17.11	16.83
03:00	24	30.41	47.29	49.01	11.95	19.19	19.37	57	30.41	47.29	49.01	11.95	19.19	19.37
04:00	24	31.95	46.69	48.26	12.87	18.12	16.72	57	31.95	46.69	48.26	12.87	18.12	16.72
05:00	24	25.94	36.69	42.71	8.76	12.21	10.74	57	25.94	36.69	42.71	8.76	12.21	10.74
06:00	24	25.02	44.22	36.16	6.91	13.62	6.47	57	25.02	44.22	36.16	6.91	13.62	6.47
07:00	24	22.82	41.64	28.29	7.44	13.35	6.52	57	22.82	41.64	28.29	7.44	13.35	6.52
08:00	24	18.41	41.51	32.27	8.77	12.64	9.03	57	18.41	41.51	32.27	8.77	12.64	9.03
09:00	24	16.85	44.70	32.31	10.43	16.03	18.10	57	16.85	44.70	32.31	10.43	16.03	18.10
10:00	24	13.48	53.00	32.45	11.46	24.21	21.70	57	13.48	53.00	32.45	11.46	24.21	21.70
11:00	24	19.65	57.94	40.54	11.33	24.81	27.12	57	19.65	57.94	40.54	11.33	24.81	27.12
12:00	24	16.89	60.92	41.79	12.66	27.24	27.42	57	16.89	60.92	41.79	12.66	27.24	27.42
13:00	24	32.39	60.16	46.90	15.53	27.19	27.30	57	32.39	60.16	46.90	15.53	27.19	27.30
14:00	24	27.63	56.70	57.17	14.29	26.06	30.27	57	27.63	56.70	57.17	14.29	26.06	30.27
15:00	24	35.87	74.98	70.65	18.39	31.81	34.27	57	35.87	74.98	70.65	18.39	31.81	34.27
16:00	24	42.05	82.88	71.36	16.19	29.42	28.58	57	42.05	82.88	71.36	16.19	29.42	28.58
17:00	24	56.55	75.34	89.28	18.78	27.04	29.53	57	56.55	75.34	89.28	18.78	27.04	29.53
18:00	24	80.44	101.45	120.20	21.64	26.79	32.46	57	80.44	101.45	120.20	21.64	26.79	32.46
19:00	24	81.37	108.90	132.50	19.95	27.84	31.57	57	81.37	108.90	132.50	19.95	27.84	31.57
20:00	24	75.30	115.03	130.01	21.94	35.51	33.35	57	75.30	115.03	130.01	21.94	35.51	33.35
21:00	24	72.05	103.25	122.93	17.82	31.07	33.14	57	72.05	103.25	122.93	17.82	31.07	33.14
22:00	24	60.46	84.86	98.06	16.48	28.36	26.43	57	60.46	84.86	98.06	16.48	28.36	26.43
23:00	24	53.94	65.43	77.08	15.40	23.10	18.98	57	53.94	65.43	77.08	15.40	23.10	18.98
24:00	24	41.90	60.52	68.18	14.40	26.37	21.86	57	41.90	60.52	68.18	14.40	26.37	21.86
00:00	30	33.38	53.31	53.18	15.52	18.61	17.19	58	38.28	61.15	61.00	17.80	21.34	19.71
01:00	30	27.08	45.82	49.13	12.07	16.45	16.12	58	31.06	52.56	56.36	13.85	18.87	18.49
02:00	30	29.34	37.45	44.48	12.31	14.92	14.67	58	33.65	42.96	51.02	14.12	17.11	16.83
03:00	30	26.52	41.23	42.73	10.42	16.73	16.89	58	30.41	47.29	49.01	11.95	19.19	19.37
04:00	30	27.85	40.70	42.08	11.22	15.80	14.58	58	31.95	46.69	48.26	12.87	18.12	16.72
05:00	30	22.62	31.99	37.24	7.64	10.65	9.37	58	25.94	36.69	42.71	8.76	12.21	10.74
06:00	30	21.81	38.56	31.53	6.02	11.87	5.64	58	25.02	44.22	36.16	6.91	13.62	6.47

07:00	30	19.90	36.30	24.67	6.48	11.63	5.68	58	22.82	41.64	28.29	7.44	13.35	6.52
08:00	30	16.05	36.19	28.13	7.65	11.02	7.87	58	18.41	41.51	32.27	8.77	12.64	9.03
09:00	30	14.69	38.97	28.17	9.09	13.98	15.78	58	16.85	44.70	32.31	10.43	16.03	18.10
10:00	30	11.76	46.21	28.29	9.99	21.10	18.92	58	13.48	53.00	32.45	11.46	24.21	21.70
11:00	30	17.13	50.51	35.35	9.88	21.63	23.64	58	19.65	57.94	40.54	11.33	24.81	27.12
12:00	30	14.73	53.12	36.43	11.04	23.75	23.90	58	16.89	60.92	41.79	12.66	27.24	27.42
13:00	30	28.24	52.45	40.89	13.54	23.71	23.80	58	32.39	60.16	46.90	15.53	27.19	27.30
14:00	30	24.08	49.43	49.84	12.46	22.72	26.39	58	27.63	56.70	57.17	14.29	26.06	30.27
15:00	30	31.27	65.38	61.59	16.04	27.73	29.88	58	35.87	74.98	70.65	18.39	31.81	34.27
16:00	30	36.66	72.25	62.22	14.11	25.65	24.91	58	42.05	82.88	71.36	16.19	29.42	28.58
17:00	30	49.30	65.68	77.84	16.37	23.57	25.75	58	56.55	75.34	89.28	18.78	27.04	29.53
18:00	30	70.13	88.45	104.79	18.87	23.36	28.30	58	80.44	101.45	120.20	21.64	26.79	32.46
19:00	30	70.94	94.94	115.52	17.39	24.27	27.52	58	81.37	108.90	132.50	19.95	27.84	31.57
20:00	30	65.65	100.29	113.35	19.13	30.96	29.07	58	75.30	115.03	130.01	21.94	35.51	33.35
21:00	30	62.82	90.02	107.18	15.54	27.09	28.90	58	72.05	103.25	122.93	17.82	31.07	33.14
22:00	30	52.71	73.99	85.49	14.37	24.72	23.04	58	60.46	84.86	98.06	16.48	28.36	26.43
23:00	30	47.03	57.05	67.20	13.43	20.14	16.55	58	53.94	65.43	77.08	15.40	23.10	18.98
24:00	30	36.53	52.76	59.45	12.56	22.99	19.06	58	41.90	60.52	68.18	14.40	26.37	21.86
00:00	34	38.28	61.15	61.00	17.80	21.34	19.71	59	38.28	61.15	61.00	17.80	21.34	19.71
01:00	34	31.06	52.56	56.36	13.85	18.87	18.49	59	31.06	52.56	56.36	13.85	18.87	18.49
02:00	34	33.65	42.96	51.02	14.12	17.11	16.83	59	33.65	42.96	51.02	14.12	17.11	16.83
03:00	34	30.41	47.29	49.01	11.95	19.19	19.37	59	30.41	47.29	49.01	11.95	19.19	19.37
04:00	34	31.95	46.69	48.26	12.87	18.12	16.72	59	31.95	46.69	48.26	12.87	18.12	16.72
05:00	34	25.94	36.69	42.71	8.76	12.21	10.74	59	25.94	36.69	42.71	8.76	12.21	10.74
06:00	34	25.02	44.22	36.16	6.91	13.62	6.47	59	25.02	44.22	36.16	6.91	13.62	6.47
07:00	34	22.82	41.64	28.29	7.44	13.35	6.52	59	22.82	41.64	28.29	7.44	13.35	6.52
08:00	34	18.41	41.51	32.27	8.77	12.64	9.03	59	18.41	41.51	32.27	8.77	12.64	9.03
09:00	34	16.85	44.70	32.31	10.43	16.03	18.10	59	16.85	44.70	32.31	10.43	16.03	18.10
10:00	34	13.48	53.00	32.45	11.46	24.21	21.70	59	13.48	53.00	32.45	11.46	24.21	21.70
11:00	34	19.65	57.94	40.54	11.33	24.81	27.12	59	19.65	57.94	40.54	11.33	24.81	27.12

12:00	34	16.89	60.92	41.79	12.66	27.24	27.42	59	16.89	60.92	41.79	12.66	27.24	27.42
13:00	34	32.39	60.16	46.90	15.53	27.19	27.30	59	32.39	60.16	46.90	15.53	27.19	27.30
14:00	34	27.63	56.70	57.17	14.29	26.06	30.27	59	27.63	56.70	57.17	14.29	26.06	30.27
15:00	34	35.87	74.98	70.65	18.39	31.81	34.27	59	35.87	74.98	70.65	18.39	31.81	34.27
16:00	34	42.05	82.88	71.36	16.19	29.42	28.58	59	42.05	82.88	71.36	16.19	29.42	28.58
17:00	34	56.55	75.34	89.28	18.78	27.04	29.53	59	56.55	75.34	89.28	18.78	27.04	29.53
18:00	34	80.44	101.45	120.20	21.64	26.79	32.46	59	80.44	101.45	120.20	21.64	26.79	32.46
19:00	34	81.37	108.90	132.50	19.95	27.84	31.57	59	81.37	108.90	132.50	19.95	27.84	31.57
20:00	34	75.30	115.03	130.01	21.94	35.51	33.35	59	75.30	115.03	130.01	21.94	35.51	33.35
21:00	34	72.05	103.25	122.93	17.82	31.07	33.14	59	72.05	103.25	122.93	17.82	31.07	33.14
22:00	34	60.46	84.86	98.06	16.48	28.36	26.43	59	60.46	84.86	98.06	16.48	28.36	26.43
23:00	34	53.94	65.43	77.08	15.40	23.10	18.98	59	53.94	65.43	77.08	15.40	23.10	18.98
24:00	34	41.90	60.52	68.18	14.40	26.37	21.86	59	41.90	60.52	68.18	14.40	26.37	21.86
00:00	35	38.28	61.15	61.00	17.80	21.34	19.71							
01:00	35	31.06	52.56	56.36	13.85	18.87	18.49							
02:00	35	33.65	42.96	51.02	14.12	17.11	16.83							
03:00	35	30.41	47.29	49.01	11.95	19.19	19.37							
04:00	35	31.95	46.69	48.26	12.87	18.12	16.72							
05:00	35	25.94	36.69	42.71	8.76	12.21	10.74							
06:00	35	25.02	44.22	36.16	6.91	13.62	6.47							
07:00	35	22.82	41.64	28.29	7.44	13.35	6.52							
08:00	35	18.41	41.51	32.27	8.77	12.64	9.03							
09:00	35	16.85	44.70	32.31	10.43	16.03	18.10							
10:00	35	13.48	53.00	32.45	11.46	24.21	21.70							
11:00	35	19.65	57.94	40.54	11.33	24.81	27.12							
12:00	35	16.89	60.92	41.79	12.66	27.24	27.42							
13:00	35	32.39	60.16	46.90	15.53	27.19	27.30							
14:00	35	27.63	56.70	57.17	14.29	26.06	30.27							
15:00	35	35.87	74.98	70.65	18.39	31.81	34.27							
16:00	35	42.05	82.88	71.36	16.19	29.42	28.58							

17:00	35	56.55	75.34	89.28	18.78	27.04	29.53							
18:00	35	80.44	101.45	120.20	21.64	26.79	32.46							
19:00	35	81.37	108.90	132.50	19.95	27.84	31.57							
20:00	35	75.30	115.03	130.01	21.94	35.51	33.35							
21:00	35	72.05	103.25	122.93	17.82	31.07	33.14							
22:00	35	60.46	84.86	98.06	16.48	28.36	26.43							
23:00	35	53.94	65.43	77.08	15.40	23.10	18.98							
24:00	35	41.90	60.52	68.18	14.40	26.37	21.86							